DOCTOR OF PHILOSOPHY

Characterisation of the localisation and function of the Bacillus subtilis YuaB protein during biofilm formation

Ostrowski, Adam

Award date:
2012

University of Dundee
Division of Molecular Microbiology

Characterisation of the localisation and function of the *Bacillus subtilis* YuaB protein during biofilm formation

Adam Ostrowski

A thesis submitted for the degree for Doctor of philosophy

September 2012

Declaration

I declare that I am the author of this thesis. Unless otherwise stated, all references cited have been consulted by myself. I declare that the experiments of which the thesis is a record of have been conducted by myself and that any work conducted by other researchers has been noted accordingly. I declare that the thesis has not been previously accepted for a higher degree.

Adam Ostrowski

(Candidate)

Dr Nicola R. Stanley-Wall

(Supervisor)

Acknowledgements

First of all, the greatest Thank You goes to Nicola for accepting me into her lab after what could possibly be one of the most bizarre interviews of the year and for her guidance, help and supervision over the past 4 years. I learned from you more than I could list if asked. We had our differences and misunderstandings but I think we worked through it all pretty well and have ended on a high.

All this would not have happened without all of the people in the NSW lab, both past and present. You guys make being here a fantastic experience and turn hard work into a really good fun. Keep it going this way! Taryn, you deserve special thanks for bearing with me, my moods and constant nagging for something over all those years and most of all for becoming a fantastic friend. Laura, you appeared in my little world in one of the most difficult times and not only did you not run away but you kept supporting and cheering me up for these long months. Thank you!

All the MMB people, many thanks to all of you too. I'm sure I asked every one of you for something at least once and you're a great bunch of people that are fun to be around. I must mention Jackie, who keeps all of us safe from self-inflicted harm and keeps the entire division going, and all that with a smile. Many thanks to Angela and Alan for helping me with my work and sharing their knowledge and experiences with me.

I also want to thank my family for their support in all of my decisions, many of which were difficult for them. I also thank all of my former teachers and mentors. I wouldn't be who I am without any them.

Last, but by far not the least, I'm so grateful to Michael for his strongest never-ending support through every hard moment, every doubt and every tear. You're so much more than I could ever hope for and I wouldn't be able to do any of this without you.

Publications

Ostrowski, A., Mehlert, A., Prescott, A., Kiley, T. B., Stanley-Wall, N. R. (2011). YuaB functions synergistically with the exopolysaccharide and TasA amyloid fibres to allow biofilm formation by *Bacillus subtilis*. Journal of Bacteriology 193(18): 4821-4831

Ostrowski, A., Hobley, L., Porter, M., Prescott, A., Penman, G., Swedlow, J. R., van Aalten, D. M. F., Stanley-Wall, N. R. (2012) BslA (YuaB) forms higher order structures in *Bacillus subtilis* biofilms. (In preparation)

Abstract

Bacteria can actively communicate and interact with each other to establish multicellular communities. Many of these processes involve functional differentiation of cells into specialised subpopulations by expression of varying genetic programmes. This leads to division of labour between the arising subpopulations of cells in the community. One type of such community is the biofilm, which is composed of microbial cells enclosed in a biopolymeric matrix. Such biofilms can be formed in a large range of environments from sea beds to animal tissues. *Bacillus subtilis* is a soil dwelling Gram-positive rod that was shown to closely interact with plants and establish a protective symbiosis by formation of biofilms on the roots. The biofilm matrix synthesised by *B. subtilis* is composed of the exopolysaccharide, for which the chemical structure is not yet established, and a protein TasA that forms amyloid-like fibres spanning between the cells and anchored to the cells by an accessory protein TapA. A third protein of unknown function, YuaB, has also been shown to be necessary for establishment of a biofilm. However, the mechanism of function for YuaB has not been elucidated. The data presented in this report focus on the role played by YuaB during formation of the biofilm. By analysis of cell differentiation patterns YuaB was shown to be required for maturation of the biofilm. The localisation of YuaB is identified in two “subtypes” of biofilm, a biofilm pellicle floating on the air-liquid interface and complex colonies formed on solid surfaces. This is achieved using a combination of biofilm fractionation combined with Western blotting and a newly developed method for immuno-fluorescent labelling of biofilm proteins. YuaB acts in synergy with the exopolysaccharide and TasA, as both components of the biofilm matrix are synthesised in the absence of YuaB but the biofilm is not made. The initial structural characterisation of YuaB is presented based on *in silico* predictions and physiological and biophysical analysis of the mutations introduced into the sequence of YuaB. The experimental data is concluded with a hypothesis that YuaB forms a hydrophobic protective layer necessary for support of the structure of the matured biofilm.

General abbreviations

AbDil	Antibody diluent
AHL	Acyl-homoserine lactones
AI-2	Autoinducer type 2
API	Application programming interface
APS	Ammonium persulphate
ATP	Adenosine 5'-triphosphate
AU	Arbitrary units
Bap	Biofilm associated proteins
Bhp	Bap homologous proteins
BSA	Bovine serum albumin
CD	Circular dichroism
CF	Cystic fibrosis
CFU	Colony forming units
CLSM	Confocal laser scanning microscopy
Cml	Chloramphenicol
ddH_2O	Double distilled water
DNA	Deoxyribonucleic acid
dNTP	Deoxyribonucleotide triphosphates
e. g.	*Exempli gratia* (*lat.* For example)
ECL	Enhanced chemiluminescence
eDNA	Extracellular DNA

EDTA	Ethylenediaminetetraacetic acid
EGTA	Ethylene glycol tetraacetic acid
EPS	Exopolysaccharide
et al.	*Et alii* (*lat.* And others)
FPLC	Fast performance liquid chromatography
GFP	Green fluorescent protein
GlcNAc	*N*-acetylglucosamine
GST	Glutathione transferase S
hEGF	Human Epithelial growth factor
HIS_6	Hexahistidine
i. e.	*Id est* (*lat.* That is)
IgG	Immunoglobulin fraction G
IPTG	Isopropyl β-D-1-thiogalactopyranoside
Kan	Kanamycin
Lat.	Latin
LB	Lysogeny Broth (Luria-Bertani broth)
LC-MS-MS	Liquid chromatography – mass spectrometry
MLS	Macrolides, lincosamides and streptogramins
MSgg	Minimal salts glutamic acid glycerol (Media)
MS-TOF	Mass spectrometry – time of flight
MWCO	Molecular weight cut off
OD_{600}	Optical density measured at wavelength 600 nm

PAGE	Polyacrylamide gel electrophoresis
PBS	Phosphate buffered saline
PCR	Polymerase chain reaction
PEL	*pel* locus (*P. aeruginosa* polysaccharide)
PFA	Paraformaldehyde
PGPR	Plant growth-promoting rhizobacteria
PNAG	β-1,6-*N*-acetyl-D-glucosamine
PSI	Pounds per square inch
PSL	Polysaccharide locus (*P. aeruginosa* polysaccharide)
PVDF	Polyvinylidene fluoride
QS	Quorum sensing
ROI	Region of interest
SDS	Sodium dodecyl sulphate
Sp	Subspecies
Spc	Spectinomycin
TAE	Tris acetic acid EDTA
TAFI	Thin aggregative fimbriae
TBS	Tris buffered saline
TEM	Transmission electron microscopy
TEMED	N,N,N',N'-tetramethylethylenediamine
Tet	Tetracycline
TEV	Tobacco etch virus

TY	Tryptone Yeast extract (media)
U	Unit
UV	Ultra violet
v/v	Volume to volume
w/v	Weight to volume

Table of contents

Table of figures

List of tables

1. Introduction

1.1. Bacteria as multicellular organisms

1.1.1. Bacterial life in the laboratory and in the wild

Since methods for cultivating pure bacterial cultures were established by Robert Koch in the late XIXth century, bacteriologists worldwide have traditionally propagated bacterial strains either in shaking liquid media or as single colonies on solidified growth media. Indeed, this approach has allowed for the development of numerous methods for bacterial species identification, genetic manipulation, as well as a comprehensive understanding of bacterial physiology and biochemistry (Madigan *et al.*, 2000). Consequently, cultures of pure strains of microorganisms are the basis of many biotechnological processes, allowing for fast and clean production of various products from enzymes to biopolymers (Morikawa, 2006). However, maintaining a pure microbial culture is possible only in the laboratory environment and is a phenomenon that does not (generally) exist in the natural environment.

1.1.1.1. Social life of bacteria in the natural environment

Outside the laboratory, bacteria typically co-exist in mixed multispecies populations. Here they are governed by identical ecological mechanisms as populations of any other living organisms (Costerton *et al.*, 1987). Bacteria are capable of communicating and establishing competitive, cooperative, mutualistic and even parasitic relationships (Shapiro, 1998, Gonzalez-Pastor *et al.*, 2003, Bassler & Losick, 2006, Aguilar *et al.*, 2007, Sockett, 2009, Kearns, 2010), which are a form of multicellular lifestyle of bacteria. The multicellular behaviour of bacteria occurs not

only in the complex communities of unrelated species, but is also observed in monospecies populations (Shapiro, 1998). In this case multicellularity is defined as the ability of the community of bacterial cells to communicate, actively direct the development of the community, coordinate growth, movement and biochemistry as well as division of labour (Shapiro, 1998).

The differentiation of a monoclonal population into various cell types has been shown for many different phyla of prokaryotes (Shapiro, 1998). One classic example are the cyanobacteria. Many species of the Cyanobacteria phylum grow in the form of long filaments of clonally identical cells. Despite the identical genetic blueprint, a distinct cell type, known as a heterocyst, periodically develops in the filament. These differentiated cells are dedicated to nitrogen fixation and are biochemically distinct from their genetic siblings (Adams, 1997). Another example of cellular differentiation within bacterial community can be drawn from *Streptomyces*. These filamentous Gram-positive bacteria differentiate the vegetative filaments into aerial hyphae which rise above the vegetative hyphae to produce dormant spores (Chater & Losick, 1997). Not only do these new hyphae undergo specialization into spore producers to ensure prevalence of the entire community, but the vegetative hyphae provide nutrients for the growing aerial hyphae by localised lysis (Chater & Losick, 1997). Finally, probably the best described example of multicellularity in bacteria is from the genus *Myxococcus*. *Myxococcus* species are best known for their ability to form fruiting bodies (Shimkets & Dworkin, 1997). These macrostructures are formed by a population of cells which have gathered in one place by directed motility. During active accumulation of bacterial cells, some cells remain motile and organise spatially to form the outer structure of a fruiting body. In contrast, the cells localised in the centre of

the fruiting body are organised in a much looser manner. These cells become immotile to begin differentiation into dormant and resistant spores (Shimkets & Dworkin, 1997). The examples of cyanobacteria, *Streptomyces,* and *Myxococcus* show the ability of the individual isogenic cells within a larger community to co-operate and contribute towards the benefit of entire community. The emergence of morphologically and biochemically diverse cell types from genetically identical population of bacteria resembles the differentiation observed in, and thought by many to be restricted to, higher organisms. The discovery of this phenomenon in many bacterial species was possible only due to development of cytological methods such as expression monitoring with fluorescent proteins on a single cell level (Figure 1.1). These methods allowed for direct observation of differentiation of cells with modest phenotypes, from the rest of the population, that are not apparent to the naked eye. Thus the development of these new methods has allowed for a better understanding of the widespread nature of multicellularity in prokaryotes.

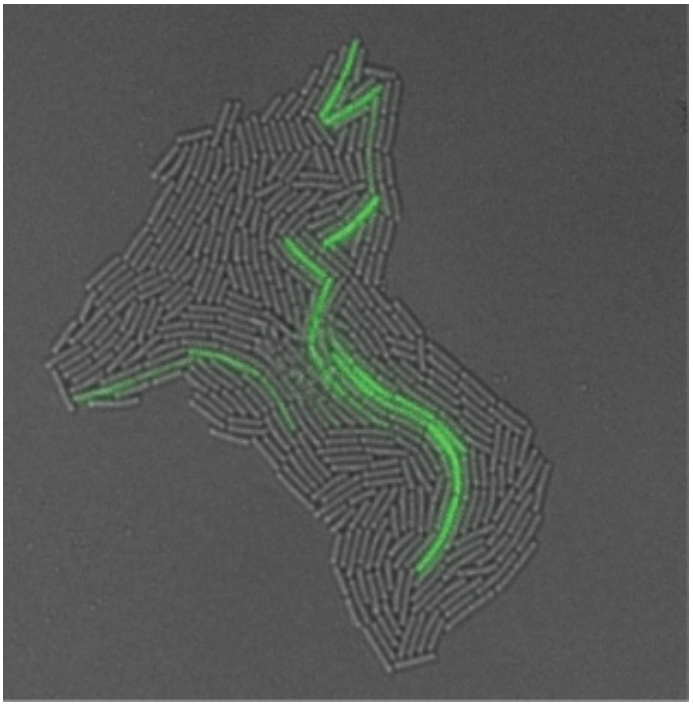

Figure 1.1 Bacteria in a multicellular community undergo differentiation into different cell types. A subpopulation of cells of *B. subtilis* expressing biofilm matrix genes (indicated by green fluorescence) emerges from generally non-fluorescent population (V. Marlow).

1.1.1.2. Laboratory strains lose multicellular features

The complexity of multispecies interactions, and the strength of environmental pressure to maintain the ability to interact with other species, became apparent when the wild isolates of bacteria were compared to domesticated strains (Fux *et al.*, 2005b). The domesticated, or laboratory, strains were shown to contain multiple frame shift mutations in the sequences of encoded genes, often leading to loss of function of the impacted genes. These mutations were introduced either by prolonged cultivation of strains in the laboratory (away from environmental pressure) and were exacerbated by the selection of phenotypes favouring lack of synthesis of extracellular matrix to ease laboratory proceedings; or by random mutagenesis during experimentation, which gave rise to traits desired in the laboratory (Fux *et al.*, 2005b, McLoon *et al.*, 2011). As a result, many of the laboratory strains have lost the ability to undertake some types of

multicellular behaviours observed in the wild isolates (Fux *et al.*, 2005b, Patrick & Kearns, 2009, Kearns, 2010, McLoon *et al.*, 2011).

1.1.2. Intercellular signalling

The study of bacteria-to-bacteria and bacteria-to-environment relationships is difficult outside the laboratory environment, where experimental conditions cannot be maintained stably and the naturally varying environmental factors affect the experimental readout. Fortunately, many simplified variations on the behaviour of the wild bacteria can be observed in laboratory conditions (Aguilar *et al.*, 2007). This opens a gateway to allow us to understand how an individual species of bacteria changes and adapts to the life in a community, rather than as single, dispersed cells in a nutrient medium. Understanding the genetic and physiological adaptation of individual species of bacteria will allow for a better understanding of interspecies processes observed in the natural environment.

1.1.2.1. Bacteria communicate using diffusible molecules

Multicellular behaviours exhibited by bacteria are a consequence of the cells responding to various environmental cues, perhaps to enhance the chances of survival in rapidly changing conditions (Shapiro, 1998, Aguilar *et al.*, 2007). However, any cooperative behaviour requires a capability of communication between individuals. The first report of bacterial interspecies communication was observed in *Vibrio fischeri* (Hastings & Nealson, 1977). An acyl-homoserine lactone produced by this bacterium is detected by a dedicated sensory protein LuxR that activates the expression of genes required for bioluminescence (Engebrecht & Silverman, 1984). Since then, similar systems have been described in various Gram-negative bacteria (Bassler & Losick,

2006). In principle, Gram-negative bacteria synthesise homoserine lactones (AHL) with various side chain lengths and modifications specific for their own species (Figure 1.2A) (Bassler, 2002). These lactones freely pass through bacterial membranes. Once a threshold concentration is reached, the presence of the signalling molecule, called the autoinducer, is detected by a cognate sensory protein triggering genetic regulatory cascade (Schauder & Bassler, 2001). An analogous system exists in Gram-positive bacteria; however, in this case short peptides are typically used as signal molecules (Figure 1.2B) (Bassler & Losick, 2006). Additionally, a two-component system is used as a sensor for the autoinducer detection (Kleerebezem *et al.*, 1997). However, one thought that should be kept in mind is that both these systems are species-specific methods of chemical communication, and therefore are not suitable for coordination of cooperative multispecies communities.

1.1.2.2. Interspecies cross-talk of bacteria

In a mixed-species community, certain member species can be more prevalent than others, but the entire community must coordinate their biochemistry to optimise the processes driving the community (Shank & Kolter, 2009). As a microbial community can contain both Gram-positive and Gram-negative species, no species-specific quorum sensing system can be used for coordinating all of the community members simultaneously. There is, however, a third type of a signal molecule called the type 2 autoinducer (AI-2) (Bassler *et al.*, 1997, Schauder & Bassler, 2001). The AI-2 was initially discovered in *Vibrio harveyi*, a close relative of *V. fischeri*, which encodes a non-canonical AHL-driven quorum sensing system (Bassler *et al.*, 1993, Bassler *et al.*, 1994). *V. harveyi* encodes a protein LuxS responsible for synthesis of furanone (Figure 1.2C) which is a proposed second intercellular signalling molecules, the autoinducer

type 2 (Schauder & Bassler, 2001). The AI-2 is detected by a sensory two-component system, similar to those of Gram-positive bacteria (Schauder & Bassler, 2001). More importantly, homologues of the *luxS* gene were found in over 30 species of both Gram-negative and Gram-positive bacteria. This suggests that the AI-2 system is a chemical language that is widely used by bacteria to assess the member numbers of different species residing in the same ecological niche (Bassler & Losick, 2006).

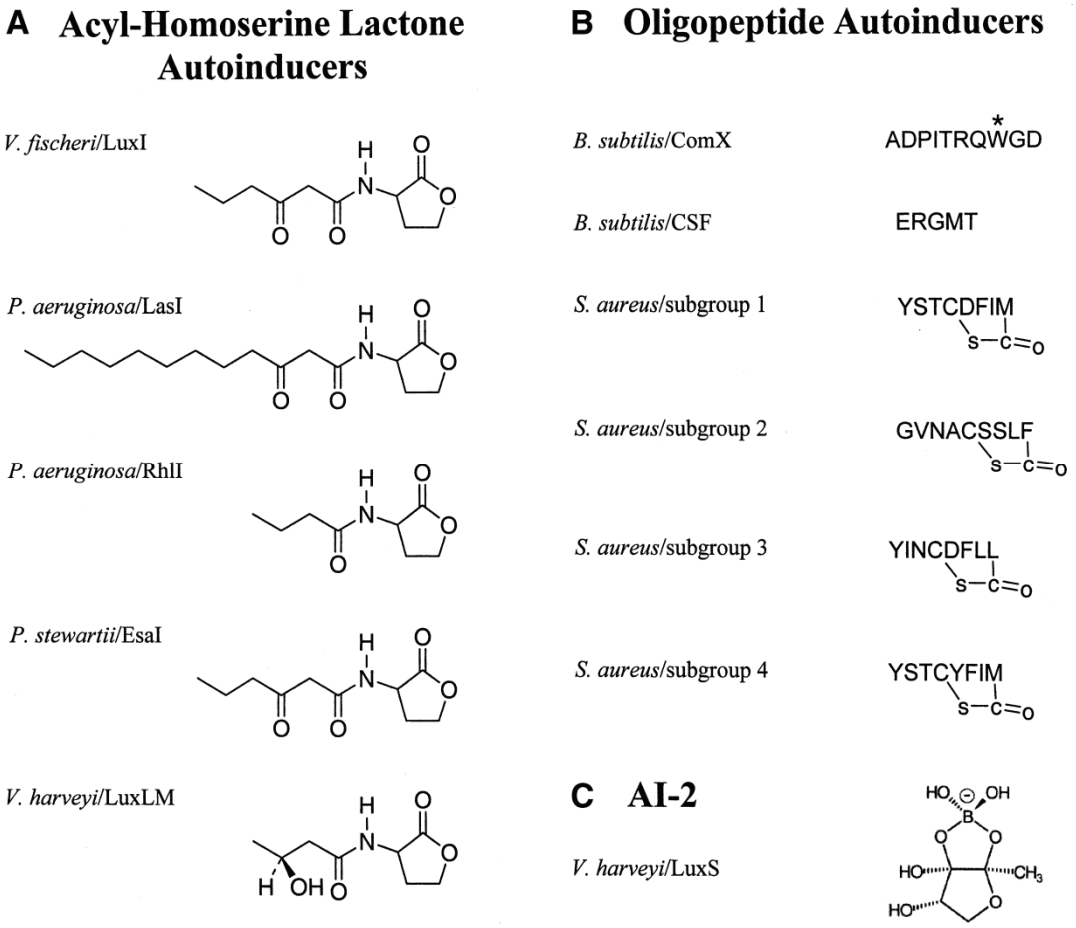

Figure 1.2 The variety of quorum sensing molecules. (**A**) Acyl-homoserine lactones produced by Gram-negative bacteria. (**B**) Oligopeptide pheromones of Gram-Positive bacteria. (**C**) An example of a furanone used as a type 2 autoinducer. Adapted from (Bassler, 2002).

The presence of two types of intercellular communication between bacteria, the species-specific AHL or peptide mediated systems in Gram-negative and Gram-positive species respectively, and the interspecies AI-2 mediated system, allow bacteria to sense the overall quorum of the surrounding community and gauge the

appropriate biochemical response to the dynamically changing environment (Schauder & Bassler, 2001). There are various examples of molecular processes triggered by the high cell density detected via quorum sensing. These include, but are not restricted to the aforementioned initiation of expression genes required for bioluminescence of *V. fischeri*, which takes place in light organs of various aquatic organisms; production of virulence factors by *e.g. Staphylococcus aureus* (Ji *et al.*, 1995), *Pseudomonas aeruginosa* (Latifi *et al.*, 1995, Winson *et al.*, 1995) and *Pectobacterium carotovorum* (Jones *et al.*, 1993); or natural competence for uptake of extracellular DNA by *Bacillus subtilis* (Solomon *et al.*, 1996) and *Streptococcus pneumoniae* (Pestova *et al.*, 1996).

1.1.2.3. Intercellular signalling unrelated to quorum sensing

Recently several other signalling mechanisms have been described that are not based on classical quorum sensing. These mechanisms can be illustrated in the model organism *Bacillus subtilis*. First, the surface tension-reducing surfactin produced by *B. subtilis* was shown to be used by *B. subtilis* as a signalling molecule (Lopez *et al.*, 2009a, Lopez *et al.*, 2009d). Moreover, the same surfactant was also shown to affect the multicellular development of other organisms without causing growth inhibition (Straight *et al.*, 2006). Surfactin is produced only by a subpopulation of cells in the community and is released to the environment (Lopez *et al.*, 2009d). As a surface active compound, surfactin rapidly spreads on the surface (Arima *et al.*, 1968) and comes in contact with more cells in the community than those responsible for its production (Lopez *et al.*, 2009a). Surfactin was proposed as a paracrine signalling molecule.

A second mechanism with regulatory effect on the multicellular behaviour of *B. subtilis* is the production of toxins aimed at cells of its own, and other species, known as cannibalism (Gonzalez-Pastor *et al.*, 2003). The purpose of cannibalism is to provide a boost of nutrients to the entire community. This is achieved by sacrificing a subpopulation that is not resistant to the toxins, thus cannibalism is a type of social behaviour itself. The cannibalistic subpopulation of cells produces extracellular toxins affecting their immediate microbial neighbours. As a result, the non-cannibalistic, and susceptible, cells lyse and release valuable nutrients to the environment. The nutritional boost delays entry into sporulation, thus further affecting differentiation of cells (Gonzalez-Pastor *et al.*, 2003). However, the cannibalistic cells must be resistant to their own toxins. The resistance is achieved by synthesis of immunity proteins (Gonzalez-Pastor *et al.*, 2003). The presence of cannibalism toxins in the environment can additionally be used as a form of signalling. It has been shown that a subpopulation of *B. subtilis* cells can react to the toxins secreted by members of other species from the *Bacillus* genus. As a result this population differentiate into a biofilm forming subpopulation (Shank *et al.*, 2011). The biofilm formation is outlined in more detail in the Sections 1.1.4 and 1.2. Furthermore, a similar reaction was demonstrated in response to the presence of antibiotics, which can also promote biofilm formation (Lopez *et al.*, 2009c). In general, studies like the ones exemplified above elucidate the complex signalling that govern microbial behaviour (Aguilar *et al.*, 2007, Karatan & Watnick, 2009, Shank & Kolter, 2011).

1.1.3. Co-ordinated movement

The coordinated effort of the bacterial community is not only triggered by chemical cues, but also by the environment itself (Kearns, 2010). One such type of

behaviour seems to be swarming motility. Swarming motility occurs on semi-solid surfaces in high density of cells (Kearns, 2010). The genetic circuitry responsible for the transition into swarming motility, in the majority of bacterial species, is regulated by a "master regulator" protein; however, the master regulators of different species share very little similarity between each other (Kearns, 2010). Currently, the greatest insight to swarming is available at the level of cellular morphology. Just like swimming motility, swarming is dependent on rotation of flagella to propel the cell (Kohler *et al.*, 2000, Harshey, 2003, Kearns & Losick, 2003, Rather, 2005). However, there are defined characteristics associated with swarming that distinguish it from swimming motility. These are defined below.

Firstly, swarming motility requires peritrichal flagellation of the cell, which is not a requirement for swimming motility. Even species such as *P. aeruginosa,* with only one polar flagellum, synthesise additional flagella in the stage preceding swarming, called a "swarming lag" (Kohler *et al.*, 2000, Kearns, 2010). Secondly, unlike single cells swimming in a liquid environment, the cells in a swarm traverse the semi-solid surfaces as loosely associated cell rafts (Kearns & Losick, 2003, Jones *et al.*, 2004, Julkowska *et al.*, 2004). It is not known exactly how the cells in the swarm rafts are associated. But what is known is that the cells, at least in some cases, can be actively recruited to the rafts or dissociated from them as the swarm progresses (Kearns & Losick, 2003). Furthermore, the cells that leave a swarming raft quickly become immotile, which suggests that rafting is tightly coupled with swarming motility (Kearns, 2010). The third requirement for swarming to occur is synthesis of a surfactant which reduces the surface tension allowing for easy movement of bacterial cells on the solid surface (Kearns, 2010). The surfactants produced are species specific and belong to several

families of chemical compounds. For example they can be lipopeptides like surfactin or serrawettin produced by *B. subtilis* (Kearns & Losick, 2003, Julkowska *et al.*, 2005) and *S. marcescens* (Matsuyama *et al.*, 1992) respectively or rhamnolipids of *P. aeruginosa* (Kohler *et al.*, 2000). Species of bacteria which exhibit swarming behaviour, but do not synthesise surfactants, are able to swarm only on surfaces of inherently lowered surface tension (Kearns, 2010).

The general reason of swarming motility in the natural environment is still unknown, but it is proposed to be an escape mechanism as swarming cells can move with significant speed of 2 – 10 μm/s (Kearns, 2010). It is also of interest to note that an increased antibiotic resistance was observed in swarming cells in comparison to their swimming counterparts (Overhage *et al.*, 2008). Perhaps the additional phenotypes accompanying the swarming motility are an indication of other changes to the cell physiology that can occur concurrently in a multicellular community.

1.1.4. Bacterial metropolis

It is logical to predict that various environmental cues will trigger different types of response from the microbial community. A noteworthy example, in addition to swarming motility, is formation of complex multicellular communities of cells enclosed in a robust extracellular matrix, that are known as biofilms (Costerton *et al.*, 1987, Costerton *et al.*, 1994, Costerton *et al.*, 1995, Lopez *et al.*, 2010). Biofilm formation is additionally an example of a process that depends on microbial communication (Davies *et al.*, 1998, Hardie & Heurlier, 2008). The capability to form a biofilm has been reported for a number of species and is believed to be the main form of bacterial growth in the natural environment (Costerton *et al.*, 1995). Biofilms are

found in rivers, lakes and sea beds or floating as bacterial mats (Costerton *et al.*, 1987). Successful colonisation of man-made environments by bacteria, such as water pipes or submerged metal constructions, is also possible thanks to the capability to form a biofilm (Costerton *et al.*, 1994). The high adhesive properties of biofilms and their chemical resistance are significant obstacles to attempts of removing such biofilms. Furthermore, biocorrosion can be caused by prolonged exposure of artificial materials to biofilms (Figure 1.3) (Costerton *et al.*, 1994).

1.1.4.1. Bacterial biofilms are ubiquitous in the environment

Formation of structurally complex biofilm communities allow bacteria to thrive in environments inaccessible to any other organisms. Prokaryotes of various kinds are found to exist in biofilms in extreme environments such as acid ponds, where the pH nears 0, and in hot oceanic vents with water reaching boiling temperatures (Davey & O'Toole G, 2000). The unusual chemical resistance of the biofilm matrix to non-specific defence mechanisms of higher organisms has also allowed for colonisation, and the subsequent development of symbiosis, between bacteria and the host organisms. For example, biofilms are found in guts of higher animals where the biofilm protects bacteria from digestive enzymes (Macfarlane & Dillon, 2007). Furthermore, biofilms can be formed on plant roots where bacteria can acquire nutrients in otherwise nutrient-poor soil (Davey & O'Toole G, 2000).

Despite the abundance of biofilms in the natural environment, the postulate of bacteria predominantly existing in organised and highly structured communities is in contradiction to the long standing view on bacteria as single, independent cells dispersed in liquid media where they can move freely or form bioactive sediments

(Costerton *et al.*, 1987). However, a single cell in the environment is exposed to external conditions which, in most cases, are far from ideal physiological conditions in which bacteria are grown in the laboratory. Biofilms therefore allow for the adaptation of the surrounding environment, immobilising bacterial cells in most beneficial environment and allowing undisturbed occupation of the infection site. Both plant and animal tissues can be colonised by the biofilm-producing bacteria, where the biofilm matrix protects the biofilm-enclosed population of cells from the natural defences of the host and chemical and pharmacological treatments (Costerton *et al.*, 1987, Costerton *et al.*, 1994, Davey & O'Toole G, 2000, Morikawa, 2006). The prevalence of biofilms in nature, and the capability of bacteria to adjust the conditions within the biofilm matrix, also caused the biofilms to emerge as a new and serious complication in the industrialised world (Flemming *et al.*, 2009). This will be discussed in more detail in the next section.

1.1.4.2. Microbial biofilms impact industrial processes and medicine

Due to the ability to form biofilms on abiotic surfaces, marine microbes became an unpredicted factor that greatly increases the rate of metal deterioration in marine vessels (Figure 1.3). The submerged hulls of ships are now coated with substances aimed at reducing the settlement of bacteria (Costerton *et al.*, 1994, Branda *et al.*, 2005). Nonetheless, constant treatment of deposits of marine microbes on the submerged metal surfaces is necessary to prolong the lifespan of these constructions (Beech & Sunner, 2004). The same property of biofilms – the ability to adhere to abiotic surfaces – is the source of common complication in medicine (Costerton *et al.*, 1999). Bacterial biofilms are found to form on surfaces of medical implants and instrumentations (Figure 1.3) that are not correctly sterilised (Costerton *et al.*, 1999,

Hall-Stoodley *et al.*, 2004). As these biofilms are formed in the hospital environment, they can harbour the most dangerous of infection factors such as multidrug resistant strains of bacteria (Costerton *et al.*, 1999). Implantation of an implant colonised by biofilm-forming bacteria is in fact a common cause for post-surgical chronic infections (Costerton *et al.*, 1999, Hall-Stoodley *et al.*, 2004). This is caused in part by low penetration of the biofilm matrix by both immune system and pharmacological drugs (Lopez *et al.*, 2009c, Kaplan, 2011).

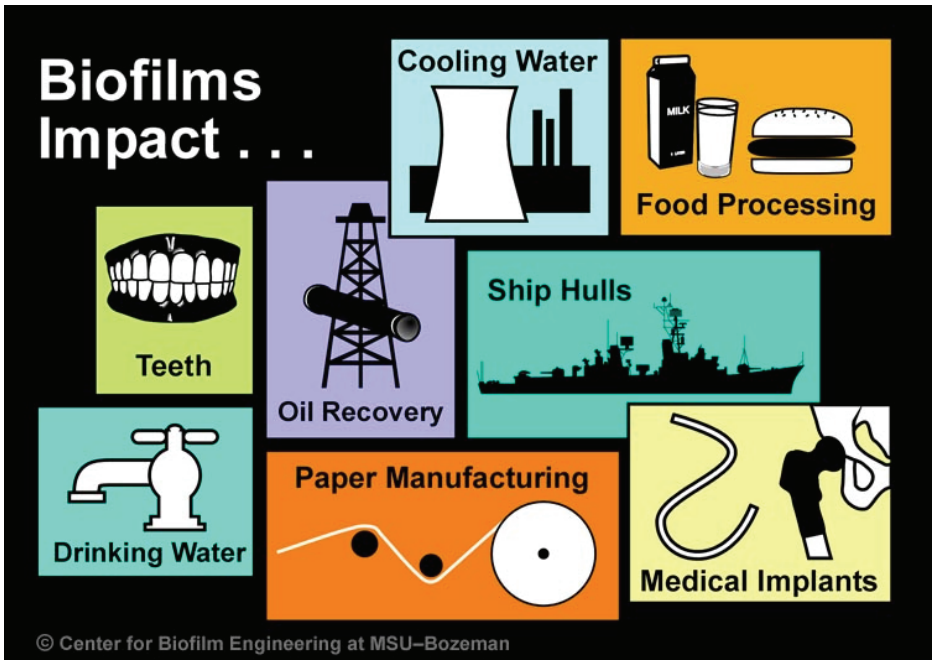

Figure 1.3 Biofilm formation has negative impact on medicine and technology. Examples of various fields negatively affected by biofilms are shown. Image courtesy of Montana State University Center for Biofilm Engineering.

Dental plaque is another type of biofilm commonly associated with health problems (Figure 1.3). This unique type of biofilm is inhabited by over 500 different species (Paster *et al.*, 2001) and is strongly calcified (Schroeder, 1969, White, 1997) which makes its removal particularly difficult. Another example of a multispecies biofilm with a high impact on human health is the biofilm established in lungs of cystic fibrosis (CF) patients (Costerton, 1984). The CF patients suffer of continuous lung

infections promoted by accumulation of mucous in the lung epithelium, which is easily colonised by bacteria (Costerton, 2001). One of the common etiological agents of lung infections is *P. aeruginosa* (Hall-Stoodley *et al.*, 2004). This species is also commonly the first to establish a biofilm within the mucous layer which is than populated by other opportunistic bacteria. The examples include, but are not restricted to *Burkholderia cepacia, Staphylococcus aureus, Heamophilus influenzae* and many more (Hogardt *et al.*, 2000).

1.1.4.3. Application of biofilms in biotechnology and biocontrol

The same properties of biofilms that cause disease and damage: adhesiveness, resistance to external factors, and the ability of the inhabiting bacteria to manipulate the conditions within the biofilm are targets for application in biotechnology. For example, various plant growth-promoting (PGPR) bacteria are known to form biofilms on the roots of plants. Many of the PGPR species also are able of producing various antibiotics (Ramey *et al.*, 2004, Morikawa, 2006, Danhorn & Fuqua, 2007, Nagorska *et al.*, 2007). The bactericidal properties of antibiotics, combined with the physical barrier of the biofilm, are beneficial to the host plant preventing pathogenic species of microorganisms from establishing infection in the plant. Already some species, like *B. thuringiensis* and *B. subtilis,* are commonly used in some countries as protective additives in mass-produced fertilisers (Morikawa, 2006). Furthermore, it is hoped that the natural stability of conditions within a biofilm can be exploited to utilise biofilms as natural bioreactors for the mass production of enzymes and other biotechnology products (Cheng *et al.*, 2010). This, accompanied by the natural adhesion of biofilms, could be used to immobilise such a bioreactor and ease the application of feed-batch reactor types (Cheng *et al.*, 2010). Finally, probably the widest application of biofilms is

found in the sewage plants, as the active sediments used for neutralisation of biological waste produced worldwide. Biological sewage treatment plants entirely depend on the multispecies communities of bacteria inhabiting the sludge sediment (Nicolella *et al.*, 2000), which are capable of decomposing organic matter. These bacteria exist in a form of biofilm, which prevents the bacteria from washing away. Thus the bacterial biofilm is an integral part of the waste treatment bioreactor (Wagner *et al.*, 2002).

1.2. The biofilm matrix

The presence of an extracellular matrix is a common feature of all biofilms (Costerton *et al.*, 1987). The matrix provides protection and allows residing bacteria to tailor the biofilm environment to their own needs by secretion of various bioactive compounds (Costerton *et al.*, 1987, Costerton *et al.*, 1994, Costerton *et al.*, 1995, Branda *et al.*, 2005, Flemming & Wingender, 2010). The biofilm matrix is formed from several types of biopolymers. The most common are proteins, exopolysaccharide and extracellular DNA (eDNA) (Flemming & Wingender, 2010). The presence of the biofilm matrix provides a survival advantage to the biofilm dwelling bacteria. For example, the biofilm matrix formed by pathogens is a physical barrier that the cells of the host's immune system cannot easily penetrate. Similarly, the biofilm matrix of the aquatic species provides tight binding of the community to the floor of the occupied reservoir and protects the cells from being washed away by water currents (Costerton *et al.*, 1987, Costerton *et al.*, 1995). In the case of multispecies biofilms, different conditions are established in different layers of the biofilm by the metabolic needs and products of the residing species (Figure 1.4) (Costerton *et al.*, 1987). Among the factors influenced within the biofilm are the control over pH and oxygen availability, as well as

oxidizing, and reducing conditions and availability of nutrients (Davey & O'Toole G, 2000).

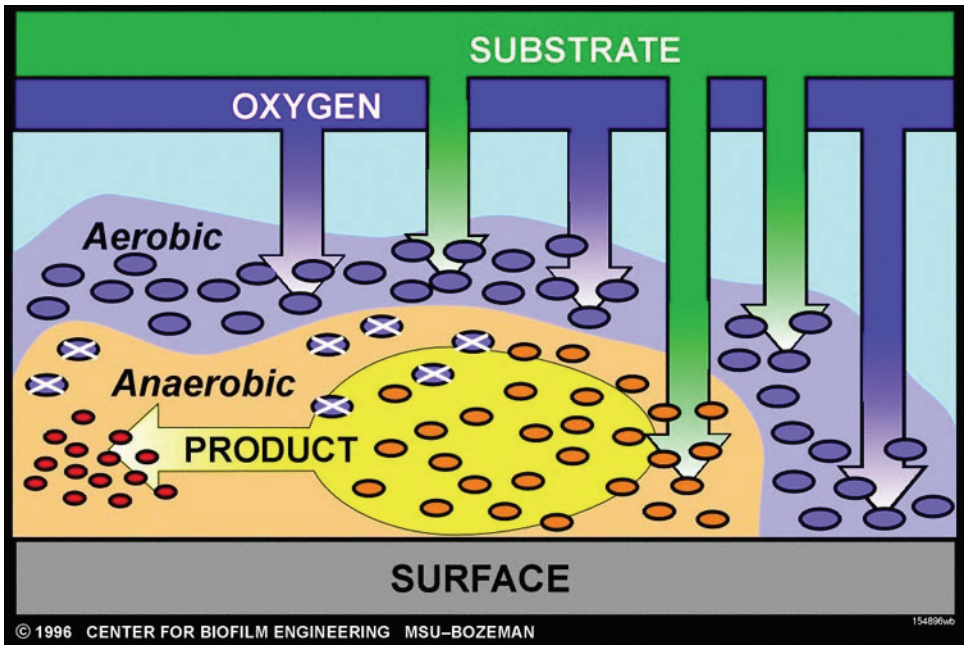

Figure 1.4 Schematic representation of a multicellular biofilm attached to a solid surface. Aerobic species utilise oxygen from the environment and allow for development of anaerobic conditions within the biofilm. Both aerobic and anaerobic species benefit from the nutrient substrates, which freely penetrate the biofilm matrix and allow for localised biochemical processes. Image courtesy of Montana State University Center for Biofilm Engineering.

Depending on the community forming the biofilm, the components of the biofilm matrix can be provided by one or more species dwelling in the biofilm (Flemming & Wingender, 2010). As a result, the composition of individual biofilm matrices varies significantly. However, the universal property of each of the unique combination of biopolymers comprising biofilm matrices is the ability to provide robustness, adhesiveness and resistance (Branda *et al.*, 2005). To allow for these features, all components of the matrix must be present in the correct concentration and produced at the adequate stage of polymerisation for biofilm to be formed properly (Lopez *et al.*, 2010). In the absence of any of the matrix components the biofilm is not formed. Additionally, an excess of any of the components causes strong alterations in the biofilm morphology (Flemming & Wingender, 2010). The following

section is dedicated to general description of biopolymers found in the biofilm matrix and their characteristics.

1.2.1. Exopolysaccharides

1.2.1.1. Function and detection of bacterial polysaccharides

Bacterial polysaccharides have been the subject of scientific interest for a long time, as the synthesis of polysaccharides is essential for bacterial physiology (Neidhaedt *et al.*, 1990). Two examples of essential polysaccharides include the peptidoglycan: *N*-acetylglucosamine linked with *N*-muramic acid that is cross-linked by short peptides and which is a fundamental component of the cell wall (Cooper, 1991, Scheffers, 2007) and lipopolysaccharides that are the major component of the outer membrane of Gram-negative bacteria (Madigan *et al.*, 2000).

Many bacterial polysaccharides are immunological determinants that allow for effective recognition and elimination of pathogens by the immune system (Morrison & Ryan, 1979). These features make bacterial polysaccharides an interesting target for novel drugs and vaccines (Nagy & Pal, 2008, Pollard *et al.*, 2009). However, the chemical nature of polysaccharides makes them a very difficult subject of study. Detection of saccharides is possible only by colorimetric chemical reactions or immunological assays using lectins which add significant difficulty to chromatography-based assays, especially size exclusion chromatography (Varki *et al.*, 2008). Furthermore, the chemical nature of polysaccharide linkage requires prior knowledge on the composition of the investigated polysaccharide before the structural studies can be performed (Varki *et al.*, 2008). There is also no universal assay allowing for detection and identification of all possible monosaccharides comprising the

polysaccharide (Varki *et al.*, 2008). For these reasons, relatively little is known about the exopolysaccharides comprising biofilm matrices.

1.2.1.2. Biofilm matrix of P. aeruginosa *contains three exopolysaccharides*

The biofilm of *P. aeruginosa* is probably the best studied system due to the impact of this organism on the well-being of cystic fibrosis patients. Three exopolysaccharides are known to be components of *P. aeruginosa* biofilm matrix: alginate, PSL and PEL (Figure 1.5) (Mann & Wozniak, 2012). Initially alginate was thought to be the main, and essential EPS, of the *P. aeruginosa* biofilm (Evans & Linker, 1973). This was due to the prevalence of the mucoid strains of *P. aeruginosa* that are isolated from sputum samples of CF patients (Boucher *et al.*, 1997, Mann & Wozniak, 2012). The mucoid strains of *P. aeruginosa* have been shown to overproduce alginate, (Hentzer *et al.*, 2001). However, in non-mucoid strains, alginate plays only a secondary role in biofilm matrix formation (Wozniak *et al.*, 2003). The biofilm matrix of non-mucoid strains of *P. aeruginosa* is comprised mostly of two polysaccharides: PSL, containing repeating units of a neutral, branched pentasaccharide consisting of D-glucose, D-mannose and L-rhamnose monosaccharides (Figure 1.5C) (Ma *et al.*, 2007, Byrd *et al.*, 2009); and another polysaccharide of unknown chemical composition, known as PEL (Friedman & Kolter, 2004a, Friedman & Kolter, 2004b, Colvin *et al.*, 2011). PSL was first identified as essential for biofilm formation in a non-mucoid strain of *P. aeruginosa,* as the disruption in the *psl* (polysaccharide synthesis locus) abolished biofilm formation (Jackson *et al.*, 2004). The importance of PEL was initially identified by the inability of *pel* (pellicle formation) deletion mutants to maintain cell-to-cell interactions during pellicle formation (Friedman & Kolter, 2004a). Both PEL and PSL

exopolysaccharides were shown to be required for biofilm formation by *P. aeruginosa*, but the importance of each individual polysaccharide is dependent on particular isolate and in some cases can be redundant (Colvin *et al.*, 2011).

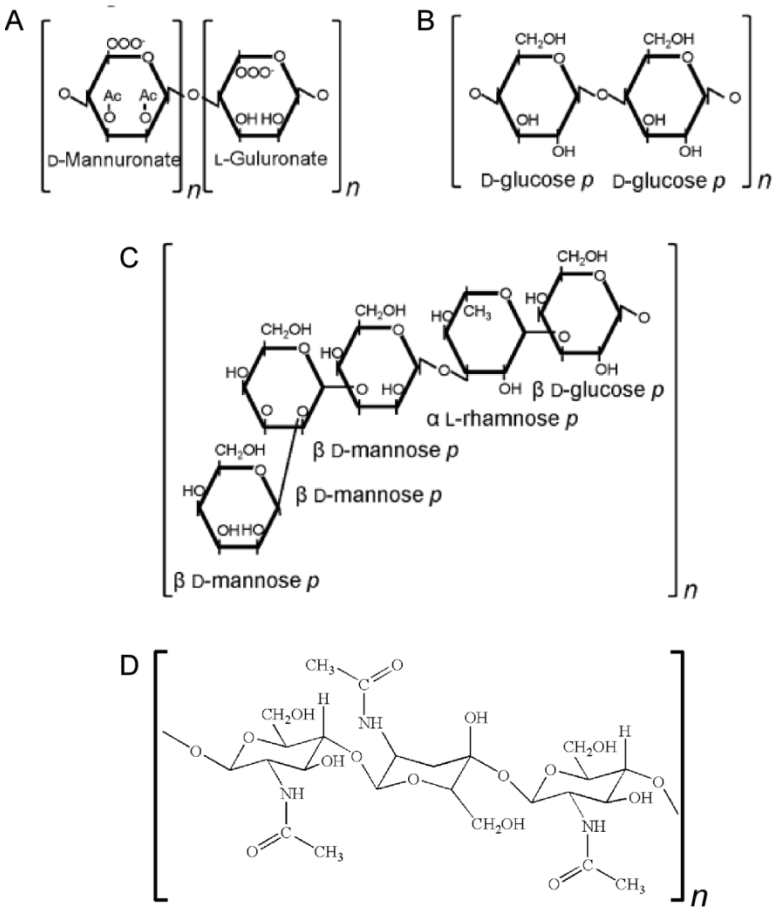

Figure 1.5 Examples of exopolysaccharides found in bacterial biofilms. (**A**) Alginate, (**B**) cellulose, (**C**) PSL, (**D**) PNAG. Images **A-C** adapted from (Mann & Wozniak, 2012), image **D** sourced from Wikimedia.

1.2.1.3. E. coli *synthesises several types of exopolysaccharides*

Synthesis of multiple types of EPS for the formation of a functional biofilm is not restricted to *P. aeruginosa,* as will be illustrated below. The full genome sequence of multiple strains of *E. coli* identify operons required for the synthesis of 3 independent polysaccharides: colanic acid, cellulose and poly-β-1,6-*N*-acetyl-D-glucosamine (PNAG) (Figure 1.5D) (Karatan & Watnick, 2009). It is unknown, however,

if all these polysaccharides are produced concurrently in the biofilms of *E. coli* or if synthesis of a particular EPS favoured by certain environmental conditions.

Colanic acid was observed to be the main polysaccharide in the biofilm matrix of the laboratory strain *E. coli* K-12 (Stevenson *et al.*, 1996). Mutants in the *wca* locus, responsible for synthesis of colonic acid, form one or two-cell layer thick, dense biofilms, whereas the mother strain is capable of formation of thick biofilms (Danese *et al.*, 2000). The defect in biofilm formation in the absence of the colanic acid can be overcome by overexpression of curli. Curli are a type of fimbriae involved in adhesion during biofilm formation by *E. coli,* and will be discussed in Section 1.2.2.2. When colanic acid is made, overexpressed curli enhances biofilm formation even further (Prigent-Combaret *et al.*, 2000). The second type of EPS used by *E. coli* in biofilm formation is cellulose (Figure 1.5B) (Zogaj *et al.*, 2001). Cellulose is also synthesised by some strains of *Salmonella enterica* sv Typhimurium and other of *Enterobacteriaceae* during formation of a biofilm (Karatan & Watnick, 2009). As in the case of colanic acid, the presence of cellulose in the biofilm matrix does not appear to be equally important in all strains of *E. coli* and *S. enterica* (Karatan & Watnick, 2009). This probably reflects the different requirements defined by the niche environments inhabited by these bacteria.

1.2.1.4. PNAG is an EPS used by various bacterial species

The exopolysaccharides described above: alginate, PEL, PSL and colanic acid are types of EPS that are specific to one species (or very few very closely related species) of bacteria. In contrast, cellulose is an EPS that is synthesised by several enterobacteria, but it has not been reported to be important in biofilm formation of

other families of bacteria (Karatan & Watnick, 2009). The narrow range of bacterial species using a given type of EPS in biofilm formation is characteristic for most biofilms. PNAG (poly-β-1,6-*N*-acetyl-D-glucosamine) (Figure 1.5D) is a noteworthy exception from this rule. PNAG was shown to be present in biofilms of various species including *E. coli, S. epidermidis, S. aureus, Yersinia pestis, Actinobacillus spp., Aggregatibacter actinomycetemcomitans,* and *Bordetella spp* (Karatan & Watnick, 2009). As such a widely distributed EPS, PNAG is among the most studied types of EPS. The majority of genes in the gene clusters responsible for PNAG synthesis across all species are orthologous, which suggests a common ancestry (Itoh *et al.*, 2005). In all cases, PNAG synthesis clusters include glucosamine transferases required for polymerisation of PNAG (Gerke *et al.*, 1998). Furthermore, upon its export, PNAG is associated directly with cell wall or is located to the cell envelope (Karatan & Watnick, 2009). Deacetylation of GlcNAc moieties is also a common process during PNAG synthesis, but the reasons for the GlcNAc deacetylation varies. For example, in the biofilms formed by the *Staphylococcus* species, PNAG deacetylation allows for anchoring to the cell wall (Vuong *et al.*, 2004), whereas in *E. coli* deacetylation is required for PNAG export (Itoh *et al.*, 2008). The significant differences in the function of the similar modification of the same EPS synthesised by different species highlights the importance of studies of EPS in a broad range of microorganisms. Only through the analysis of individual types of EPS can broad conclusions on the function EPS be drawn.

1.2.1.5. Various types of EPS have similar functions in the biofilm

Despite large variability in the types of EPS synthesized by different bacterial species, the presence of EPS in the biofilm matrix is required for the structural development of the biofilm. In all cases, examined strains deficient in EPS synthesis are

only able to form a very thin layer biofilms, where the thickness is comparable to 1-2 cells (Flemming & Wingender, 2010). This suggests that the function of the EPS is in mediating cell-to-cell interactions; as was shown for PEL (Friedman & Kolter, 2004a). In addition to intercellular interactions, an EPS can perform various physical and chemical functions in a biofilm, for example attachment of bacteria to the surface where the biofilm is to be established (Branda *et al.*, 2005).

Due to the biophysical properties, many polysaccharides have strong sorption properties in addition to the adhesive properties. These absorptive properties enable the EPS to store water and keep the cells in the biofilm well hydrated (Flemming & Wingender, 2010). The EPS can also be used as a nutrient gathering array, or a sink for excess energy, which can be later recovered by hydrolysis of the EPS (Flemming & Wingender, 2010). Furthermore, polysaccharides are generally chemically inert which make them a perfect shield which protects the biofilm-dwelling cells from harsh environment outside the biofilm matrix (Costerton *et al.*, 1987, Costerton *et al.*, 1994, Branda *et al.*, 2005, Flemming & Wingender, 2010). In all cases however, an interaction between EPS and protein components of the biofilm matrix are required to establish the biofilm community successfully.

1.2.2. Extracellular proteins

The main tool for transforming the surrounding environment employed by bacteria is the secretion of proteins that have either enzymatic or structural properties. Secreted enzymes allow bacteria to extract nutrients from the neighbouring biological matter, like plant or animal tissues (Morikawa, 2006). The secretion of structural proteins also allows for attachment by use of various adhesins

and the establishment of a biofilm, which will protect bacterial cells from being removed from the occupied niche (Morikawa, 2006). Furthermore, the three-dimensional nature of the biofilm matrix can be used to immobilize enzymes and localise them to the site where the highest productivity can be achieved (Flemming & Wingender, 2010).

1.2.2.1. Extracellular proteins stabilise the biofilm matrix

Various cell surface-associated proteins produced by bacteria have a capability to bind polysaccharides. For example, LecA and LecB are two cell surface-associated lectins produced by *P. aeruginosa* that have been implicated in biofilm formation (Tielker *et al.*, 2005, Diggle *et al.*, 2006). Another protein secreted by *P. aeruginosa*, CdrA, was shown to directly bind to the PSL EPS and is thought to be responsible for cross-linking of PSL during biofilm formation (Borlee *et al.*, 2010). Moreover, in last decade a family of large biofilm associated proteins (Bap) has been described (Lasa & Penades, 2006). Bap proteins contain multiple tandem repeats in the middle section of the sequence, which puts them among the largest bacterial proteins (Lasa & Penades, 2006). They are anchored to either cell wall of Gram-positive bacteria or the outer membrane of Gram-negative bacteria (Lasa & Penades, 2006). Bap-like proteins were shown to be important in biofilm formation and in establishing of the structure of the biofilm matrix (Cucarella *et al.*, 2001). Bap protein was initially described in the *S. aureus* V329 but its homologues were found in various other species. These include *Streptococcus pyogenes, Enterococcus faecalis, Staphylococcus epidermidis, Pseudomonas putida, Bordetella bronchiseptica*, *Escherichia coli* and *Burkholderia cepacia* (Toledo-Arana *et al.*, 2001, Huber *et al.*, 2002, Hinsa *et al.*, 2003, Latasa *et al.*, 2005, Roux *et al.*, 2005, Tormo *et al.*, 2005). Interestingly, Bap is not found in human

pathogenic strains of *S. aureus* (Lasa & Penades, 2006), but several of sequenced strains of pathogenic *S. aureus* indicate presence of a Bap homologous protein Bhp performing a function similar to Bap (Tormo *et al.*, 2005). Another interesting feature of Bap-like proteins is the fact that the central multiple repeats region shows a high β-strand content (Lasa & Penades, 2006). These domains are required for functionality of the Bap-like proteins through a yet unknown mechanism (Latasa *et al.*, 2005).

1.2.2.2. Amyloid proteins are common in biofilms

Although not directly related to the Bap proteins, other β-rich proteins involved in biofilm formation have been shown to form amyloid fibres (Sunde *et al.*, 1997). Two of the most studied examples are the curli fibrils formed by *E. coli* (Figure 1.6) (Chapman *et al.*, 2002) and the TasA protein found in the biofilm matrix of *B. subtilis* (Figure 1.14) (Romero *et al.*, 2010). TasA is described in detail in Section 1.6.2. The synthesis of *E. coli* curli is dependent on the *csg* genes which encode structural and regulatory proteins of curli (Hammar *et al.*, 1995). Furthermore, genes homologous to *csg* were found in *Salmonella enterica*, encoding monomers of fimbriae known as TAFI (thin aggregative fimbriae) (Collinson *et al.*, 1996, Romling *et al.*, 1998a), indicating a requirement for the amyloid proteins in biofilms of different species. TasA, curli, and TAFI are capable of binding the dye Congo Red which is specific to amyloid fibres due to their quaternary structure (Hammar *et al.*, 1995, Romling *et al.*, 1998a, Romero *et al.*, 2010). Purified bacterial amyloid proteins increase fluorescence of thioflavin T and form long fibres when observed under a microscope (Romero *et al.*, 2010, Dueholm *et al.*, 2011). Curli and TAFI mediate cell attachment to abiotic surfaces during initial stages of biofilm formation (Romling *et al.*, 1998b, Prigent-Combaret *et al.*, 2000). These fibrils also seem to be required for the cell-to-cell contact in biofilms (Prigent-

Combaret *et al.*, 2000). Furthermore, similarly to TasA, curli and TAFI appear to form a structural scaffold onto which the EPS can be attached to form a fully developed, robust biofilm matrix (Prigent-Combaret *et al.*, 2000, Barnhart & Chapman, 2006, Romero *et al.*, 2010). Another functional amyloid-like fibril protein FapC was also identified in the genomes of many *Pseudomonas* species. These proteins were also indirectly shown to be involved in biofilm formation (Dueholm *et al.*, 2010).

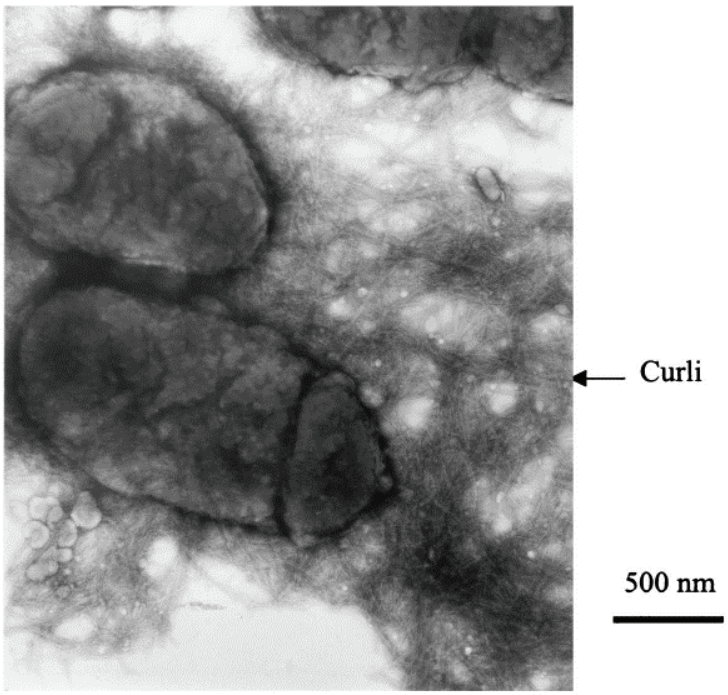

Figure 1.6 Cells of *E. coli* extracted from a surface attached biofilm and imaged with TEM. The arrow indicates negatively stained amyloid fibres formed by curli fibrils stretching from the cells. Taken from (Prigent-Combaret *et al.*, 1999).

1.2.2.3. Biofilm proteins allow for the modification of established biofilms and adaptation of the environment

Once a biofilm matrix is established, the resident bacterial community does not become dormant. The biofilm matrix can be expanded by growth of the population already dwelling in the biofilm as well as cells joining or leaving already established communities (Costerton *et al.*, 1987). For such changes to occur, modifications to the biofilm matrix are required. Multiple types of proteins are secreted by bacteria to the

extracellular environment and under biofilm conditions these proteins may become associated with the biofilm matrix (Flemming & Wingender, 2010). To rebuild a biofilm matrix its components must be first degraded to be replaced by newly synthesised structures. This is achieved through the various proteinases and glycosylases secreted by bacteria (Flemming & Wingender, 2010). The same enzymes can be used to degrade the components of the biofilm matrix during starvation to obtain additional nutrients that were accumulated in biopolymers during formation of the biofilm.

In addition to modification of the biofilm structure, a large number of peptidases, glycosilases, proteinases, ribonucleases, lipases, esterases and other enzymes can be immobilized on the EPS and used to modify the ecological niche occupied by the biofilm cells (Flemming & Wingender, 2010). These enzymes are used to degrade biological and synthetic polymers in the immediate neighbourhood of the biofilm and have also been shown to take part in biocorrosion, bioweathering and bioremediation (Beech & Sunner, 2004, Singh *et al.*, 2006, Mapelli *et al.*, 2012). The association of enzymes with the polysaccharides of the biofilm matrix was shown to increase the stability of the enzymes and to increase their processivity [as reviewed in (Flemming & Wingender, 2010)].

1.2.3. Extracellular DNA

Extracellular DNA (eDNA) was discovered as an important building block of biofilms (Whitchurch *et al.*, 2002). Initially eDNA was believed to be a product of a spontaneous cell lysis and not to be a structural component of the biofilm matrix (Sutherland, 2001). However, Whitchurch and colleagues (2002) showed that eDNA is required for development of the biofilm structure of *P. aeruginosa*. Since then, eDNA

was found in biofilms of various strains and was shown to be involved in biofilm formation (Flemming & Wingender, 2010). However, the function of eDNA seems to vary from species to species. In some cases eDNA is a structural part of the biofilm matrix (*e. g. P. aeruginosa, S. aureus*) (Izano *et al.*, 2008), in other situations it acts as an adhesin (*e. g. B. cereus*) (Vilain *et al.*, 2009). eDNA has also been shown to be a factor contributing to the dispersal of motile progeny from the sessile cells of *Caulobacter crescentus* biofilms (Berne *et al.*, 2010).

The mechanisms of export of eDNA to the extracellular space seems to vary between species as well. In many cases it is not clear if eDNA is actively exported from the cells or is it a product of cell lysis (Flemming & Wingender, 2010). For example, a study of the sequence differences between eDNA and chromosomal DNA revealed some variation in the sequences, favouring the active transport hypothesis (Bockelmann *et al.*, 2006), whereas in another study (Steinberger & Holden, 2005) eDNA was shown to be identical to chromosomal DNA. In case of *B. subtilis,* involvement of eDNA in biofilm formation was shown only indirectly (Nijland *et al.*, 2010). Biofilm formation of *B. subtilis* is inhibited if the cells are incubated under biofilm forming condition in presence of DNases. This is in agreement with unpublished results (A. Ostrowski).

1.3. *Bacillus subtilis* is a model organism for Gram-positive bacteria

1.3.1. B. subtilis *is a well-studied model organism used in biotechnology*

The soil, and the plants rhizosphere in particular, is rich in microbial life (Madigan *et al.*, 2000). One of the many Gram-positive and Gram-negative bacteria

that can be isolated from the rhizosphere is a Gram-positive rod *Bacillus subtilis.* First described by Ferdinand Cohn in 1877 (Cohn, 1877), *B. subtilis* is now one of the most widely studied bacteria and also arguably one of the best described organisms in the world (Graumann, 2007). It is a non-pathogenic bacterium with a wide temperature tolerance spanning from +14 to +50 °C. However, it is routinely cultured in laboratory conditions at 37 °C in rich media like Lysogeny Broth (also known as Luria-Bertani broth) (Bertani, 1951, Bertani, 2004). In these conditions the generation time of *B. subtilis* is close to 25 minutes which makes *B. subtilis* a very easy organism to cultivate. Moreover, wild strains of *B. subtilis* are prototrophs allowing for cultivation in minimal defined media expanding even further the array of microbiological methods applicable to the work with *B. subtilis* (Harwood & Cutting, 1990).

1.3.1.1. B. subtilis *is related to many pathogenic species*

B. subtilis is a close relative of pathogenic *Bacillus cereus* and *Bacillus anthracis* species, as well as of the insect pathogen *Bacillus thuringiensis* (Drobniewski, 1993). The phylogenic placement of *B. subtilis* among pathogenic species, combined with the lack of pathogenicity of *B. subtilis* itself, makes it an ideal model for study of the general physiology and biochemistry of the *Bacillus* genus. Furthermore, in 1997 the full genome sequence of *B. subtilis* strain 168 was published (Kunst *et al.*, 1997). The analysis of the genome that followed revealed significant similarities between *B. subtilis* and other *Firmicutes* like *Streptococcus mutans and Staphylococcus pyogenes* for which *B. subtilis* gained use as a model organism as well (Harwood, 2003).

1.3.1.2. Application of B. subtilis *in biotechnology*

The extensive knowledge on the genetics of *B. subtilis* and the availability of the robust genetic manipulation methodologies for this bacterium made it an attractive subject for development of biotechnological applications (see below). Furthermore, a variety of naturally produced compounds can be easily extracted from *B. subtilis* cultures. These include the antibiotics subtilisin and bacitracin (Stein, 2005); a very potent surfactant called surfactin (Arima *et al.*, 1968); and a variety of proteases (Gupta *et al.*, 2002). Moreover, *B. subtilis sp natto* is widely used in Japan for production of fermented soybean food product Natto. The ease of genetic manipulation of *B. subtilis* allowed for the introduction of novel biochemical traits that can be exploited in biotechnology. For example, *B. subtilis* found its use in the production of such recombinant products like proinsulin (Olmos-Soto & Contreras-Flores, 2003), hEGF (Lam *et al.*, 1998) and streptavidin (Wu & Wong, 2002). The attractiveness of *B. subtilis* as an industrial strain has encouraged further, and extensive, research of the biology and biochemistry of various isolates of *B. subtilis* which resulted in multiple discoveries, some of which are discussed below.

1.3.2. Bacillus subtilis *is a plant growth-promoting bacterium*

1.3.2.1. B. subtilis *as biocontrol agent*

B. subtilis has not only found application in biotechnology as a host for recombinant processes, but it is also considered a plant growth-promoting rhizobacterium (PGPR) (Nagorska *et al.*, 2007). In addition to the ability to produce antibiotics, *B. subtilis* synthesises many other compounds that have been shown to possess anti-microbial activity, including surfactin. The antimicrobial activity of

surfactin is most likely the result of interaction of surfactin with bacterial cytoplasmic membranes, which leads to destabilisation of the membranes (Kolter, 2010). Another group of lipopeptides with antimicrobial activity synthesised by *B. subtilis,* and other species from the *Bacillus* genus, are iturins (Besson *et al.*, 1976). Iturins, despite limited antibacterial activity, were shown to be potent antifungal compounds (Stein, 2005). These cyclic lipopeptides disrupt the fungal cell membrane and cause leakage of electrolytes from the cytoplasm (Stein, 2005).

Not only can *B. subtilis* promote the growth of bacteria by secretion of antibiotics, and thus control the growth of pathogenic bacteria, but it is able to provide a physical protection by forming biofilms on the roots of host plants as well (Bais *et al.*, 2004). The plant-associated biofilm is a robust physical barrier that blocks the attachment to, and penetration of, plant tissues by pathogenic species (Bais *et al.*, 2004). At the same time the growth of the host plant is not impaired suggesting a symbiotic relationship between the bacterium and the plant (Nagorska *et al.*, 2007). The variety of beneficial traits of *B. subtilis* makes it an interesting target for development for application in agriculture.

1.3.3. Application of B. subtilis *in medicine and biotechnology*

In addition to appliclation of *B. subtilis* as a model organisms for traditional microbiology, a novel medical application for this bacterium was described. The spores formed by *B. subtilis* were found to be an interesting new vaccine delivery system (Duc le *et al.*, 2003b). *B. subtilis* itself is a non-pathogenic species, but it was found to induce an immune response in mice (Duc le *et al.*, 2003b). The spores of *B. subtilis* are able to pass through the gastrointestinal system and germinate into viable cells in the bowel in

the mice model (Duc le *et al.*, 2003b, Tam *et al.*, 2006). During spore formation various proteins are targeted to the coat of the spore. The spore coat is the most exterior part of the spore, protecting the cortex and the core (Driks, 2002) and also provides the interface between the spore and the external environment. Therefore, presentation of a target immunological determinant on the spore coat is a promising tool for induction of immune response. A number of attempts were made where recombinant immunological epitopes from pathogens like *B. anthracis* (Duc le *et al.*, 2007) or *Helicobacter acinonychis* (Hinc *et al.*, 2010) were expressed in the mother cells of *B. subtilis* and subsequently presented on the coat of the endospore. Initial reports show promising results of successful expression and targeting of proteins, and causing an immune response as well (Duc le *et al.*, 2003b). To increase the attractiveness of *B. subtilis* as a vaccine delivery system, an alternative approach was proposed. In this case the orally administered spores travel to the small intestine, where they can germinate. The resulting vegetative cells express the recombinant epitope and present it on the cell wall after germination allowing for detection by the immune system of the host (Duc le *et al.*, 2003a). However, none of these methods has become a mainstream method for vaccination delivery so far.

1.4.Multicellular behaviour of *Bacillus subtilis*

For many years, *B. subtilis* was known to undertake several quorum sensing-regulated processes including natural competence for uptake of foreign DNA, antibiotic production and the formation of biochemically dormant and environmentally resistant spores (Aguilar *et al.*, 2007). During later investigation, *B. subtilis* has also been shown to exhibit many more forms of multicellular behaviour. These include swarming motility, a coordinated movement on semi-solid surfaces

(Kearns & Losick, 2003); cannibalism that allows bacteria to obtain additional nutrients by killing a susceptible subpopulation of the genetically identical population (Gonzalez-Pastor *et al.*, 2003); exoprotease production (Msadek, 1999); poly-γ-glutamic acid synthesis (Stanley & Lazazzera, 2005) and formation of multicellular biofilm (Branda *et al.*, 2001). Moreover, it has been observed that the array of multicellular behaviour exhibited by different strains of *B. subtilis* varies and this fact was attributed to the genetic differences (McLoon *et al.*, 2011). Due to the large variety of the multicellular behaviours, *B. subtilis* is a comprehensive model organism for studying the social interactions within the bacterial culture. Furthermore, such diversity implies a requirement for a complex regulatory network to govern these behaviours. Indeed such a network is present in *B. subtilis* and is outlined below.

During vegetative growth the cells of *B. subtilis* are exposed to various extracellular signals. Despite the fact that the entire community is exposed to these signals, only in a subpopulation of cells is a genetic reaction triggered (Lopez & Kolter, 2010). As a result, differential gene expression is initiated in these cells, and a subpopulation with a distinct phenotype arises from the genetically identical population. The rise of the new subpopulation can be monitored using fluorescent protein transcriptional fusions to the promoter regions of interest and visualised by flow cytometry or fluorescent microscopy (Figure 1.1) (Fujita *et al.*, 2005, Veening *et al.*, 2005). In fact, most multicellular processes exhibited by *B. subtilis* take part in only a subpopulation of cells (Lopez *et al.*, 2009b, Lopez & Kolter, 2010). The division of labour is particularly well illustrated in the complex biofilm communities. During biofilm formation, several subpopulations of cells emerge in a process that is regulated in both space and time. This process is described in more detail in Section 1.6.1.1.

Furthermore, the importance of successful differentiation into diverse cell subpopulations is emphasised by the example of laboratory strains, which are impaired in cell differentiation and hence do not perform many of multicellular processes.

1.4.1. Laboratory strains of B. subtilis *show reduced multicellular behaviour*

The research focusing on the comparative physiology and genetics of the domesticated *B. subtilis* strain 168, sequenced by Kunst and colleagues (1997), and its parental wild isolate *B. subtilis* NCIB3610 Marburg (hereafter referred to as 3610) has revealed significant genetic and physiological differences between these strains (McLoon *et al.*, 2011). It was long known, that the strain 168 is auxotrophic for tryptophan synthesis and that it contains multiple mutations introduced by Burkholder and Giles during their experiments involving irradiation with UV (Burkholder & Giles, 1947). Other strains derived from strain 168, such as the laboratory strain *B. subtilis* PY79, were generated by continuous propagation in laboratories and have accumulated further mutations (McLoon *et al.*, 2011). However, only recently have a number of mutations affecting the multicellular types of behaviour of *B. subtilis* been described. The strain 168 was shown to carry loss-of-sense mutations in multiple genes involved in multicellular behaviour (McLoon *et al.*, 2011). Among the genes inactive in the strain 168 are genes *sfp* and *swrA* which are required for surfactin synthesis and swarming motility (Nakano *et al.*, 1992, Kearns *et al.*, 2004, Patrick & Kearns, 2009). These mutations not only cause lack of swarming phenotype but also impair biofilm formation (McLoon *et al.*, 2011). Biofilm formation in laboratory strains is also affected by other mutations carried by these strains. Laboratory strains were shown to carry a

frame shift in the *epsC* gene resulting in an inability to synthesise the exopolysaccharide component of the biofilm matrix (see Section 1.6.3.1) (McLoon *et al.*, 2011). Among interrupted genes in the laboratory strains are not only biosynthetic genes but also regions with regulatory functions. An example can be the promoter region of the *degQ* gene, which product is required for maximal activity of the DegU response regulator causing pleiotropic effects on the multicellular behaviour of *B. subtilis* (See Section 1.5.2). Due to the large number of mutations incorporated into the genomes of laboratory strains, these strains are deemed to be less valuable in the study of the multicellular behaviours of bacteria than the wild isolates (Fux *et al.*, 2005b). However, some mutations acquired by the laboratory strains have in fact enhanced their application in molecular biology. An example of such a mechanism is genetic competence naturally expressed by *B. subtilis* (Spizizen, 1958), which is greatly enhanced in the laboratory strains (Anagnostopoulos & Spizizen, 1961).

1.5.The genetic circuitry driving the biofilm formation of *B. subtilis*

1.5.1. The environmental and genetic triggers of biofilm formation

B. subtilis is able to form biofilms at the interface of air and liquid, called pellicles; on solid surfaces, in the form of complex colonies (Figure 1.12) (Branda *et al.*, 2001); and on the surfaces of plant roots (Bais *et al.*, 2004, Chen *et al.*, 2012). Additionally, the laboratory strain *B. subtilis* JH642 is capable of forming a form of a biofilm that tightly adheres to abiotic surfaces (Hamon & Lazazzera, 2001, Hamon *et al.*, 2004, Terra *et al.*, 2012). Biofilm formation has been shown to be possible during growth in a broad spectrum of media, both rich and minimal (Branda *et al.*, 2001, Hamon & Lazazzera, 2001, Nagorska *et al.*, 2008). This fact undermined the initial

hypothesis, that biofilm formation is triggered by starvation (Hamon & Lazazzera, 2001). The emerging view from current literature is that biofilm formation is stimulated by various diffusible substances in response to cell density, rather than the nutritional conditions (Lopez & Kolter, 2010). Furthermore, the detection of these chemical and environmental signals causes the transition from a motile lifestyle to biofilm formation in only a subset of cells in the population (Chai *et al.*, 2008, Lopez *et al.*, 2009b, Lopez *et al.*, 2009d, Lopez & Kolter, 2010). Therefore, biofilm formation is an example of multicellular behaviour of bacteria resulting from the functional differentiation of cells. Differentiation of *B. subtilis* cells during biofilm formation is governed by two regulatory proteins: namely Spo0A and DegU. These regulatory pathways are discussed in following sections.

1.5.1.1. Spo0A controls two parallel pathways regulating biofilm formation

Spo0A is a global regulator of multicellular behaviour in *B. subtilis* that is active in its phosphorylated form (Spo0A~P) (Burbulys *et al.*, 1991, Fujita *et al.*, 2005). The effect of Spo0A~P depends strictly on the intracellular level of Spo0A~P (Fujita *et al.*, 2005). In simple terms the signal cascade starts with the sensory kinases, KinA, KinB, KinC, KinD or KinE (Jiang *et al.*, 2000). The signal is transduced to Spo0A by a multicomponent phosphorelay (Figure 1.7) (Burbulys *et al.*, 1991). The phosphotransferase Spo0B is the final protein in the phosphorelay that directly phosphorylates Spo0A (Burbulys *et al.*, 1991). The balance between phosphorylated and unphosphorylated Spo0A is maintained by the Spo0E phosphatase (Figure 1.7) (Ohlsen *et al.*, 1994), alongside other phosphatases (Perego, 2001).

In addition to control of the level of Spo0A~P by dephosphorylation, the balance of phosphorylated to unphosphorylated forms of Spo0A partially depends on which kinase has initiated the signal transduction. It was demonstrated, that KinC promotes low kinetics of Spo0A phosphorylation, and thus a low level of Spo0A~P in the cell (Lopez *et al.*, 2009a); whereas KinD causes accumulation of high levels of Spo0A~P (Aguilar *et al.*, 2010). The genes required for biofilm formation are activated in response to signal from KinC (Lopez *et al.*, 2009d). In comparison KinD was shown to be the checkpoint kinase linking biofilm formation and sporulation, which is initiated in presence of high levels of Spo0A~P (Aguilar *et al.*, 2010). The contribution of KinA and KinB is not clear but these kinases were also implicated in activation of biofilm formation and sporulation (Perego *et al.*, 1988a, Trach & Hoch, 1993, LeDeaux *et al.*, 1995, McLoon *et al.*, 2010). The nature of the environmental signals perceived by these sensory kinases is poorly understood. However, KinC was demonstrated to respond to potassium leakage from the cell (Lopez *et al.*, 2009a). This could be triggered by lipopeptides, like surfactin, which cause destabilisation of the cytoplasmic membranes (Lopez *et al.*, 2009d).

1.5.1.2. Low levels of Spo0A~P activate biofilm formation

The concentration-dependent regulation by Spo0A~P is based on the differential binding to the promoters of genes expressed at a low or high concentration of Spo0A~P (Fujita *et al.*, 2005). Genes which promoter elements contain a high affinity binding site for Spo0A~P are influenced by Spo0A~P on its low intracellular levels and activate biofilm formation. In contrast, the promoter regions with low affinity to Spo0A~P are controlled when the intracellular levels of Spo0A~P are high. When the

level of Spo0A~P is high sporulation is stimulated. Additionally biofilm formation is inhibited in the conditions of high concentrations of Spo0A~P (Chai *et al.*, 2011).

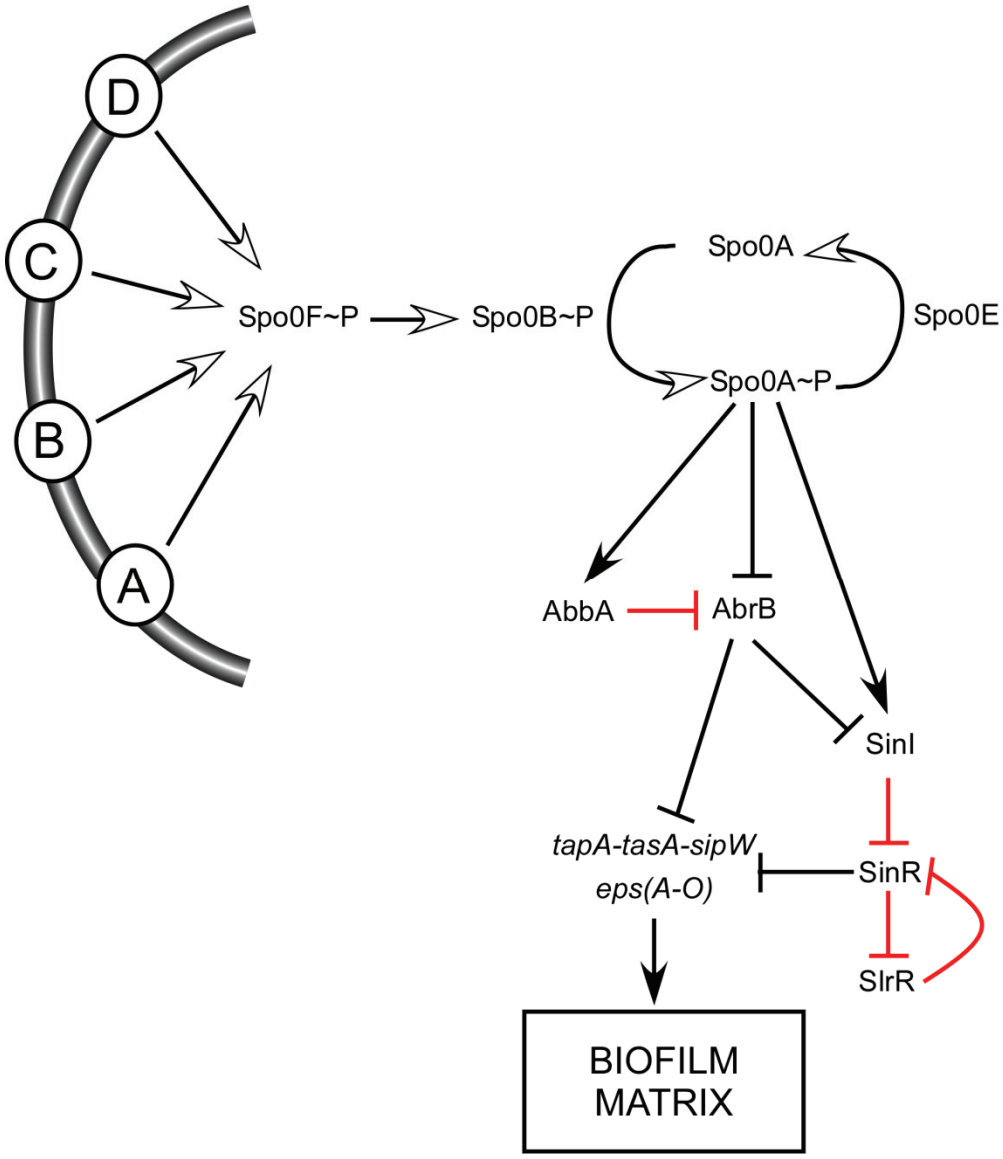

Figure 1.7 Spo0A~P regulates biofilm formation through two parallel pathways. A, B, C and D represent membrane-bound sensory kinases KinA, KinB, KinC and KinD respectively. Phopsho-transfer interactions are marked with white head arrows. Expression activation events are marked with black head arrows and expression repression with black T-bars. Red T-bars represent protein-protein inhibition. Genes are signified by italics.

When Spo0A~P is present on low levels within a cell, two parallel pathways of antirepression are activated which are required to be released for biofilm formation (Figure 1.7). The first pathway is governed by the global regulator protein AbrB (Greene & Spiegelman, 1996, Molle *et al.*, 2003, Fujita *et al.*, 2005). AbrB is

proteolytically unstable, thus repression of transcription of *abrB* by Spo0A~P leads to rapid depletion of AbrB in the cell and activation of genes under AbrB repression (Greene & Spiegelman, 1996, O'Reilly & Devine, 1997, Fujita *et al.*, 2005). Among genes regulated by AbrB is a three-gene operon *tapA-sipW-tasA* (Hamon *et al.*, 2004) (hereafter the *tapA* operon) which encodes proteins required for the synthesis of the biofilm matrix (Branda *et al.*, 2006); the 15-gene operon *epsABCDEFGHIJKLMNO* (hereafter the *eps* operon) (Chumsakul *et al.*, 2010) required for exopolysaccharide synthesis (Figure 1.7) (Kearns *et al.*, 2005) and the *yuaB* gene, which was also shown to be required for biofilm formation (Figure 1.10 and Section 1.7.1) (Kobayashi, 2007b, Verhamme *et al.*, 2009). As mentioned above, Spo0A~P can activate gene expression as well as repress it. One of the genes where expression is activated by low levels of Spo0A~P, is *abbA* (antirepressor of AbrB A). The *abbA* gene encodes a small antagonist protein of AbrB (Figure 1.7) (Banse *et al.*, 2008). AbbA binds AbrB and inhibits the DNA binding properties of AbrB, which leads to antirepression of AbrB-controlled genes (Banse *et al.*, 2008). Therefore, Spo0A~P inhibits the AbrB repression in two ways: by direct binding to the *abrB* promoter and inhibiting translation of *abrB*; and by activating an antagonist protein AbbA which inhibits the activity of AbrB (Banse *et al.*, 2008).

The second pathway activating biofilm formation that is also stimulated by low levels of Spo0A~P, is the pathway controlling the activity of the transcriptional repressor SinR (Chu *et al.*, 2006). SinR is encoded as part of a two gene operon with SinI (Gaur *et al.*, 1988). SinI is a Spo0A~P regulated antagonist of a constitutively expressed repressor protein SinR (Bai *et al.*, 1993). Similarly to AbrB, SinR directly inhibits expression of genes required for establishing of the biofilm matrix (Chu *et al.*,

2006); namely the *tapA* operon and the *eps* operon, (Figure 1.7). Thus when Spo0A~P is activated SinR-mediated inhibition is released.

1.5.1.3. SinR is a part of a bistable switch

In addition to regulation by SinI, the activity of SinR is regulated by a hybrid protein SlrR, resembling both SinI and SinR (Kobayashi, 2008, Chai *et al.*, 2009, Chai *et al.*, 2010). The gene encoding SlrR (*slrR*) is directly repressed by SinR (Figure 1.8), thus in conditions of planktonic growth, when Spo0A is not phosphorylated, SlrR is not produced (Chai *et al.*, 2010). In biofilm forming conditions, the repression of *slrR* by SinR is alleviated by production of SinI. SlrR is then able to bind to SinR and inhibit the binding of SinR to the *slrR* promoter, thus locking the cell in a state when SlrR is constantly produced (Figure 1.8) (Chai *et al.*, 2009). SlrR also promotes transcription from the *tapA* and *epsA* promoters by interaction with SinR and thus alleviation of SinR-mediated repression (Kobayashi, 2008, Chai *et al.*, 2009, Murray *et al.*, 2009b). Furthermore, the SinR-SlrR complex assumes novel functions and inhibits the expression of autolysins. A reduction in the level of autolysins causes the cells to form chains of incompletely separated cells and additionally indirectly inhibits motility of cells in the static cultures (Figure 1.8) (Chai *et al.*, 2010). Cell chaining is one of the characteristic phenotypes accompanying biofilm formation [see Section 3.2 and (Kobayashi, 2007a)]. It is important to note that only in a subpopulation of cells is the level of Spo0A~P compatible with controlling these pathways. Therefore, the self-enforcing SinR-SlrR feedback loop locks a subpopulation of cells that have initiated biofilm formation in this state, thus ensures the bistability of the biofilm population (Chai *et al.*, 2010).

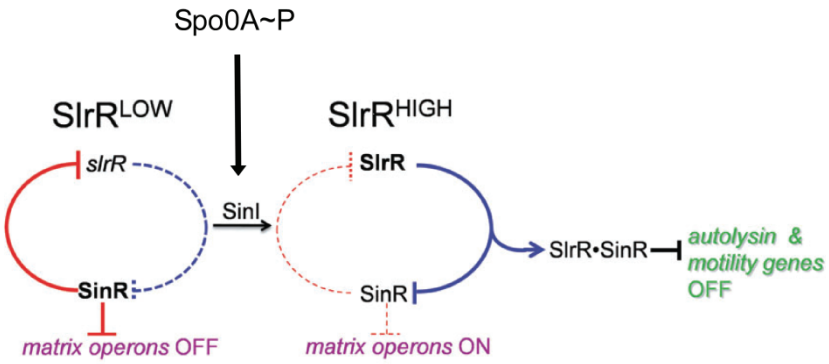

Figure 1.8 Spo0A~P influences the SlrR switch leading to generation of biofilm producing subpopulation. Dashed arrows indicate translation. Solid lines represent two pathways leading to motile cells (red) or sessile, matrix producing cells (blue). Black T-bars represent expression repression. SlrR·SinR denotes the SlrR-SinR protein complex. Genes are signified by italics. Adapted from (Chai *et al.*, 2010).

1.5.2. DegU-mediated control of multicellular behaviour of B. subtilis

1.5.2.1. Activity of DegU is regulated by DegS

DegU also controls biofilm formation (Kobayashi, 2007b, Verhamme *et al.*, 2007). DegU is a response regulator of the protein kinase DegS, which together form a two-component regulatory system [for review see (Murray *et al.*, 2009a)]. The majority of sensory kinases forming the two-component systems are anchored to the cell membrane and monitor the extracellular environment to detect a particular signal (Fabret *et al.*, 1999). However, DegS is an unusual sensor kinase as it is located in the cytoplasm rather than anchored in the cytoplasmic membrane (Meile *et al.*, 2006). As a cytoplasmic sensory protein, DegS is likely to respond to changes in the physiological conditions within the cytoplasm. A genome-wide transcriptional profiling in high salinity conditions demonstrated an impact on transcription of number of genes within the DegS-DegU regulon indirectly implicating DegS in sensing of osmolarity (Ruzal & Sanchez-Rivas, 1998). However, no direct signal stimulating autophosphorylation of DegS has been elucidated so far.

Despite the fact, the environmental signal activating the kinase activity of DegS remaining elusive, significant progress was made in the study of the signal transduction through the DegS-DegU system. Upon signal detection, DegS dimerises and autophosphorylates (Msadek *et al.*, 1990, Dahl *et al.*, 1991). The kinase activity of DegS allows for the transfer of the phospho-moiety onto DegU (Dahl *et al.*, 1991). This process is enhanced by the small protein DegQ (Kobayashi, 2007b). The activity of DegQ is required for DegU~P-dependent activation of biofilm formation (Stanley & Lazazzera, 2005, Kobayashi, 2007b). Prior to phosphorylation, DegU is also active as a transcription regulator. It is able to bind inverted repeat sequences in the promoter regions of target genes, like the promoter of *comK* that is needed for genetic competence (van Sinderen & Venema, 1994, Hamoen *et al.*, 2000, Shimane & Ogura, 2004). When DegU becomes phosphorylated (hereafter DegU~P) by DegS, the DNA binding activity of DegU is altered to enable binding of tandem repeat sequences, of which an example is found in the promoter region of *aprE* encoding an extracellular protease (Shimane & Ogura, 2004).

1.5.2.2. DegU~P binds to promoters with different affinity

The DegS-DegU regulatory system controls a variety of multicellular behaviours of *B. subtilis* including: swimming motility, genetic competence, swarming motility, biofilm formation and exoprotease production (Msadek *et al.*, 1990, Dubnau *et al.*, 1994, Amati *et al.*, 2004, Stanley & Lazazzera, 2005, Verhamme *et al.*, 2007, Verhamme *et al.*, 2009). The regulation of gene expression by DegU~P is not only dependent on the phosphorylation state, but also on the intracellular concentration proportion between the phosphorylated and unphosphorylated DegU (Verhamme *et al.*, 2007, Murray *et al.*, 2009a). Unfortunately it is currently impossible to directly measure the

concentration of DegU~P *in vivo.* However, a concentration-dependent effect on the phenotype was shown (Verhamme *et al.*, 2007). Similarly to Spo0A~P dependent promoter regions, promoters regulated by DegU~P have different affinity for binding of the response regulator (Shimane & Ogura, 2004). Therefore it is presumed that promoters with strong affinity are bound by DegU~P at low concentrations, the promoters with low affinity are reacting with DegU~P at high concentration of the phosphorylated DegU and finally the promoter regions with intermediate affinity are regulated by intermediate concentrations of DegU~P (Verhamme *et al.*, 2007, Tsukahara & Ogura, 2008).

1.5.2.3. Biofilm formation is stimulated by intermediate levels of DegU~P but inhibited by high levels of DegU~P

The existence of DegU and DegU~P dependent promoters, that respond to different concentrations of phosphorylated DegU, has allowed for the development of a regulatory network that is able to controll multiple types of behaviours (Figure 1.9) (Murray *et al.*, 2009a). The regulation by DegU is based on differential promoter region binding and the balance between phosphorylated and unphosphorylated forms of DegU. In consequence, the unphosphorylated DegU activates genes required for genetic competence by activation of *comK* expression (Ogura & Tanaka, 1996). When DegU is phosphorylated by DegS and maintained in low concentration, genes required for swarming motility are activated (Verhamme *et al.*, 2007). As the ratio of DegU to DegU~P changes in favour of the phosphorylated form, the genes required for biofilm formation, *yuaB* and *yvcA* (see Section 1.7.1) are activated (Figure 1.9 and Figure 1.10) (Kobayashi, 2007b, Verhamme *et al.*, 2007, Verhamme *et al.*, 2009). Finally, when DegU~P reaches high intracellular levels and the level of unphosphorylated DegU is

very low, the genes required for swarming and biofilm formation are inhibited. Simultaneously, transcription of genes encoding extracellular proteases, like *bpr* and *aprE*, are activated (Figure 1.9) (Mukai *et al.*, 1990, Tsukahara & Ogura, 2007, Verhamme *et al.*, 2007). The high level of DegU~P is probably caused by reception of an environmental signal promoting escape from the currently occupied ecological niche (Verhamme *et al.*, 2007). The production of extracellular proteases is potentially the mechanism allowing the biofilm enclosed cells to degrade the biofilm matrix. The inhibition of transcription of biofilm formation genes, which takes place at the same time, allows for faster degradation of the extracellular matrix and faster escape. Once the biofilm matrix is completely degraded, the persisting motile subpopulation can continue the search for more a favourable niche (Verhamme *et al.*, 2007).

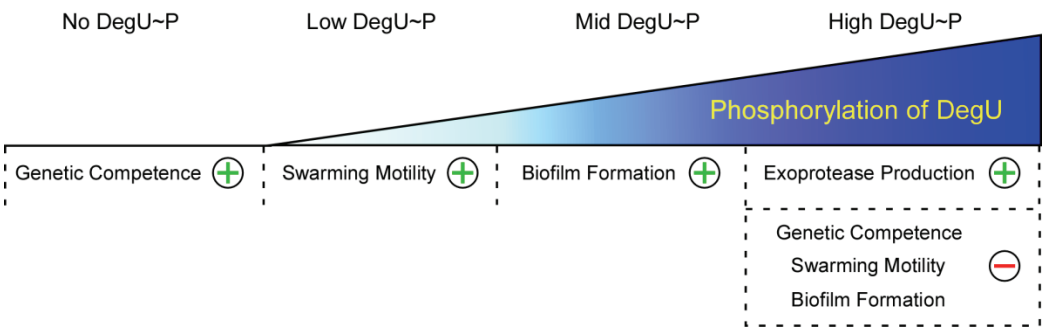

Figure 1.9 DegU regulates different types of multicellular behaviour depending on its phosphorylation state. A simplified schematic illustrating differential effects of DegU and DegU~P promoting and inhibiting different multicellular behaviours of *B. subtilis*. The green "plus" sign indicates activation and the red "minus" sign indicates inhibition accordingly to the intracellular concentration of DegU~P shown. (T. B. Kiley)

1.5.3. YuaB is jointly regulated by Spo0A and DegU regulators

One of the genes activated by the intermediate levels of DegU~P is a monocistronic gene *yuaB* (Verhamme *et al.*, 2007). Interestingly, the expression of *yuaB* was found to be regulated by AbrB in addition to the DegU~P-mediated

regulation (Figure 1.10) (Verhamme *et al.*, 2009). The AbrB-mediated regulation is most probably direct, as AbrB is able to bind to the *yuaB* promoter region *in vitro* (Verhamme *et al.*, 2009). In contrast, DegU~P-mediated regulation appears to be indirect. That said, inactivation of DegU causes complete loss of *yuaB* expression (Verhamme *et al.*, 2009). Additionally, ectopic DegU-independent expression of *yuaB* is sufficient to overcome the DegU mutation and restore biofilm formation defect associated with DegU deletion (Figure 1.11); thus *yuaB* is probably the main target of DegU~P during biofilm formation.

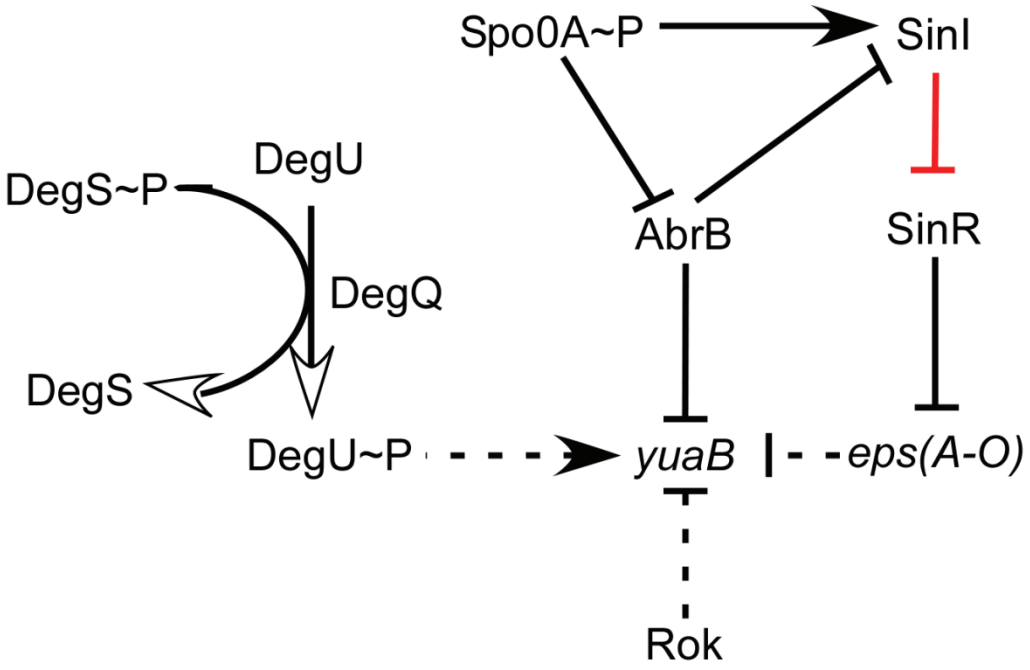

Figure 1.10 Expression of *yuaB* is regulated by multiple factors during biofilm formation. Phopsho-transfer interactions are marked with white head arrows. Expression activation events are marked with black head arrows and expression repression with black T-bars. Red T-Bars represent protein-protein inhibition. Solid lines represent direct interaction, whereas the dashed arrows represent indirect interactions. Genes are signified by italics.

Expression of *yuaB* is also indirectly regulated by SinR (Verhamme *et al.*, 2009) and Rok (Kovacs & Kuipers, 2011) (Figure 1.10**Figure 1.10**). The EPS synthesis pathway, or its member proteins, seems to be the link between SinR regulation and *yuaB* expression, as mutants in *epsG* show significant reduction in *yuaB* expression in the *sinR* genetic background (Figure 1.10) (Verhamme *et al.*, 2009). However, no effect on YuaB expression was seen when *epsG* was mutated in the background of a laboratory strain (Kovacs & Kuipers, 2011). Rok is an AbrB-dependent regulatory protein found to bind to the AT-rich fragments of DNA (Strauch *et al.*, 1989). Mutation of *rok* was found to inhibit expression of *yuaB* during biofilm formation in one of the laboratory strains of *B. subtilis* (Kovacs & Kuipers, 2011). However, the mechanism of this regulation is not known.

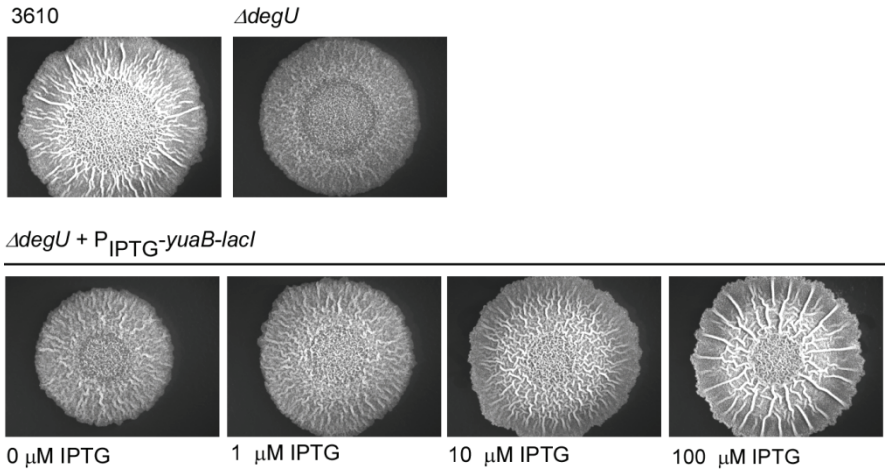

Figure 1.11 Ectopic expression of YuaB is sufficient to overcome the biofilm defect caused by lack of DegU. The complex colonies of the *degU* mutant strain carrying an IPTG-inducible allele of *yuaB* (NRS2298) were grown on MSgg agar plate supplemented with IPTG as indicated. The resulting complex colony morphologies are compared to that of the wild type (3610) and the *degU* mutant (NRS1314). (Ostrowski *et al.*, 2011)

1.6.The structural components of the biofilm matrix of *B. subtilis.*

1.6.1. B. subtilis *forms biofilms on air-liquid interfaces and solid surfaces*

The first report of a "biofilm" formed in the cultures of *B. subtilis* comes from Ferdinand Cohn (Cohn, 1877). Although the existence of biofilms as a concept was not known at the time, Cohn described a development of a thin and delicate film on top of standing cultures after 2 days of incubation. These films, with time, gained "a slimy-flocculent or scaly character" while becoming more turbid (Cohn, 1877, McLoon *et al.*, 2011). Despite this clear description, biofilm formation by *B. subtilis* was not investigated until the reports by Branda *et al.* and Hamon & Lazazzera in 2001.

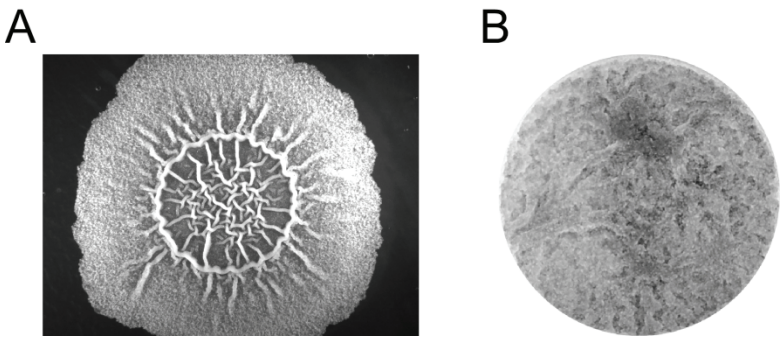

Figure 1.12 Two types of biofilms formed by *Bacillus subtilis*. A complex colony formed on a solid surface (**A**) and a biofilm pellicle formed on an air-liquid interface (**B**).

1.6.1.1. *Distinct subpopulations of cells inhabit the biofilm matrix of* B. subtilis

Analysis of gene expression specific for various multicellular behaviours of *B. subtilis* revealed spatial and temporal differences in the population composition within the biofilm (Figure 1.13) (Vlamakis *et al.*, 2008). The development of the biofilm begins from a population of motile cells, from which the subpopulation of matrix producing cells emerge (Figure 1.13) (Vlamakis *et al.*, 2008). This subpopulation synthesises the

TasA protein component of the matrix (described in Section 1.6.2) and the EPS (described in Section 1.6.3). Interestingly, both components of the biofilm matrix can be synthesised by different cells and the resulting biopolymers are shared by the entire community (Branda *et al.*, 2006). Furthermore, the motile subpopulation remains present at the bottom of the biofilm throughout the biofilm development (Vlamakis *et al.*, 2008). It was hypothesised that the persistence of the motile cell in the generally sessile biofilm community would allow for a fast escape of cells, should the environmental conditions turn to less favourable. Finally, the matrix producing cells differentiate further to give rise to the subpopulation of sporulating cells (Vlamakis *et al.*, 2008). Interestingly, the differentiation of cells into sporulating cells rarely occurs from the motile cells and the preferred sporulation sites are located at the tips of the aerial projections known as “fruiting body-like” structures (Figure 1.13) (Branda *et al.*, 2001, Vlamakis *et al.*, 2008). A possible explanation is that the entry into sporulation is partially driven by starvation and that the aerial projections are the parts of the biofilm most remote from the nutrient substratum. Hence sporulation is promoted in the aerial projections from matrix producing cells, not from the subpopulation of motile cells present predominantly at the interface with the substratum (Vlamakis *et al.*, 2008, Lopez *et al.*, 2009b).

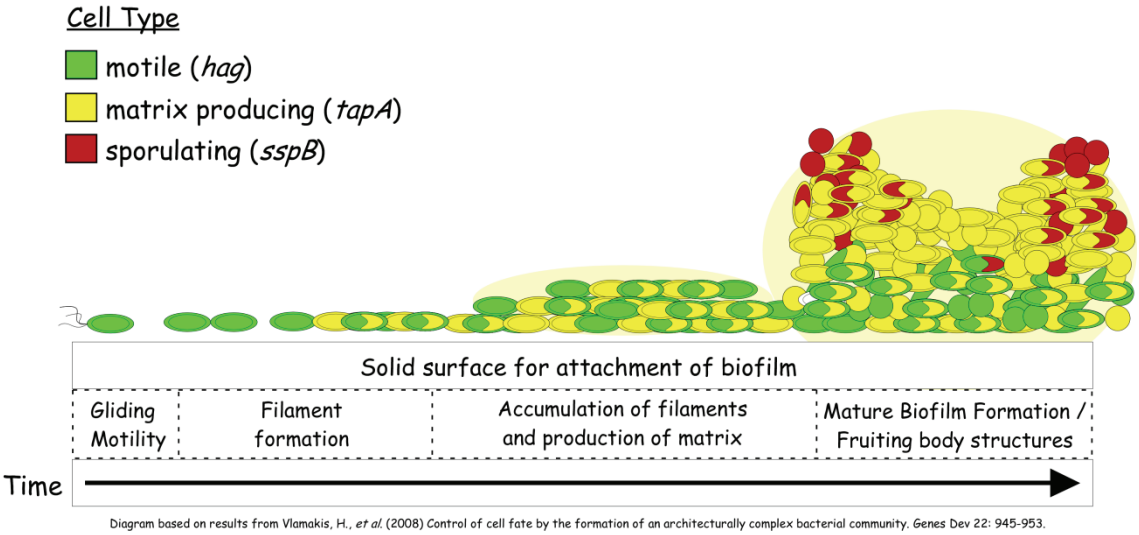

Figure 1.13 Formation of biofilm proceeded through defined spatio-temporal stages. From the population of motile cells (showed in green) a subpopulation of matrix producing cells (shown in yellow) differentiates. The cells accumulate through division and produce biofilm matrix. The final stage of biofilm development is marked by differentiation of sporulating cell (shown in red) at the tips of the fruiting body-like aerial projections. Based on (Vlamakis *et al.*, 2008, Lopez *et al.*, 2009b) (Taryn B. Kiley).

Differentiation into sporulating cells is mostly dependent on the Spo0A~P regulated processes (Lopez *et al.*, 2009b). However, the existence of the matrix producing cells is also dependent on DegU~P regulation (Verhamme *et al.*, 2007) (Marlow *et al.* in review). As DegU~P regulates also the transcription of the exoprotease synthesis genes, it is plausible to assume, that the population of protease producers will be present in a biofilm as well. The ecological reason for existence of such a population would be (*i*) ability to degrade the proteins in the environment as a nutrient source (Lopez & Kolter, 2010); (*ii*) to degrade the biofilm matrix and allow the motile cells to leave the unfavourable environment (Verhamme *et al.*, 2007). The investigation into the regulation of cell fate in the biofilm by DegU revealed that DegU~P affects the frequency of switching between different genetic programmes (Marlow *et al.* in review). In conclusion, the population of cells within the biofilm is undergoing constant and dynamic adaptation to the current state of the biofilm

development and environmental conditions. The study of these mechanisms allows for a completely new insight into the dynamics of bacterial social behaviour.

Despite extensive knowledge of the regulatory networks governing the development of the biofilm communities and the fate of cells inhabiting the biofilm, not much is known about the dynamics of the biofilm matrix assembly. In fact, only recently the first information on biophysical properties of the TasA protein component of the matrix were published (Romero *et al.*, 2010). The exopolysaccharide component of the biofilm matrix remains undescribed. Similarly the mechanistic function of other genes indicated in biofilm formation, like DegU~P-regulated *yuaB* and *yvcA* (Verhamme *et al.*, 2009), are poorly understood. The following sections are a review of the current state of knowledge on the composition of the biofilm matrix and the function and interaction between the individual components of the matrix.

1.6.2. The TasA amyloid fibres.

1.6.2.1. TasA is the first described amyloid protein produced by B. subtilis

As described in Section 1.2.2, extracellular proteins located in the biofilm matrix perform a structural role as adhesins of cells to the substrate or allow for cell-to-cell connections. TasA protein was identified as a secreted protein which is predominantly located within the biofilm matrix during formation by *B. subtilis* (Branda *et al.*, 2006). Deletion of the *tasA* gene causes a loss of biofilm complexity and reduces chaining of the biofilm producing cells (Branda *et al.*, 2006). Scanning electron microscopy images revealed significant changes to the biofilm matrix in the strain that does not produce TasA. Thus TasA was determined to be the main protein component of the biofilm matrix (Branda *et al.*, 2006). Interestingly, during purification of TasA

directly from *B. subtilis* biofilms, TasA did not elute from size exclusion column in the expected fractions. The theoretical molecular mass of TasA is ~28 kDa, but TasA was found to elute in the void volume suggesting significantly larger mass of the protein (Romero *et al.*, 2010). Following this, TasA was subjected to immuno-gold detection and transmission electron microscopy (TEM). These experiments have shown that TasA form fibril-like structures in pellicles of *B. subtilis* (Figure 1.14) (Romero *et al.*, 2010). The authors hypothesised that TasA forms amyloid fibres in the biofilm matrix. Purified TasA was shown to bind Congo red dye (Romero *et al.*, 2010), which is an indication of presence of amyloid structures in the analysed samples (Klunk *et al.*, 1999). Indeed amyloid fibre formation by TasA was confirmed by *in vitro* polymerisation assays and binding of Thioflavin T, another amyloid-specific dye (Klunk *et al.*, 1999, Romero *et al.*, 2010). Furthermore, complex colonies of wild type *B. subtilis* stain red when grown on an agar media supplemented with Congo red and this feature is not exhibited by the *tasA* mutant (Romero *et al.*, 2010).

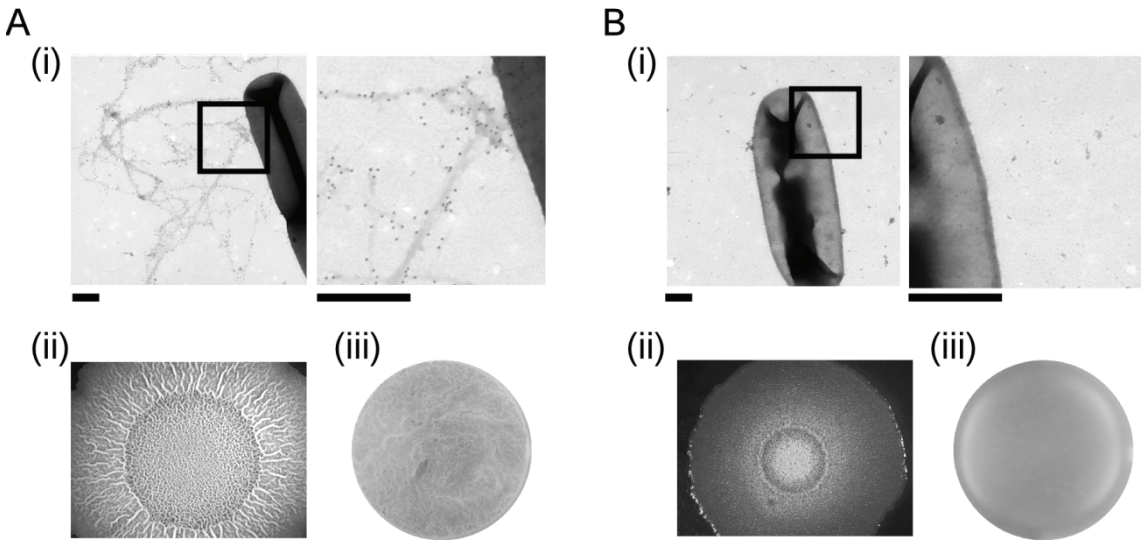

Figure 1.14 TasA forms amyloid fibres required for biofilm formation. Analysis of the biofilms formed by (**A**) wild type and (**B**) *tasA* mutant strains. (**i**) The amyloid fibres of TasA were immuno-gold labelled in cells extracted from biofilm forming conditions. Strains unable to produced EPS were used (NRS2450 and NRS2451 respectively) to avoid electron-thick background. Images in the right panel are the magnification of the boxed area in the left panel. Scale bars represent 0.5 µm. Effects of TasA deletion on the complex colony (**ii**) and biofilm pellicle (**iii**) formation by the wild type (3610) (**A**) and *tasA* (NRS2415) (**B**) strains. Based on the results from (Branda *et al.*, 2006) and (Romero *et al.*, 2010). Images by A. Ostrowski.

1.6.2.2. TasA provides structural scaffold to the biofilm

The polymerisation features of TasA allowed for classification of TasA as the first amyloid protein described in the biofilm matrix of *B. subtilis* (Romero *et al.*, 2010). However, biofilms of *B. subtilis* 3610 are known not to adhere to abiotic surfaces and the complex colonies are easily lifted from the agar surface. Therefore, it was unlikely, that TasA is a surface adhesin; as it was observed for other biofilm amyloids, such as curli fimbriae isolated from *E. coli* (Vidal *et al.*, 1998). In fact the formation of biofilms by *B. subtilis* has been shown to be dependent on the lipoprotein surfactin. Surfactin is not only a signalling molecule but is also required for spatial spreading of the growing biofilm (Seminara *et al.*, 2012). Surfactin has also been proven to be the factor that allows the biofilm to "climb" the walls of a vessel when grown in liquid media (Angelini *et al.*, 2009). For these reasons, it is plausible to assume, that the predominant function of TasA in the biofilm matrix is to provide cell-to-cell binding and a structural

scaffold on which the exopolysaccharide can be polymerised to provide the coherent structure of the biofilm. This conclusion is supported by the finding that TasA is not required for formation of surface-adhered biofilms by laboratory strains of *B. subtilis* (Hamon *et al.*, 2004, Terra *et al.*, 2012).

1.6.2.3. TapA is the nucleation inducing protein for TasA

Many amyloid-forming proteins interact with another protein while in the monomeric state (Wang & Chapman, 2008, Dueholm *et al.*, 2011). This interaction promotes transition of the amyloid protein from a monomer to polymer (Larsen *et al.*, 2007). Once polymerisation begins, further subunits of the amyloid fibre can be added to the growing structure without assistance from the accessory protein (Hammer *et al.*, 2007). TasA is encoded in a three-gene operon *tapA-sipW-tasA* (Stover & Driks, 1999b). The first gene in this operon was shown to encode a small protein TapA (TasA accessory protein A, previously known as YqxM) that can be found in the cell wall (Romero *et al.*, 2011). TapA has been shown to promote polymerisation of TasA (Romero *et al.*, 2011). Using TEM and immuno-gold labelling TapA was also shown to be a minor component of the TasA fibre, probably an artefact of the TasA polymer nucleation (Romero *et al.*, 2011). Interestingly, TapA has also been shown to be responsible for the attachment of the TasA fibres to the cell wall. Furthermore, the purified TasA can be added to the suspension of the cells producing TapA. This allows attachment of the TasA fibres to the cells and formation of a wild type biofilm. Evidence also suggests that interaction with TapA is necessary for at least stability, if not synthesis, of TasA. In the absence of TapA very few detached fibres of TasA were observed and minimal amount of TasA was detectable by Western blotting (Romero *et al.*, 2011).

1.6.2.4. TasA and TapA require the signal peptidase SipW

The N-termini of TasA and TapA contain export signal peptides, most likely directing these proteins to the Sec general secretion pathway (Stover & Driks, 1999c). The proteins exported through the Sec pathway and to be released from the cell must be processed by a signal peptidase (Yamane *et al.*, 2004). SipW, the middle gene in the *tapA* operon, is such a peptidase (Stover & Driks, 1999a). SipW has been demonstrated to be required for processing and secretion of TasA and TapA. In the absence of SipW, TasA is trapped in the cell, whereas TapA is not secreted and not found in cells (Stover & Driks, 1999c). This suggests that TapA that is not secreted is rapidly degraded. In both cases, in the absence of SipW these proteins are not found in the media or biofilm matrix (Branda *et al.*, 2006).

In addition to the signal peptidase function, SipW was also shown to be required for formation of the surface-associated biofilm by the laboratory strain *B. subtilis* JH642 (Terra *et al.*, 2012). In this system, the signal peptidase function of SipW is not required for biofilm formation. However, a second function of SipW was described in this study, which links SipW to regulation of the expression of the *eps* operon. It was demonstrated, that the C-terminus of SipW conveys an expression regulator function that is genetically separable from the peptidase activity. These findings identified SipW as a dual-role signal peptidase (Terra *et al.*, 2012).

1.6.3. The exopolysaccharide component of the biofilm matrix

1.6.3.1. The eps *operon encodes machinery for EPS synthesis*

The second typical component of biofilm matrix found across all biofilms is an exopolysaccharide (EPS) (Flemming & Wingender, 2010). In general, once the growing

biofilm is attached to the substratum, the EPS is believed to settle on the matrix proteins allowing for development of structural integrity of the growing biofilm (Flemming & Wingender, 2010). Despite the fact that the structures of many bacterial polysaccharides have been described to date (as described in Section 1.2.1), the composition of the EPS synthesised by *B. subtilis* remains unknown. During the first investigation into biofilm formation by *B. subtilis,* two genes encoded within a 15-gene operon *yveK-yvfF* were identified as required for formation of biofilms (Branda *et al.*, 2001). The analysis of protein sequences encoded by the *yveK-yvfF* operon revealed significant similarities to the known proteins involved in synthesis of the capsular polysaccharides and exopolysaccharides in other species (Table 1.1). Therefore the *yveK-yvfF* operon was renamed *epsABCDEFGHIJKLMNO* (the *eps* operon) (Kearns *et al.*, 2005). In addition to the proteins encoded by the *eps* operon, other proteins, encoded by genes that are located in different locations on the chromosome, have been implicated in the synthesis of the EPS. For example it was demonstrated that the EPS is not produced in the absence of a UDP-glucose-4-epimerase GalE (Pozsgai *et al.*, 2012). Other genes involved in saccharide modification, or similar to saccharide modifying enzymes, were shown to affect biofilm formation as well. These include alpha-phosphoglucomutase PgcA (Branda *et al.*, 2004, Lazarevic *et al.*, 2005) and a homologue of EpsH, a putative polysaccharide pyruvyl transferase YxaB (Nagorska *et al.*, 2008). However, it is unclear how these proteins contribute to the synthesis of EPS.

The entire *eps* operon forms a single transcriptional unit (Kunst *et al.*, 1997, Kearns *et al.*, 2005, Irnov & Winkler, 2010). That said, three transcription terminators are located within the coding region of *epsF* (Irnov & Winkler, 2010). In biofilm forming conditions, not only is the repression by AbrB and SinR alleviated, but additionally a

small intrinsic regulatory RNA is present within the *eps* transcript that facilitates antitermination at *epsF*. This regulatory RNA, termed EAR – eps associated RNA, is a section of the polycistronic mRNA located between transcripts of *epsB* and *epsC* genes. The EAR element was demonstrated to assume a complex secondary structure which facilitates the transcripton of the distal *eps* genes (Irnov & Winkler, 2010).

1.6.3.2. EpsA and EpsB are putative protein kinase modulator and tyrosine protein kinase

Based on the protein primary sequence comparison, putative functions can be assigned to the Eps proteins (Table 1.1). EpsA and EpsB are predicted to be a protein kinase modulator and a protein tyrosine kinase respectively (Mijakovic *et al.*, 2003). In Gram-positive bacteria, the regulatory kinase modulator is encoded by a separate gene which is co-transcribed with the gene encoding the cognate kinase (Grangeasse *et al.*, 2007). While EpsA is predicted to be such a kinase activity modulator located in the cell membrane and regulating activity of EpsB, phosphorylation of EpsB was only observed when it was overexpressed in *E. coli* and was not shown *in vitro* or in *B. subtilis.* Despite this fact, EpsB is predicted to be modifying one or more of the Eps proteins on a posttranslational level, thus influencing EPS synthesis (Mijakovic *et al.*, 2003)(NSW unpublished data).

Table 1.1 Predicted or known function of EpsA – EpsO.

Protein	Size [1]	Putative function	References
EpsA	234	EpsB-kinase modulator	(Mijakovic *et al.*, 2003, Kearns *et al.*, 2005)
EpsB	227	Protein tyrosine kinase	(Mijakovic *et al.*, 2003, Kearns *et al.*, 2005)
EpsC	598	Putative UDP-*N*-acetylglucosamine 4,6 dehydratase (PF02719)	(Ivanova *et al.*, 2003, Kearns *et al.*, 2005)
EpsD	381	Glycosyl transferase family 1 (PF00534)	(Kearns *et al.*, 2005)
EpsE	278	Flagella motor-stator separation, Glycosyl transferase family 2 (PF00535)	(Kearns *et al.*, 2005, Blair *et al.*, 2008, Guttenplan *et al.*, 2010)
EpsF	384	Glycosyl transferase family 1 (PF00534)	(Kearns *et al.*, 2005)
EpsG	367	Extracellular polysaccharide synthesis enzyme	(Branda *et al.*, 2001, Ren *et al.*, 2004, Kearns *et al.*, 2005)
EpsH	344	Putative glycosyl transferase family 2 (PF00535)	(Branda *et al.*, 2001, Ren *et al.*, 2004, Kearns *et al.*, 2005)
EpsI	358	Putative polysaccharide pyruvyl transferase (PF04230)	(Kearns *et al.*, 2005)
EpsJ	344	Putative glycosyl transferase family 2 (PF00535)	(Kearns *et al.*, 2005)
EpsK	505	Putative exopolysaccharide exporter (PF01943)	(Kearns *et al.*, 2005)
EpsL	202	Putative exopolysaccharide exporter (PF02397)	(Kearns *et al.*, 2005)
EpsM	216	Putative *O*-acetyl transferase	(Kearns *et al.*, 2005)
EpsN	388	Putative amino transferase (PF01041)	(Kearns *et al.*, 2005, Nagorska *et al.*, 2008)
EpsO	322	Putative pyruvyl transferase (PF04230)	(Kearns *et al.*, 2005, Nagorska *et al.*, 2008)

[1.] Size represented by number of amino acids.

1.6.3.3. EpsE is a bifunctional protein

The proteins encoded downstream from EpsB within the *eps* operon are predicted to be involved in the biosynthesis or transport of exopolysaccharides (Table 1.1). Although no biochemical information is available on the majority of these

proteins, the outstanding example is EpsE, which was shown to contain two genetically separable activities during biofilm formation (Guttenplan *et al.*, 2010). EpsE was shown to bind to the FliG protein within the stator of the flagellum (Blair *et al.*, 2008). EpsE binding to FliG is mediated by the residues K106 to K113 (Guttenplan *et al.*, 2010) and causes a change of conformation of FliG which uncouples the flagellum stator from the motor (Blair *et al.*, 2008). Thus the energy transfer from the stator to the rotor is stopped. As a result, EpsE enables the transition of cells from the motile to non-motile state. This transition is required for establishing the biofilm matrix (Blair *et al.*, 2008). Second function of EpsE is involved in the EPS synthesis (Guttenplan *et al.*, 2010). The EPS synthesis function of EpsE is mediated by a region homologous to glycosyltransferases. A number of mutations within this region were shown to inhibit biofilm formation but not the clutch activity of EpsE (Guttenplan *et al.*, 2010), thus demonstrating the bifunctional nature of the protein.

1.6.3.4. EPS is a large polymer of unknown structure

As already mentioned, the chemical structure of the exopolysaccharide is unknown. The presence of EPS within biofilm matrix can be demonstrated by extraction of the biofilm matrix fraction from pellicles and resolution of the concentrated fraction by SDS-PAGE. The resolved polysaccharide can be stained in several ways. The first image of EPS resolved by electrophoresis was published by Guttenplan *et al.* (2010) where a large polymer dependent on the *eps* that was resistant to nuclease and proteinase treatment was isolated. This is in line with experiments conducted during this project (Figure 1.15). However, on both occasions EPS was only identified as “a band that did not leave the stacking gel […], corresponding with high molecular weight substance” (Guttenplan *et al.*, 2010).

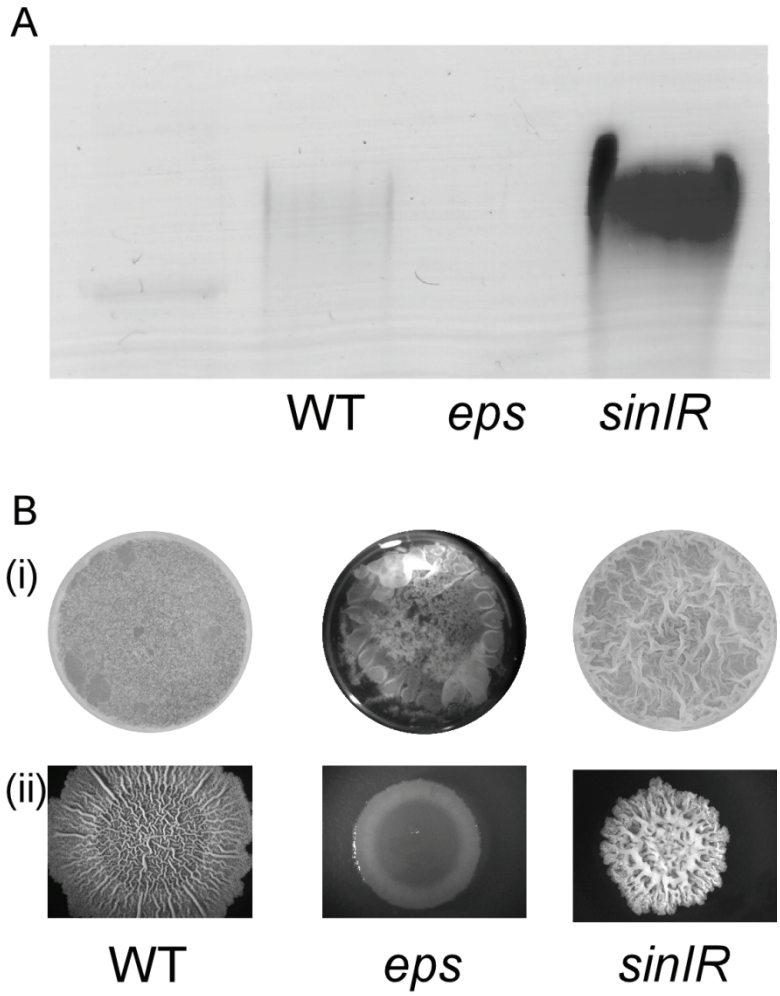

Figure 1.15 Exopolysaccharide is a functional component of the biofilm matrix of *B. subtilis*. (**A**) The biofilm matrix fractions of the wild type (3610), *eps* mutant (NRS2450) and *sinIR* (DS9) were resolved in SDS-PAGE and stained against carbohydrates. (**B**) The biofilm morphology of (**i**) the biofilm pellicle and (**ii**) complex colonies of the wild type (3610), *eps* mutant (NRS2450) strain lacking the EPS and *sinIR* (DS9) strain overproducing the EPS is presented. Results from (Chu *et al.*, 2006) and (Guttenplan *et al.*, 2010). Images A. Ostrowski.

1.7. A small protein of unknown function, YuaB, is required for biofilm formation.

1.7.1. The DegU-regulated protein YuaB is required for biofilm formation

During the last 11 years investigating biofilm formation by *B. subtilis* many genes were found to be needed for the formation of a biofilm. This research revealed one DegU~P regulated gene *yuaB* involved in formation of the biofilm, in addition to TasA and EPS components of the biofilm matrix (Stanley & Lazazzera, 2005, Kobayashi, 2007b, Verhamme *et al.*, 2007). YuaB is a small protein that does not resemble any known proteins when compared at the primary amino acid sequence. No putative biochemical domains can be assigned to the sequence of YuaB (Kobayashi, 2007b, Verhamme *et al.*, 2009). However, by application of software based on a neural network approach, in this case SignalP, a putative signal peptide at the N-terminus was identified (Kobayashi, 2007b). YuaB is predicted to be targeted to the Sec general secretory pathway with the signal peptide cleavage site between residues A28 and A29. Consistent with this, YuaB was identified in a secretome-wide study of *B. subtilis* as a secreted protein (Antelmann *et al.*, 2001). Disruption of the *yuaB* gene causes a loss of biofilm formation in both the complex colony and pellicle biofilm subtypes (Figure 1.16), the phenotypes of which are remarkably different from those caused by either *tasA* or *eps* mutations (compare to Figure 1.14 and Figure 1.15) (Kobayashi, 2007b, Verhamme *et al.*, 2009). Therefore it was assumed that YuaB contributes to biofilm formation in a distinct manner.

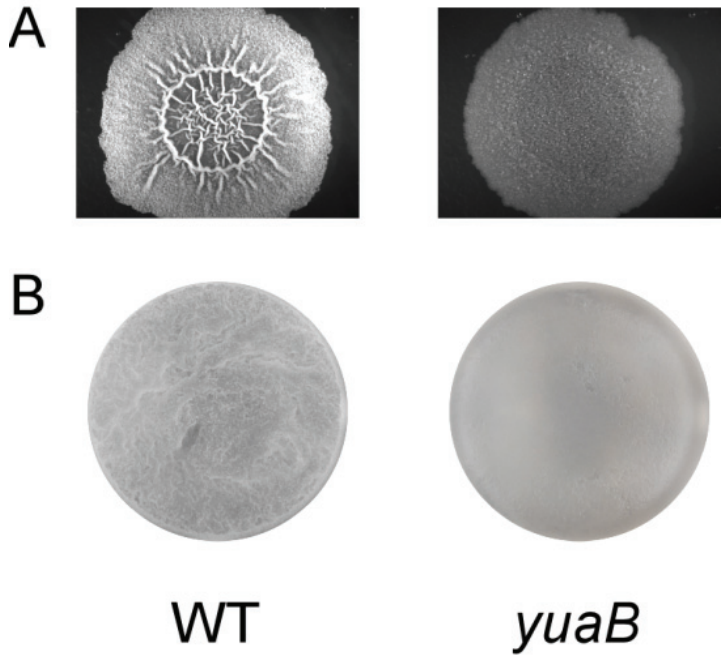

Figure 1.16 YuaB is required for biofilm formation. The *yuaB* mutant strain (NRS2097) is unable to form a biofilm of a complexity comparable to that of the wild type in (**A**) complex colonies (**B**) or biofilm pellicles in comparison to the wild type (3610) strain. Results from (Kobayashi, 2007b) and (Verhamme *et al.*, 2009). Images by A. Ostrowski.

1.8. Aims of the project

The involvement of YuaB in biofilm formation has been shown by two groups (Kobayashi, 2007b, Verhamme *et al.*, 2009). However, no conclusion on the mechanism of YuaB function could be drawn. The goal of this project was to provide biophysical and biochemical insight into function performed by YuaB during the development of the biofilm. The individual aims included:

- Identification of the localisation of YuaB in the biofilm;
- Identification of the essential fragments of YuaB needed for its activity;
- To elucidate the relationship between YuaB and the known components of the biofilm matrix;
- Identification of the mechanism of how YuaB facilitates to biofilm formation.

2. YuaB acts synergistically with TasA and EPS to allow biofilm formation

2.1. Introduction

Formation of a biofilm is ultimately dependent on the production and secretion of biopolymeric constituents of the biofilm matrix. In the case of *B. subtilis* these are the amyloid protein TasA (Romero *et al.*, 2010) and an exopolysaccharide (EPS) (Branda *et al.*, 2001, Kearns *et al.*, 2005). These biopolymers need to interact with one another to form a robust network which will provide a structural support for the growing biofilm. Furthermore, a third uncharacterised protein, called YuaB, was shown to be required for biofilm formation in addition to TasA and the EPS (Kobayashi, 2007b, Verhamme *et al.*, 2009). During studies to further understand the contribution of YuaB to biofilm formation I have identified YuaB as a secreted protein that functions independently from TasA and EPS. In this chapter I present an initial characterisation of YuaB and conclude by proposing that it acts synergistically with the two known components of the biofilm matrix to allow for the full maturation of the biofilm.

2.2. YuaB is required for spore formation in the biofilm

During biofilm formation, the cells of *B. subtilis* cells undergo a differentiation process that results in the emergence of three subpopulations of cells: motile cells, biofilm matrix-producing cells, and sporulating cells (Vlamakis *et al.*, 2008). The population of sporulating cells is the last one to emerge. This final stage of cell type differentiation is dependent on the establishment of a fully developed, and robust, biofilm matrix. It is deemed to mark the maturation of the biofilm (Vlamakis *et al.*, 2008, Aguilar *et al.*, 2010). Therefore the sporulation frequency in the biofilm can be

used as an indicator of biofilm maturity (Vlamakis *et al.*, 2008). The biofilm morphotype of the *yuaB* mutant strain (NRS2097) lacks the structural complexity apparent in the wild type strain (Figure 1.16) (Kobayashi, 2007b, Verhamme *et al.*, 2009). Similar changes in the biofilm complexity are associated with inability of a given strain to form a mature biofilm (Lopez *et al.*, 2010). Using the sporulation frequency as a proxy, the maturity of the biofilm formed in the absence of YuaB was assessed. After 72h of incubation, the sporulation rate of the *yuaB* mutant (NRS2097) was 13% ± 3% and was 6-fold lower than that of the wild type (3610) (81% ±3%, n=3 $P<0.001$) (Figure 2.1). The sporulation rate of the *yuaB* mutant returned to the wild type levels upon expression of *yuaB* from an IPTG-driven promoter $P_{hy\text{-}spank}$ introduced at an ectopic position *amyE* on the chromosome (NRS2299). It should be noted that a 2-fold decrease in the total number of colony forming units (CFU) in the biofilm of the *yuaB* strain (NRS2097) was detected. The reduction in the cell density in biofilm cultures formed by strains deficient in biofilm matrix synthesis has been independently detected previously (Aguilar *et al.*, 2010).

The genetic pathways responsible for activation of biofilm formation and sporulation are linked through the regulatory protein Spo0A (Hamon & Lazazzera, 2001, Aguilar *et al.*, 2010). In response to environmental cues, Spo0A can be phosphorylated and achieve ratios of phosphorylated to unphosphorylated Spo0A specific for activation of biofilm formation or sporulation (Fujita *et al.*, 2005). Additionally expression of YuaB is partially regulated by Spo0A-dependent expression repressor protein AbrB (Verhamme *et al.*, 2009). Thus it was important to rule out a possibility that the difference in the sporulation rate between the *yuaB* mutant (NRS2097) and the wild type is caused by a block in sporulation pathway rather than

caused by a defect in biofilm matrix synthesis. To do this the sporulation frequency of the *yuaB* mutant was assessed in the liquid culture. To ensure that similar nutrition conditions were provided as those present in the biofilm cultures, and thus similar expression profiles, a biofilm promoting medium, MSgg, was used. Unlike in biofilm forming conditions, the cells were incubated with vigorous shaking so that the 3-dimensional structure in the biofilm matrix could not be established. Under these conditions, after 72h incubation, the sporulation rate of the *yuaB* mutant was found to be 94% ±2%, which was not statistically different from that of the wild type (3610) (96% ±2%) (Figure 2.1). Taken together, these results indicate that the decrease in the sporulation frequency in the biofilm forming conditions in the absence of YuaB is not caused by disruption of the sporulation pathway but is a consequence of deficiency in the assembly of the biofilm matrix. Therefore YuaB is required for maturation of the biofilm.

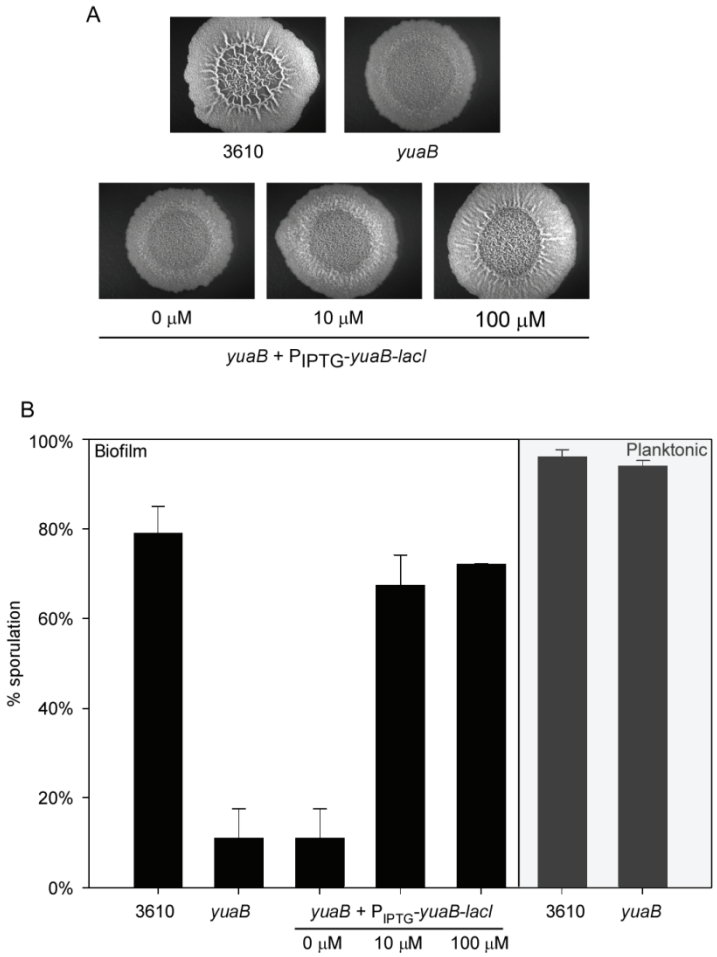

Figure 2.1 Sporulation rate is affected by *yuaB* mutation in biofilm forming conditions but not in the planktonic growth conditions. The biofilm phenotypes of the analysed strains are presented (**A**). Sporulation in biofilm was used to assess the maturity of biofilm of the wild type (3610), the *yuaB* (NRS2097) mutant and the complemented *yuaB* strain (*yuaB* + P_{IPTG}-*yuaB-lacI*) (NRS2299) (**B**). The decreased sporulation rate of the *yuaB* mutant indicates lack of biofilm maturity and can be complemented by an ectopic expression of YuaB (left panel). YuaB is not required for sporulation during planktonic growth (right, light grey panel).

2.3. Purification of recombinant YuaB and TasA and antibody generation

Having shown that YuaB is required for the assembly of the biofilm matrix, it was of interest to elucidate the localisation of YuaB in the biofilm. One possible method for the identification of protein localisation in the biofilm is biofilm fractionation followed by immuno-detection of proteins by Western blot (Branda *et al.*, 2006). For this purpose the ability of immuno-detecting YuaB was required. The first possibility explored was to construct a recombinant variant of YuaB fused to a FLAG epitope on the C-terminus. The resulting protein was able to complement for the

lack of the wild type YuaB, if expressed ectopically (Figure 2.2). However, the FLAG epitope was not detectable by Western blot for unknown reasons (Data not shown). A possible explanation was that the C-terminus of YuaB is processed by unknown factors, which causes cleavage of the FLAG epitope; or that the C-terminus is hidden within the folded molecule of YuaB, hence the FLAG epitope is inaccessible to the antibody.

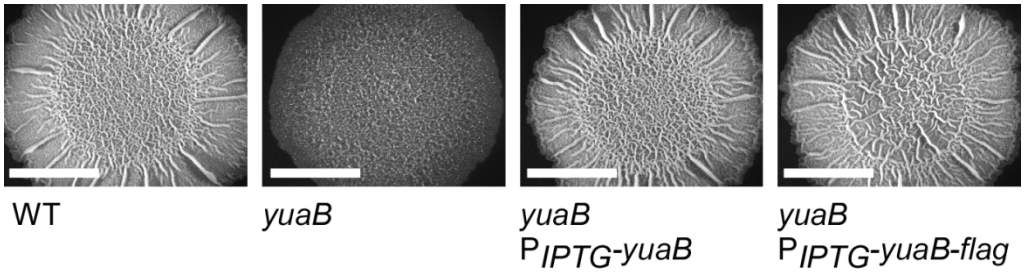

Figure 2.2 FLAG-tagged YuaB complements the *yuaB* mutant phenotype. Complex colonies of wild type (3610), *yuaB* mutant (NRS2097), *yuaB* mutant complemented with wild type *yuaB* (NRS2299) and *yuaB* mutant complemented with FLAG-tagged *yuaB* (NRS2397) were grown on MSgg agar supplemented with 25 µM IPTG at 30 °C over 48 h. The images show representative colonies formed by each strain. The scale bar is 1 cm.

Therefore, the method of choice to enable immunological detection of YuaB was to raise antibodies against purified YuaB. For this purpose a vector was constructed for *E. coli* expression of YuaB tagged with a hexahistidine tag. At the same time it was decided to establish suitable conditions for crystallisation of YuaB. The amino acid sequence of YuaB is not similar to any proteins of known structure. It was proposed that YuaB might be a protein of new and unknown fold, therefore structural information on YuaB would provide important information for understanding its function during biofilm formation.

2.3.1. Purification of C-terminally His_6-tagged YuaB

To express YuaB in the cytoplasm of *E. coli*, an allele of *yuaB* missing the predicted signal peptide and carrying a His_6-tag was introduced into pQE-60 to construct pNW610 (see Materials and Methods). The expression and solubility of the

tagged YuaB was tested by induction of expression with 100 µM IPTG for 2h and the samples of induced and uninduced cells were collected. Inclusion bodies were isolated from the cytoplasm of the cells to assess solubility of the recombinant protein. The isolated fractions were analysed by SDS-PAGE (Figure 2.3).

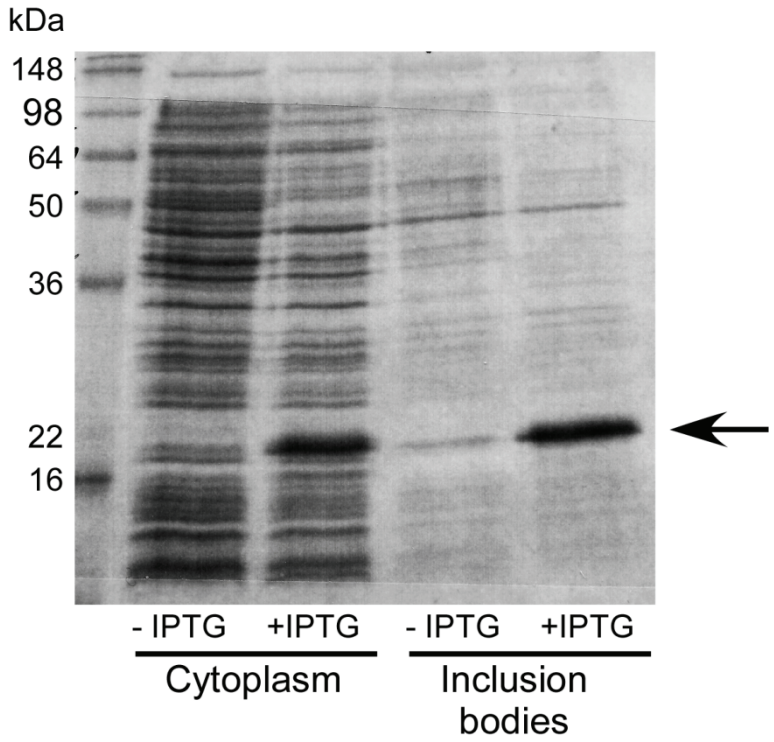

Figure 2.3 YuaB-His_6 is partially soluble when expressed in *E. coli*. The cytoplasm and the inclusion bodies fractions from cells carrying a vector for expression of YuaB-His_6 with and without induction were resolved by running on a 12% SDS-PAGE. The band corresponding to the mass of the recombinant YuaB-His_6 is marked with an arrow. Molecular mass sizes are indicated according to a protein size standard SeeBlue2.

The expressed protein was found to be soluble at a sufficient level to be affinity-purified. Large scale overexpression in a total volume of 6 L was conducted as described in the Materials and Methods (Section 5.5.3) and using expression induction with 100 µM IPTG. The protein was purified from the cell lysate using His-Trap HP columns (GE Healthcare) and eluted with a gradient of imidazole. The resulting fractions were analysed by SDS-PAGE (Figure 2.4).

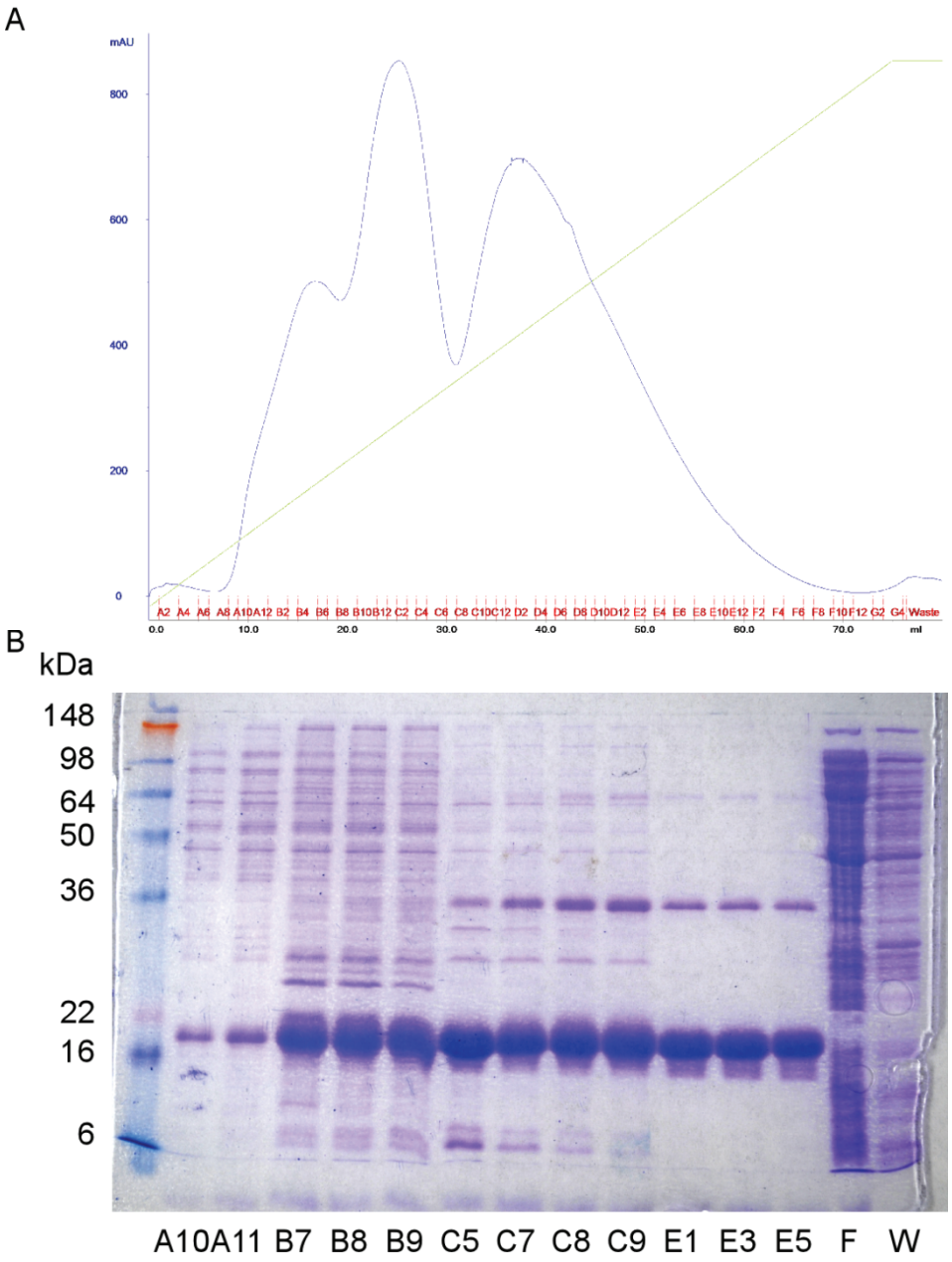

Figure 2.4 Purification of YuaB-His_6 construct. (**A**) FPLC trace of purification. The blue line represents A_{280} of the purified sample, the Y axis is the A_{280} scale in arbitrary units. The green line represents the imidazole gradient from 25 mM to 500 mM. The collected fractions are indicated on the X axis. (**B**) SDS-PAGE analysis of the selected fractions collected during chromatography. The first lane is the protein size marker. The relative protein sizes are indicated. Fraction numbers are indicated below lanes accordingly to the X axis in (**A**). F is the flowthrough fraction of unbound protein. W is the column wash of the unbound sample.

The size of YuaB-His_6 protein after purification was calculated at 17.6 kDa. After purification a predominant band running at the size corresponding to ~20 kDa was found and was subjected to gel filtration using Superdex75 gel filtration column (Figure 2.5).

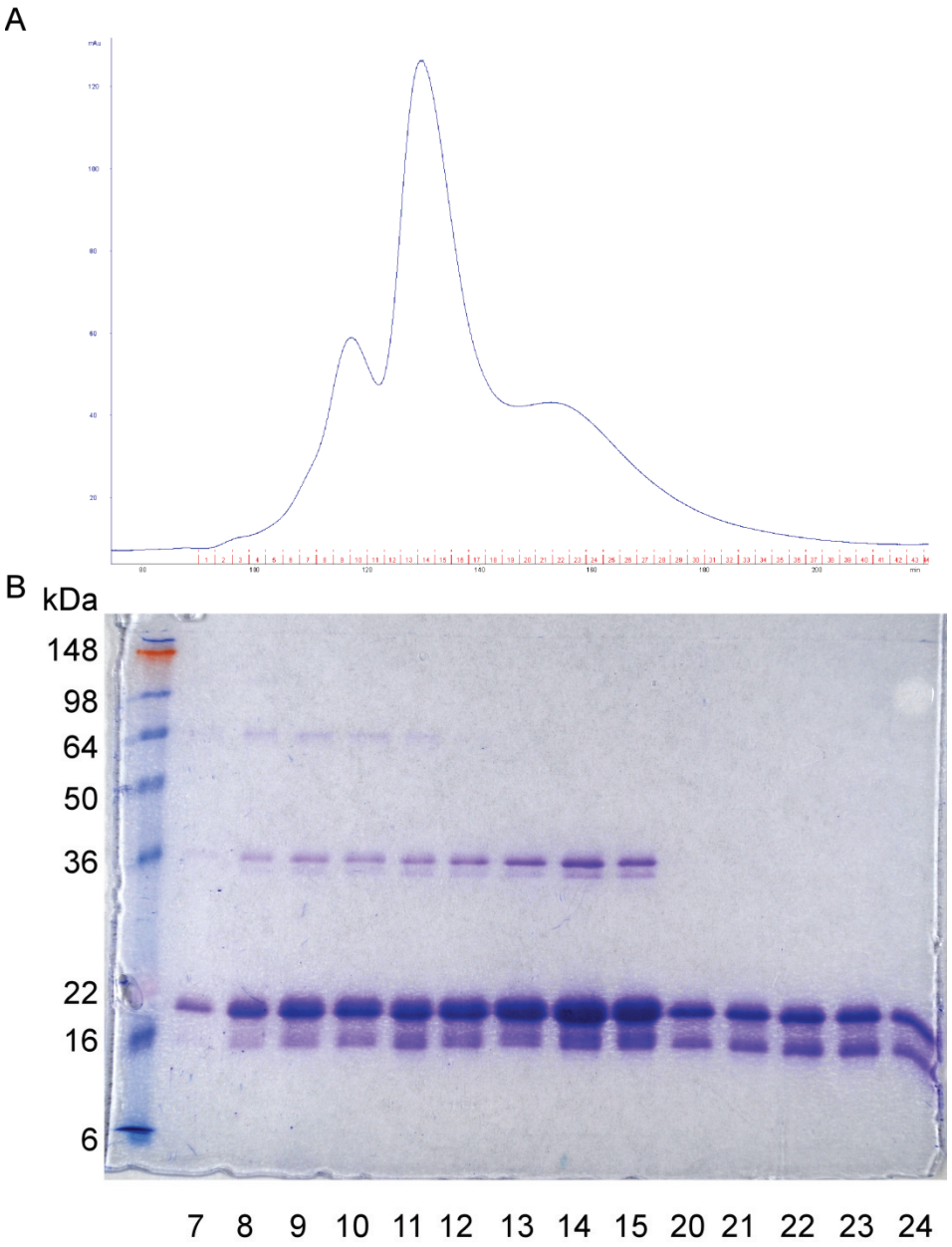

Figure 2.5 Size exclusion chromatography of YuaB-His_6 construct. (**A**) FPLC trace of the chromatography. The blue line represents A_{280} of the sample, the Y axis is the A_{280} scale in arbitrary units. The collected fractions are indicated on the X axis. (**B**) SDS-PAGE analysis of the selected fractions collected during chromatography. The first lane is the protein size marker. The relative protein sizes are indicated. Fraction numbers are indicated below lanes accordingly to the X axis in (**A**).

The predominant peak in the gel filtration trace (Figure 2.5, fractions 12 – 20) contained the protein seen on the SDS-PAGE following affinity chromatography, and a band corresponding to dimer size of the purified protein. However, and in addition to the bands discussed above, a smaller band with size corresponding to ~16 kDa was found as well. It was assumed that the smaller band that was not seen after affinity

chromatography, is a degradation product of YuaB. To confirm this, both bands were excised from the gel and identified using liquid chromatography – mass spectrometry (LC-MS-MS). Indeed both were identified as YuaB, therefore the samples of pure protein were used to raise polyclonal antibodies against YuaB in rabbits.

2.3.2. Identification of instability site in YuaB and purification optimisation

The instability of the YuaB-His_6 construct made it unsuitable for crystallisation; therefore the site of instability was identified. The small change of the protein mass indicated that only a small portion of the overall protein was lost. The impacted terminus of the protein was identified by sequencing of the N-terminus by Edman's degradation. The lower molecular mass product was excised and submitted for sequencing. This revealed an intact sequence of the first 6 amino acids of the construct. It was therefore concluded that the instability occurs at the C-terminus and could be caused by the presence of the His_6 tag, which was not cleaved off during purification. To eliminate the option that the instability of the protein was caused by C-terminal fusion; a construct of YuaB with N-terminus fused to glutathione transferase S (GST) was constructed in the expression vector pNW619. The fusion protein was purified using glutathione-conjugated beads and the GST was cleaved off from YuaB. The proteins were separated by gel filtration. However, disappointingly the separation of YuaB into two forms was seen on the gel (Figure 2.6).

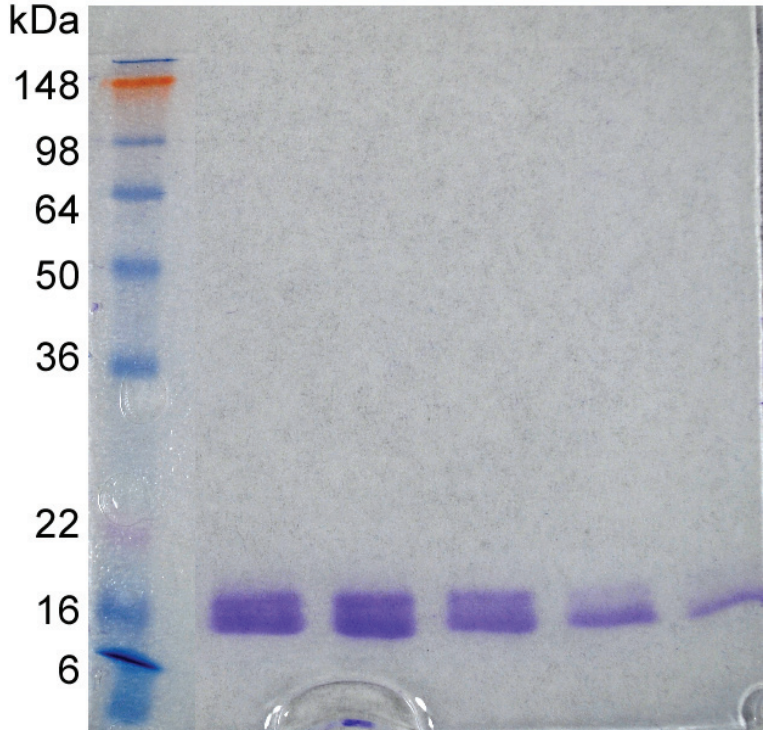

Figure 2.6 YuaB cleaved off from GST is unstable. Examples of fractions of purified YuaB after cleavage of GST and size exclusion chromatography. The first lane is the protein size marker. The relative protein sizes are indicated. The following lanes represent degradation of YuaB during chromatography.

Due to the fact that the C-terminus of YuaB became unstable after purification, it was concluded that the instability is caused by the nature of the protein itself. A hypothesis was drawn that the two cysteine residues in positions C_{178} and C_{180} are contributing to the instability of the purified protein. This was confirmed by comparison of size of both forms of the protein by mass spectrometry – time of flight (MS-TOF) analysis. MS-TOF identified the size of the lower molecular mass form to correspond to that of the full construct missing the His_6 and 5 amino acids from the sequence of YuaB itself. Therefore a new construct of $YuaB_{29\text{-}176}$ N-terminally fused to the His_6-GFP tag separated with the tobacco etch virus (TEV) protease site was constructed (pNW632). A His_6 tag was favoured over a GST tag due to possibility of automatisation of the purification process. However, it was found that the His_6-GFP tag cannot be cleaved from YuaB after purification, probably due to inaccessibility of the

cleavage site. At this point further attempts of YuaB purification using His_6 tag was abandoned. Previous attempts of YuaB purification using the GST fusion proved to be successful in obtaining a pure protein. Therefore a stop codon was introduced in the P_{177} position of the YuaB harboured in pNW619 to generate a GST-$YuaB_{29\text{-}176}$ construct in pNW634. The GST-$YuaB_{29\text{-}176}$ fusion was purified using glutathione-conjugated beads and the GST tag was successfully cleaved off using PreScission protease (GE Healthcare) (Figure 2.7) and a pure protein was obtained after size exclusion chromatography to remove the remaining GST contamination (Figure 2.8). The resulting protein remained stable and was used in further proceedings.

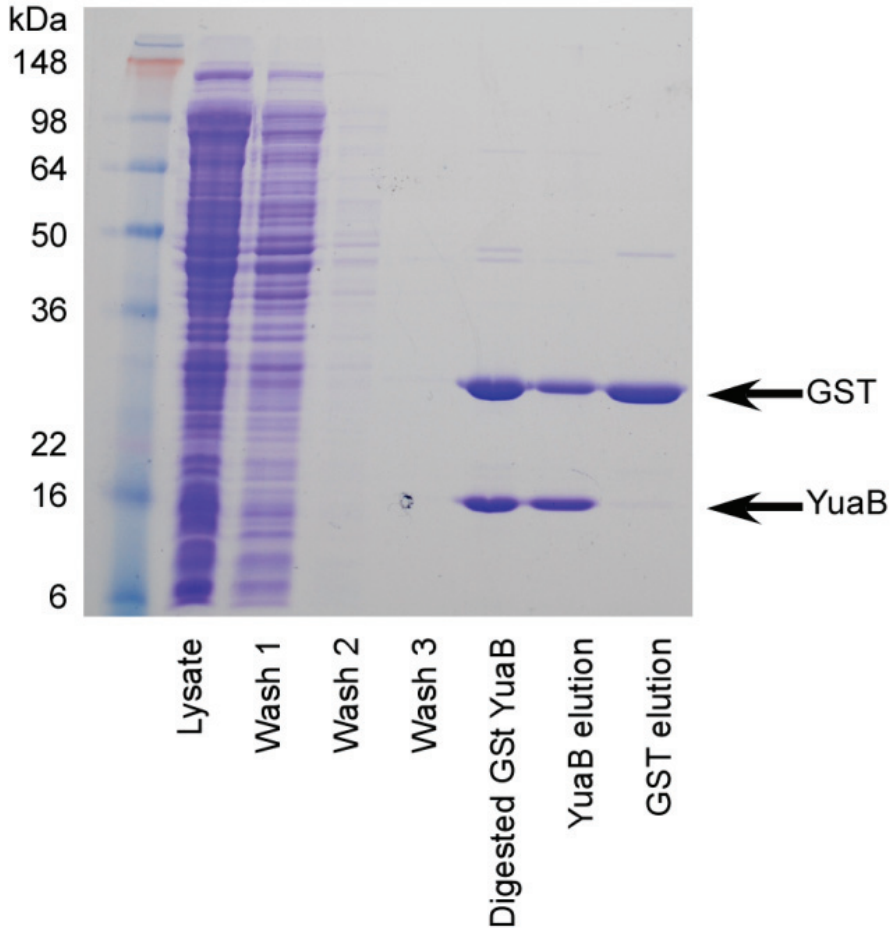

Figure 2.7 SDS-PAGE analysis of fractions after purification and cleavage of GST-$YuaB_{29\text{-}176}$ fusion protein. The first lane is the protein size marker. The relative protein sizes are indicated. The fractions are indicated below lanes. GST and YuaB bands are indicated. The "YuaB elution" fraction was used for size exclusion chromatography.

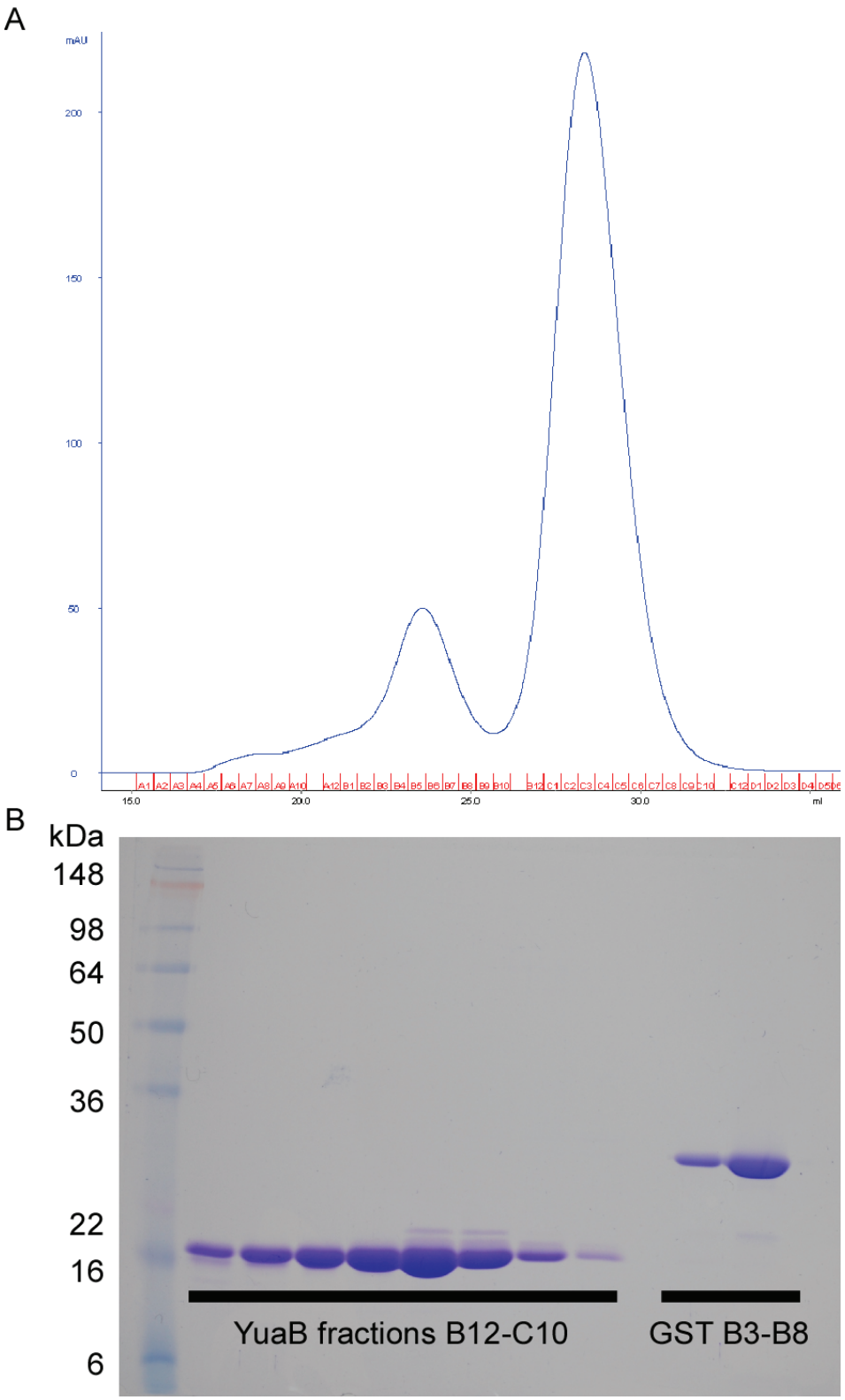

Figure 2.8 Size exclusion chromatography of cleaved GST and $YuaB_{29-176}$ proteins. (**A**) FPLC trace of the chromatography. The blue line represents A_{280} of the sample, the Y axis is the A_{280} scale in arbitrary units. The collected fractions are indicated on the X axis. (**B**) SDS-PAGE analysis of the selected fractions collected during chromatography. The first lane is the protein size marker. The relative protein sizes are indicated. Fraction numbers are indicated below lanes accordingly to the X axis in (**A**).

2.3.3. The purified and analysed variants of YuaB are active in vivo

During optimisation of the recombinant YuaB, to increase the stability of the protein after purification, a 5 amino acid truncation was introduced. To exclude the possibility that the protein purified for crystallography did not represent an active YuaB, a similar truncation was introduced into recombinant YuaB expressed in *B. subtilis.* The activity of YuaB truncated at the C-terminus [$YuaB_{\Delta 172\text{-}181}$ (NRS2957)] in biofilm formation was tested by complementation of the *yuaB* mutant phenotype. The truncated version of YuaB was able to restore the biofilm phenotype to the same levels as the wild type YuaB (Figure 2.9). Therefore it was concluded that the purified YuaB resembles an active protein.

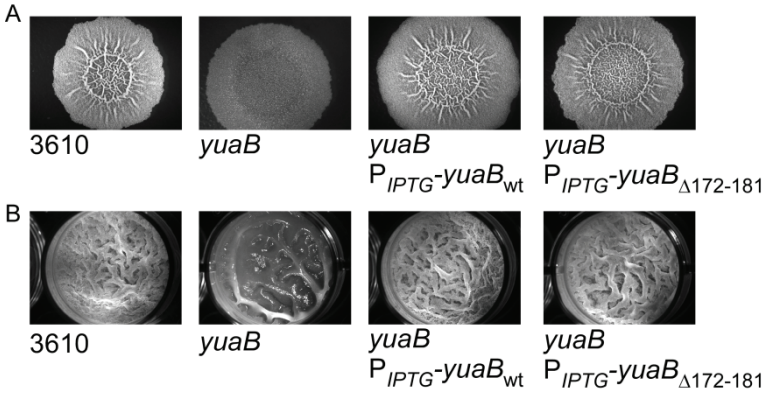

Figure 2.9 The C-terminal 10 amino acid residues of YuaB are not required for YuaB function in the biofilm. Strains shown are wild type (3610), the *yuaB* mutant (NRS2097), the *yuaB* mutant complemented with wild type YuaB (*yuaB*, *amyE*::P_{IPTG}-*yuaB-lacI*; NRS2299) and the *yuaB* mutant complemented with YuaB lacking the C-terminal 10amino acids (*yuaB*, *amyE*::P_{IPTG} -$yuaB_{\Delta 172\text{-}181}$-*lacI;* NRS2957). (**A**) Complex colonies were grown for 48 hours at 30 °C and (**B**) pellicles were grown for 72 hours at 25 °C, all in the presence of 25 µM IPTG.

2.3.4. Attempts to crystallise YuaB

The YuaB purification yield was found to be approximately 5 mg/ml in 50 ml of final purification product obtained from 8 L of bacterial culture (see Materials and Methods). The resulting protein was also found to be very soluble as the maximum concentration obtained was 120 mg/ml of pure YuaB. To optimise crystallisation

conditions for YuaB, a range of protein concentrations was used from 20 to 120 mg/ml. To screen for optimum conditions a range for crystallisation, Crystal Screen, Index, PEG/Ion and Natrix kits (Hampton Scientific) were used. However, none of the conditions tested resulted in precipitation or crystallisation of purified YuaB. As an alternative, Morpheus screen (Molecular Dimensions) was used. Using several conditions included in this screen small two-dimensional crystals were found. An array of conditions with subtle variations in the concentration of each component, including protein concentration, was prepared and tested for improvement in crystallisation. However, larger crystals were not found in any of the customised crystallisation conditions. As the easily accessible and basic procedures for crystallising YuaB were unsuccessful, the protein crystallisation project was handed over to crystallographers Dr George Penmann and Dr Francesco Rao (DVA, College of Life Sciences, Dundee). In retrospect, the difficulties we had in crystallising YuaB are perhaps not surprising in the light of the results to be presented in Chapter 3 and the Discussion.

2.3.5. Purification of anti-YuaB antibody

The final bleed of anti-YuaB antiserum received after immunisation of rabbits with purified YuaB was found to be reactive against multiple proteins from *B. subtilis* (Figure 2.10). To purify the YuaB-specific antibodies from the antiserum, an affinity column with immobilised YuaB, which was used as an antigen for immunisation of rabbits, was prepared according to the protocol obtained from Mr. Ellis Jaffray (RTH, College of Life Sciences, Dundee). The anti-serum was applied to the column and the purified antibody was collected (see Section 5.5.8). The purified antibody was tested for detection of YuaB on cell lysate from *B. subtilis* and was found to be suitable for immuno-detection (Figure 2.10).

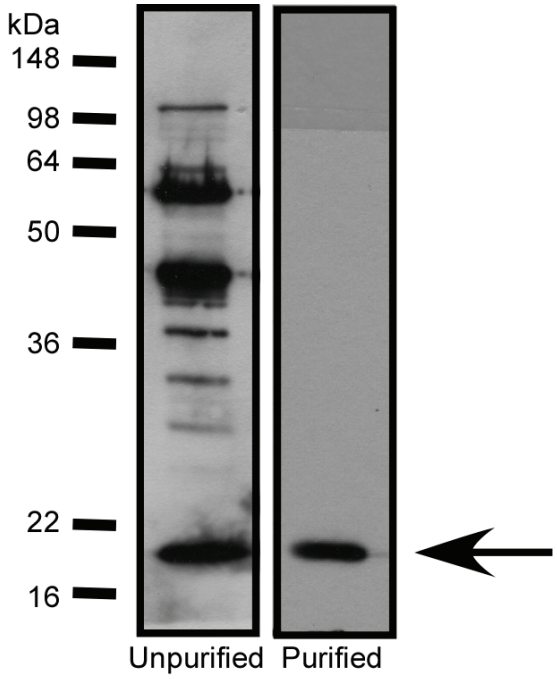

Figure 2.10 Immuno-purified antibody against YuaB detects only YuaB. The lysate from cells extracted from a biofilm was exposed to unpurified (left panel) and purified (right panel) antibodies raised against YuaB. The band of the mass corresponding to YuaB is indicated with an arrow. Relative molecular masses according to a protein standard are indicated.

2.3.6. Purification of TasA for antibody production

To develop a detection method for TasA in the biofilm and cell samples, an anti-TasA antibody was generated. For this purpose an allele of *tasA* lacking the putative signal peptide was fused to *gst* to yield an overexpression vector pNW548. The fusion protein was overexpressed and purified using glutathione beads as described in Materials and Methods (Section 5.5.3.2). The resulting protein was cleaved with PreScission protease to release TasA from the fusion protein, which was subsequently purified using negative binding of cleaved off GST and of the protease to the regenerated glutathione beads which resulted in isolation of pure TasA (Figure 2.11).

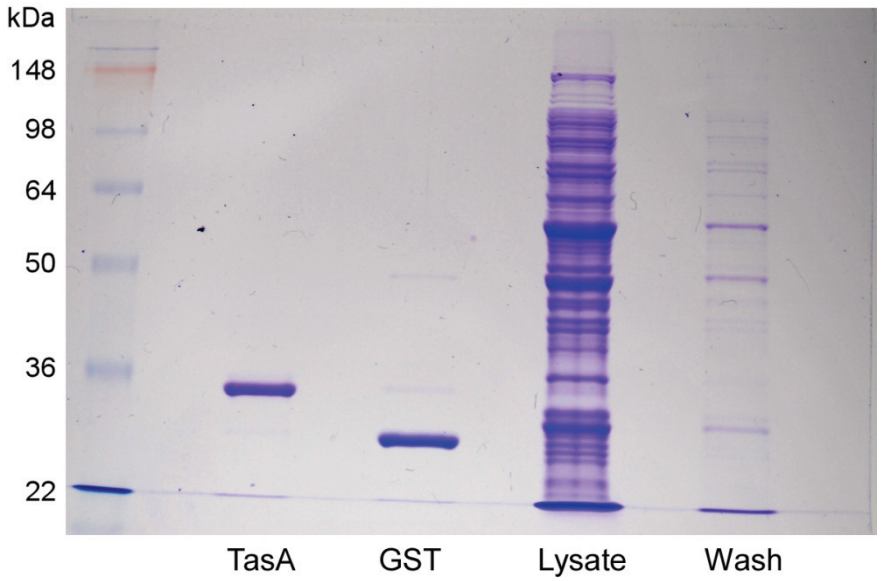

Figure 2.11 TasA purification using GST-TasA fusion. The purity of isolated TasA and GST after enzymatic cleavage was analysed by SDS-PAGE. Lanes with resolved purified proteins as well as the cell lysate and the wash of unbound protein are indicated. The first lane is the protein size marker. The relative protein sizes are indicated.

The purified protein was identified using LC-MS-MS as TasA and was sent for immunisation of rabbits to raise anti-TasA antibodies. The received antiserum was tested for reactivity against TasA and was found to be suitable for use without further purification (Figure 2.12).

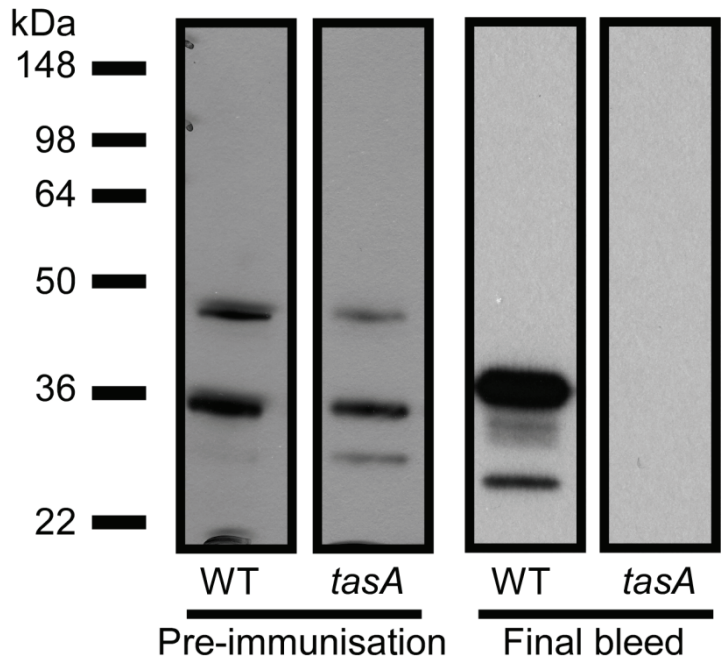

Figure 2.12 The TasA specific antiserum detects TasA in cell lysates. The lysates of wild type and *tasA* mutant cells extracted from biofilms were exposed to antisera samples taken prior to first immunisation and after final bleed of rabbits. Relative molecular masses according to a protein standard are indicated.

2.4.YuaB can be found in the cell wall

2.4.1. Localisation of YuaB in biofilm pellicle by Western blotting

The major protein component of the biofilm matrix, TasA, is secreted to the extracellular matrix during biofilm formation (Branda *et al.*, 2006). During its transport across cell membrane, TasA is processed by a specific signal peptidase SipW and anchored to the cell wall by TapA which allows for the polymerisation of TasA into functional amyloid fibrils (Stover & Driks, 1999c, Branda *et al.*, 2006, Romero *et al.*, 2010, Romero *et al.*, 2011). Similarly to TasA, YuaB was identified as a secreted protein during a secretome-wide study of *B. subtilis* (Antelmann *et al.*, 2001). Additionally, an *in silico* prediction performed during this study using the SignalP programme (Petersen *et al.*, 2011) showed the presence of a signal sequence on the N-terminus of YuaB, directing this protein to the general secretion pathway Sec (Figure 2.15). A signal

peptidase site was detected between residues A_{28} and A_{29} which resulted in an estimate of the molecular mass of the mature YuaB of 16.4 kDa. Based on this prediction, it was hypothesised that YuaB can be secreted to the biofilm matrix where it takes part in the formation and/or stabilisation of a functional biofilm matrix. To test whether YuaB is a novel component of the biofilm matrix, fractionation of biofilm pellicles into growth medium, biofilm matrix and biofilm-enclosed cells was performed and the localisation of YuaB was identified in the individual fractions using Western blot (Figure 2.13) (Branda *et al.*, 2006).

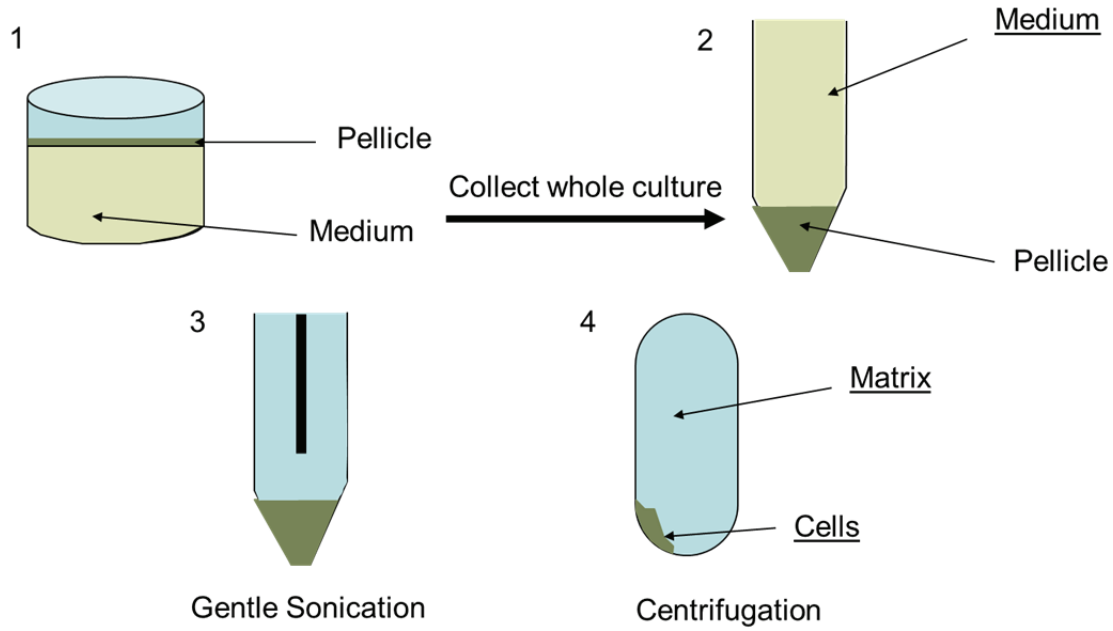

Figure 2.13 Schematic representation of biofilm pellicle fractionation. The entire biofilm culture (1) is collected by centrifugation where the supernatant becomes the isolated growth medium fraction (2). The pellet is subjected to a mild sonication (3) to dissolve the biofilm matrix (4) which can be isolated from the cellular fraction (4). The individual isolated fractions are underlined in appropriate isolation steps.

During immuno-blotting against YuaB, preceded by biofilm fractionation, a band corresponding in size to the mature YuaB was detected exclusively in the fraction representing biofilm-enclosed cells. This band was not found in fractions obtained from biofilm pellicles formed by the *yuaB* strain (NRS2097) and was returned upon complementation of *yuaB* from an ectopically expressed copy of *yuaB* (NRS2299)

(Figure 2.14). To verify if the cells remained intact throughout fractionation procedure, an antibody against membrane-bound ATP synthase subunit A (AtpB) was used (Hahne *et al.*, 2008). The presence of AtpB-specific band only in the cellular fraction confirmed, that the cells did not lyse (Figure 2.14). These results led to the conclusion that YuaB is cell-associated and were in contradiction to the proteomic study during which YuaB was detected in the growth media. However, this could be explained by the fact that the experiments conducted by Antelmann *et al.* (2001) were performed using rich LB media and planktonic growth conditions, whereas the experiments presented here involve usage of minimal defined media and biofilm formation conditions.

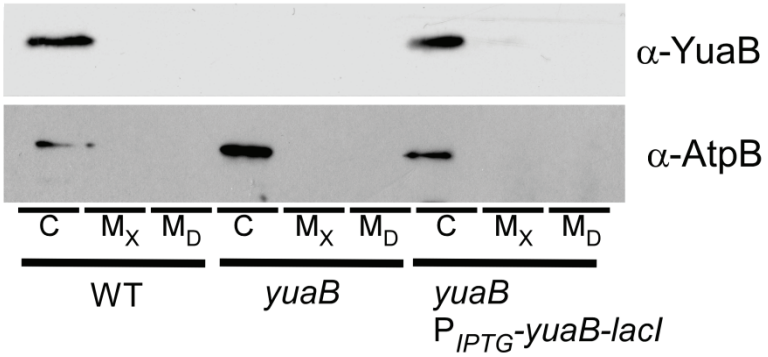

Figure 2.14 YuaB is associated with biofilm enclosed cells. Wild type (3610), *yuaB* mutant (NRS2097) and complemented strain *yuaB* + *amyE*::$P_{hy\text{-}spank}$-*yuaB-lacI* (NRS2299) pellicles were separated into cell (C), matrix (M_X) and growth medium (M_D) fractions. Localisation of YuaB was determined by Western blotting.

2.4.2. The N-terminus of YuaB is a functional signal peptide

The results of YuaB localisation by Western blotting led to the hypothesis that during biofilm formation YuaB is exported from the cell upon its synthesis but remains in the close vicinity of the cell, perhaps anchored in the cell wall. To test this, a series of experiments was designed to firstly confirm that YuaB is indeed a secreted protein and secondly to verify localisation of YuaB to the cell wall. To test whether YuaB has to be exported from the cell to contribute to biofilm formation, a signal peptide swapping experiment was designed.

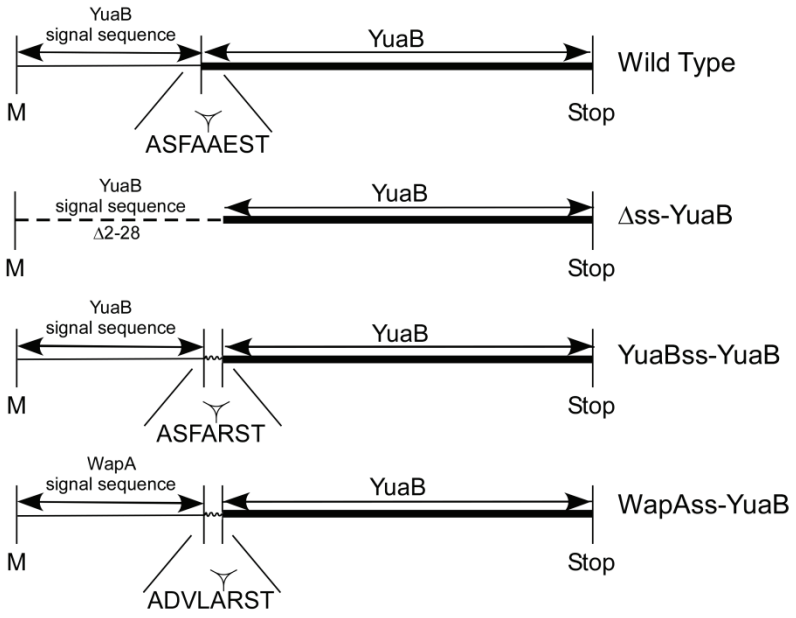

Figure 2.15 Schematics of constructs used to test if YuaB is a secreted protein are presented. 'M' represents the methionine translation initiation codon; the inverted arrow represents the predicted signal peptide cleavage site beneath which the amino acid sequence surrounding the site is provided; the YuaB mature region is indicated by a thick line and the signal sequences are indicated as appropriate. For full details of the plasmid construction see Materials and Methods.

A variant of YuaB was designed such that the DNA fragment encoding the putative signal peptide predicted by SignalP was removed (Figure 2.15). Ectopic expression of the truncated YuaB in the *yuaB* deletion background (NRS2446) was not sufficient to restore the wild type biofilm morphology, unlike when the wild type YuaB is expressed (NRS2299) (compare Figure 2.17A and B). However, the version of YuaB lacking the signal peptide can no longer be detected by Western blot, probably due to proteolytic activity in the cytoplasm (Figure 2.16).

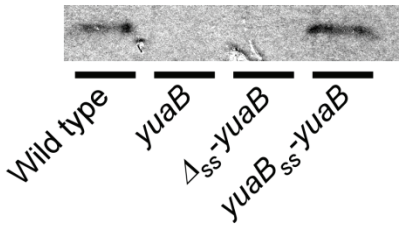

Figure 2.16 YuaB lacking a signal peptide is not stable. Proteins were extracted from complex colonies of the wild type (3610), *yuaB* mutant (NRS2097), *yuaB* mutant expressing an allele of *yuaB* lacking the signal peptide (NRS2446) and the reconstructed *yuaB* (NRS2447).

To confirm that the signal peptide was the element required for the stability and export of YuaB, the DNA fragment encoding the YuaB signal peptide was subcloned to the vaiant of YuaB containing the mature fragment discussed above (NRS2447). The reconstruction of YuaB resulted in a two amino acid change in the vicinity to the signal peptidase cleavage site (Figure 2.15). Nonetheless, the signal peptidase cleavage site was still recognisable by SignalP in the sequence of recombinant YuaB. Furthermore, upon expression of the reconstructed recombinant YuaB in the genetic background of the *yuaB* mutant (NRS2447), the wild type biofilm morphology was restored (Figure 2.17C) and the corresponding band was detected by Western blot (Figure 2.16). To verify that the rescue of the wild type phenotype by the reconstructed YuaB is an effect of YuaB being exported from the cell, a chimeric protein was designed in which the DNA encoding the predicted signal peptide was exchanged to the DNA of signal sequence from a well characterised cell wall protein WapA (Foster, 1993) (Figure 2.15). The chimeric WapA-YuaB protein (NRS2448) was able to restore biofilm formation to the *yuaB* mutant with the same efficiency as the wild type YuaB (Figure 2.17D). In conclusion, YuaB is a secreted protein that contributes to biofilm formation after its export from the cytoplasm.

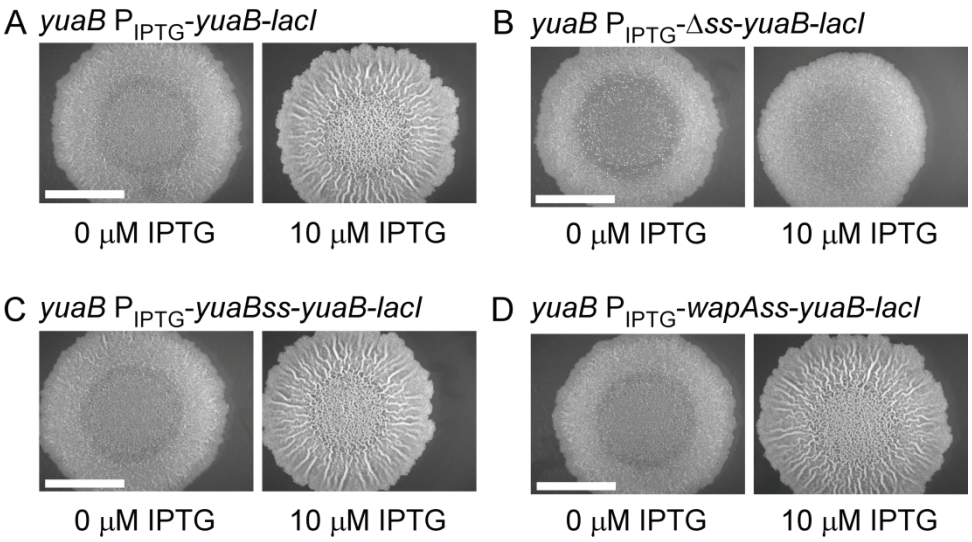

Figure 2.17 YuaB contains a functional signal peptide. Representative images of biofilms formed after 48 hours incubation at 37 °C on solidified MSgg medium, in the presence or absence of 10 μM IPTG as indicated, by the yuaB mutant carrying at the *amyE* locus under the control of the IPTG inducible promoter $P_{hy\text{-}spank}$ (**A**) wild type *yuaB* allele (NRS2299), (**B**) an allele of *yuaB* lacking the N-terminal signal sequence (NRS2446); (**C**) a recombinant *yuaB* signal sequence-*yuaB* construct (NRS2447); and (**D**) a *wapA* signal sequence-*yuaB* recombinant protein (NRS2448). Scale bars are 1cm.

The data discussed above indicate that YuaB is a protein that has to be secreted from the cytoplasm during biofilm formation, but does not leave the immediate vicinity of the cell. Furthermore, YuaB contains no recurring transmembrane domains and the predicted signal sequence cleavage site was assigned a high prediction score by SignalP software which makes it unlikely to be a membrane protein. To test if YuaB is localised to the cell wall after being secreted from the cytoplasm, the cells extracted from biofilm pellicles were subjected to washes with high molarity lithium chloride. Lithium chloride wash of whole cells is a method established for isolation of non-covalently bound cell wall proteins. The method was initially used for preparation of active autolysins from *B. subtilis* cells and was shown not to affect the integrity of cell membrane (Brown, 1973). The fraction of cell wall proteins obtained after cell washes was analysed for presence of YuaB by Western blot and compared to the whole cell extracts. Strong YuaB bands were detected in both fractions obtained from the wild type cells (Figure 2.18).

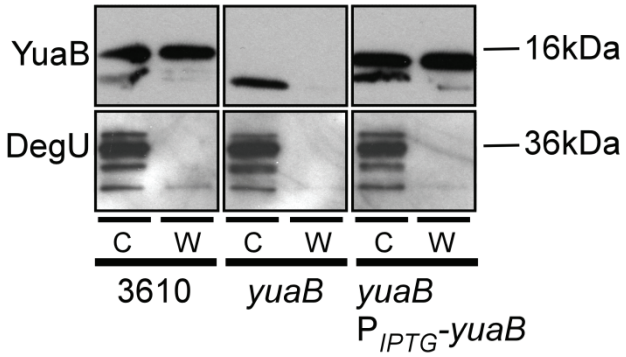

Figure 2.18 YuaB is non-covalently bound to the cell wall. Cells from wild type (3610), *yuaB* mutant (NRS2097) and complemented strain *yuaB + amyE::*$P_{hy\text{-}spank}$*-yuaB-lacI* (NRS2299) pellicles were extracted and subjected to a lithium chloride wash to isolate proteins non-covalently bound to the cell wall. Localisation of YuaB was determined by Western Blot. YuaB was detected in both cellular (C) and cell wall wash (W) fractions, whereas the cytoplasmic response regulator DegU could be detected only in the cytoplasmic fraction. Protein sizes are indicated by size markers.

Similarly to the observations from the biofilm fractionation, no band corresponding in mass to processed YuaB was found in the fractions prepared from the *yuaB* mutant and the bands were present in the fractions prepared from the *yuaB* mutant complemented with an ectopic copy of *yuaB*. In this experiment cell lysis was controlled for using an antibody against the cytoplasmic response regulator DegU (Msadek *et al.*, 1990). In all cases DegU was detected at equal levels exclusively in the fractions representing cytoplasm but not in the cell wall washes (Figure 2.18).

2.4.3. Localisation of YuaB in biofilm cells by transmission electron microscopy

To confirm the finding that YuaB is localised to the cell wall of the cells growing in a biofilm, a transmission electron microscopy (TEM) linked with immuno-gold labelling of YuaB approach was utilised. The cells extracted from 24 h old biofilm cultures were frozen and cross-sectioned. The resulting ribbons of sectioned cells were attached to TEM grids, immuno-labelled with YuaB-specific antibody and the labelling was followed with incubation with gold-conjugated protein A. As the result, the YuaB

protein labelled with an antibody is visible as a dark spot on TEM micrographs. It should be noted that this method requires usage of cells that do not synthesise EPS due to the fact the EPS is an electron-thick material obscuring images obtained using TEM (Romero *et al.*, 2010). Therefore, all strains used for purpose of this analysis carry an *eps(A-O)::tet* insertion. For the YuaB-positive strain (NRS2450) gold particles representing YuaB labelling were associated with the cell wall (Figure 2.19A). The abundance of detected labelling was low, but this is in line with previous reports indicating that the transcription from the *yuaB* promoter is relatively low [Section 3.2.3 and (Kovacs & Kuipers, 2011)]. Furthermore, the gold labelling associated with the cell wall was not found in the YuaB-negative control strain (NRS2452) (Figure 2.19B).

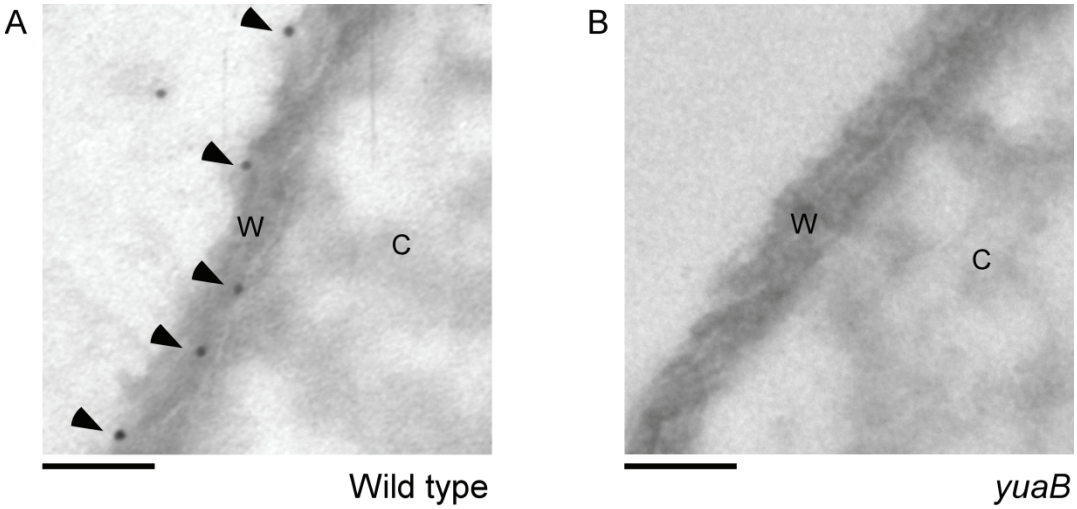

Figure 2.19 Immuno-gold labelled YuaB in the cell wall (TEM imaging). The cells "wild type" for *yuaB* (NRS2450) (**A**) and mutant for yuaB (NRS2452) (**B**) were collected from early stage biofilms. YuaB was visualised by immuno-gold labelling and can be seen as dark spots indicated by the arrow heads. The images show fragments of cell wall (W) and cytoplasm (C) of representative cells of each strain. The scale bars represent 0.1µm.

The quantification of YuaB foci was performed using an interactive software tool written in Matlab which accessed images stored in OMERO via the OMERO API (Allan *et al.*, 2012). Points labelled as 'cell wall', 'cytoplasm' or 'extracellular space' were marked as appropriate on each image where gold particles indicated foci of YuaB.

Another point labelled as 'cell' marked each bacterium in an image. The number of individual points with each label was automatically counted across data sets of images. The number of points each group of labels was normalised to the number of cells in each data set. The foci assigned to cytoplasmic and cell wall groups were compared for the YuaB-positive strain (NRS2450). The majority of foci in the YuaB-positive strain was associated with the cell wall rather than the cytoplasm ($P<0.001$). The comparison was repeated for quantified data of foci associated with the cell wall and cytoplasm of the YuaB-negative strain (NRS2452). No statistically significant difference was found ($P=0.643$). The number of foci associated with the cell wall of the YuaB-positive strain was significantly higher than that of the YuaB-negative strain ($P<0.001$). The number of foci observed in the extracellular space was not strain-dependent ($P=0.077$) and was accounted to non-specific labelling.

In summary, the N-terminus of the primary amino acid sequence of YuaB constitutes a functional signal peptide which is required for the activity of YuaB. However, in the biofilm pellicle mode of biofilm formation YuaB remains closely associated with the cells extracted from the biofilm. The TEM observations confirm that YuaB is being secreted from the cytoplasm, but the majority of YuaB can be found in association with the peptidoglycan; therefore it was concluded that YuaB is a cell wall-associated protein.

2.5. Overproduction of TasA and EPS cannot compensate for the absence of YuaB

Expression of *tapA* and *eps* operons encoding proteins required for assembly of the biofilm matrix is repressed by two regulatory proteins, AbrB and SinR (Hamon *et al.*, 2004, Kearns *et al.*, 2005). The alleviation of the AbrB and SinR-mediated repression is dependent on the Spo0A and SlrR proteins (Hamon & Lazazzera, 2001, Chai *et al.*, 2010) and results in a bimodal expression of *tapA* and *eps* operons in the biofilm culture (Chai *et al.*, 2008). Additionally deletion of either *abrB* or *sinR* leads to overproduction of the TasA amyloid fibres and the EPS (Hamon *et al.*, 2004, Kearns *et al.*, 2005, Branda *et al.*, 2006). It was tested if overproduction of TasA amyloid fibres and EPS is sufficient to overcome the biofilm defect caused by the absence of YuaB. This was achieved by uncoupling the expression of *tapA* and *eps* operons from AbrB and SinR control. For this purpose *yuaB* was deleted from the *abrB* (NRS2276) and *sinIR* (NRS2291) strain backgrounds. It was predicted that if YuaB was essential for biofilm formation to proceed, a reduction in biofilm architecture would be observed in the double mutant strains. Consistent with this assumption, deletion of *yuaB* from the *abrB* mutant (NRS2276) led to a reduction in the complexity of the biofilm architecture exhibited by both the pellicle and the colony. This phenotype could be specifically complemented by introduction of the *amyE*::$P_{hy\text{-}spank}$-*yuaB*-*lacI* construct in the presence of the inducer IPTG (NRS2748) (Figure 2.20A). Deletion of *yuaB* from the *sinIR* mutant background (NRS2291) also reduced the complexity of the pellicle formed. The raised ridges and furrows characteristic of the absence of SinR did not develop. Introduction of the ectopically expressed *yuaB* under an IPTG-inducible promoter $P_{hy\text{-}spank}$ to the *yuaB sinIR* strain restored the furrows and raised ridges to the pellicle

formed in the presence of IPTG (NRS2749) (Figure 2.20D). On solid media the alteration in morphology between the *yuaB sinIR* (NRS2291) and *sinIR* (DS93) strains was apparent but was more subtle, than when the *yuaB abrB* double mutant and its parental *abrB* mutant strain were compared (Figure 2.21(i) D and F). This difference presumably reflects the difference in the level of EPS and TasA produced in the *abrB* (Hamon *et al.*, 2004, Chu *et al.*, 2008) and *sinIR* (Chu *et al.*, 2006) mutant backgrounds.

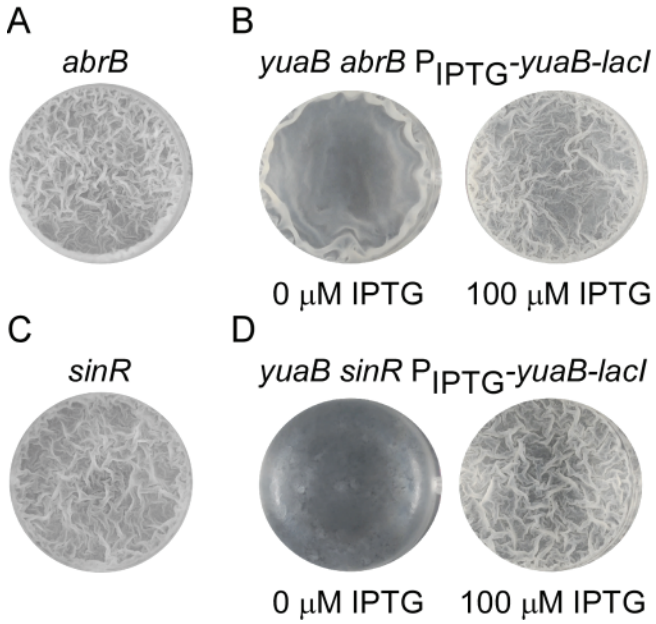

Figure 2.20 Overproduction of TasA and the exopolysaccharide cannot compensate for the absence of YuaB. Representative images of the pellicle formed after 24 hours incubation at 37 °C in MSgg by matrix overproducing strains (**A**) *abrB* (NRS1647) and (**C**) *sinIR* (DS93) are presented. The representative pellicles formed after 24 hours incubation at 37 °C in MSgg in the presence and absence of 100 μM IPTG are shown for (**B**) *yuaB::cat abrB amyE*::P$_{hy\text{-}spank}$-*yuaB-lacI* (NRS2748) and (**D**) *yuaB::cat sinIR amyE*::P$_{hy\text{-}spank}$-*yuaB-lacI* (NRS2749).

To rule out the possibility that the reduced complexity of the *yuaB abrB* and *yuaB sinIR* strains was somehow linked to a reduction in expression from either the *eps* or *tapA* promoters, the level of transcription was determined at the single cell level by flow cytometry using a P$_{epsA}$-*gfp* and a P$_{tapA}$-*gfp* transcriptional reporter fusion. It is known that deletion of either *abrB* or *sinR* increases transcription from the *epsA* and *tapA* promoters and this is manifested by an increase in the number of cells that

transcribe these operons and the level of expression (Lopez *et al.*, 2009b). It was found that deletion of *yuaB* did not negatively influence the transcription profile from either the *epsA* promoter in the absence of AbrB (NRS2302) where there were 40% ±10% of GFP-positive cells compared to 44% ±9% (P=0.676) in the *abrB* mutant mother strain (NRS2296) or *tapA* promoter (NRS2426) where 54% ±6% was expressing GFP in comparison to 66% ±4% (P=0.098) in the *abrB* mutant (NRS2418) (Figure 2.21(iii) and (iv)). Similarly expression of the *epsA* operon was observed in 82% ±8% of cells of the *yuaB sinIR* double mutant (NRS2428) in comparison to 88% ±6% (p=0.374) in the *sinIR* mutant (NRS2427) and 68% ±17% of *gfp* expressing cells from *tapA* promoter were detected in the *yuaB sinIR* double mutant (NRS2430) and 76% ±21% (p=0.672) in the *sinIR* single mutant (NRS2429) (Figure 2.21(iii) and (iv)). Therefore the loss of complexity of biofilm formed by the *yuaB abrB* and *yuaB sinIR* mutant strains was not a consequence of a reduction in transcription of the *eps* and *tapA* operons. The simplest explanation for these findings is that the YuaB is required in addition to EPS and TasA to allow biofilm maturation.

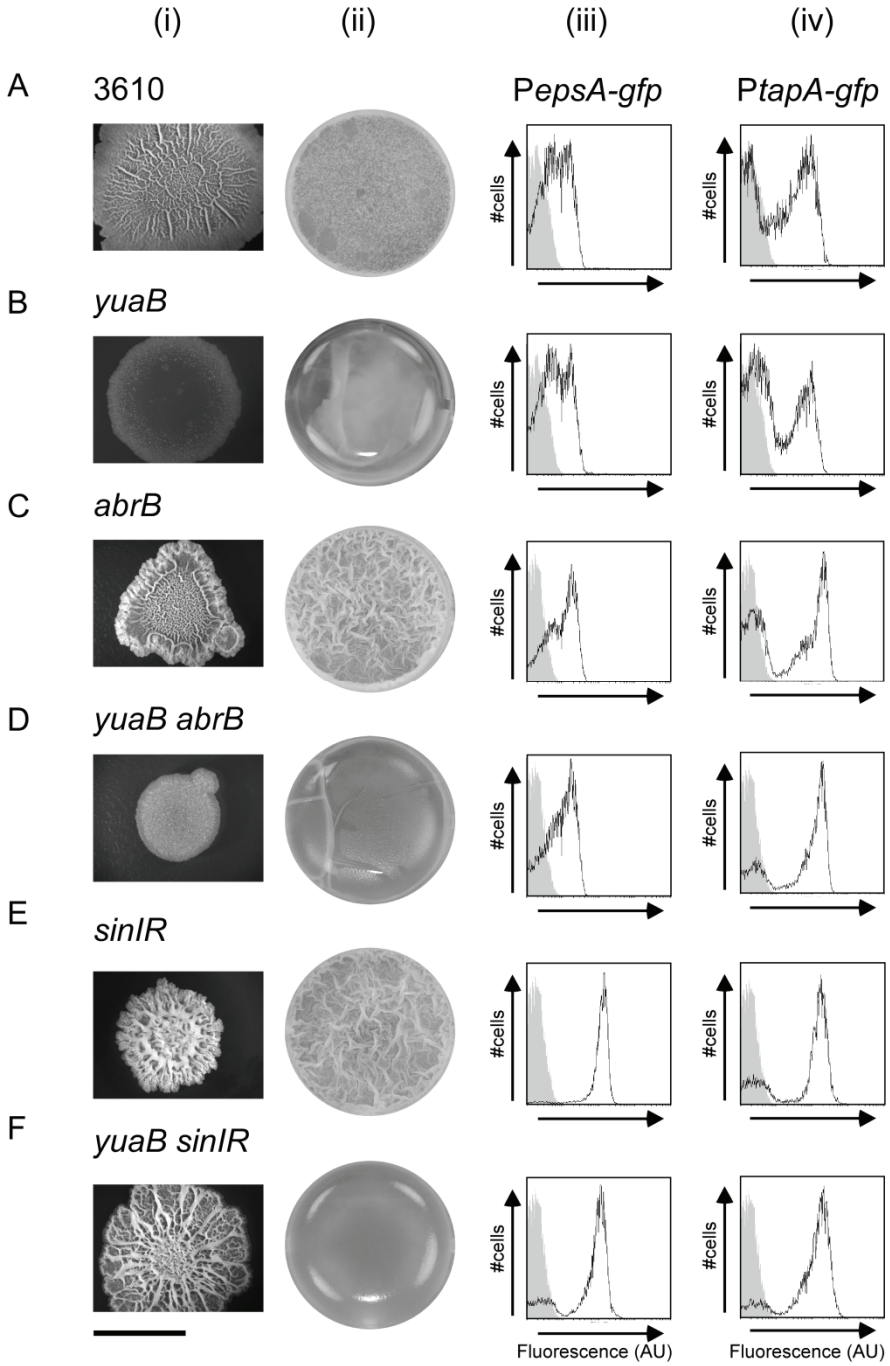

Figure 2.21 YuaB does not affect transcription from the *epsA* and *tapA* promoters. (**A**) Wild type (3610), (**B**) *yuaB* (NRS2097); (**C**) *abrB* (NRS1647); (**D**) *yuaB abrB* (NRS2276); (**E**) *sinIR* (DS93); (F) *yuaB sinIR* (NRS2291). In column (**i**) representative images of colony morphology after 48 hours incubation at 37 °C are shown. In column (**ii**) representative images of the pellicle formed after 24 hours incubation at 37 °C in MSgg are shown. The scale bar is 1 cm. The graphs provide representative flow cytometry data where the level of expression from the *epsA* promoter (column **iii**) and *tapA* promoter (column **iv**) was measured after 18 hours incubation on MSgg plates. (See materials and methods for full details). The x-axis of each graph represents the level of fluorescence in arbitrary units (AU) in the logarithmic scale. The y-axis of each graph represents the number of cells. For each graph the fluorescence profile generated by the non-fluorescent control strain 3610 is shown as the light grey peak.

2.6. YuaB benefits all members of the biofilm

The data presented above show that YuaB is a secreted protein that remains associated with the cell wall via non-covalent binding, is not affecting regulation of the known biofilm matrix components and its absence cannot be overcame by TasA and EPS alone. Basing on these findings, a hypothesis was drawn that YuaB, TasA and EPS are all needed for biofilm maturation. As products of genes expressed in a bimodal fashion, TasA and EPS are synthesised only by a subpopulation of cells in the biofilm (Chai *et al.*, 2008). Branda *et al.* (2006) have shown that upon secretion into the biofilm matrix, TasA and EPS are shared by all cells in the community (Figure 2.22A). To establish if the functionality of YuaB could also be shared within the biofilm community, despite being localised to the cell wall and expressed by all cells in the biofilm [see Section 3.2.3 and (Kovacs & Kuipers, 2011)], a following approach was taken. A strain carrying mutations in the *eps* operon and the *tasA* gene (NRS2451), therefore producing YuaB but not the biofilm matrix components, and a strain unable to produce YuaB (NRS2097), but supplying EPS and TasA fibres to the community, were grown in a co-culture. A mature biofilm, as depicted by complex architecture, was observed to form when the co-culture was grown on solid media (Figure 2.22E). The specificity of the biofilm complexity rescue due to YuaB was tested by co-culturing the *yuaB* mutant with a *tasA eps yuaB* triple mutant (NRS2453). The resulting biofilm exhibited morphology identical to that of a pure *yuaB* mutant (NRS2097) culture (Figure 2.22F).

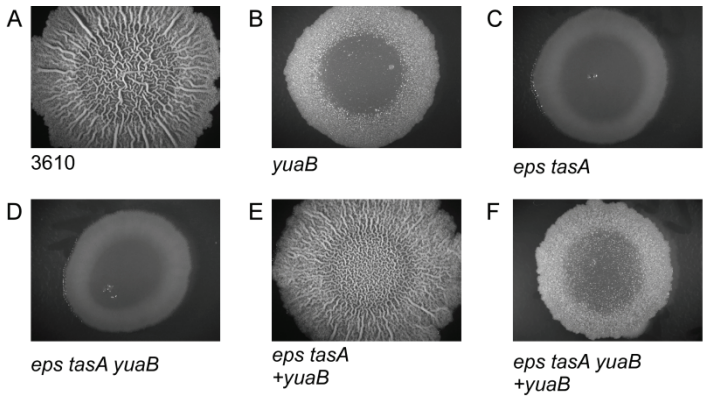

Figure 2.22 Wild type biofilm formation can be restored on co-culture. Representative images of colony morphology after 48 hours incubation at 37 ^{o}C and pellicles after 96 hours incubation at 25 ^{o}C are shown. (**A**) wild type (3610); (**B**) *yuaB* (NRS2097); (**C**) *eps tasA* (NRS2451); (**D**) *eps tasA yuaB* (NRS2453); (**E**) *eps tasA* (NRS2451) co cultured with the *yuaB* mutant (NRS2097); (**F**) *eps tasA yuaB* (NRS2453) co-cultured with the *yuaB* mutant (NRS2097).

The maturity of the biofilm formed was confirmed by assessing the sporulation frequency of the co-cultured *yuaB* (NRS2097) strain with the *tasA eps* double mutant (NRS2451) and *tasA eps yuaB* triple mutant (NRS2453). The sporulation rate of the *yuaB* and *tasA eps* co-culture has reached 82% ±8% which is comparable to the sporulation rate observed for the wild type strain (81% ±3%, section 2.2) (Figure 2.23A). The sporulation rate of the co-culture of the *yuaB* strain to the triple mutant was 20% ±8%. To further verify if the biofilm after co-culture was composed of equal numbers of the *yuaB* and *eps tasA* strain cells, the experiment was repeated where the *yuaB* mutant (NRS2097) was replaced with a *yuaB* mutant constitutively expressing *gfp* (NRS2417). The morphology of the biofilm from co-culture of the *tasA eps* (NRS2451) strain and *yuaB gfp*$^{+}$ (NRS2417) was identical to that seen previously. The cells were extracted from the complex colony after 30h incubation and the ratio of fluorescent to non-fluorescent cells was calculated by flow cytometry (Figure 2.23B). The mature biofilm co-culture was composed of 52% of fluorescent bacteria confirming even growth of strains in the biofilm. Additionally the extracted members of the co-culture were enumerated using antibiotic resistances associated with mutations carried by

each of the strains. The strain to strain ratio in the co-culture of the *tasA eps* mutant (NRS2451) with the *yuaB* mutant (NRS2097) was 0.67 and the ratio of co-culture of the *yuaB tasA eps* mutant (NRS2453) with the *yuaB* mutant (NRS2097) was 0.63.

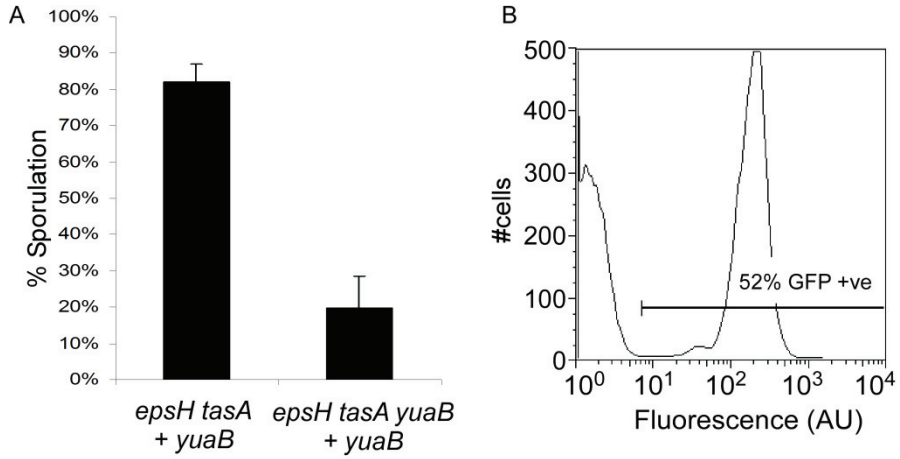

Figure 2.23 The mature biofilm is restored if YuaB is synthesised by 50% of the population. (**A**) Sporulation ratio, representing the maturity of the biofilm, in a co-culture of the *tasA eps* (NRS2450) mutant and the *yuaB* (NRS2097) mutant in comparison to the co-culture deficient in YuaB (NRS2453 with NRS2097). (**B**) Flow cytometry of the *eps tasA* strain (NRS2451) co-cultured with the *yuaB* GFP positive strain (NRS2417) after 30 hours incubation on solid media at 37^{o}C. The percentage of GFP-positive cells is indicated and represents the number of *yuaB* cells in the biofilm.

Interestingly, when the co-culture experiment was repeated in the biofilm pellicle growth conditions, the complementation capabilities of mixed cultures were lower (Figure 2.24E). It was assumed, that this can be caused by a reduced concentration of YuaB in the co-culture in comparison to a pure culture of a wild type strain. This would be caused by the fact that *yuaB* is naturally expressed by all cells in the biofilm [Section 3.2.3 and (Kovacs & Kuipers, 2011)], not a subset of cells as it the case with *tapA* and *eps* operons. Therefore a mixed culture of cells expressing *yuaB* and those that do not would result in a 2-fold decrease in YuaB concentration per cell in the culture. To compensate for this, a strain was constructed where an additional copy of a complete *yuaB* gene including the promoter region was inserted into a non-essential locus *amyE* in a *tasA eps(A-O)* double mutant (NRS2980). This synthetic

strain, when grown in a monoculture, exhibited a phenotype identical to that seen in a previously used *tasA eps(A-O)* mutant (NRS2450). When the synthetic strain expressing additional copy of the *yuaB* gene (NRS2980) was added to the *yuaB* mutant (NRS2097) in a co-culture, the resulting biofilm phenotype was an intermediate between a wild type and that of a *yuaB* mutant monoculture (Figure 2.24E).

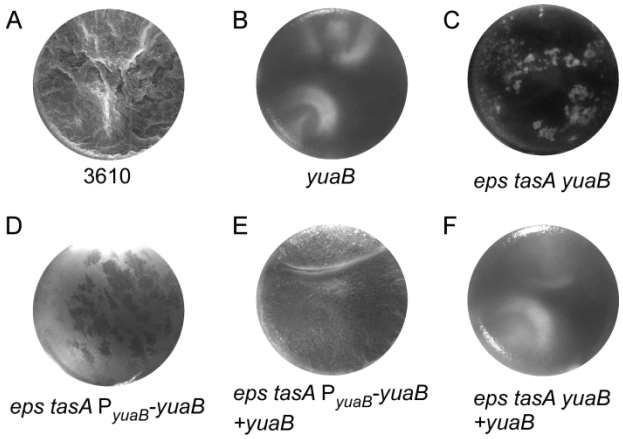

Figure 2.24 Wild type biofilm formation can be partially restored on co-culture in pellicle biofilms. Representative images of pellicles after 96 hours incubation at 25°C are shown. (**A**) wild type (3610); (**B**); *yuaB* (NRS2097); (C) *eps tasA yuaB* (NRS2453); (**D**) *eps tasA* P_{yuaB}-*yuaB* (NRS2980); (E) *eps tasA* P_{yuaB}-*yuaB* (NRS2980) co cultured with the *yuaB* mutant (NRS2097); (**F**) *eps tasA yuaB* (NRS2453) co-cultured with the *yuaB* mutant (NRS2097).

This experiment was interpreted so that in a biofilm pellicle culture the effects of YuaB can be shared in the culture, as a YuaB-specific effect on biofilm was observed, but the effects are not as strong as those seen in a complex colony. A potential explanation was drawn, that this might be caused by differences in the cell density and packaging of cells between the pellicle and complex colony. Specifically, the denser packaging of cells in a complex colony would allow for better interaction between YuaB contained in cell walls of some cells with the cells that do not express YuaB. Further experiments described in the following sections of this thesis allowed for better understanding of this mechanism. These are outlined in the Section 3.2 and the Discussion.

2.7. YuaB does not affect production of EPS or TasA

YuaB was clearly shown to be needed for biofilm formation and its absence cannot be compensated for by overproduction of the components of the biofilm matrix, namely TasA fibres and the EPS. To start elucidating the mechanism of YuaB function, two hypotheses were drawn. First, that YuaB influenced EPS biosynthesis and second that YuaB controlled TasA biosynthesis or localisation. Previous experiments showed that YuaB does not affect the transcription of the *tapA* or *eps* operons in the *abrB* and *sinIR* genetic backgrounds (Figure 2.21), but the expression profiles from these promoter regions were also compared in the wild type and *yuaB* backgrounds to ensure that this is not the case (data not shown). This transcriptional analysis was followed by analysis of EPS and TasA production to confirm correct localisation and assembly of these biofilm matrix components.

2.7.1. YuaB is not required for EPS biosynthesis.

The *eps* operon encodes 15 proteins that are required for synthesis of the exopolysaccharide (Kearns *et al.*, 2005). The biochemical function of individual Eps proteins was so far mostly predicted using protein sequence homology (see Section 1.6.3.1 for details). However, it was shown on multiple occasions that strains carrying mutations in the *eps* genes, or those that are unable to express the *eps* operon altogether, are unable to form biofilms due to lack of EPS synthesis (Branda *et al.*, 2001, Branda *et al.*, 2004, Kearns *et al.*, 2005, Guttenplan *et al.*, 2010, Nagorska *et al.*, 2010). Additionally, the expression of the *eps* operon is bimodal (Chai *et al.*, 2008), therefore it was plausible that YuaB, as a surface protein, is influencing the genetic regulation of the *eps* operon upstream from AbrB and SinR, thus affecting the synthesis of the EPS.

To elucidate if YuaB is required for synthesis, assembly or stability of the EPS, the biofilm matrix fractions, containing the EPS, from the pellicles formed by the wild type (3610), *yuaB* (NRS2097) and *eps* (NRS2450), as well as from *sinIR* (DS93) and *yuaB sinIR* (NRS2291) strains were isolated. The fractions were concentrated by lyophilisation and resolved in a gradient polyacrylamide gel and stained using Schiff's reagent which is a carbohydrate-specific reagent (Segrest & Jackson, 1972) (Figure 2.25). It should be noted, that the Schiff's reagent will detect glycosylated proteins as well as polysaccharides resolved in a gel. Therefore the staining pattern was complex as several protein bands were detected as well as smeary entities which usually are accounted to free polysaccharides. Due to this fact the comparison of the wild type extracts to the extracts from the *eps* mutant (EPS-negative) and the *sinIR* mutant (overproducing EPS) were necessary and extremely helpful. The major band identified to be missing from the *eps* sample and to be significantly stronger in the *sinIR* sample was a band running >148 kDa according to a protein standard (Figure 2.25). It has to be noted that due to the chemical structure of polysaccharides they do not react with SDS as proteins do, therefore the surface charge of molecules resolved in the gel is not equilibrated. This results not only with smearing of the sample but also in the fact that the size of polysaccharides estimated in a gel according to a protein marker is on average 2-fold larger than the true size of the polymer (Segrest *et al.*, 1971).

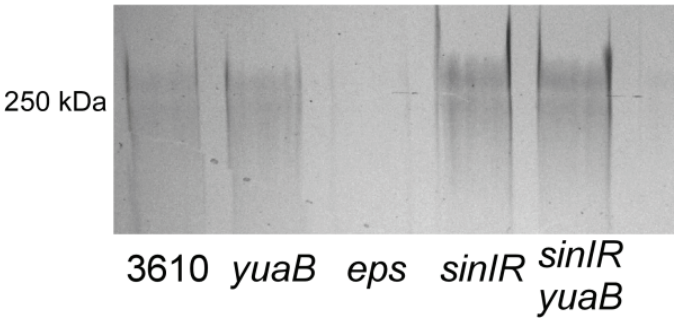

Figure 2.25 YuaB is not required for the production of the EPS. EPS was extracted from the biofilm pellicles of the wild type (3610), *yuaB* (NRS2097), *eps* (NRS2450), *sinIR* (DS93) and *sinIR yuaB* (NRS2291) mutants, resolved by SDS-PAGE and stained using Schiff's method.

The comparison of the EPS staining pattern extracted from the *yuaB* mutant (NRS2097) was no different from that of the wild type strain (3610) (Figure 2.25). The major band was found to be of the same size proving correct polymerisation of the EPS. Also no additional bands of lower molecular mass were seen; therefore no obvious premature degradation occurred. It was hypothesised, that any potential changes in the size of the EPS will be more noticeable in the *sinIR* background due to the larger amounts of EPS produced by this strain. However, the staining pattern of the samples from *sinIR* (DS93) and *sinIR yuaB* (NRS2291) were indistinguishable (Figure 2.25). It was concluded from these experiments that YuaB is not affecting the size or stability of the EPS synthesised. However, it was not possible to eliminate possibilities that the *yuaB* mutation is affecting the linkage of the individual monosaccharides comprising the EPS.

2.7.2. TasA amyloid fibres are correctly assembled and localised in the absence of YuaB

To verify if TasA is correctly synthesised, localised and assembled into amyloid fibres in the absence of YuaB, two approaches were taken. Firstly, biofilm fractionation coupled with Western blotting was performed to analyse synthesis levels and

localisation of TasA. Secondly immuno-gold labelling of TasA followed by transmission electron microscopy (TEM), as described by Romero & Kolter (2010), allowed for analysis of TasA amyloid fibres. The biofilm pellicles were fractionated into fractions representing whole cells, biofilm matrix and growth medium (Figure 2.13). The immuno-blot analysis of fractions revealed predominant presence of TasA in the cellular fraction and in the biofilm matrix of the wild type biofilm (Figure 2.26). This is in line of the original data presented by Branda *et al.* (2006). The small band detected in the growth medium fraction can be accounted for TasA fibres detached from the biofilm (Romero *et al.*, 2010). The analysis of the fractions obtained from the biofilm pellicle formed by the *yuaB* mutant (NRS2097) revealed identical pattern of bands of similar intensity (Figure 2.26). It should be noted that despite the fact TasA polymerises into amyloid fibres in the biofilm, in all immuno-blots performed during this project as well as those published in the literature, the TasA band is found to be corresponding to the molecular mass of a TasA monomer, which is 26 kDa (Serrano *et al.*, 1999, Stover & Driks, 1999c, Branda *et al.*, 2006). The *tasA* strain (NRS2415) was used as a negative control where no bands corresponding to TasA molecular mass was detected. Therefore it was concluded that YuaB is not required for synthesis of TasA or its export and correct localisation to the biofilm matrix.

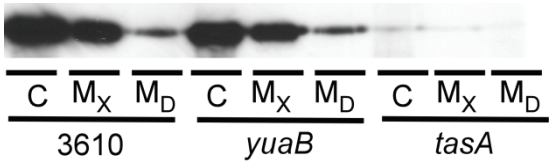

Figure 2.26 YuaB is not required for synthesis or export of TasA to the biofilm matrix. Pellicles of the wild type (3610), *yuaB* mutant (NRS2097) and *tasA* mutant (NRS2415) were collected and separated into cell (C), matrix (M_X) and growth medium (M_D) fractions. Localisation of TasA was identified by Western blotting.

Upon its export from the cytoplasm and processing by the SipW peptidase (Serrano *et al.*, 1999, Branda *et al.*, 2006), TasA polymerises into amyloid fibres (Romero *et al.*, 2010) and is anchored to the cell wall by the accessory protein TapA (Romero *et al.*, 2011). These fibres can be observed by TEM upon labelling of TasA with antibodies and visualising using gold-conjugated protein G (Romero *et al.*, 2010). To identify if YuaB is involved in the polymerisation and anchoring of TasA, microscopical analysis of TasA fibres was performed. To avoid the electron-thick background caused by the EPS, strains defective in the synthesis of EPS were used (Romero *et al.*, 2010) as described in section 2.4.3. It was shown previously that a defect in EPS synthesis does not affect polymerisation or anchoring of TasA (Romero *et al.*, 2010). The TasA fibres decorated with gold particles were clearly visible in the specimen prepared from the "wild type" strain (NRS2450) culture (Figure 2.27). Identical labelling was detected in the *yuaB* mutant (NRS2452), but not when the *tasA* control strain (NRS2451) was used (Figure 2.27). Due to the fact that no difference in the assembly or anchoring of the TasA fibres was observed in the absence of *yuaB,* it was concluded that YuaB is not involved in the synthesis, localisation or polymerisation of TasA.

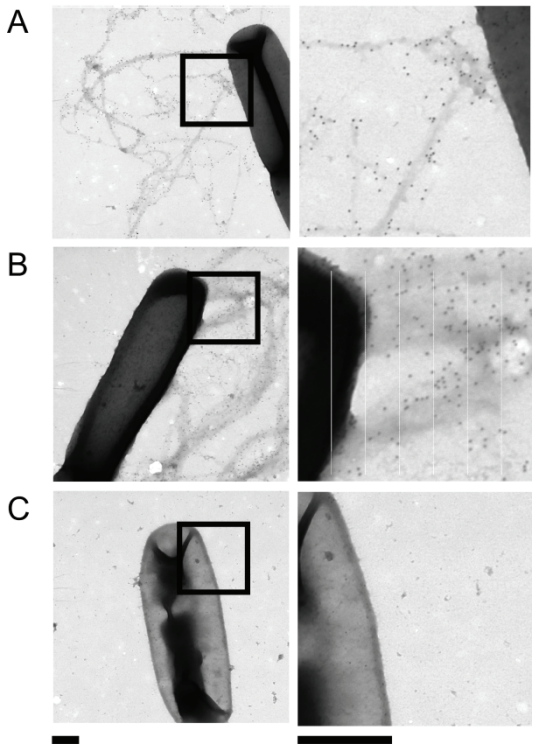

Figure 2.27 YuaB is not required for assembly and anchoring of TasA amyloid fibres. TasA fibres were visualized for the (**A**) "wild type" (NRS2450), (**B**) *yuaB* mutant (NRS2452), (**C**) and *tasA* mutant (NRS2451) by immuno-gold labelling. The images are of representative cells of each strain and surrounding extracellular space where the gold-decorated TasA fibres are visible. The images in the right hand side column represent magnifications of the left hand side images as indicated by black boxes. The scale bars represent 0.5 µm.

2.8. Summary

The principal conclusion to the experimental data presented above is that YuaB is a novel protein localised in the cell wall that acts in a synergistic manner with TasA and EPS to form a biofilm. This conclusion is based on the fact, that neither EPS nor TasA is affected by the absence of YuaB, but biofilm formation is ablated. In the absence of YuaB the sporulation rate in the biofilm, which is the marker of the final maturity of *B. subtilis* biofilm, is significantly lowered. This effect can only be complemented by controlled expression of YuaB. Therefore YuaB is required, in combination with TasA and EPS, for the maturation of the biofilm. YuaB was shown to contain a functional signal peptide, the role of which is to allow the export of YuaB from the cytoplasm. This is made clear by the fact that the signal peptide from YuaB

can be replaced by one from an unrelated protein WapA. Furthermore, YuaB detected by immuno-blotting is of lower mass then would be calculated from the sequence of the full length sequence. In fact the molecular mass of YuaB detected by Western blotting corresponds to that of the primary sequence starting after the signal peptidase cleavage site predicted by SignalP software.

Using electron microscopy, YuaB was seen to preferentially localise to the cell wall. Thus far it is not known how YuaB is anchored to the cell wall. The combined facts that YuaB does not contain the peptidoglycan binding motif LPxTG (Nguyen *et al.*, 2011, Liew *et al.*, 2012) and can be washed off the cells using high concentration salt supports the hypothesis that YuaB is bound to the cell wall via a non-covalent binding. However, to the date the anchoring partner was not identified. It is also not known how YuaB interacts with the TasA fibres and EPS to form the biofilm matrix. However, it is clear from the co-culture experiments that this interaction is necessary for biofilm formation to proceed. It is very interesting that a cell wall-associated protein not only inflicts an effect on the extracellular compartment of the biofilm matrix, but also that this effect is shared by the entire community. In the next chapter I expand on this mechanism providing a novel insight into how YuaB interacts with the remaining elements of the biofilm.

3. An *in situ* analysis of YuaB in biofilms reveals distinct localisation patterns

3.1. Introduction

In the previous chapter YuaB was identified as a cell wall-associated protein that acts in synergy with the TasA and EPS components of the biofilm matrix. To gain further insight into how individual components of the biofilm (TasA, EPS, the cells and YuaB) interact, it was of interest to characterise the nature of YuaB function within a biofilm. For this purpose a method for *in situ* detection of biofilm proteins, based on immuno-fluorescence labelling, was developed. This allowed for imaging of YuaB directly in the biofilm using confocal laser scanning microscopy (CLSM) in both pellicle and complex colony types of the biofilm. The ability to image protein localisation *in situ* in the biofilm was a significant improvement over methods used previously (immuno-gold labelling and TEM). Unlike previously, a fully developed biofilm could be imaged. Additionally, this is the first, to our knowledge, attempt of high magnification with high resolution imaging of complex colonies formed by *B. subtilis*.

The work presented in this chapter was conducted in close collaboration with Dr Laura Hobley. I thank her for help and useful discussion.

3.2. *In situ* localisation of YuaB in pellicles and complex colonies

3.2.1. YuaB is located at the liquid-cell interface

Previous reports have shown that the cells of *B. subtilis* form long chains of cells via an incomplete cell separation during biofilm formation (Branda *et al.*, 2006). It was also shown that the *degU* mutant is impaired in cell chaining (Kobayashi, 2007a).

Knowning that *yuaB* is the main target of DegU during biofilm formation (Section 1.7.1) and that YuaB is a cell wall-associated protein (Section 2.4), it was hypothesised that YuaB is responsible for cell-to-cell association within the biofilm. Indeed in a CLSM image of cells extracted from pellicles, a clear disarrangement of cells can be seen in the pellicle formed by the *yuaB* mutant in comparison to that of the wild type strain (Figure 3.1). To investigate if YuaB is directly involved in arrangement of cells in a pellicle, a method for detection of YuaB within the biofilm was developed. The fully developed pellicles were settled down on a microscope cover slip, which was precoated with Concavalin A to allow for binding of cells to the glass (Figure 3.1). Concavalin A is a lectin extracted from *Canavalia ensiformis* and is specifically binding mannose-containing polycarbohydrates (Goldstein *et al.*, 1965); therefore Concavalin A binds cell walls of Gram-positive bacteria, including *B. subtilis* (Doyle & Birdsell, 1972).

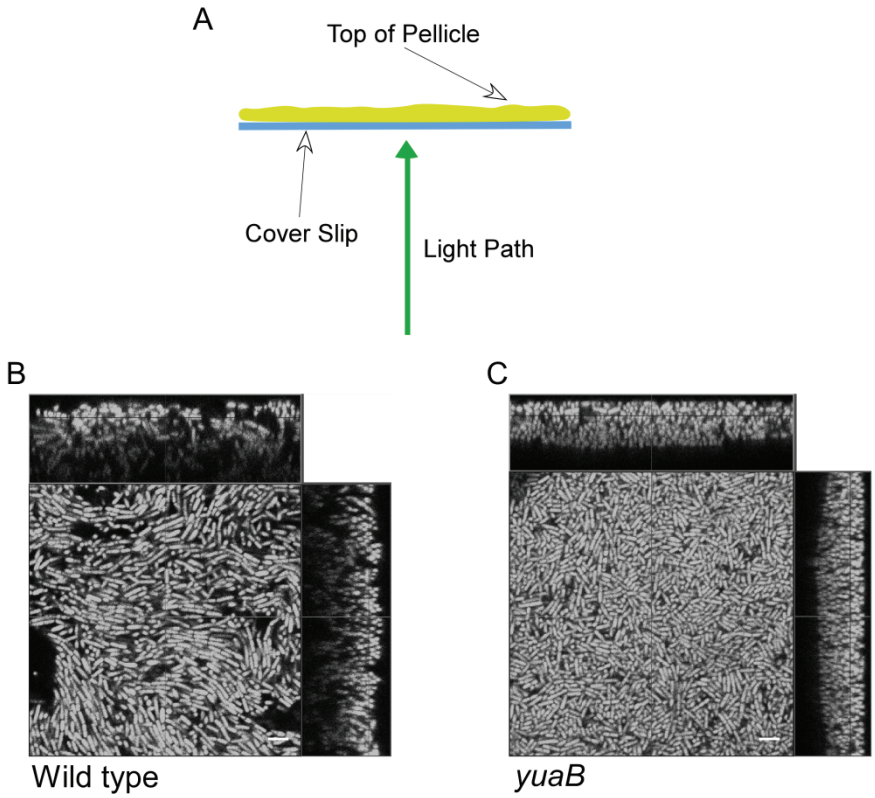

Figure 3.1 YuaB is required for cell alignment in a biofilm pellicle. (**A**) Schematic representation of biofilm pellicle preparation for imaging using CLSM. The pellicle (shown in light green) settled on a microscope coverslip (shown in blue) and immobilised with Concavalin A was imaged from the bottom to the top. The light path is indicated by a green arrow. (**B**) Orthogonal views of biofilm pellicles captured with CLSM of the wild type strain (NRS1473) and (**C**) the *yuaB* mutant (NRS3812). The XY fields represent the same relative Z plane of each pellicle. Scale bars represent 5 µm.

The preparation of pellicles for imaging involves fixation with paraformaldehyde (PFA) and multiple washes (as detailed in Section 5.4.11). These proceedings may cause significant loss of the sample; therefore a reference measurement of an intact biofilm was required. The pellicles of the wild type strain modified to constitutively express GFP were settled on Concavalin A-coated slides and mounted onto microscope slides with a cavity, to protect the structure of the biofilm. The pellicles mounted on the microscope slides were imaged by CLSM with acquisition of Z sections starting from the bottom of the pellicle towards the top (Figure 3.1A). The obtained images were uploaded to OMERO image analysis software (Allan *et al.*, 2012) and the depth of the pellicles was measured (Figure 3.2A). The average depth of

pellicles was 20.5 ± 1.7 µm (n=5). Having measured the thickness of a live biofilm, the thickness of a biofilm after immuno-labelling was measured. The pellicles of GFP-expressing wild type strain (NRS1473) were settled on cover slips and fixed with PFA. The immobilised biofilm was fixed and exposed to YuaB-specific primary antibody and subsequently fluorescently-labelled secondary antibodies. The slides were imaged and analysed as described above and in Section 5.4.11. The depth of the immuno-labelled ("processed") pellicle was measured for 17.1 ± 1.2 µm (n=5). Furthermore, the patterning and organisation of cells in the pellicles could not be distinguished between the processed and unprocessed pellicles (Figure 3.2). These findings indicate that sample processing does not significantly affect the structure of the wild type pellicle.

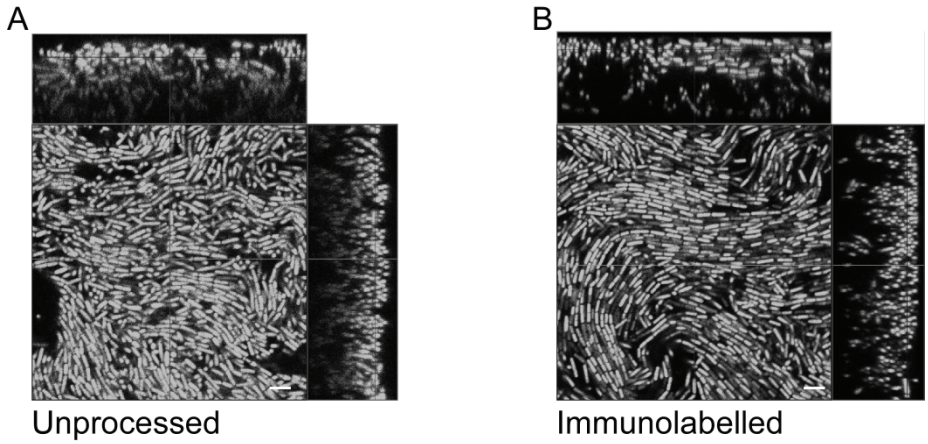

Figure 3.2 Pellicle processing for immuno-fluorescence does not disrupt the overall structure of the biofilm. Orthogonal views of biofilm pellicles of the wild type strain (NRS1473) imaged (**A**) live or after (**B**) immuno-labelling. The XY fields represent the same relative Z plane of each pellicle. Scale bars represent 5 µm.

Next, the spatial labelling pattern of YuaB was analysed (Figure 3.3). In the images of the wild type pellicles, YuaB was found in direct contact with the cells, as predicted (Figure 3.3A). In fact, in the high magnification images, the outline of cells surrounded by YuaB is clearly visible in the DyLight594 fluorescence channel, representing YuaB (Figure 3.3B). Furthermore, a "network" formed by YuaB around the

biofilm-enclosed cells was revealed. Unexpectedly however, the YuaB signal was found to be localised to the base of the pellicle, corresponding to the liquid-cell interface, and was not found in the deeper parts or the top of the pellicle (Figure 3.3A). The staining was shown to be specific, as no or very little, fluorescence was observed in the YuaB channel in specimen prepared from the *yuaB* mutant biofilms (Figure 3.3 C and D). The YuaB signal returned upon ectopic expression of *yuaB* under the control of an IPTG-driven promoter (Figure 3.22A). Additionally, a characteristic pattern of chaining cells within the wild type biofilm was observed upon return of YuaB (Figure 3.22A). Interestingly, in the cells enclosed in a pellicle formed by the *yuaB* mutant strain formed visually distinct chains that failed to form bundles, as seen for the wild type (data not shown). This supports the hypothesis that YuaB is required for cell-to-cell interactions in a biofilm. Note that due to the nature of CLSM and the size of the cell chain bundles, these structures are not clearly visible in the images in Figure 3.3. Since the cell chain bundles are formed by multiple aggregating cells, 3-dimensional image rendering would be required to visualise this structure. The chaining and bundling of cells in a pellicle was also previously observed in a different isolate of *B. subtilis* ATCC6051 (Kobayashi, 2007a, Kobayashi, 2007b). However, in this report, mutation of *yuaB* did not affect chaining of cells (Kobayashi, 2007b). Nonetheless, this can be caused by differences in the biofilm formation between the 3610 and ATCC6051 strains, which were shown on the genetic level (Kobayashi, 2008, Chai *et al.*, 2009).

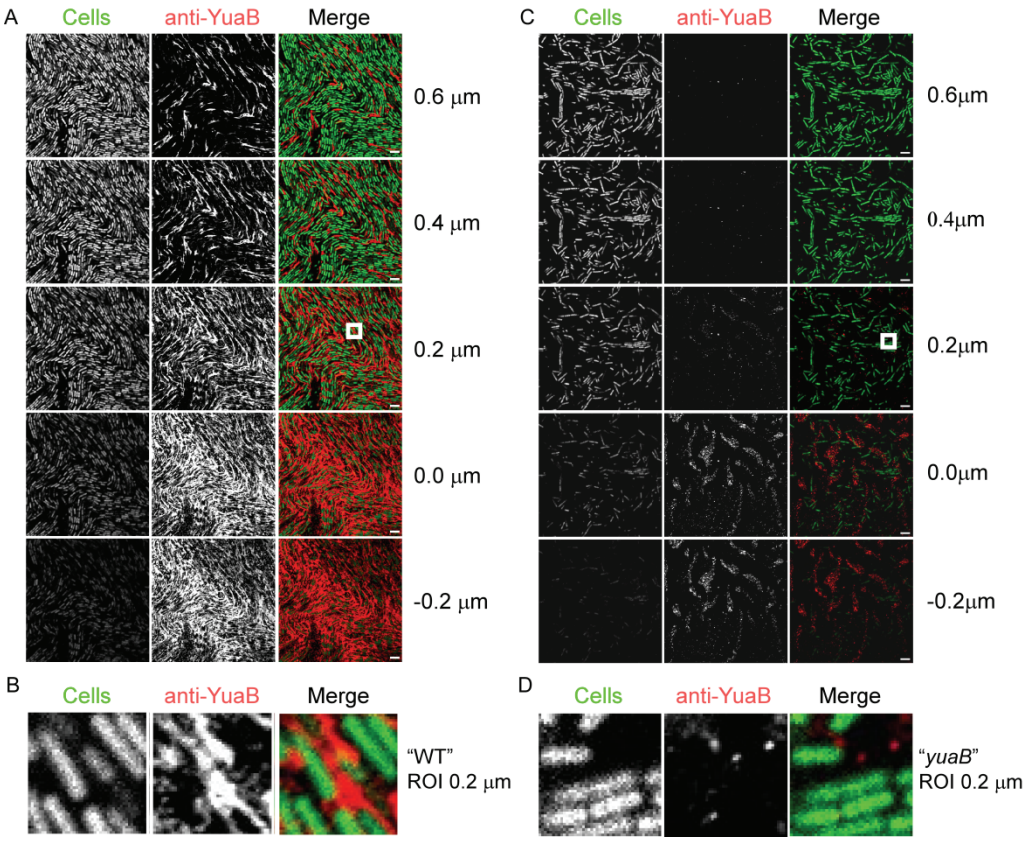

Figure 3.3 *In situ* analysis of YuaB localisation in the pellicle biofilm. CLSM images of pellicles of (**A** and **B**) the wild type strain (NRS1473) and (**C** and **D**) the *yuaB* mutant (NRS3812) after immuno-labelling against YuaB. Fluorescence from the GFP within the cells is presented in white in the left hand columns or false coloured green in the merged images. Fluorescence associated with DyLight594, representing immuno-labelled YuaB is presented in white in the middle columns or false coloured red in the merged images. **B** and **D** represent the regions of interest highlighted by the white box in the parts **A** and **C** respectively. The scale bars are 5 µm.

3.2.2. Automated analysis of YuaB localisation

To objectively assess YuaB abundance at the liquid-cell interface in the biofilm pellicles, fluorescence of the Z-sections for channels representing the cells and YuaB was quantified. For purpose of this analysis, the base of the pellicle was identified as the first Z-section where the cells become visible. This section was arbitrarily marked as 0 µm position of the pellicle (*e. g.* Figure 3.3A, 0 µm image). It was found that YuaB occupied loosely defined areas in the image stack. Furthermore, the fluorescence signal intensity varied between the acquired images due to non-quantitative preparation of the specimen. Therefore, fluorescence intensity analysis could not be used to quantify the amount of YuaB present in each sample. As an alternative, a

measurement of signal-positive pixels in each channel in each Z-section was conducted. The resulting values were plotted against the distance from the biofilm depth (Figure 3.4) and the area under the curve was calculated to quantify the total abundance of signal-positive pixels across the biofilm (Table 3.1). Analysis of vertical sections through the pellicle indicated that YuaB-specific staining penetrated on average from 0.4 μm below the base cell layer, to 4 μm above the base cell layer into the developing wild type pellicle (Figure 3.4A). Furthermore, the YuaB signal present at the base of the wild type pellicle (*e.g.* Figure 3.3C, 0 μm image and Figure 3.4B) covered on average 25% of the field of view.

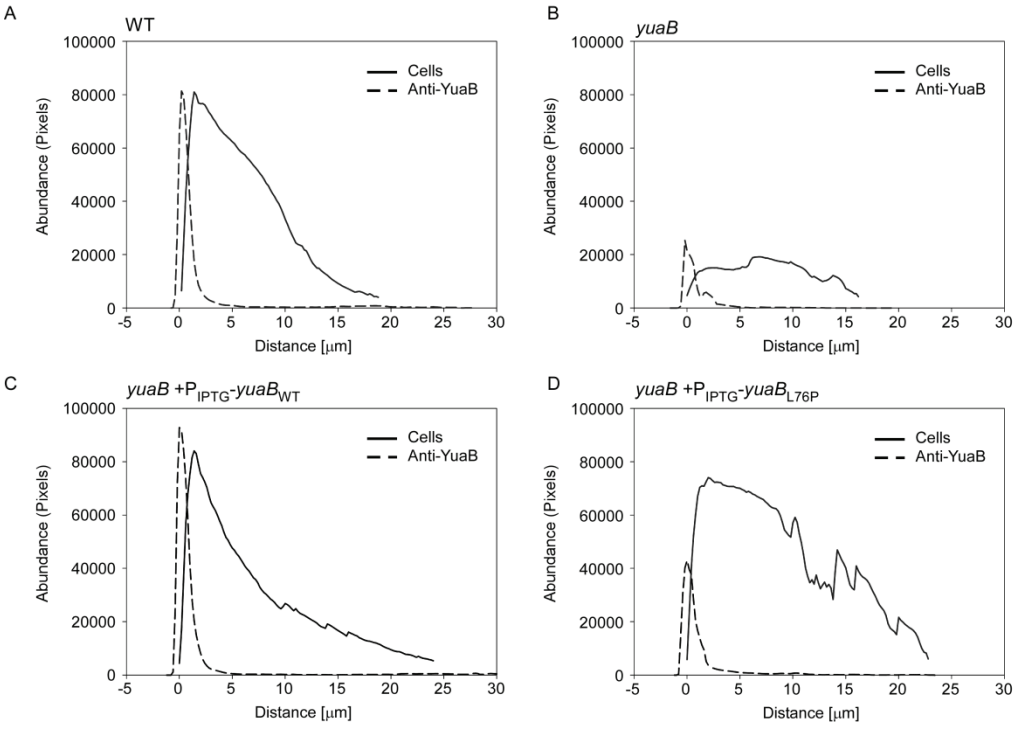

Figure 3.4 YuaB abundance analysis throughout the depth of the pellicle biofilm. Average values of abundance of the fluorescent signal for GFP, depicting cells in the biofilm as a solid line, and DyLight594, representing immuno-labelled YuaB as a dashed line, in each of the Z-sections acquired from (**A**) wild type cells (3610 *sacA::*P_{IPTG}*-gfp*; NRS1473), (**B**) the *yuaB* mutant strain (*yuaB sacA::*P_{IPTG}*-gfp*; NRS3812), (**C**) the *yuaB* mutant strain complemented by wild type YuaB (*yuaB amyE::*P_{IPTG}*-yuaB-lacI sacA::*P_{IPTG}*-gfp;* NRS3790), (**D**) the *yuaB* mutant strain complemented by $YuaB_{L76P}$ (*yuaB amyE::*P_{IPTG}*-yuaB*$_{L76P}$*-lacI sacA::*P_{IPTG}*-gfp;* NRS3948). The signal abundance was calculated from pixel population for each of the XY-images and plotted against the depth (Z-section number) of the biofilm where 0 μm depicts the first Z-section containing GFP signal.

Table 3.1 Average integration values of the abundance of signal-positive pixels in the DyLight594 channel, representing YuaB.

Strain	**Total pixel abundance**	**Statistic comparison to wild type[1]**
Wild type	109578	N/A
yuaB	26248	P<0.0001
yuaB P_{IPTG}-*yuaB*$_{WT}$	134435	P>0.05
yuaB P_{IPTG}-*yuaB*$_{L76P}$	72897	P<0.05

[1] The P values were calculated using Welch's *t*-test for samples with unequal variance.

This bespoke analysis was validated by control experiments. In the absence of primary antibody the mean signal intensity in the DyLight594 channel was 2% of that measured in the presence of the primary antibody (Figure 3.5A) and the distribution of pixels identified by the automatic analysis tool as "signal positive" resembled that expected of background noise (Figure 3.5B). Furthermore, the analysis of the residual fluorescence in the immuno-labelled pellicles of the *yuaB* mutant (Figure 3.3B) and the wild type that was not exposed to the primary antibody (Figure 3.5A) did not show the result in the same distinctive distribution. Moreover, comparison of the mean total abundance of signal-positive pixels in the DyLight594 channel measured in the *yuaB* pellicle, to that calculated for the wild type pellicle, showed a significantly lower value of signal abundance (P<0.0001) (Table 3.1). Therefore, the staining of YuaB observed in the wild type pellicle was deemed specific. Additionally, as expected in the presence of the ectopic copy of *yuaB,* the abundance of the signal in the DyLight594 channel (representing YuaB labelling) returned back to the level similar to that of the wild type strain (Figure 3.4C and Table 3.1)

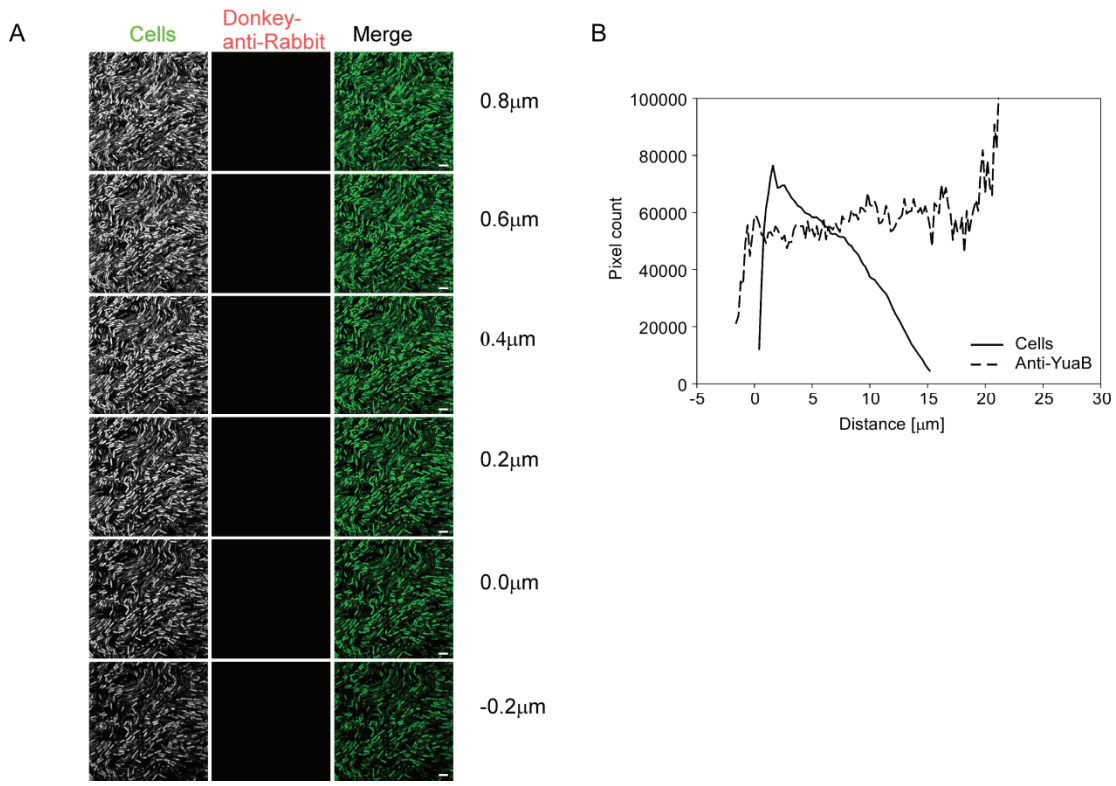

Figure 3.5 Immuno-fluorescence without the primary antibody. (**A**) CLSM images of pellicles of strain NRS1473 (3610, sacA::P_{IPTG}-*gfp*) after processing for immuno-labelling lacking the primary antibody. Fluorescence from the GFP within the cells is presented in white in the left hand columns or false coloured green in the merged image. Fluorescence associated with DyLight594 is presented in white in the middle columns or false coloured red in the merged image. The scale bar is 5 µm. (**B**) Average values of abundance of the fluorescent signal for GFP, depicting cells in the biofilm as a solid line, and DyLight594 in each of the Z-section acquired from the wild type cells (3610, sacA::P_{IPTG}-*gfp*; NRS1473) after immuno-fluorescence staining lacking the primary antibody.

3.2.3. Expression from the yuaB *promoter is unimodal*

In biofilm pellicles YuaB is associated with the cell wall of the cells located at the base of the pellicle. As very little YuaB was found in the higher sections of the pellicle it was possible that YuaB is expressed only in the subpopulation of cells occupying the lower sections of the pellicle. This would put YuaB in the large group of bimodally expressed proteins involved in the multicellular lifestyle of *B.* subtilis (Lopez *et al.*, 2009b). To test if the expression of *yuaB* is indeed bimodal, the *gfp* gene was cloned under the control of the P_{yuaB} promoter and introduced into the wild type (NRS2289) and *yuaB* mutant (NRS2292) strains. The cells were extracted from complex colonies 14 to 48 hours post inoculation. The cells were separated from each other

using mild sonication, so that the cells do not lyse but the surrounding biofilm matrix is disrupted and the fluorescence of individual cells was measured using flow cytometry (Figure 3.6). To compensate for the autofluorescence of cells, a sample of non-fluorescent wild type cells extracted from biofilms of equal age was used as a negative control. The fluorescence histogram obtained from the wild type cells was used to define the boundaries of fluorescence originating from the cells rather than the fluorescent reporter.

During the time course, the fluorescence corresponding to expression from the *yuaB* promoter was detected in both wild type and *yuaB* strains, which indicates that YuaB is not a self-regulating protein. The signal was detectable as early as after 14 h after inoculation. The fluorescence level remained largely unchanged throughout the experiment and the samples after 48 h incubation showed the same level of fluorescence as at the beginning of the experiment (Figure 3.6). In conclusion the expression of the *yuaB* gene is unimodal throughout biofilm formation and YuaB does not affect its own expression.

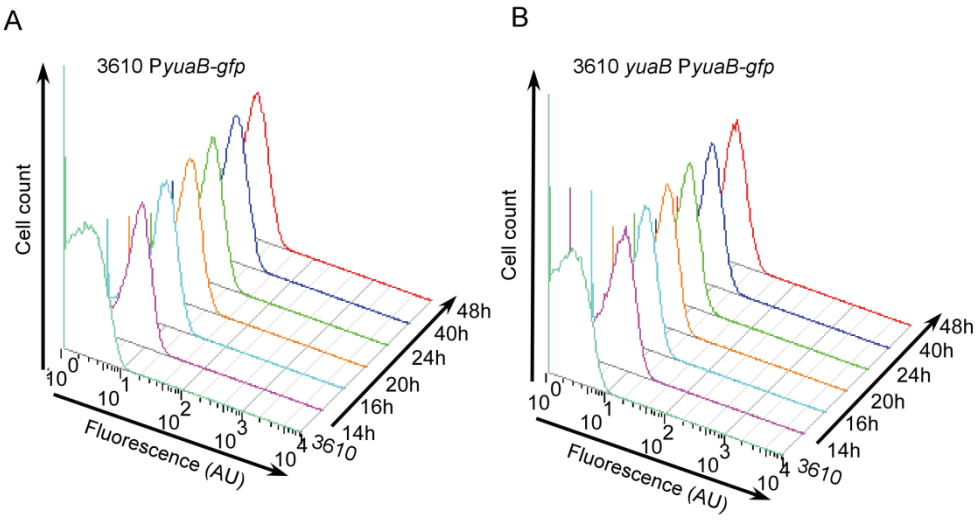

Figure 3.6 Expression of GFP under regulation of the *yuaB* promoter measured by flow cytometry is unimodal. Cells expressing GFP under the *yuaB* promoter were extracted from complex colonies of (**A**) the wild type (NRS2289) and (**B**) the *yuaB* mutant (NRS2292) after 14, 16, 20, 24, 40 and 48 h incubation at 37 °C. The GFP fluorescence was measured by flow cytometry against a non-fluorescent parental strain. The fluorescent values are presented in arbitrary units.

3.2.4. YuaB coats the air-cell and agar-cell interfaces of a complex colony

The finding that YuaB specifically localises to the base of the biofilm pellicle was surprising, as YuaB was shown to be expressed by all cells within the biofilm. To elucidate if this effect is specific to the pellicle, a method for immuno-labelling of proteins within a complex colony was developed. Briefly, a fully developed colony was snap-frozen in liquid nitrogen in presence of a cryo-preservative and sectioned using a cryomicrotome (Figure 3.7) (Vlamakis *et al.*, 2008).

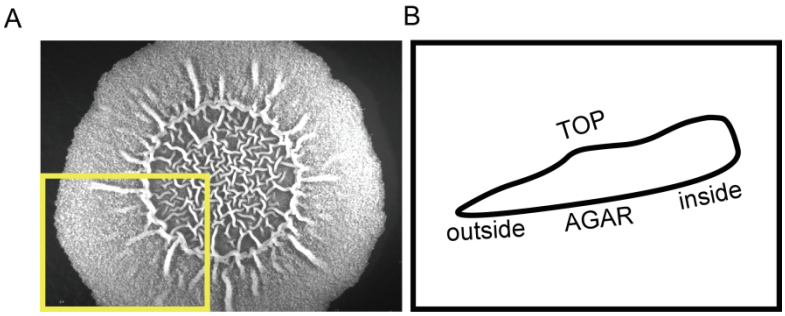

Figure 3.7 Schematic representation of complex colony section preparation for immuno-labelling. (**A**) A complex colony formed by the wild type strain (3610). The yellow box exemplifies the section removed for cryo-sectioning. (**B**) Diagrammatic representation of a cryo-sectioned sample orientation mounted on a microscope slide.

The resulting sections were placed on a microscope slide, where the colony sections were immuno-labelled in the same way as were pellicles. Strikingly, the majority of YuaB was found to form a tight layer surrounding the complex colony (Figure 3.8A). The YuaB layer was visible at both the top air-cell and the bottom agar-cell interfaces. On the top surface, only small protrusions of fluorescence from the YuaB staining were found to penetrate into the deeper parts of the colony (Figure 3.8A). In line with the immuno-fluorescence analysis of pellicles, the YuaB labelling was not visible in the *yuaB* mutant indicating the specificity in the assay (Figure 3.8B).

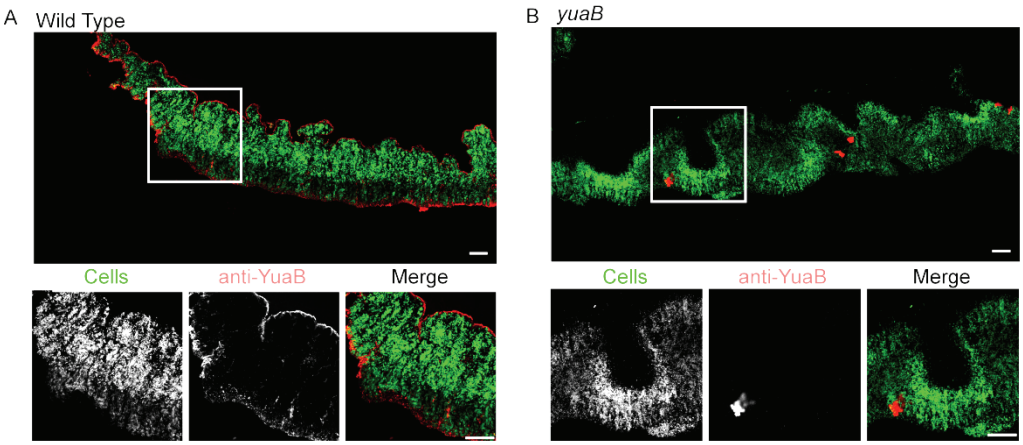

Figure 3.8 *In situ* analysis of YuaB localisation in the complex colony biofilm. CLSM images of complex colonies formed by (**A**) the wild type (NRS1473) or the (**B**) *yuaB* mutant strain (NRS2812). The cells express GFP for visualisation purposes. The smaller images show the regions highlighted by the white box at higher magnification. Fluorescence associated with GFP within the cells is shown in green in the large panels and in the merged images and in white in the left hand higher magnification images. Fluorescence associated with DyLight594, representing immuno-labelled YuaB staining is shown in red in the large panels and merged images, and in white in the central higher magnification images. The scale bars represent 50 µm.

3.2.5. YuaB is located within the matrix of the colony biofilm but is cell-associated in the pellicle

To investigate the whether the striking differences between YuaB localisation patterns in pellicles and complex colonies were an indication of fundamental differences between these types of biofilm, and if these differences affected the cell-YuaB association, the localisation of YuaB within complex colonies was analysed using

biofilm fractionation and Western blotting. In the biofilm pellicle YuaB was found to be associated with the cell wall (Section 2.4 and Figure 2.19), not with the TasA-containing biofilm matrix. This is consistent with the novel *in situ* immuno-fluorescence analysis indicating cell-association if YuaB in pellicles (Figure 3.3). In contrast, after fractionation of the complex colonies into the biofilm matrix and cell fraction, a large proportion of YuaB was found to be located within the biofilm matrix fraction (Figure 3.9); again consistent with the *in situ* immuno-fluorescence analysis (Figure 3.8). In each case the biofilm matrix was defined based on the localisation of the amyloid biofilm matrix protein TasA (Branda *et al.*, 2006). Cell lysis was controlled for using an antibody against membrane-bound protein AtpB (Hahne *et al.*, 2008). The data presented above indicate that YuaB is cell-wall associated within the pellicle biofilm, but located in the biofilm matrix in complex colonies. The cause of this difference is unknown; however, it is plausible that, during pellicle formation, another protein is present that acts as an anchor for YuaB. Consequently, such a protein must be absent from the complex colonies to allow release of YuaB to the biofilm matrix.

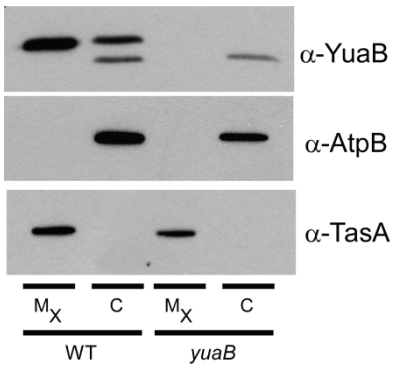

Figure 3.9 YuaB localisation in the complex colony analysed by fractionation and Western blotting. Complex colonies of the wild type (3610) and the *yuaB* mutant strain (NRS2097) were separated into cell (C) and matrix (M_X) fractions. The localisation of YuaB was determined by Western blotting, by comparison with the amyloid-fibre protein TasA and the membrane-bound AtpB, which was used as a control for cell lysis.

3.3. YuaB is a hypothetical amyloid-like protein

3.3.1. YuaB confers Congo Red binding properties

The *in situ* immuno-fluorescence-CLSM analysis of YuaB localisation indicates the possibility of YuaB forming higher order structures, self-polymerising or self-segregating in the biofilm. The self-polymerising proteins commonly found in biofilms are amyloid fibre forming proteins (Larsen *et al.*, 2007), like the matrix protein TasA (Romero *et al.*, 2010). It was of interest to verify if the structures, which visually resemble higher order organisation, visible in the images of YuaB possess amyloid-like properties. To investigate this possibility, a common feature of amyloid proteins, to bind the amyloid-specific dye Congo Red, was tested. TasA was previously shown to bind Congo Red *in vitro* and *in vivo* as the complex colonies grown on media supplemented with Congo Red turn red in colour (Figure 3.10A) (Romero *et al.*, 2010). The wild type (3610) and the *yuaB* mutant (NRS2097) strains were grown on an MSgg agar plate supplemented with the Congo Red dye (Section 5.2.1), with *tasA* (NRS2415) strain as a control, to investigate the YuaB-dependent Congo Red binding. Similarly to the *tasA* mutant, the *yuaB* colony did not stain red, which suggests YuaB having amyloid-like properties (Figure 3.10B). It is noteworthy, that the TasA fibres are assembled in the absence of YuaB (Section 2.7.2, Figure 2.26); therefore the reduction in Congo Red binding by the *yuaB* mutant is specific to the absence of YuaB. Furthermore, analysis of the *tasA yuaB* double mutant (NRS2425) indicated that the residual red staining apparent in the *tasA* mutant was YuaB-dependent (Figure 3.10), further supporting the conclusion that YuaB may have amyloid-like properties.

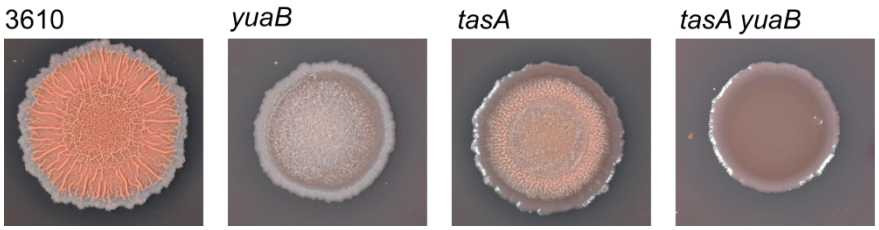

Figure 3.10 Congo red staining of complex colonies of wild type (3610), *yuaB* (NRS2097), *tasA* (NRS2415) and *tasA yuaB* (NRS2425) mutant strains. Colonies were grown at 30 °C for 48 hours in the presence of 20 μg/ml Congo red dye with 10 μg/ml Coomassie blue G-250.

3.3.2. In silico analysis of potential amyloidogenic or aggregation domains in YuaB

Amyloid proteins contain short stretches of amino acids, arranged into β-strand structures, which allow for amyloid fibre formation *in vivo* and *in vitro* (Sunde *et al.*, 1997). As the primary amino acid sequence of YuaB does not resemble the sequence of any proteins with a known structure, homology modelling of YuaB structure was not possible. As an alternative, a secondary structure prediction server PsiPred was employed, which calculates the predicted structures using a neural network approach (McGuffin *et al.*, 2000). The *in silico* prediction of the secondary structure of YuaB predicted the presence of multiple β-strands (38 % of the overall sequence, Figure 3.11). The predicted β-strands are indicated as arrows in the Figure 3.11. To identify any potential amyloidogenic or aggregation domains in YuaB, three prediction programmes were utilised: Aggrescan (Conchillo-Sole *et al.*, 2007), FoldAmyloid (Garbuzynskiy *et al.*, 2010) and TANGO (Fernandez-Escamilla *et al.*, 2004). These algorithms identified slightly different amyloidogenic or aggregation-prone sequences within the mature region of YuaB, which is the region starting after the predicted signal peptidase cleavage at the residue A_{28} (Figure 3.11). Noteworthy was the correlation between the aggregation-prone regions prediction and the β-strands prediction by PsiPred (Figure 3.11). A similar correlation was seen between the β-rich

regions of TasA and aggregation regions in TasA as predicted by PsiPred and Aggrescan respectively (Figure 3.12). To verify these predictions, the orthologues of YuaB, identified by BLAST (Altschul *et al.*, 1997) in different species of the *Bacillus* genus, were analysed. In all cases similar predictions were obtained (Figure 3.13). Together with the specific Congo Red staining and conservation of hypothetical aggregation Hot Spots, these data support the hypothesis that YuaB has certain amyloid-like properties.

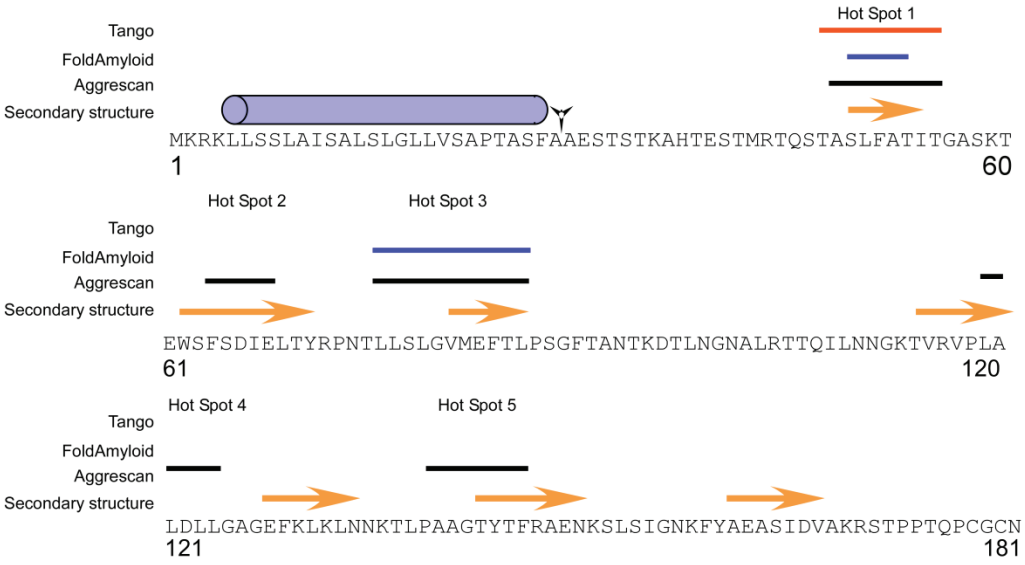

Figure 3.11 Full sequence of YuaB. From top to bottom: Amyloidogenic/aggregation-prone regions (marked by solid lines) predicted by the indicated programmes, the Hot Spots predicted by Aggrescan are annotated; the secondary structure as predicted by PsiPred, the α-helix is indicated with a purple cylinder, the β-sheets are indicated with yellow arrows. The signal peptide cleavage site is indicated with the black arrow head. The amino acid residue numbers are indicated.

A

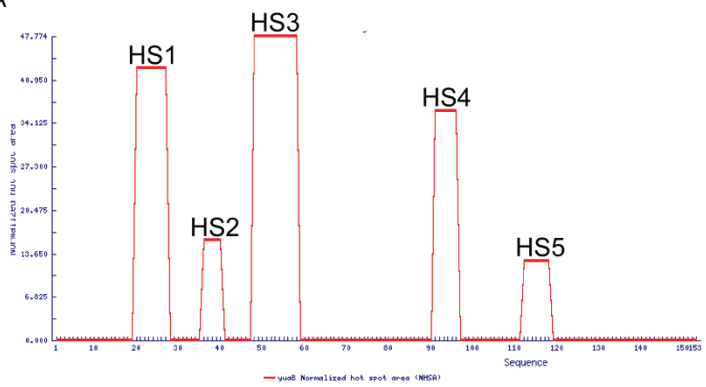

B

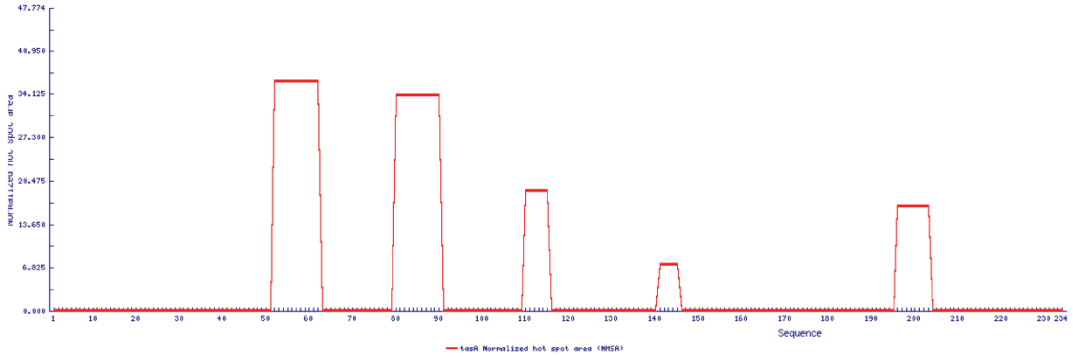

C

MGMKKKLSLGVASAALGLALVGGG**TWAAFN**DIKSKDA**TFASGTLDLSA**KENSASVNLSNLKPGD**KLTKDFQFEN**NGSLAI
KEVLMALNYGDFKANGGSNTSPEDFLSQF**EVTLLTV**GKEGGNGYPKNIILDDANLKDLYLMSAKNDAAAAEKIKKQIDPK
FLNASGKVNVATIDGKTAPEYDGVPKTPTDFDQ**VQMEIQFKD**DKTKDEKGLMVQNKYQGN**SIKLQFSFEAT**QWNGLTIKK
DHTDKDGYVKENEKAHSEDKN

Figure 3.12 Aggregation domain predictions for YuaB and the amyloid-fibre protein TasA. Aggrescan predictions of potential aggregation hot spots of the mature protein sequence (as predicted by SignalP) for (**A**) YuaB and (**B**) TasA. (**C**) The complete protein sequence of the amyloid-fibre protein TasA; highlighted in yellow are the predicted aggregation hotspots as predicted by Aggrescan in bold are beta-sheets and underlined are alpha helices as predicted by PsiPred.

3.4. Mutations of *yuaB* can be complemented by orthologues of YuaB

BLAST sequence searches with YuaB from *B. subtilis* identified potential orthologues in closely related species: namely *B. licheniformis, B. amyloliquefaciens* and *B. pumilus* (Figure 3.13 and Table 3.2). Additionally, a homologue of *yuaB,* the *yweA* gene, is encoded within the genome of *B. subtilis,* which encodes a secreted protein of unknown function (Antelmann *et al.*, 2001, Kobayashi, 2007b). The ability of the orthologous genes to complement the biofilm defect caused by the *yuaB* mutation was tested. To achieve this, the coding region of each orthologue was introduced at

the heterologous *amyE* site on the chromosome under the control of the IPTG inducible promoter $P_{hy\text{-}spank}$. The ability to complement the *yuaB* deletion phenotype by each of the orthologues was assessed by the restoration of colony morphology, pellicle formation, and by the recovery of spore formation (Branda *et al.*, 2006, Vlamakis *et al.*, 2008). With the exception of YweA, all orthologues of YuaB were able to restore the wild type morphology of the biofilm in the absence of the endogenous YuaB (Figure 3.14). Furthermore, the level of sporulation in the mature biofilms was restored to a level near that of the wild type, indicative of a functional biofilm matrix being formed (Figure 3.14).

Figure 3.13 Protein sequence of YuaB from *B. subtilis* 3610 aligned with orthologues: YweA from *B. subtilis* 3610 and YuaB from each of *B. licheniformis* DSM13, *B. amyloliquefaciens* FZB42 and *B. pumilis* SAFR-032. The region highlighted in yellow is the signal sequence to the predicted cleavage site, the predicted aggregation hotspots identified by Aggrescan are highlighted in blue (Hot Spots 1 and 3) and grey (Hot spots 2, 4 and 5). The asterisk (*) marks the L76 residue at the start of Hot Spot 3 in *B. subtilis* YuaB, and the grey arrows indicate predicted beta-sheets.

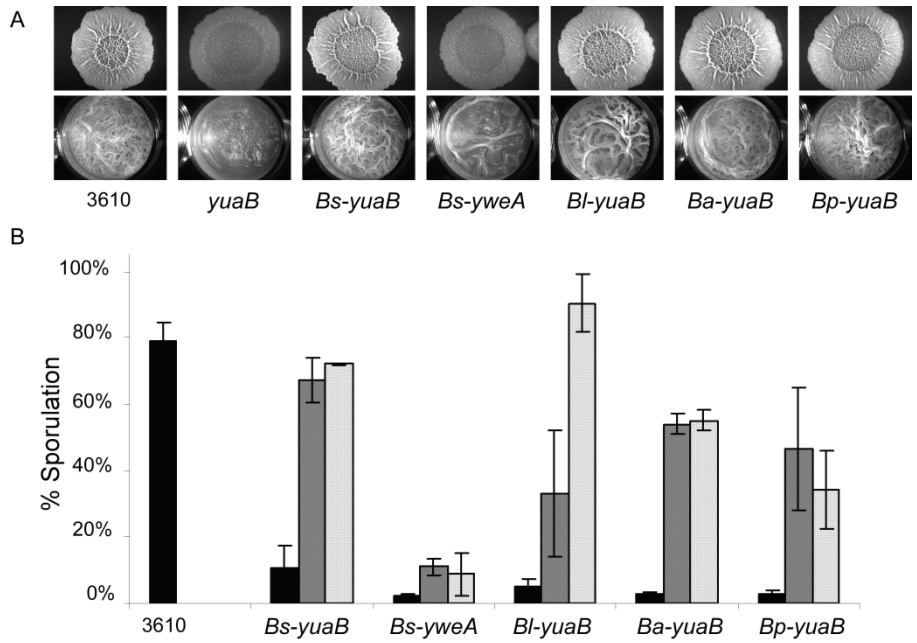

Figure 3.14 The homologues of YuaB can restore biofilm formation and maturation. (**A**) Complex colony and pellicle formation by strains expressing orthologues of YuaB upon IPTG induction (at 25 μM) from the P*hy-spank* promoter at the *amyE* location on the chromosome. Strains imaged are: 3610 (wild type NCIB3610), the *yuaB* mutant (NRS2097) and the *yuaB* mutant complemented with *B. subtilis* YuaB (*Bs-yuaB*; NRS2299), *B. subtilis* YweA (*Bs-yweA*; NRS2412), *B. licheniformis* YuaB (*Bl-yuaB*; NRS2414), *B. amyloliquefaciens* YuaB (*Ba-yuaB*; NRS2458) and *B. pumilis* YuaB (Bp-yuaB; NRS2464). Colonies were grown at 30 °C for 48 hours and pellicles at 25 °C for 72 hours before being imaged. (**B**) The average percentage sporulation after 72 hours under biofilm formation are plotted for the strains detailed above; the concentration of inducer used in the analysis is 0 μM (black bars), 10 μM (dark grey bars) and 50 μM (light grey bars). The error bars represent the standard error of the mean. Pellicle images acquired by Dr Laura Hobley.

Table 3.2 Amino acid sequence identity and similarity between the homologues of YuaB

Complementation protein	**% identity (% similarity)[a]**
YuaB *B. licheniformis*	64.3 (78)
YuaB *B. amyloquefaciens*	73.2 (81.4)
YuaB *B. pumilus*	55.1 (70.8)
YweA *B. subtilis*	55.1 (62.6)

[a] The percentage similarity and identity was obtained using pairwise protein-protein BLAST analysis across the entire length of the protein (Altschul *et al.*, 1997).

The possible explanation of the inability of YweA to complement for the absence of YuaB is the absence of 15 N-terminal amino acids after the putative signal peptide in the sequence of YweA in comparison to the amino acid sequence of YuaB (Figure 3.13). To identify if reinstating the fragment missing from the sequence of YweA will allow YweA to facilitate biofilm formation, a hybrid YuaB-YweA protein was constructed so that DNA sequence encoding the signal peptide and the sequence absent from the native YweA was fused to DNA of the mature YweA. The hybrid gene was placed under the control of an IPTG-inducible promoter and introduced to the *yuaB* mutant (NRS3001). However, the expression of the hybrid YuaB-YweA protein did not restore the biofilm formation to the *yuaB* mutant strain (Figure 3.15). The reason for which neither YweA nor the hybrid protein were able to complement for the absence of YuaB was not established. Nonetheless, this result is in agreement with previous findings that YweA does not take part in biofilm formation (Kobayashi, 2007b).

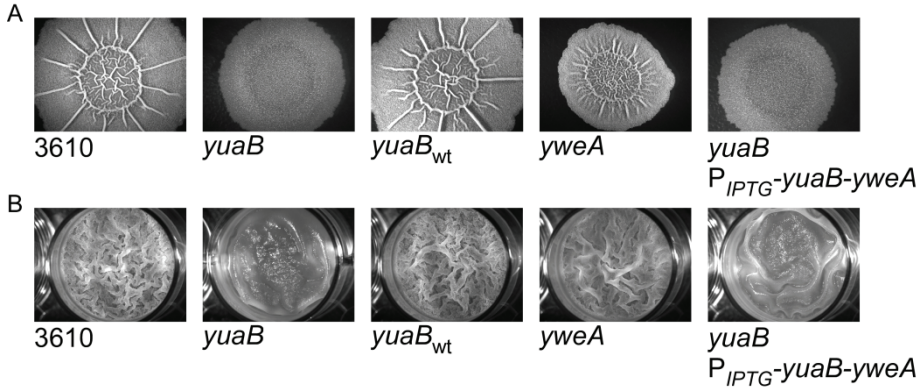

Figure 3.15 Deletion of *yweA* does not affect biofilm formation and a chimeric YuaB-YweA protein cannot restore biofilm formation in a *yuaB* mutant. Strains shown are wild type (3610), the *yuaB* mutant (NRS2097), the *yuaB* mutant complemented with wild-type YuaB (*yuaB*, *amyE*::P_{IPTG}-*yuaB-lacI*; NRS2299), the *yweA* mutant (NRS2405) and the *yuaB* mutant complemented with the chimeric YuaB-YweA protein (*yuaB*, *amyE*::P_{IPTG} *-yuaB-yweA-lacI ;* NRS3001). (**A**) Complex colonies were grown for 48 hours at 30 °C and (**B**) pellicles were grown for 72 hours at 25 °C, all in the presence of 25 µM IPTG.

3.5. Identification of regions of YuaB required for function

3.5.1. Site directed mutagenesis of the aggregation Hot Spots

To further investigate the requirement of the potential YuaB aggregation domains for biofilm formation, a series of site directed mutations was constructed. The mutations were designed so that a single amino acid substitution would reduce the predicted aggregation properties of YuaB in the most strongly predicted sites: Hot Spot1 and Hot Spot3 as predicted by Aggrescan (Figure 3.12). The following mutations were constructed: *i*) YuaB A_{48}SLFATIT_{55} to A_{48}SAAAAIT_{55} (NRS3819); and *ii*) YuaB L_{76}LSLGVMEFTL_{86} to L_{76}LSAAAAAATL_{86}. (NRS3960) which replaced the central amino acids in Hot Spot 1 and 3 with alanine residues respectively; *iii*) $YuaB_{F51P}$ (NRS3821); and *iv*) $YuaB_{L76P}$ (NRS3809) which were designed to perturb Hot Spots 1 and 3 respectively by introduction of a proline (Figure 3.16A) (Conchillo-Sole *et al.*, 2007). As mentioned above, the aggregation Hot Spots are located in the YuaB sequence fragments predicted to be β-strands. Introduction of a proline residue within a β-strand ($YuaB_{F51P}$, Figure 3.16) or at either end of a β-strand ($YuaB_{L76P}$, Figure 3.16) will destabilise the local secondary structure causing loss of the putative aggregation properties (Dr Francesco Rao, personal communication) (Conchillo-Sole *et al.*, 2007). The proline substitutions were accompanied by mutations in the same residue predicted to have no impact on the aggregation profile: $YuaB_{F51Y}$ (NRS3811) and $YuaB_{L76I}$ (NRS3820) respectively.

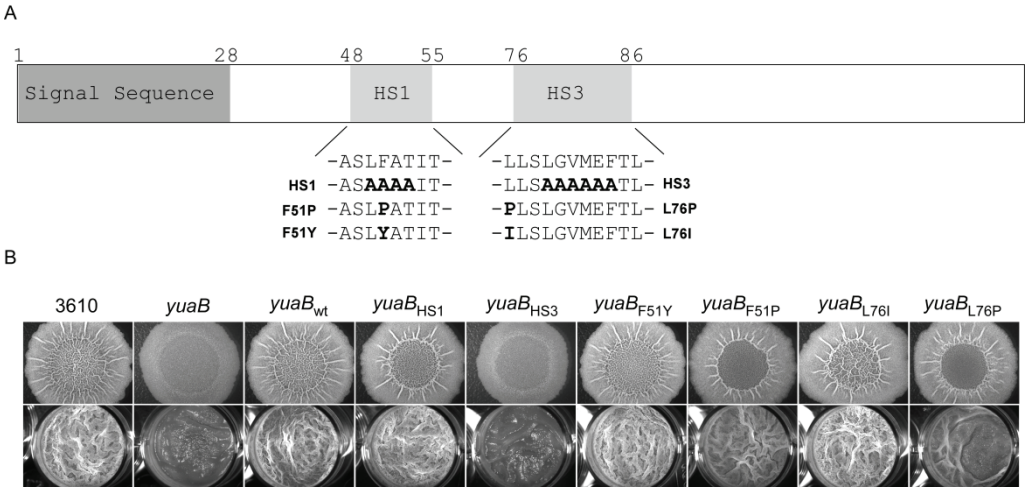

Figure 3.16 Predicted aggregation hot spots are important for YuaB function. (**A**) Diagrammatic representation of the YuaB protein sequence, showing the location of the predicted aggregation hot spots 1 and 3, and the site-directed mutations made in these areas. (**B**) Complex colony and pellicle formation by strains expressing mutated forms of YuaB upon IPTG induction (at 25 µM) from the P*hy-spank* promoter at the *amyE* location on the chromosome. Strains imaged are: wild type (3610), *yuaB* mutant (NRS2097), and the *yuaB* mutant complemented with wild type YuaB (NRS2299), $YuaB_{HS1}$ (NRS3819), $YuaB_{HS3}$ (NRS3960), $YuaB_{F51Y}$ (NRS3811), $YuaB_{F51P}$ (NRS3821), $YuaB_{L76I}$ (NRS3820) and $YuaB_{L76P}$ (NRS3809). Colonies were grown at 30 °C for 48 hours and pellicles at 25 °C for 72 hours before being imaged. Images and figure by Dr Laura Hobley.

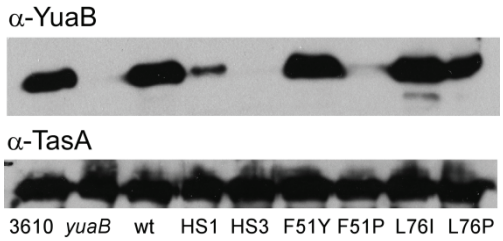

Figure 3.17 Western blot analysis of YuaB and TasA proteins in the complex colonies for each YuaB hotspot mutant [as in (Figure 3.16)], colonies were again grown for 48 hours at 30 °C. (Dr Laura Hobley)

The capability of the mutant alleles of *yuaB* to complement the *yuaB* biofilm minus phenotype was assessed by assaying pellicle formation and complex colony development. The level of protein produced was monitored by Western blotting compared with that generated by the wild type *yuaB* allele under the control of the same promoter (Figure 3.17). It was determined that the alanine substitutions in Hot Spot 1 had no effect on either complex colony or pellicle morphology, despite a reduction in the level of the $YuaB_{HS1}$ protein compared with the wild type complement (Figure 3.16 and Figure 3.17). In contrast, replacing the Hot Spot 3 central amino acids

with alanine residues resulted in colonies and pellicles with a YuaB-null phenotype (Figure 3.16). Western blot analysis indicated that this was a consequence of the $YuaB_{HS3}$ protein either not being made, or not being stable, as no protein could be detected (Figure 3.17). Mutation of the F_{51} residue (found in the centre of Hot Spot 1) to a proline resulted in an altered colony phenotype, and a slightly impaired pellicle phenotype (Figure 3.16). This was, however, also associated with significantly reduced (but still detectable) protein levels (Figure 3.17). The instability in the protein was specific to the $F_{51}P$ mutation as the control, $F_{51}Y$ mutation, resulted in wild-type biofilm morphology and wild type protein levels (Figure 3.16 and Figure 3.17). Mutation of the first amino acid of Hot Spot 3, L_{76}, to a proline also resulted in an altered colony phenotype, particularly in the central region of the colony (Figure 3.18). The $L_{76}P$ mutation was also associated with a *yuaB* mutant-like pellicle morphotype. The effect was specific to the introduction of proline, as the $L_{76}I$ substitution mutant of YuaB restored wild type colony and pellicle morphology to the *yuaB* mutant strain (Figure 3.16). Western blot analysis indicated that the $YuaB_{L76P}$ protein was made at near wild-type levels (Figure 3.17). Thus the alteration in the ability to complement the *yuaB* biofilm morphology seen in this strain was due to the change in the predicted aggregation Hot Spot and not due to reduced protein production or stability. As the $L_{76}P$ mutation caused the most significant alteration to the morphology of the biofilm, that was not the consequence of a reduction in protein production, it was chosen for further analysis to assess the nature of the impact.

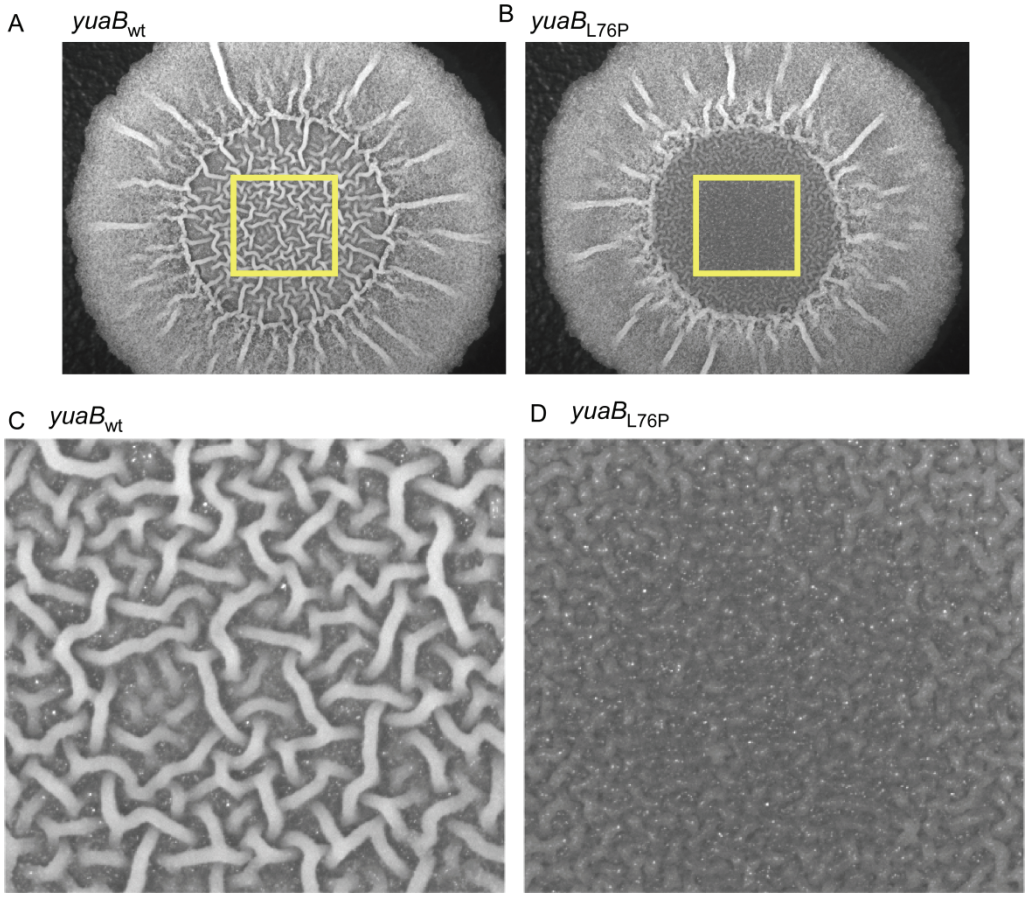

Figure 3.18 Leucine 76 of YuaB is needed for function. Strains imaged are: the *yuaB* mutant complemented with wild type (**A** & **C**) YuaB (NRS2299) and (**B** & **D**) $YuaB_{L76P}$ (NRS3809). Colonies were grown at 30 °C on MSgg medium supplemented with 25 μm IPTG for 48 hours before being imaged.

3.5.2. Mutation of leucine 76 does not alter secondary structure of recombinant protein

The proteins used in the following analyses were expressed and purified by Dr George Penman. Mutation of leucine 76 to proline blocked the ability of $YuaB_{L76P}$ to facilitate biofilm formation and altered the ability of *B. subtilis* to form a complex colony (Figure 3.18). It was plausible that the reduction of biofilm complexity was a consequence of gross alterations in the secondary structure of the protein; therefore the overall secondary and tertiary structures of the wild type YuaB and the $YuaB_{L76P}$ mutant proteins were compared by circular dichroism (CD) spectroscopy analysis of purified proteins. Spectrometric analysis of purified YuaB protein supported the *in*

silico secondary structure prediction and 7% helix, 33% strand, 60% disordered structure was detected. Analysis of the $YuaB_{L76P}$ recombinant protein detected only a minor change in secondary structure content of $YuaB_{L76P}$ (6% helix, 34% strand and 59% disordered structure). Moreover, the comparison of the near UV spectra of the wild type YuaB and $YuaB_{L76P}$ proteins confirmed that the overall tertiary structures remained unchanged (Figure 3.19). Thus no significant change in the secondary structure was observed; demonstrating that the introduction of the proline at position L_{76} has specific, rather than pleiotropic, effects on YuaB folding and thus function.

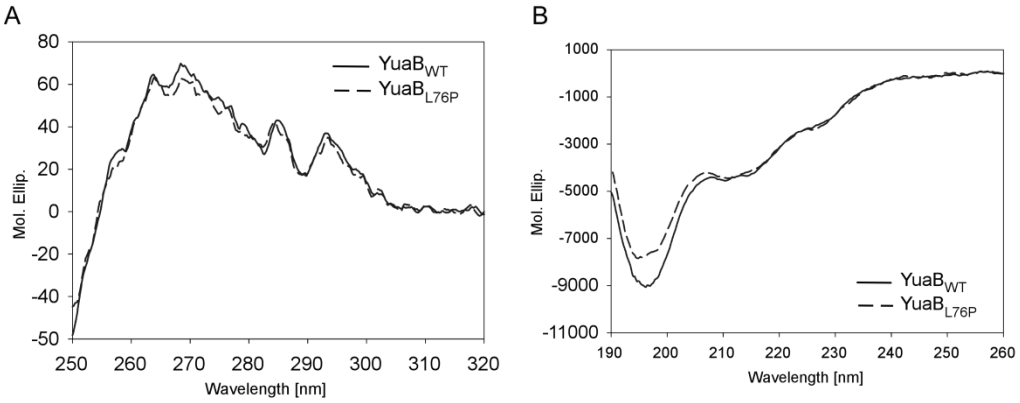

Figure 3.19 The overall structure of $YuaB_{L76P}$ is similar to that of the wild type YuaB. (**A**) A near UV spectrum and (**B**) Circular dichroism spectroscopy of purified wild type YuaB and $YuaB_{L76P}$ proteins showing only minor changes to topology in the $L_{76}P$ mutant protein.

3.6. Mutation of leucine 76 to proline affects localisation of YuaB

3.6.1. Mutation of leucine 76 to proline disrupts YuaB-cell association

In the pellicle biofilm YuaB is cell-associated and prevalent at the base of the biofilm (Section 3.2.1, Figure 3.3). The presence of $YuaB_{L76P}$ reduced the ability of *B. subtilis* to form a pellicle biofilm despite the protein being produced and folded in a manner equivalent to the wild type protein (Figure 3.17 and Figure 3.19). Therefore, it was plausible that the $L_{76}P$ mutation may disrupt the YuaB-cell association observed in the pellicle. The cell-association of $YuaB_{L76P}$ in pellicles was tested by biofilm

fractionation and Western blotting. In contrast to the wild type protein, the localisation profile of $YuaB_{L76P}$ showed that the mutated protein is no longer associated with the cells but is released to the growth media (Figure 3.20). These findings suggest that leucine 76 in YuaB is essential for the cell association of YuaB, and without this interaction, YuaB is released into the biofilm matrix and subsequently into the growth media.

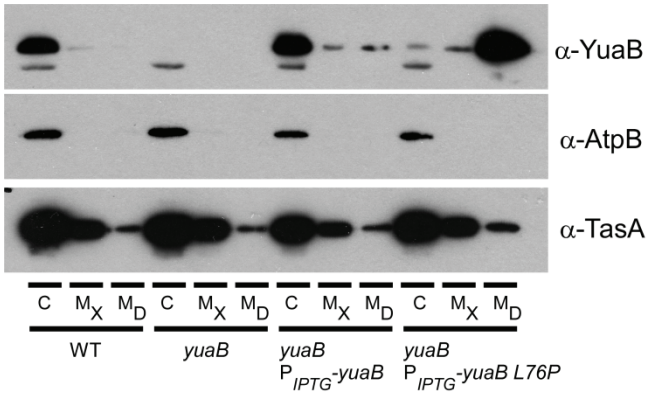

Figure 3.20 $YuaB_{L76P}$ localisation in the analysed by fractionation and Western blotting. Wild type (3610), the *yuaB* mutant (NRS2097) and the *yuaB* mutant strain complemented by either wild type YuaB (*yuaB*, *amyE*::P_{IPTG}-*yuaB*-*lacI*; NRS2299) or $YuaB_{L76P}$ (*yuaB*, *amyE*::P_{IPTG}-*yuaB*$_{L76P}$-*lacI*; NRS3809) strain pellicles were separated into cell (C), matrix (M_X) and growth medium (M_D) fractions. The localisation of YuaB was determined by Western blotting, by comparison with the amyloid-fibre protein TasA and the membrane-bound AtpB, which was used as a control for cell lysis.

3.6.2. $YuaB_{L76P}$ does not form uniform raft at the base of the pellicles

To determine the impact of mutating leucine at position 76 to proline on the localisation of $YuaB_{L76P}$ *in situ*, immuno-fluorescence combined with CSLM was used. The first striking observation was that $YuaB_{L76P}$ is unable to restore the spatial arrangement of the cells characteristic for the wild type biofilm (Figure 3.21). Consistent with the Western blot of the fractionated pellicle (Figure 3.20), $YuaB_{L76P}$ had an altered localisation profile by comparison with the wild type protein (Figure 3.22). $YuaB_{L76P}$ specific staining no longer coated along, and between, the cells in the pellicle in the relatively uniform manner seen for the wild type protein (Figure 3.22), rather

the fluorescence was punctate, and lacked the high level of association with the cells that was observed in the wild type pellicle. This correlated with a significant reduction in the abundance of the $YuaB_{L76P}$ stained material across a field of view (compare Figure 3.4D). However, despite these differences, the $YuaB_{L76P}$ staining remained prevalent at the base of the pellicle at the liquid-cell interface (Figure 3.4D and Figure 3.22).

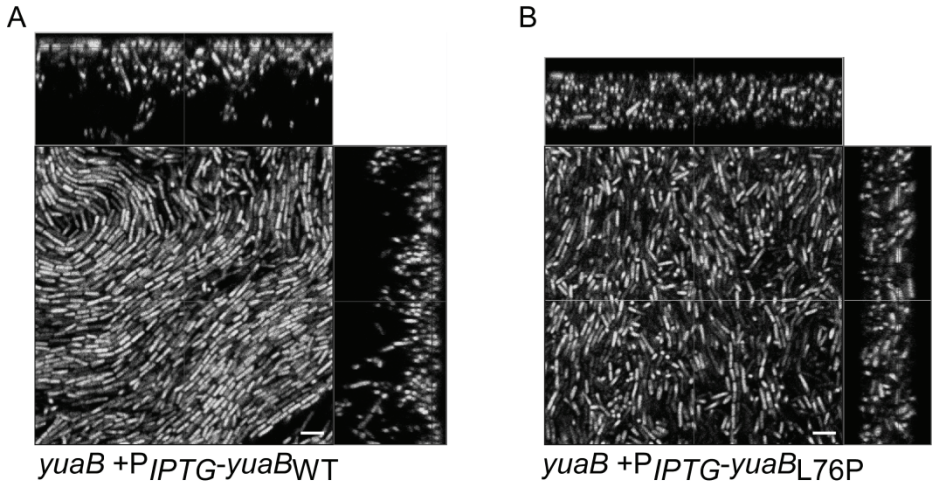

Figure 3.21 $YuaB_{L76P}$ does not restore cell alignment in the biofilm pellicle. Orthogonal views of biofilm pellicles captured with CLSM of the *yuaB* mutant complemented by either (**A**) wild type YuaB (NRS3790) or by (**B**) $YuaB_{L76P}$ (NRS3948). The XY fields represent the same relative Z plane of each pellicle. Scale bars represent 5 µm.

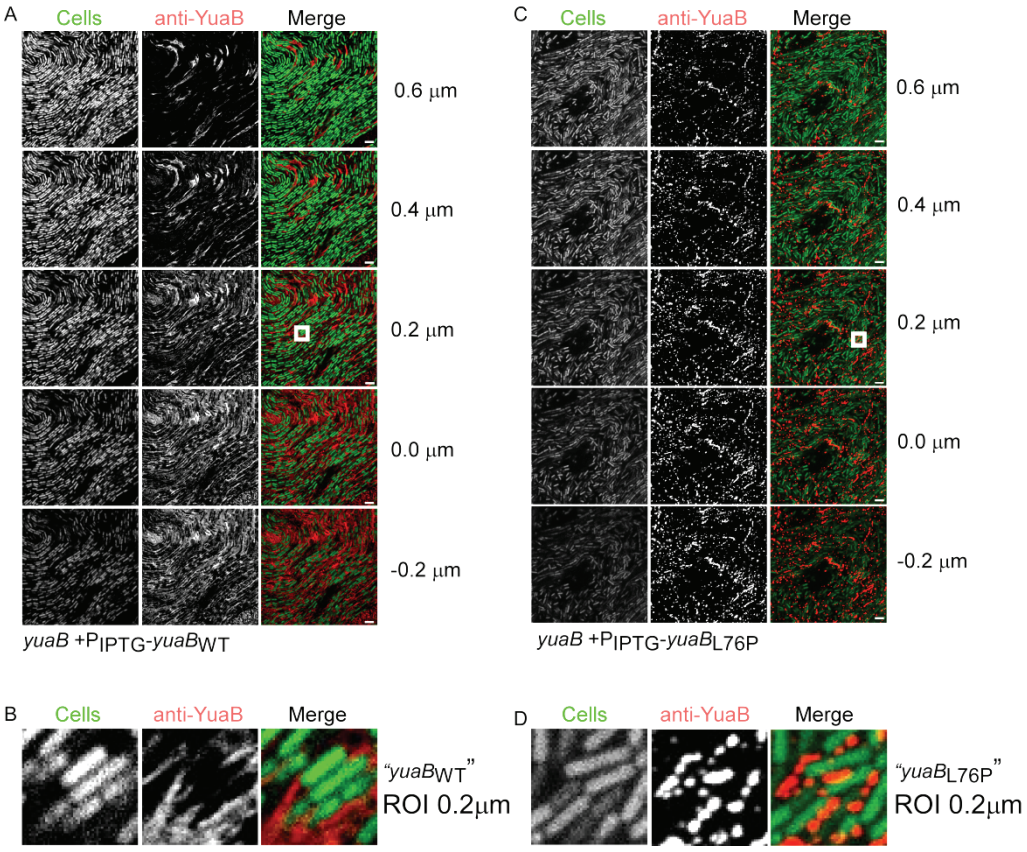

Figure 3.22 *In situ* localisation of YuaB$_{L76P}$ in the pellicle biofilm by immuno-fluorescent staining. CLSM images of pellicles of the *yuaB* mutant strain complemented by either wild type YuaB (**A** and **B**) or by YuaB$_{L76P}$ (**C** and **D**). Fluorescence from the GFP within the cells is presented in white in the left hand columns or false coloured green in the merged image, whilst fluorescence associated with DyLight594, representing immuno-labelled YuaB staining is presented in white in the middle columns or false coloured red in the merged image. (**B** and **D**) represent the regions of interest highlighted by the white box in part **A** and **C** respectively at a higher magnification. The scale bars represent 5 μm.

3.6.3. YuaB$_{L76P}$ is more diffused in complex colonies

The L$_{76}$P mutation disrupts formation of the raft by YuaB in pellicles. It was of interest to test whether similar effect of this mutation is the cause of the reduced complexity of complex colonies formed in presence of YuaB$_{L76P}$. To test this complex colonies formed by the strain expressing YuaB$_{L76P}$ (NRS3948) were subjected to microsectioning, and YuaB$_{L76P}$ was visualised using immuno-fluorescence. Unlike the wild type YuaB protein, the YuaB$_{L76P}$ mutant protein was found to form a thick and distorted layer around the cells (Figure 3.23B). Furthermore protrusions of YuaB$_{L76P}$ stained material into the cell biomass could be seen. These findings indicate that

leucine 76 is required to allow YuaB to form a tight coat around the colony, which was hypothesised to confer a protective function [see Section 4.1.3.2 and (Kobayashi & Iwano, 2012)].

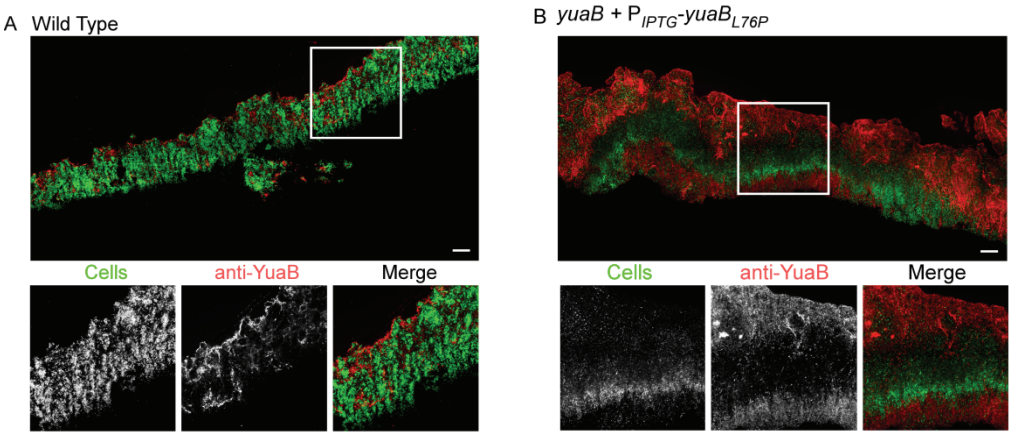

Figure 3.23 *In situ* analysis of $YuaB_{L76P}$ localisation in the complex colony biofilm. Confocal scanning laser microscopy images of a cross-section of a complex colonies formed by (**A**) the wild type (NRS1497) or (**B**) the *yuaB* mutant strain complemented by $YuaB_{L76P}$ (*yuaB*, *amyE*::P_{IPTG}-*yuaB*$_{L76P}$-*lacI*, *sacA*::P_{IPTG}-*gfp*; NRS3948). The smaller images show the region of interest highlighted by the white box at higher magnification. Fluorescence from the GFP within the cells is shown in green in the large panel and in the merged image, and white in the left hand image at higher magnification. Fluorescence associated with DyLight594, representing immuno-labelled YuaB staining is shown in red in the large panel and merged image, and white in the central higher magnification image. The scale bars represent 50 µm.

3.7. Summary

The two principal findings presented in this chapter are: *i*) YuaB is associated with the cell in biofilm pellicles but is released to the biofilm matrix in complex colonies; and *ii*) the dual type localisation of YuaB indicates that the pellicle and complex colony are two distinct types of a biofilm formed by *B. subtilis*. Furthermore, YuaB was shown to form visually larger structures which could be indicative of aggregation or amyloid formation. Despite the fact that YuaB exhibits several amyloidogenic-like properties, *i. e.* Congo Red binding and presence of aggregation-prone Hot Spots, the results presented above are preliminary. To date YuaB was not seen to form amyloid fibres *in vitro* that could be monitored either with direct TEM observation or by spectroscopy, as it was shown for TasA (Romero *et al.*, 2010). Basing

on the information available, the hypothesis of YuaB forming amyloid-like structures cannot be dismissed. However, it is likely that YuaB forms aggregates of a so far unknown nature, structure of which does not resemble amyloid fibres (see Section 4.2).

Furthermore, YuaB was shown to be self-segregating to the interfaces of the biofilm with the liquid substratum in the case of biofilm pellicles and to the air-cells and agar-cells interfaces of the complex colonies. How YuaB localises to these interfaces is currently unknown. However, the association of YuaB to the pellicle-enclosed cells might be an indication of an unknown binding partner that is produced in the pellicle, but absent in complex colonies, where YuaB can be released from the immediate vicinity of the cells. Additionally, a single amino acid substitution of leucine 76 to proline was shown to be able to abolish the self-segregation and aggregation-like properties of YuaB without inflicting major changes to the conformation of the protein. This mutation also abolished the cell-association of YuaB in biofilm pellicles, which may infer the loss of interaction capabilities with the partner protein in this mode of biofilm formation.

A major contribution to the methodology of biofilm protein investigation is the adaptation of the immuno-fluorescent labelling of biofilm proteins for localisation *in situ*. A similar study was recently published where immuno-fluorescence was used to localise proteins within the biofilm formed by *Vibrio cholerae* attached to solid surfaces (Absalon *et al.*, 2011). However, to our knowledge, the first example of immuno-fluorescence and high resolution microscopy of a biofilm formed on a liquid surface and that of the complex colony is presented in this thesis.

4. Discussion

The biofilm matrix formed by *Bacillus subtilis* is comprised of two structural components, the TasA amyloid fibre forming protein and the exopolysaccharide (Branda *et al.*, 2004, Kearns *et al.*, 2005, Branda *et al.*, 2006). However, the data presented in this study clearly show that these components alone are not sufficient to establish a functional, fully mature biofilm. In addition to the aforementioned structural components, a small protein called YuaB is required for maturation of the biofilm. The absence of YuaB results in severe reduction in biofilm-dependent sporulation (Figure 2.1). This is the result of a reduction in the final differentiation of the sporulating cells from the biofilm matrix producing cells, which normally marks the final stage of *B. subtilis* biofilm formation (Vlamakis *et al.*, 2008). However, the biofilm formation defect is not caused by the absence of either TasA or EPS, as both matrix components are synthesised and assembled correctly in the *yuaB* mutant biofilm (Figure 2.25, Figure 2.26 and Figure 2.27). Therefore, YuaB is the third factor required for assembly of the biofilm matrix, and it acts in synergy with TasA and the EPS. This work was published in the Journal of Bacteriology (Appendix D).

4.1. YuaB shows two distinct localisation profiles in the biofilm

4.1.1. Localisation of YuaB depends on the type of biofilm formed

To interact with the extracellular components of the biofilm matrix, YuaB must be exposed to the extracellular environment. Indeed YuaB was predicted to contain an N-terminal signal peptide directing it to the Sec general secretion pathway (Figure 2.15) and was identified as a member of the secretome of *B. subtilis* (Antelmann *et al.*, 2001). The presence of the signal peptide and the requirement for YuaB to be secreted from the cell was confirmed by genetic manipulation of the signal peptide. This

included an exchange of the native signal peptide with one of an unrelated secreted protein, WapA (Figure 2.15). Interestingly, analysis of the localisation of YuaB in the biofilm revealed two profiles, which are defined by the "type" of biofilm formed. In the pellicle biofilm at the air-liquid interface, YuaB was found to be cell wall-associated by immuno-gold labelling of early stage pellicles linked with TEM. This result was confirmed by biofilm fractionation and Western blotting of mature pellicles and by *in situ* biofilm protein visualisation using immuno-fluorescence labelling and CLSM. Each of these methods indicates an association of YuaB with the biofilm enclosed cells throughout the development of the pellicle. Contrary to this, fractionation of fully matured complex colonies revealed that YuaB was released from the cells and located predominantly in the biofilm matrix (Figure 3.9). This localisation pattern was also seen in complex colonies throughout colony development (data not shown). *In situ* analysis of YuaB localisation in this biofilm "subtype" revealed a distinct layer of YuaB at both the agar-cell and air-cell interfaces (Figure 3.8). These findings confirmed that YuaB is not associated with the cell wall of cells in the complex colony.

The reason for differential localisation of YuaB in the biofilm subtypes is unknown. Furthermore, it is not known how YuaB is associated with the cell wall in the pellicles. Extracellular proteins that are covalently bound to cell walls of Gram-positive bacteria typically contain an LPxTG peptidoglycan binding motif (Nguyen *et al.*, 2011). However, such a motif is not found in the primary amino acid sequence of YuaB (Figure 3.11). Moreover, YuaB can easily be dissociated from the cell wall in high osmolarity conditions (Figure 2.18). These are the conditions that have been shown to promote dissociation of proteins non-covalently bound to the cell wall (Brown, 1973). Therefore one possible explanation is a requirement for an unknown binding partner that keeps

YuaB anchored to the cell. This would need to be absent from the complex colony subtype of biofilm. It would be of interest to attempt to isolate any partner proteins using co-immuno precipitation experiments.

4.1.2. YuaB forms a "raft" at the base of a pellicle

The methods for detection of biofilm proteins applied to date in the study of *B. subtilis* biofilms are based on methodology resulting in disruption of the native biofilm structure (Branda *et al.*, 2006, Romero *et al.*, 2010). Therefore, these methods are not suitable for analysing the localisation of a protein in the context of the biofilm as a whole. A widely used method of imaging whole biofilms is confocal laser scanning microscopy, most commonly applied to study biofilms with high adhesive properties, such as those formed by *E. coli* or *P. aeruginosa* (Tolker-Nielsen *et al.*, 2000, Reisner *et al.*, 2003). However, with the exception of laboratory strains (Terra *et al.*, 2012), *B. subtilis* forms biofilms that do not adhere to abiotic surfaces in laboratory conditions. Therefore, a new method of sample preparation for confocal microscopy was required for biofilm-wide observation of the *B. subtilis* biofilm structure. The mannose-binding lectin Concavalin A was found to provide sufficient binding of the developed biofilms to glass coverslips to allow for application of more traditional immuno-labelling techniques.

Using a methodology that combined specific labelling of proteins and high resolution microscopy, YuaB was seen to form a raft at the base of the pellicle in which the cells seemed to be embedded (Figure 3.3). The novel imaging technique applied to capture the 4-dimensional images of pellicles allowed for mathematical analysis of YuaB localisation. Penetration of YuaB-specific staining in the biofilm was quantified by assessing the signal-positive pixels throughout the stack of acquired Z-sections. This

analysis revealed that the majority of YuaB is located directly below the cell layer and engulfs only the first cells at the liquid interface of the pellicle (Figure 3.4 and Figure 4.1). Analysis of the cell orientation in the pellicle demonstrated that the absence of the YuaB layer caused disarrangement of the cells in the biofilm (Figure 3.1). It will be of interest to identify if localisation of YuaB is directly linked to presence or polymerisation of TasA, or the EPS, since YuaB acts in synergy with both of these macromolecules. First attempts to detect TasA *in situ* in the biofilm were unsuccessful, as the TasA-specific antibody was unsuitable for immuno-fluorescence methodology (data not shown). To the best of our knowledge, a technique similar to the one described above, was applied only once in the past (Absalon *et al.*, 2011). However, the analysed biofilm was that of *Vibrio cholerae,* which naturally adheres to glass surfaces, and the data presented was of lower resolution then that obtained in the experiments described here. Therefore, the pellicle imaging technique described here is a significant improvement in the field of biofilm protein detection.

The finding that YuaB is located exclusively to the base of a biofilm pellicle was surprising, as YuaB has been shown to be transcribed by all of the cells in the biofilm [Section 3.2.3 and (Kovacs & Kuipers, 2011)]. The mechanism promoting such a specific localisation of a protein that is produced by the entire community, but also associated with the cell wall in some circumstances, is unknown. A possible explanation is that YuaB is secreted by all cells in the pellicle and subsequently bound to the cell wall by a bimodally expressed anchor protein that is located at the base of the pellicle. However, this hypothesis is unlikely. This is due to the lack of complementation of the pellicle morphology during co-culture experiments where 50% of the biofilm population expressed *yuaB* (See below and section 2.6). The cause of this contradiction

remains unknown. Currently the immuno-fluorescence CLSM method is being developed further to allow for simultaneous detection of YuaB and TasA proteins to investigate the mutual effects on localisation, function and interaction between these two proteins in a mature biofilm.

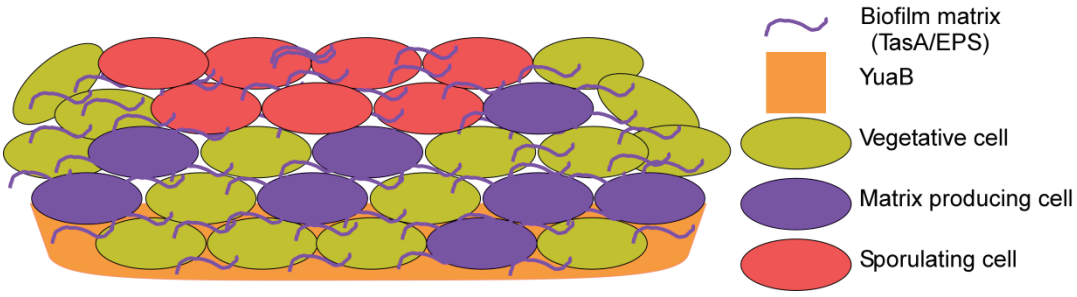

Figure 4.1 Schematic representation of a mature biofilm pellicle. The YuaB "raft" (shown in orange) supports the pellicle structure at the base of the pellicle where the subpopulation of cells is dedicated to synthesise the biofilm matrix (shown in purple). The mature structure of the pellicle allows for differentiation of sporulating cells (shown in red).

4.1.3. YuaB forms an interface layer in complex colonies

The localisation of YuaB in the complex colony form of biofilm was identified using cryo-sectioning of mature complex colonies. This allowed visualisation of proteins in the biofilm sections using specific fluorescently labelled antibodies. As was the case with imaging of pellicles, the images of complex colonies presented in this work are of significantly higher resolution than any results present in the literature to date [see examples in (Vlamakis *et al.*, 2008, Lopez & Kolter, 2010, Kobayashi & Iwano, 2012)]. The combination of the immuno-detection of proteins and high resolution microscopy allowed for the identification of an interface layer formed by YuaB in complex colonies. It is not known how YuaB is targeted to the interfaces of the complex colony. However, it once again highlights how a product of a unimodally transcribed gene can display a distinct spatial localisation profile in a mature biofilm. It

will be of interest to learn if other proteins involved in biofilm formation in different species also display similar localisation profiles.

4.1.3.1. YuaB is a shared resource in complex colonies

The TasA amyloid fibres and the EPS components of the biofilm matrix can be shared by the entire community (Branda *et al.*, 2006). Analogous experiments, to determine if YuaB can be shared between the members of the biofilm, have shown that this was the case for complex colonies but not for pellicles (Figure 2.22 and Figure 2.24). Only partial restoration of the pellicle formation was observed, even when the expression of YuaB was increased in the subpopulation of YuaB-positive cells (Section 2.6). At the time, these experimental results could not be explained. However, the discovery that YuaB is released from the cells during complex colony formation, but not pellicle formation, explains these findings (Figure 4.2). That said, the mechanism driving the localisation of YuaB to the surface and the base of the complex colony is not known. It can, however, be concluded that once YuaB is released from the cells it can be shared between all cells in the complex colony. Thus YuaB represents a third communal resource for the cells in the biofilm.

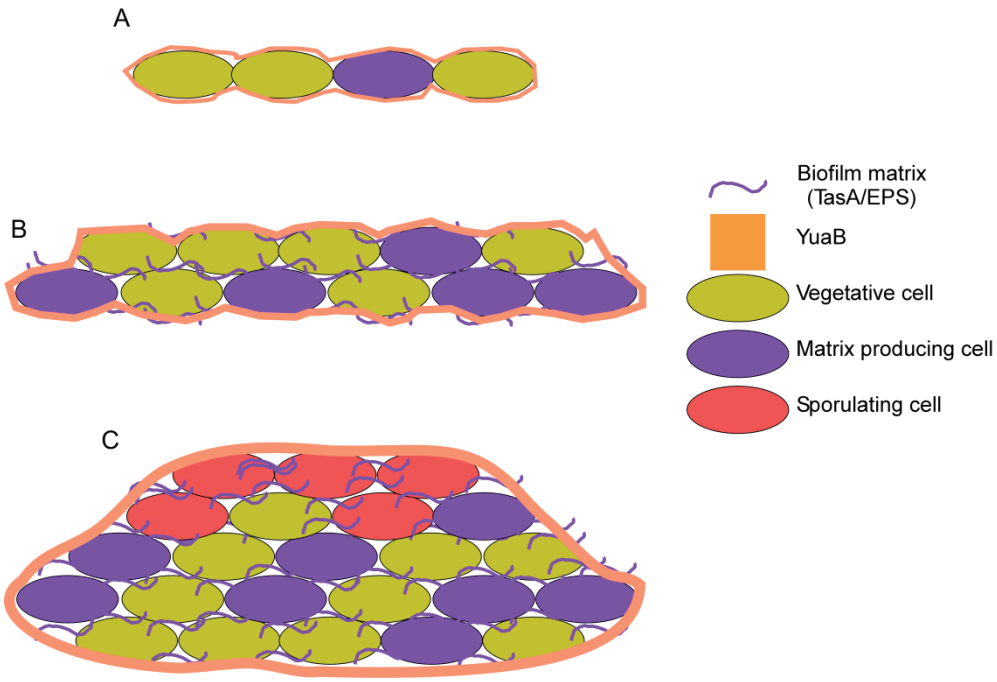

Figure 4.2 Schematic representation of major stages in complex colony development. (**A**) The first matrix producing cells (shown in purple) differentiate from the motile cells (green). The YuaB coat is produced from early stages of biofilm formation. (**B**) The differentiation continues and the biofilm matrix is produced as the colony develops. (**C**) The mature complex colony comprised of cells held together by the biofilm matrix and surrounded by the YuaB coat. The final subpopulation of sporulating cells (shown in red) has emerged and the spore-containing aerial projections are lifted above the surface of the colony.

4.1.3.2. Does YuaB form a hydrophobic barrier?

The wild type biofilm of *B. subtilis* was shown to be a hydrophobic structure (Epstein *et al.*, 2011). This explains the growth on the surface of the liquid media as pellicles, rather than as a submerged biofilm and hydrophobicity of complex colonies (Epstein *et al.*, 2011). The hydrophobicity of the biofilm was mostly attributed to the presence of the EPS in the biofilm matrix (Epstein *et al.*, 2011). However, taking the fact that YuaB localises specifically to the cell-liquid interface in the pellicles and forms a surface layer of the colonies, we speculated that YuaB may contribute to the hydrophobic properties of the biofilm. In this case, the layer of YuaB formed on top and at the base of the colonies would act to protect the cells from the external environment and enhance the overall cohesion of the biofilm. Similarly, the YuaB "raft" formed at the base of the pellicles would allow the cells to form bundles of

chains required for formation of this biofilm subtype. Furthermore, the hydrophobic barrier, formed by YuaB, would support the superstructure of the biofilm on top of the liquid medium. This is yet to be tested experimentally in this laboratory.

4.2. YuaB shows aggregation properties

The immuno-fluorescence CLSM images of both pellicles and complex colonies show YuaB as large fields of seemingly connected material, which can be interpreted as YuaB forming higher order structures. Consistently with this, Dr Francesco Rao (DVA lab) has seen a transient formation of a "skin" or a "layer" of protein on top of solutions of YuaB purified for crystallisation purposes (data not shown). These findings led to the hypothesis that the monomers of YuaB associate with each other to form a structure of a higher order of organisation. The *in silico* analysis of the amino acid sequence of YuaB provided potential confirmation of this hypothesis by identification of putative aggregation-promoting Hot Spots (Section 3.3.2).

4.2.1. In vitro *analysis of polymerisation of YuaB*

YuaB is predicted to contain aggregation-prone regions that were calculated by three independent programmes and labelled Hot Spot 1 to Hot Spot 5 (Figure 3.11). Therefore it is probable that aggregation Hot Spots mediate formation of the higher order structures by YuaB. Indeed, a single amino acid mutation $L_{76}P$, located in the Hot Spot 3, is sufficient to cause lack of aggregation of $YuaB_{L76P}$ which leads to disruption in biofilm formation (Section 3.6). The *in situ* analysis of $YuaB_{L76P}$ localisation indicates that it is unable to form the "raft" at the base of pellicles and is significantly more diffused in complex colonies in comparison to the wild type protein (Figure 3.22 and Figure 3.23). As the overall secondary structure of the protein remains unaffected by the $L_{76}P$ mutation, it can be concluded that the functional aggregation Hot Spots are

essential for the activity of YuaB. However, we are currently not able to assess polymerisation of YuaB *in vitro,* as discussed below.

It was plausible that the aggregation Hot Spots promote polymerisation of YuaB into amyloid fibres. This can be tested using circular dichroism (Blanco *et al.*, 2012), Congo red binding (Klunk *et al.*, 1999) or Thioflavin T fluorescence increase analysis (Saeed & Fine, 1967). However, for any of these methods to be successful, a fully functional purified protein must be obtained. During this project, attempts were made to complement for the absence of endogenic YuaB by addition of purified protein to the developing biofilm. However, these attempts were unsuccessful (data not shown). Nonetheless, the protein samples were analysed by circular dichroism and for Thioflavin T binding to verify the potential formation of amyloid-like fibres. However, no amyloid-specific properties could be detected (data not shown). The *in silico* analysis performed by Dr Francesco Rao, for the purposes of establishing an optimal construct for purification purposes, revealed the presence of highly disordered fragments on the N- and C-terminus of YuaB that are indicated in Figure 4.3. Therefore a new construct was designed so that the terminal disordered fragments were not expressed (Figure 4.3). The newly designed protein also failed to complement the absence of endogenous YuaB in the biofilm (data not shown). The reason why the attempts to complement the mutation of YuaB with ectopically added protein were unsuccessful is not clear. However, a possible explanation is outlined in the following section.

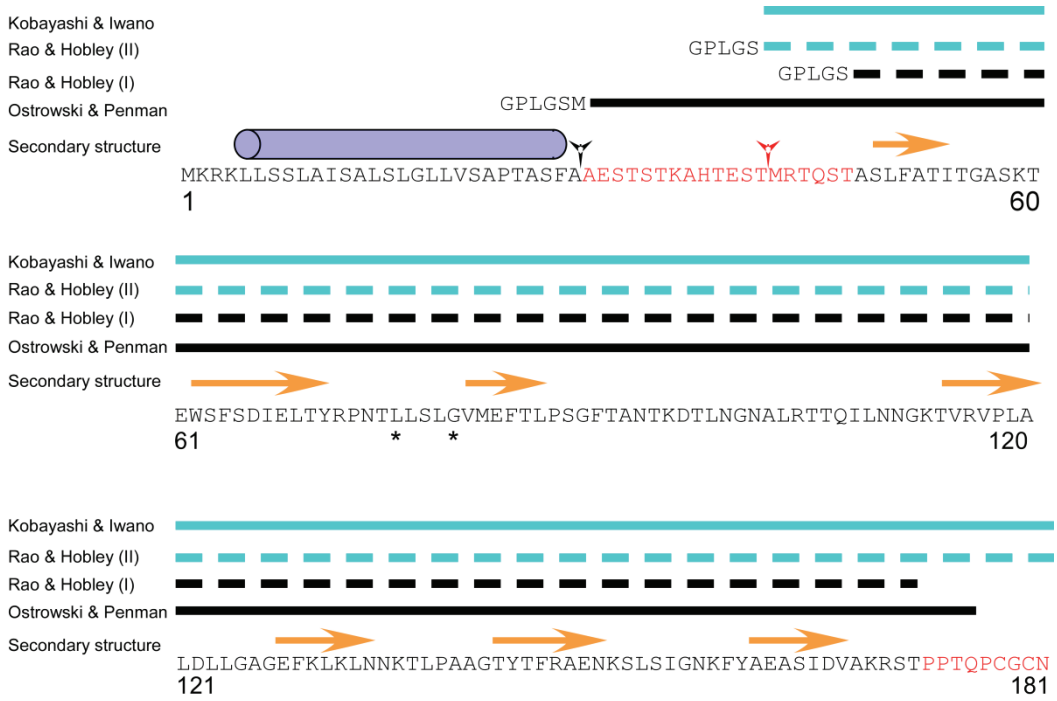

Figure 4.3 Different protein constructs used for purification and structural analysis of YuaB/BslA. The primary amino acid sequence of YuaB/BslA and the secondary structure as predicted by PsiPred are indicated. The four constructs designed by Ostrowski, Rao and Kobayashi are indicated as solid black, dashed black and blue and solid blue lines respectively. The Rao & Hobley (I) and Rao & Hobley (II) constructs were designed based on the idsordered structure prediction by Rao and by adaptation of the Kobayashi & Iwano construct for GST purification respectively. The N-terminal overhangs resulting from cloning strategy for protein purification are indicated. The signal peptidase cleavage site and the secondary processing site (predicted by Kobayashi & Iwano) are indicated as black and red arrowheads respectively. The highly disordered regions (predicted by Rao) are indicated in red. The leucine 76 and glutamine 80 residues, located in Hot Spot 3 and subjected to mutagenesis, are indicated with asterisks.

4.3. YuaB (BslA) forms a hydrophobic layer on the surface of *B. subtilis* biofilms

While the results presented in the Chapter 4 were being reviewed for publication, another laboratory published a report showing YuaB to form an amphiphilic barrier on top of the complex colonies of *B. subtilis* (Kobayashi & Iwano, 2012). The authors re-named YuaB as BslA (biofilm-surface layer protein) to reflect this property. Kobayashi and Iwano identified YuaB/BslA as a major factor contributing to the hydrophobicity of the biofilm, alongside the EPS. They showed that a strain unable to synthesise YuaB/BslA forms a biofilm that is significantly more susceptible to surface wetting (Figure 4.4). This alone supported the hypothesis of the hydrophobic barrier

formed by YuaB/BslA at the interfaces of the biofilm, which has been put forward in this thesis. Furthermore, Kobayashi and Iwano purified a YuaB/BslA variant, which was used to complement the *yuaB/bslA* mutant strain by ectopically adding the purified protein to the developing biofilm (Kobayashi & Iwano, 2012). It is assumed that the discrepancy, between the results of Kobayashi and Iwano and those presented here, in relation to the possibility of ectopic complementation of the *yuaB/bslA* mutant can be explained by the differences in the protein overexpression and purification construct. The different protein constructs used for experiments on complementation of the *yuaB/bslA* mutant are presented in Figure 4.3. The predominant difference between the construct used by Kobayashi and Iwano and those used in this study is the presence of a five amino acid overhang at the N-terminus. This is the result of the purification method. It is plausible that this N-terminal overhang inhibits the ability of YuaB/BslA to form higher structures *in vitro*. However, this possibility is yet to be tested and is ongoing work in the lab.

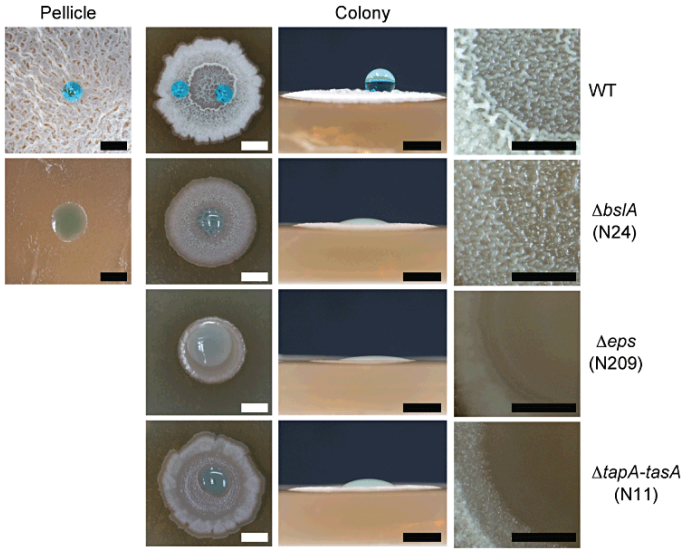

Figure 4.4 BslA(YuaB) forms a hydrophobic layer on the surface of *Bacillus subtilis* biofilms. Water drops coloured with xylene cyanol were placed on top of pellicles of the wild type and *yuaB/bslA* mutant and on complex colonies formed by the wild type, *yuaB/bslA, eps* and *tapA-tasA* mutants. The panels to the right are magnified images of complex colonies. Scale bars represent 2 mm. Taken from (Kobayashi & Iwano, 2012)

Kobayashi and Iwano used their purified YuaB/BslA protein to show polymerisation of YuaB/BslA *in vitro* into higher structures (Kobayashi & Iwano, 2012). This indirectly supports the observations from the immuno-labelling CLSM presented here. Furthermore, fluorescently labelled YuaB/BslA was successfully used to restore the wild type morphology of a complex colony and found to form a uniform layer on top of the complex colony (Figure 4.5). This is analogous to the *in situ* analysis of YuaB localisation in complex colonies presented in Section 3.2. Moreover, Kobayashi and Iwano isolated a YuaB/BslA$_{G80D}$ mutant which is unable to polymerise and cannot rescue the *yuaB/bslA* mutant phenotype. Interestingly, the glycine 80 residue is located in the middle of the Hot Spot 3, where leucine 76 is also located. L_{76} was identified in this thesis as important for the aggregation of YuaB and thus its function at the biofilm interfaces. The effects of the L_{76}P and G_{80}D mutations have very similar results on biofilm formation. This further supports the finding that Hot Spot 3 is required for functionality of YuaB/BslA. Currently attempts are being made to test if the YuaB/BslA construct described by Kobayashi and Iwano can be used in the NSW laboratory to complement the morphology of the *yuaB/bslA* mutant.

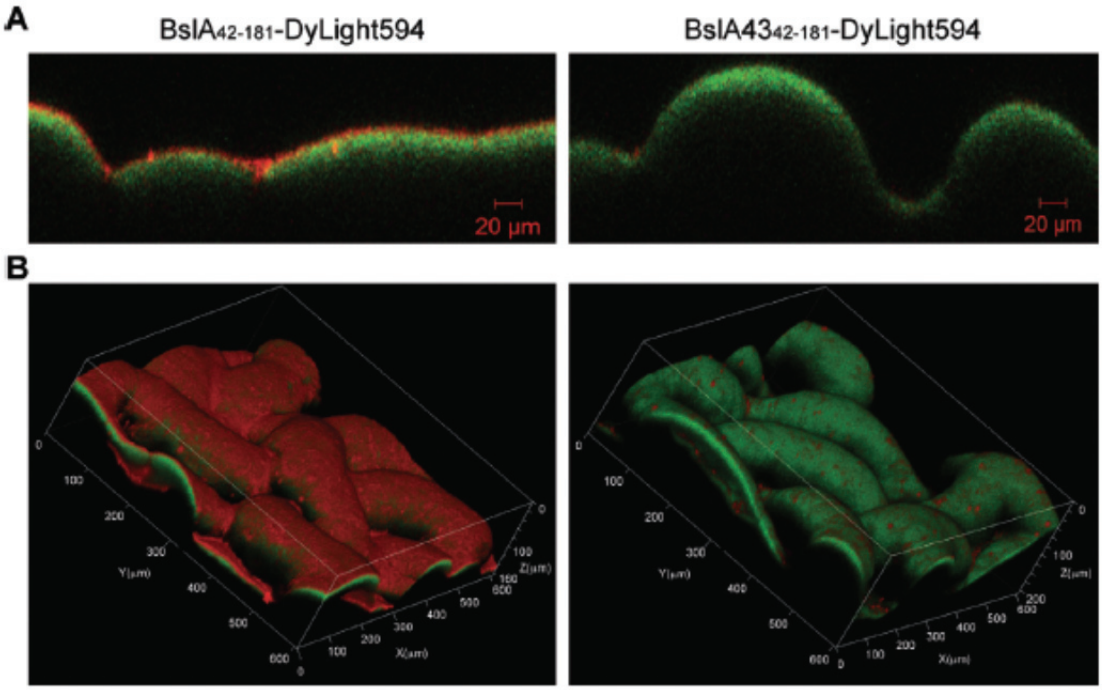

Figure 4.5 Ectopically added wild type YuaB/BslA (left panel) forms a surface layer on complex colonies, whereas the YuaB/BslA$_{G80D}$ (right panel) mutant is not functional. Purified, fluorescently labelled YuaB/BslA was added to the culture of exponentially growing cells of the *yuaB/bslA* mutant and spotted on agar-solidified medium. The central regions of resulting mature complex colonies were observed by CLSM. (**A**) Vertical section of the colonies. (**B**) Reconstructed 3-D image of the colonies. The vertical section and the 3-D reconstruction are merged images of GFP (false-coloured green) and DyLight594 (false-coloured red). Taken from (Kobayashi & Iwano, 2012).

4.4. Suggested future work

The findings presented above greatly contribute to the understanding of how the small secreted protein YuaB (recently re-named as BslA) contributes to the formation of a biofilm by *B. subtilis.* However, these results also leave many open-ended questions on the molecular mechanism of YuaB/BslA function and the nature of its interaction with the other components of the biofilm matrix and for that matter the biofilm-dwelling cells. It will be interesting to elucidate in the future if the predicted aggregation Hot Spots indeed interact with each other and what the physical nature of the resulting aggregate or polymer is? Does it form amorphic aggregates like those proposed by Kobayashi and Iwano or does it form amyloid fibres? YuaB/BslA displays a fascinating tendency not only to self-segregate to the interfaces of the biofilm, but also

to associate with the biofilm cells specifically in pellicles. Such a phenomenon suggests the presence of an unidentified protein partner that will mediate attachment to the cells. Identification of such a partner protein, or proteins, would greatly increase our understanding of protein localisation in biofilms. Finally it would shed light on the mechanism allowing a unimodally expressed protein to localise to specific parts of the biofilm.

4.5. Emerging patterns of protein interactions in the biofilm matrix

4.5.1. Proteins with similar traits to YuaB/BslA are found in different microorganisms

Proteins polymerising into higher structures are commonly found in bacterial biofilms. Examples of such polymeric proteins are amyloid fibres (Larsen *et al.*, 2007). One of the major functions of amyloid fibres in biofilms is to promote adhesion to solid surfaces (as discussed in Section 1.2.2.2). However, biofilm adhesion is not the only role played by amyloids in bacterial physiology. Some strains from the *Streptomyces* genus synthesise small secreted proteins, called chaplins (Elliot *et al.*, 2003). These proteins were found to associate with the peptidoglycan where they polymerise to form short amyloid rodlets (de Jong *et al.*, 2009). Once bound to the cell wall, chaplins form a hydrophobic barrier which lowers the surface tension of the liquid environment occupied by the mycelium (Claessen *et al.*, 2003). The reduction of surface tension allows for "lifting" of the aerial hyphae above the liquid surface. Subsequently the spore-containing filaments can be generated (Elliot *et al.*, 2003). The *in silico* analysis of the ChpH sequence, one of the chaplins from *Streptomyces coelicolor*, revealed the presence of aggregation Hot Spots (Capstick *et al.*, 2011). In summary, chaplins and YuaB share multiple similarities, including the presence of aggregation Hot Spots,

association with the cell wall and involvement in the development of multicellular structures. Therefore one might predict a similar, if not analogous, function of YuaB to that of chaplins.

Interestingly, hydrophobins that are found in various fungi are another family of proteins, which while unrelated to YuaB, possess similar characteristics (Linder *et al.*, 2005). Similarly to the chaplins and YuaB, hydrophobins are found associated to the cell wall of fungal hyphae, where they form an amphiphilic layer [reviewed in (Wosten & de Vocht, 2000)]. Analogous to the chaplins in *Streptomyces*, hydrophobins are responsible for lowering the surface tension to allow for the erection of the aerial structures (Morris *et al.*, 2011). Hydrophobins are divided into two classes *i*) those that form amyloid fibres (Class I) and *ii*) those that aggregate into non-amyloidous higher structures (Class II) (Elliot & Talbot, 2004). The Class II hydrophobins are secreted from the mycelium and accumulate at the air-liquid interface to lower the surface tension [as reviewed in (Elliot & Talbot, 2004)]. It is plausible that the accumulation of YuaB at the interfaces of complex colonies is driven by similar mechanisms.

4.5.2. Functional pairs of proteins allow biofilm formation

Metabolic analysis of various biofilm communities have shown some subpopulations of cells do not actively contribute to synthesis of the biofilm matrix (Fux *et al.*, 2005a, Vlamakis *et al.*, 2008, Lopez *et al.*, 2010, Berk *et al.*, 2012). Nonetheless, the metabolically inactive cells are surrounded by groups of active cells and the entire community benefits from the biofilm enclosure (Lopez *et al.*, 2010). Two proteins from *B. subtilis*, YuaB/BslA and TasA, co-operate with each other and with the exopolysaccharide to form a functional biofilm matrix (Ostrowski *et al.*, 2011). The biophysical properties of YuaB/BslA, and the phenotypes associated with its mutations,

place it in a small, but growing, group of biofilm proteins that can be used as a shared resource (Lopez *et al.*, 2010). Interestingly, TasA and YuaB/BslA are not the only proteins that form a "functional pair" during biofilm formation. Another example is found in *Staphylococcus* biofilms. The biofilm associated protein Bap functions as an adhesin allowing for formation of a biofilm on solid surfaces (Lasa & Penades, 2006). Homologues of Bap are found in a widespread range of microorganisms, including *Staphylococcus epidermidis* (Latasa *et al.*, 2006). *S. epidermidis* also synthesises a hydrophobic protein Aap which is needed for biofilm formation (Rohde *et al.*, 2005). Aap appears to form strands; thus it was suggested that it was responsible for developing cell-to-cell interactions over larger distances (Banner *et al.*, 2007, Kuehl *et al.*, 2009).

Recent studies have also identified two proteins synthesised by *V. cholerae*, the Bap1 and RhmA, proteins which form a functional pair during biofilm formation (Absalon *et al.*, 2011). In this background, Bap1 localises to the base of the pellicle (similarly to YuaB/BslA) to facilitate biofilm attachment and RhmA is dispersed throughout the biofilm matrix to enhance cell-to-cell interactions (Absalon *et al.*, 2011). Such function is analogous to the predicted function of TasA (Romero *et al.*, 2010). Further insight into the biofilm of *V. cholerae* revealed another protein, RbmC, which co-localises with Bap1 to further enhance biofilm formation (Berk *et al.*, 2012). This study also revealed cell clusters in the *Vibrio* biofilm surrounded by an "envelope" formed by the Bap1/RbmC proteins and the *Vibrio* polysaccharide VPS. Bap1 is therefore a second example of a protein forming a layer around the cells that in this case is required for biofilm formation by a Gram-negative bacterium.

4.6. Concluding remarks

Formation of structurally complex biofilms is a common feature of many bacterial species (Costerton *et al.*, 1987). Despite the time devoted to biofilm research, many aspects of this type of social behaviour of bacteria remain unclear. To date many different groups of proteins, polysaccharides and other biomolecules have been indicated as vital for formation of a biofilm by different species of bacteria. However, with an increase in the understanding of biofilm development, patterns of analogous mechanisms driven by genetically unrelated systems have emerged. An increasing number of proteins that form similar structures, such as amyloid fibrils, are being identified (Larsen *et al.*, 2007). Also the interactions between individual components of the biofilm matrix are becoming better understood (Flemming & Wingender, 2010). In the work presented here, yet another mechanism of protein function during biofilm formation was identified. This is the formation of a protein layer that supports and isolates the cells in the biofilm. Similar patterns are being reported for other organisms, such as *V. cholerae* (Absalon *et al.*, 2011, Berk *et al.*, 2012).

The obvious structural complexity of the biofilm has already been compared to the architecture of the eukaryotic tissue. Here cells are embedded in the extracellular matrix filled with adhesive and structural proteins functioning to protect and nurture the cells (Costerton *et al.*, 1995, Shapiro, 1998). Also similarly to the different cell types present in an animal or plant tissue, various species of bacteria can co-operate to form a biofilm where labour towards common benefit is divided not only between members of a single species (expressing different genetic programmes) but also between different species of different biochemical characteristics (Costerton *et al.*, 1987, Costerton *et al.*, 1994, Lopez *et al.*, 2010). Therefore, further analysis of molecular

interactions that lead to the establishment of a functional biofilm is key to understanding how a multispecies consortium builds a biofilm in the natural environment.

5. Materials and methods.

5.1. Bacterial strains, plasmids and oligonucleotides used in this study

All assays and experiments on the physiology and molecular biology of a biofilm were conducted in the *B. subtilis* wild isolate NCIB3610 and strains derived from NCIB3610 by phage mediated transduction. DNA constructs were integrated into *B. subtilis* chromosome using genetically competent laboratory strain 168. Plasmids were routinely maintained in *E. coli* MC1061 strain. Proteins were overexpressed and purified from *E. coli* BL21 (DE3) strain. All strains plasmids and oligonucleotides listed in this study are provided in the Appendix A.

5.2.Media and antibiotics

5.2.1. Growth media and supplements

All strains were routinely propagated and maintained in Luria-Bertani (lysogeny broth LB) broth [10 g yeast extract (Merck), 5 g NaCl (VWR), 10 g tryptone (Fisher Scientific) per litre] (Bertani, 1951, Sambrook & Russell, 2001, Bertani, 2004) at 37 °C unless stated otherwise. For all biofilm-based analysis MSgg minimal medium was used [5 mM potassium phosphate and 100 mM MOPS at pH 7.0 supplemented with 2 mM $MgCl_2$, 700 µM $CaCl_2$, 50 µM $MnCl_2$, 50 µM $FeCl_3$, 1 µM $ZnCl_2$, 2 µM thiamine, 0.5% (v/v) glycerol, 0.5% (v/v) glutamic acid after autoclaving] (Branda *et al.*, 2001).

Phage transductions were performed in TY medium (LB broth supplemented with 10 mM $MgSO_4$, 1 µM $MnSO_4$) and the post-transduction phage lysogeny was inhibited by supplementing the TY agar with 10 mM sodium citrate (Sambrook &

Russell, 2001). Media were solidified with 1.5% (w/v) agar (Invitrogen) as required. For the generation of genetically competent *B. subtilis*, cells were propagated in the SpC broth [1x T-Base, 1 mM MgSO4, 0.5% glucose (VWR), 0.2% yeast extract (Merck), 0.025% Casamino Acids, 40 µg/ml tryptophan (VWR)] and starved in SpII broth [1x T-Base, 35 mM MgSO4, 0.5% glucose (VWR), 0.1% yeast extract (Merck), 0.01% Casamino Acids, 40 µg/ml tryptophan (VWR)] (Harwood & Cutting, 1990). As required, media for growth and selection of *B. subtilis* were supplemented with following antibiotics: chloramphenicol (Duchefa Biochemie) – 5 µg/ml, kanamycin (Gibco) – 10 µg/ml, a or a combination of erythromycin (Formedium) (1 µg/ml) and lincomycin (Duchefa Biochemie) (25 µg/ml) (hereafter MLS). Selection of *E. coli* strains after transformation and maintenance of plasmids was mediated by supplementing media with ampicillin (Formedium) (100 µg/ml) and/or kanamycin (Gibco) (50 µg/ml) as required. The stock concentrations of antibiotics are outlined in Appendix B. The recombinant gene expression was induced using isopropyl β-D-1-thiogalactopyranoside (IPTG) (Formedium) at a concentration indicated in respective methods.

5.3.Molecular microbiology methods.

5.3.1. Plasmid isolation from E. coli.

Plasmids were routinely isolated from *E. coli* cells with QiaPrep Spin Miniprep Kit (Qiagen) according to the manufacturer's instructions. Briefly, a 3 ml culture of cells in LB broth supplemented with appropriate antibiotics was incubated in 37°C using a rotary shaker in borosilicate glass tubes for 3 h. The culture was collected by centrifugation (17000 g for 1 min) and lysed using alkali lysis (Sambrook & Russell, 2001) reagents provided by the manufacturer. The cell debris was removed by

centrifugation (17000 g for 10 min). The supernatant containing DNA in a high salt concentration buffer was applied to the silica-based medium in a microspin column to allow binding of the plasmid DNA to the medium. The residual DNases and salts were removed using buffers provided in the kit and the plasmid DNA was eluted from the column with ddH_2O.

5.3.2. Isolation of chromosomal DNA from B. subtilis*.*

The chromosomal DNA from *B. subtilis* was isolated and purified using phenol/chloroform method (Harwood & Cutting, 1990). Briefly, 1.5 ml of exponentially growing culture of *B. subtilis* was collected by centrifugation (3000 g for 10 min) and suspended in the lysis buffer (Appendix C) supplemented with 300 µg/ml of lysozyme (Sigma). The cells were incubated at 37 °C for 30 min to allow peptidoglycan digest by lysozyme and was followed by addition of 3.75% Sarkosyl (Sigma) (w/v) to disrupt cell membranes. The proteins in the cell lysate were precipitated by addition (1:1 ratio) of freshly made mixture of saturated and TRIS-buffered phenol at pH 6.6 (Fisher Scientific), chloroform (VWR) and isopropanol (VWR) at the ratio of 25:24:1. The sample was mixed intensively and the DNA-containing water phase and the organic phase were separated by centrifugation (17000 g for 5 min.). The extraction was repeated and DNA was precipitated with 100% ethanol in presence of 0.4 M sodium acetate as a catalyst. The precipitated DNA was collected by centrifugation (17000 g for 3 min.), washed in 70% ethanol, dried and rehydrated in ddH_2O.

5.3.3. Polymerase Chain Reaction-mediated (PCR) DNA amplification.

Amplification of DNA for cloning purposes was performed using Phusion Polymerase (Finzymes) according to manufacturer's instructions. Briefly, 50 µl

reactions were prepared using 200 µM dNTP mix (Appendix C), 0.5 µM forward and reverse primer each, 0.02 U/µl of the polymerase and 0.5 µl of the target DNA in the reaction buffer diluted to 1x concentration in water. The reaction cycle was standardised to initial DNA template melting at 98 °C for 2 min followed by 35 cycles of the template melting at 98 °C, DNA primer annealing at 65.5 °C and DNA elongation for 30 sec per kB at 72 °C. An additional elongation step of 5 min at 72 °C was added at the end of the reaction.

The PCR screening for double cross-over of the designed DNA construct into the target location on the *B. subtilis* chromosome was conducted using Taq polymerase (Qiagen) using reaction substrates as described above and 0.5 U/µl of polymerase in 20 µl reactions. Screening of *amyE* site integration was performed using primer pairs NSW12 and NSW13 or NSW872 and NSW873 (Table 7.3). Screening of *sacA* site integration was performed using primers pair NSW207 and NSW208 (Table 7.3). The typical number of cycles of Taq amplification was 25.

5.3.4. Restriction digest of DNA

All enzymatic restriction digest reactions were performed in a total volume of 50 µl using 1 µl of an appropriate restriction endonuclease (NEB), 5 µl of the suitable 10x concentrated reaction buffer supplied by the enzyme manufacturer and 15 µl of isolated plasmid DNA or 30 µl of purified PCR product. A simultaneous digest with two enzymes was used when possible. The reaction mix was incubated at 37 °C for 3 h.

5.3.5. Site-directed mutagenesis

To incorporate point mutations in the target genes, an adapted QuikChange method from Stratagene was used. The desired mutation was incorporated into the

middle of DNA primers specific to the target sequences (Appendix C). The mutation sites were flanked with at least 15 bp, complementary to the template, on each side and primers were designed so that both forward and reverse primers bind to the same location on the DNA template. Plasmids pNW512 or pNW619 (Appendix C, Table 7.2) were used as a template for the mutagenesis. The DNA amplification was then performed using Herculase II Fusion polymerase (Stratagene), 0.2 mM dNTPs mix, 0.5 µl of the DNA template and 20 ng of each DNA primer. The amplification reaction included initial template melting at 95 °C for 5 min followed by 16 cycles with the DNA template melting at 95 °C for 30 sec, primer annealing at 46 °C for 30 sec and DNA elongation at 68 °C for 15 min. The resulting DNA solution was subject to enzymatic digest with DpnI (to remove entire template DNA) for 3 h at 37 °C to remove the entire template DNA, and competent *E. coli* DH5α cells (DSTT) were transformed with 2 – 10 µl of the reaction mix. The plasmid DNA was extracted from the resulting colonies of *E. coli* and sequenced to confirm incorporation of the designed mutation. The target DNA was then excised from the vector backbone by restriction digest and cloned into the target delivery vector.

5.3.6. Gel electrophoresis of DNA and purification of DNA after enzymatic reactions

Following all enzymatic reactions, the DNA products were resolved in 1% agarose gels prepared in TAE (Appendix C). Electrophoresis was performed in TAE (Appendix C), after which the gels were stained in ethidium bromide and imaged using GelDoc XR system (Bio-Rad). The DNA bands of the desired size were excised from the gel and DNA was purified using QIAquick Gel Extraction Kit (Qiagen) according to the manufacturer's instructions. Briefly, the agarose slice was melted in the high salt

concentration buffer, which enhances DNA binding to the silica medium in the column. The immobilised DNA was washed with ethanol based wash buffer to remove remaining salts and proteins and the DNA was eluted with ddH_2O.

5.3.7. DNA ligation

The purified DNA fragments were ligated using a recombinant ligase from T4 phage (NEB). The reaction was prepared in the total volume of 20 µl typically using 2 µl of the 10x concentrated reaction buffer supplied by the enzyme manufacturer, 2 U/µl of ligase, 6 µl of the digested, purified insert DNA and 1 µl of the digested, purified vector DNA. The reaction was incubated for 2 h at room temperature.

5.3.8. DNA sequencing

All insert sequences in vectors generated with fragments amplified using PCR or after site directed mutagenesis were sequenced to confirm correctness of the sequence. Insertions into pDR111 vector were sequenced using oligonucleotides NSW872 and NSW873 (Table 7.3). All other sequences were sequenced using oligonucleotides used during cloning. The sequencing reactions were performed by DNA Sequencing and Services, DSTT, College of Life Sciences, Dundee.

5.3.9. Preparation of genetically competent E. coli *cells*

The competent *E. coli* cells were prepared using calcium chloride solution as described previously (Sambrook & Russell, 2001). The target strain of *E. coli* was inoculated to an overnight culture in LB broth to propagate. The following morning the cells were diluted 1:1000 into 500 ml of fresh LB broth and allowed to grow until cell density reached $OD_{600} \approx 0.4$. The cells were aliquoted into 50 ml centrifugation tubes,

chilled on ice for 30 min and collected by centrifugation (3000 rpm for 10 min). The cell pellet in each tube was washed in 12.5 ml of sterile ice cold 100 mM calcium chloride (VWR), collected by centrifugation and resuspended in 4 ml of sterile ice cold calcium chloride. Sterile glycerol (Fisher Scientific) was added to a final concentration of 10%, than the cells were aliquoted to Eppendorf tubes and frozen in liquid nitrogen. The competent cells were stored in -80 °C until needed.

5.3.10. E. coli *transformation*

For transformation of competent *E. coli* cells 10 µl of the ligation reaction mix was added to 100 µl of competent *E. coli* cells and incubated on ice for 30 minutes. The cells were then heat shocked for 3 min at 42 °C and placed on ice for 1 min. If ampicillin was used as the selection marker the entire transformation mix was lawn plated on ampicillin-containing LB agar plates. For selection using kanamycin, 700 µl of pre-warmed LB broth was added to the cell suspension after the heat shock and the cells were allowed to recover for 45 min at 37 °C while agitated. The cells were centrifuged for 10 min at 3000 g, resuspended in 100 µl of media and plated on kanamycin-containing LB agar plates. The plates containing transformed cells were incubated overnight at 37 °C.

5.3.11. Preparation of B. subtilis *competent cells*

The cells of the *B. subtilis* strain 168 were streaked out on an LB agar plate to single colonies and incubated overnight at 37 °C. A resulting single colony was suspended in 100 µl of LB broth and diluted 10x. The cell suspension and its dilution were lawn-plated on an LB agar plate and incubated overnight at 20 °C. The resulting cells were washed off with a wash buffer (Appendix C). The OD_{600} of the cell

suspensions was measured and the suspension with OD_{600} lower than 1 was diluted to OD_{600} = 0.01 in SpC medium. The cells were incubated at 37 °C with agitation for 5 hours. Following the incubation, the cells were diluted 1:10 in the SPII medium and were incubated for 90 min at 37 °C with agitation. The cell culture was then collected by centrifugation (3000 g for 10 min) and resuspended in 0.5 ml of the supernatant. As required, sterile glycerol was added to a final concentration of 10% and the cells were kept at -80 °C until needed.

5.3.12. Transformation of competent B. subtilis *cells*

The transformation of *B. subtilis* cells was performed as described previously (Harwood & Cutting, 1990). Briefly, 100 µl of competent cells was mixed with 100 µl of the transformation buffer (Appendix C) and 6 µl of the purified target DNA was added to the mix. The transformation mix was incubated for 30 min at 37 °C with agitation after which the mix was lawn-plated on LB agar plate supplemented with appropriate antibiotics.

5.3.13. Phage-mediated transduction of B. subtilis

The SPP1 phage transduction was conducted as described previously (Yasbin & Young, 1974, Harwood & Cutting, 1990). Briefly, prior to infection *B. subtilis* cells were grown in TY broth. The donor cells carrying the target DNA were infected with the wild type SPP1 phage and incubated for 20 minutes to allow infection. The cells were mixed with 4 ml of TY broth supplemented with 0.4% agar and poured over a TY agar plate. The plates were incubated at 37 °C for about 5 h until lysis plaques were nearly confluent. The top agar was collected and the phage was released by vortexing and centrifugation.

To introduce the DNA taken up by the phage, the recipient strains were grown overnight at 37 °C with agitation in TY broth. The cells were diluted 1:10 in fresh TY broth and 60 µl of the phage suspension was added. The cells were incubated for 30 min at 37 °C without agitation, collected by centrifugation (3000g for 10 min), resuspended in 200 µl of the supernatant and lawn-plated on TY agar plates supplemented with 10 mM sodium citrate (VWR) and suitable antibiotics. The plates were incubated overnight at 37 °C.

5.4. Bacteriology methods

5.4.1. Complex colony formation

To assess the morphology of the complex colonies, the *B. subtilis* strains were streaked out to single colonies on LB agar plates and incubated overnight at 37 °C. The following morning a single colony was inoculated to 3 ml of fresh LB broth and incubated at 37 °C with agitation for 3 h. 10 µl of the resulting culture was spotted on top of the MSgg agar supplemented with IPTG as required. The cells were allowed to dry into the agar and the plates were incubated for 48 h at 30 °C.

5.4.1.1. Congo red binding by complex colonies

To assess Congo Red binding by the complex colonies, the MSgg agar was supplemented with 20 µg/ml of Congo Red (Sigma) and 10 µg/ml of Coomassie Blue G-250 (VWR) (Romero *et al.*, 2010). The complex colonies were grown as described above.

5.4.2. Biofilm pellicle formation

To assess the morphology of biofilm pellicles, *B. subtilis* cells were prepared as described for formation of complex colonies. After the initial growth in LB broth, the cells were inoculated 1:1000 into 2 ml of MSgg broth in a 24-well microtiter plate (Greiner) and IPTG was supplemented as required. The cultures were incubated for 72 h at 25 °C.

5.4.3. Pellicle biofilm fractionation

Prior to fractionation, the biofilm pellicles were allowed to develop at 37 °C for 16 h in 10 ml of MSgg broth in 6-well microtiter dishes (Greiner). The entire biofilm culture was transferred into a 14 ml centrifuge tube (Corning) and the biofilm was separated from the growth media by centrifugation (3000 g for 10 min). The media was collected and filtered through a cellulose filter with 0.2 µm pores (Sartorius). The pelleted pellicle was resuspended in 10 ml of cold MS buffer (MSgg broth without glycerol or glutamic acid) and the biofilm matrix was disrupted by sonication (12 pulses 1 sec long with 2.5 sec intervals at 35% power, Branson Digital Sonifier) (Branda *et al.*, 2001). The released cells were collected by centrifugation (9000 g for 20 min) and the supernatant containing the biofilm matrix fraction was filtered through a cellulose filter with 0.2 µm pores (Sartorius) into a fresh tube. The collected cells were resuspended in 10 ml of MS buffer supplemented with 100 µg/ml of lysozyme (Sigma). The cells were incubated at 37 °C for 30 min to allow peptidoglycan hydrolysis by the lysozyme. 5 ml of each fraction was transferred to a fresh 14 ml centrifugation tube and mixed with 5 ml of chloroform in methanol (1:1) solution. The solutions were thoroughly mixed to precipitate all proteins and centrifuged (3000 g for 5 min) to separate organic and aqueous phases. The aqueous phase and the organic phase were

collected leaving the pellet of precipitated proteins in the tube. The pellet was washed with 100% methanol and air dried. The pellet was then suspended in 250 µl of 2x concentrated SDS-loading buffer (Appendix C).

5.4.4. Complex colonies fractionation

To separate the cells grown in complex colonies from the biofilm matrix, the complex colonies were gathered from the agar plate using a sterile loop and suspended in 500 µl of sterile PBS. The suspended colony was disrupted by passing through a 23Gx1 syringe needle 3 times followed by gentle sonication (two cycles of 12 pulses 1 sec long with 2.5 sec intervals at 35% power, Branson Digital Sonifier) (Vlamakis *et al.*, 2008, Murray *et al.*, 2009b). The cells were separated from the biofilm matrix by centrifugation at 9000 g for 10 min at 4 °C. The supernatant was retained as the biofilm matrix fraction. The cells were suspended in 500µl of BugBuster Master Mix (Novagen) and lysed according to manufacturer's instructions. The total protein concentration was measured using Bio Rad DC Protein Assay.

5.4.5. Preparation of total protein from complex colonies

To extract total protein from complex colonies, the colonies were lifted from the agar surface with a sterile loop and suspended in 500 µl of BugBuster (Novagen) supplemented with Complete EDTA-free Proteinase Inhibitor Cocktail (Roche). The colonies were passed through a 23Gx1 syringe needle and sonicated with 2 pulses 0.5 sec long at 35% power (Branson Digital Sonifier). The samples were agitated on a roller wheel for 20 min at room temperature to allow for cell lysis and the debris was removed by centrifugation (17000 g for 10 min at 4 °C). 250 µl of the protein-containing supernatant was retained for further analysis.

5.4.6. Isolation of cell wall bound proteins

To isolate the proteins non-covalently bound to the cell wall, the biofilm pellicles were grown in 10 cm Petri dishes in 25 ml of MSgg broth overnight at 37 °C. The pellicles were collected and cells extracted as described in 5.4.3. The cells were suspended in 10 ml of ice cold 5 M LiCl solution and incubated on ice for 30 minutes. The cells were collected by centrifugation (3000 g for 10 min) and the supernatant was filtered through a cellulose filter with a pore size of 0.2 µm. The proteins were precipitated using the chloroform-methanol method (5.4.3) and resuspended in 200 µl of PBS. The cells were washed 3 times in ice cold PBS and suspended in 10 ml of PBS. 1 ml of cell suspension was lysed using BugBuster (Novagen) and the cell debris was centrifuged (17000 g for 10 min at 4 °C). 750 µl of the supernatant was kept for further analysis.

5.4.7. Isolation of cells for flow cytometry analysis

The complex colonies were gathered and disrupted with a syringe needle as described in 5.4.4. The resulting cell suspension was fixed with 4% PFA in PBS for 7 minutes. The cells were collected by centrifugation (17000 g for 1 min) and washed with 1 ml of PBS. The cells were collected again and suspended in 500 µl of sterile PBS. The biofilm matrix was dissolved by gentle sonication (5.4.3) and 1 µl of the cell suspension was added to 1 ml of PBS with 1% (w/v) of BSA (VWR). Single cell fluorescence was directly measured on a BD FACS Calibur (BD Biosciences). Single cells were identified on the basis of forward and side scatter, while the GFP fluorescence was analysed using 488 nm excitation with detection at 530±30nm. Data were captured using Cell Quest™ Pro (BD Biosciences) and further analyzed using FlowJo software version 4.3. The final fluorescence value was generated by subtraction of the

geometric mean generated for the auto-fluorescence of each strain's non-fluorescent parental strain. The number of GFP positive cells was calculated as the proportion of cells that exhibited a fluorescence signal greater than that generated by their respective non-fluorescent parental strain.

5.4.8. Whole cell anti-TasA immuno-gold labelling

To visualise TasA fibres the method described by Romero *et al.* (2010) was adapted. All strains used in this analysis carry an *eps(A-O)::tet* mutation to reduce electron thick background caused by the synthesis of the EPS. Prior to labelling the cells were grown in 2 ml of liquid MSgg broth in 24-well microtitre plates for 24 h at 25 °C. Cells were aspired with a Pasteur's pipette and spotted on a glow-discharged Pioloform nickel grid. Grids were blocked in the blocking agent (PBS with 0.1% Tween-20 and 3% milk) for 20 minutes and exposed to the anti-TasA antibody at a 1:150 dilution in the blocking agent for 90 minutes. Grids were washed 3 times in PBS and exposed to Immuno-gold Conjugate Protein A (10 nm gold particles, BBInternational) at a 1:50 dilution in the blocking agent. Grids were washed in PBS followed by water and stained with 3% uranyl acetate and finally washed 5 times with water.

5.4.9. Cryo-sectioning and immuno-gold labelling of YuaB for TEM imaging

As above, all strains used in this experiment carry an *eps(A-O)::*tet mutation to eliminate synthesis of electron thick EPS (Romero *et al.*, 2010). Prior to labelling the cells were grown in 10 ml of liquid MSgg broth in 6-well microtitre plates for 24 h at 25 °C. Cells were collected by centrifugation and fixed in 4% paraformaldehyde (VWR) in piperazine-N,N'-bis(2-ethanesulfonic acid) (Sigma). The fixed pellets were transferred

to 1 M sucrose and incubated at 4 °C overnight. The cell pellets were snap-frozen in liquid nitrogen and sectioned using a Leica Ultracut EMFCS cryomicrotome into 80 nm sections. Sections were collected onto carbon-coated copper grids and blocked with 0.5% fish skin gelatine (Sigma) in PBS. For efficient labelling of YuaB, the purified YuaB-specific antibody (See 5.5.8) was concentrated 10-fold and the blocked grids were incubated in a 10µl drop of the antibody solution for 30 minutes. Grids were washed 3 times in PBS and exposed to Immuno-gold Conjugate Protein A (10 nm gold particles, BBInternational) diluted 1:50 with the blocking agent. Next the grids were washed in PBS followed by water, stained with methyl cellulose/uranyl acetate (250 µl 3% uranyl acetate in 900 µl 2% methyl cellulose) and finally washed 5 times with water.

5.4.10. Immuno-fluorescent labelling of YuaB for CLSM imaging

For the purpose of fluorescence microscopy, strains that expressed the gene encoding the green fluorescent protein from an IPTG-inducible promoter were used. Biofilm pellicles were grown in 6 well microtitre dishes (Greiner) containing 10 ml of MSgg growth medium (described above) at 37 °C for 16 h. 18 mm x 18 mm 1.5 thickness cover glasses were coated with Concavalin A (Sigma) and placed under the pellicle. The spent growth media was removed to allow the pellicle to settle on the cover glass. A 5 min incubation allowed binding of the cells to the Concavalin A. The pellicle was fixed with 150 µl of 4% PFA in PBS for 10 minutes. The slides were washed 3 times with PBS and blocked for throughout the day in 2% fish skin gelatine (Sigma) in PBS. After 3 sequential washes with PBS, 150 µl of Rabbit anti-YuaB antibody diluted 1/10 in AbDil (Appendix C) [Cramer, L., and Desai, A. (1995) (http://mitchison.med.harvard.edu/protocols/gen1.html)] was applied and coverslips were incubated overnight at 4 °C. Next, the slides were washed 3 times with PBS and

incubated for 90 min in 150 µl of DyLight594-conjugated Affinity-Purified Donkey Anti-Rabbit IgG (H+L) secondary antibody (Jackson ImmunoResearch) diluted 1/150 in AbDil. The coverslips were washed 3 times with PBS and mounted on a microscope slide on the anti-fade containing mounting medium (Appendix C) [Cramer, L., and Desai, A. (1995) (http://mitchison.med.harvard.edu/protocols/gen1.html)] and sealed with nail varnish. The slides were stored at -20 °C prior to analysis

5.4.10.1. Preparation of live biofilms

To prepare unprocessed, live pellicles for CLSM imaging, the strains were grown in 6 well microtitre dishes as described above. 22 mm x 22 mm 1.5 thickness coverslips were coated in Concavalin A (Sigma) and pellicles were settled on the coverslips as described. The coverslips were placed on top of a microscope slide with a cavity (Marienfeld), which was filled with 55 µl of PBS and sealed with nail varnish.

5.4.11. Immuno-labelling of YuaB in complex colonies for CLSM imaging

Complex colonies were grown on MSgg solidified with 1.5 % (w/v) agar as described above. A quarter section of the colony (after 48 hours growth) was excised with a No. 10 surgical scalpel and placed into O.C.T. compound (Agar Scientific) and frozen in iso-pentene chilled with liquid nitrogen. 10 µm cross-sections of the colony were cut using a Leica CM3050 S cryomicrotome. The sections were transferred onto SuperFrost Ultra Plus adhesion microscope slides (VWR). Immuno-fluorescence staining was performed as detailed above. A drop of mounting medium was applied onto a labelled section of the colony and the slide was placed under a 1.5 thickness cover glass (22mm x 22mm) and sealed with nail varnish. The slides were stored at -20°C prior to analysis.

5.4.12. Quantification of the abundance of fluorescence

To assess the abundance of fluorescence throughout the depth of the pellicle, the images acquired by confocal microscopy were stored and annotated with Regions of Interest (ROIs) in OMERO (Allan *et al.*, 2012). Following this, automated batch image analysis was performed with bespoke software written in Matlab (MathWorks) via the OMERO API (code available upon request). Briefly, for each field of view, the Z-stack of GFP (representing the cells) and DyLight594 (representing the immune-labelled YuaB) channels was downloaded into Matlab. The signal in each channel was segmented from background using the Otsu method (Otsu, 1979). For every Z-section, for each fluorescence channel, the number of segmented pixels and the total number of pixels was stored in a vector (note: the total number of pixels possible in each Z-section is 512 x 512). The first Z-section containing a signal from GFP was regarded as Z = 0 and the vectors were aligned in a matrix to generate a common reference point. The matrix of pixel counts was converted to a spread sheet. The graphs representing pixel abundance were produced in SigmaPlot 12.0 where total average pixel count per strain (a measurement of the abundance of signal) was plotted against the depth of the biofilm in μm. The average represents the n of between 10-30 independent images. The intensity of the DyLight594 channel for the wild type pellicle stained with either primary and secondary antibodies or secondary antibody only were calculated in MatLab. Images were stored in OMERO and accessed via the OMERO API. Briefly, for each image the Z-stack of DyLight594 channel was downloaded into MatLab and the fluorescence signal was segmented using the Otsu method (Otsu, 1979). The Z-section with the largest number of segmented pixels was found (equating to the peak abundance of staining) and the mean fluorescence intensity was calculated.

5.4.13. Spore quantification

To determine the percentage of sporulation, strains were grown on MSgg agar for 72 h which provided high sporulation rate (Vlamakis *et al.*, 2008). Cells were extracted from biofilms by suspending the cells in T-Base (Appendix C). The cells were disrupted by passage through a 23Gx1 syringe needle and subjected to mild sonication (5.4.4). The resulting cell preparation was serially diluted in T-base and dilutions were plated on LB agar plates to allow the total number of cells to be counted. To kill vegetative cells the diluted cell suspensions were incubated for 20 min at 80 °C prior to plating on LB agar. The number of colony forming units (CFU) was calculated for each sample and ratio of CFU from spore cultures to total number of cells was calculated. For analysing the sporulation rate from a planktonic culture, cells were grown in MSgg broth for 72 h at 37 °C with agitation to inhibit formation of the biofilm matrix. Cultures were serially diluted in T-Base and the sporulation assay was conducted as for cells extracted from biofilms.

5.5. Molecular and biochemical methods

5.5.1. Polyacrylamide gel electrophoresis of proteins and carbohydrates

Gel electrophoresis of proteins was performed using polyacrylamide gels according to a method published previously (Laemmli, 1970). The 12% or 14% resolving gels with 6% stacking gel were prepared according to the protocol from The Molecular Cloning Laboratory Handbook (Sambrook & Russell, 2001) using Mini-Protean system (Bio Rad). Electrophoresis was performed in SDS-Tris-Glycine running buffer (Appendix C) at constant electric potential of 200 V for about 1 h. To visualise

the resolved proteins gels were stained with boiling Coomassie brilliant blue (Appendix C) for 20 minutes. The unbound stain was removed by agitating the gels for 20 min in a destaining solution (Appendix C) followed by an overnight wash in ddH_2O.

Gel electrophoresis of carbohydrates was performed using 6-12% hand-poured gradient gels and the resolution method as described above. The gradient gels were made by preparing three individual mixtures of 12%, 10% and 8% acrylamide solutions (Sambrook & Russell, 2001) and overlaying the mixtures before setting. The resulting gradient gel was overlaid with a 6% stacking gel. The samples were resolved using 150 V for about 45 min and stained with the saccharide-specific Schiff's stain (Sigma) according to the published protocol (Segrest & Jackson, 1972).

5.5.2. Western blotting

Prior to protein detection by Western blotting the protein samples were resolved by SDS-PAGE as described above. For analysis of the fractionated pellicles (5.4.3) 3.5 µl of each sample was resolved in the gel. For analysis of proteins obtained from complex colonies the samples were quantified using Protein Assay DC system (Bio Rad) and 5 µg of protein from each sample was used. The resolved proteins were transferred onto a PVDF membrane (Millipore) by electroblotting using Mini-protean blotting cassettes (Bio Rad) in a Tris-Glycine transfer buffer (Appendix C) (Sambrook & Russell, 2001) at the constant current of 100 mA for 75 min. Following electroblotting, the membrane was incubated for 1 h in 3% powdered milk in TBS (Appendix C) at room temperature. This was followed by an overnight incubation in 3% powdered milk wash buffer (TBS + 0.05% Tween 20) with the primary antibodies raised against TasA at a dilution of 1:25000 or YuaB (affinity purified) at a dilution of 1:500 or AtpB

(monoclonal, murine) (AbCam) at a dilution of 1: 10000. The membrane was washed using wash buffer and incubated for 45 minutes with the secondary antibody conjugated to horseradish peroxidise (Goat anti-Rabbit (Pierce) for TasA and YuaB or Goat anti-Mouse (Pierce) for AtpB) at a dilution of 1:5000. The membrane was washed in TBS + 0.05% Tween-20, developed using ECL reagents (Appendix C) and exposed to X-ray film (Konica). The film was developed using Medical Film Processor SRX-101A (Konica Minolta).

5.5.3. Protein overexpression and purification

All protein constructs were overexpressed in *E. coli* strain BL21 (DE3) grown in LB broth. The freshly transformed cells were inoculated into an overnight culture that was incubated at 37 °C with agitation. The culture was diluted into 1 L of fresh LB broth at 1:500 dilution. The total volume of the culture was 6 to 10 litres. The cultures were incubated at 30 °C with agitation until the cell density measured at $OD_{600} \approx 0.3$. At this point the incubation temperature was lowered to 20 °C and the expression was induced with IPTG at final concentration of 100 µM. The cells were allowed to multiply overnight and were collected by centrifugation (4500 g for 45 min), washed with 50 mM Tris and collected again. The cell pellet was suspended and homogenised in 50 ml of the lysis buffer (Appendix C) per 10 L of culture. For purification of His_6-tagged proteins the lysis buffer was supplemented with 25 mM Imidazole (Sigma). The cells were lysed by two consecutive passages through French press (Thermo) set to 8000 PSI. The cell debris was removed by centrifugation (19000 g for 20 min) and the supernatant was filtered through a cellulose syringe filter with the pore size of 45 µm.

5.5.3.1. *Purification of His_6-tagged proteins*

The filtered cell lysate in the lysis buffer was loaded onto a 5 ml His-Trap HP column (GE Healthcare), equilibrated with lysis buffer, using the ACTA Purifier FPLC system (GE Healthcare). The lysate was loaded at 0.5 ml/min with pressure not exceeding 0.4 MPa. The flow-through fraction was retained for further analysis. After all the lysate has passed through the column, the column was washed with 30 ml of the filtered Buffer A (Appendix C) at a flow rate of 1 ml/min with the pressure not exceeding 0.4 MPa to wash out all unbound protein. The wash fraction was retained. The proteins bound to the column were washed out using a gradient between Buffer A and filtered Buffer B (Appendix C) with flow rate of 1 ml/min with pressure not exceeding 0.4 MPa over the period of 45 mintues, collecting elution fractions of 1 ml each during this time. The resulting fractions were analysed by SDS-PAGE.

5.5.3.2. *Purification of GST-tagged proteins*

Prior to being used for purification purposes, the glutathione-agarose beads (GE Healthcare) were washed in 50 ml of ddH_2O, collected by centrifugation (1000 g for 3 min), equilibrated in 50 ml of the lysis buffer and collected again by centrifugation. The beads were added to the cell lysate and incubated on a roller for 2 h at 4 °C. The beads in the solution were loaded into a gravity column and the flow-through fraction was collected. The beads were washed with 3x 50 ml of fresh binding buffer (Appendix C) and the wash fractions were collected. The beads were transferred to a fresh 50 ml tube and incubated on a roller with 25 ml of the elution buffer (Appendix C) for 2 h at 4 °C to uncouple the bound protein from the beads. The beads were transferred to a gravity column and the eluted protein was collected. The beads were washed with equivalent of 2 volumes of beads in the elution buffer to ensure all

of the protein was collected and the beads were regenerated with the binding buffer. The purified, GST-tagged protein was poured into a 3 kDa MWCO dialysis bag (Fisher Scientific) and 300 μg of PreScission protease (GE Healthcare) was added. The proteins were incubated with the protease whilst dialysing against 2 L of the binding buffer overnight at 4 °C. The protein mixture after cleavage was collected to a centrifuge tube and the protein precipitate was removed by centrifugation (3000 g for 10 min). The supernatant was transferred to a fresh tube and the regenerated beads were added to bind all cleaved GST and the protease, which is also GST-tagged. The beads were incubated for 2 h at 4 °C on a roller and the beads were loaded onto a gravity column. The resulting flow-through contained the purified protein. The beads were regenerated by incubation with the elution buffer and washing with the binding buffer. The fractions were analysed on an SDS-PAGE gel.

5.5.4. Size exclusion chromatography

The fractions containing the proteins of interest after purification were concentrated to 2 ml using spin concentrators with the molecular weight cut off of 10 kDa (Sartorius). The resulting protein concentrate was loaded onto an FPLC 10/120 column (GE Healthcare) packed with Superdex 75 agarose (GE Healthcare). The proteins were resolved in the column by passage of the Gel Filtration buffer (Appendix C) using the ACTA Purifier FPLC system and a flow rate of 0.4 ml/min and pressure not exceeding 0.4 MPa. 0.5 ml fractions of eluted proteins were collected and analysed by SDS-PAGE.

5.5.5. *Protein identification and sequencing*

The purified proteins were identified by excision of the protein bands from a SDS-PAGE gel and LC-MS-MS after trypsin digestion. Protein size estimation was performed using MS-TOF. The resulting peptides were identified using the MASCOT database. The sequence of the N-terminus of protein samples was determined by Edman degradation. All procedures were performed by FingerPrints Proteomics service, College of Life Sciences, Dundee.

5.5.6. *Circular dichroism*

To identify the secondary structure ratio of YuaB, the purified protein was dialysed into CD buffer (Appendix C) using 10 kDa MWCO spin concentrators (Sartorius). The close and far UV spectra of the protein samples were analysed by Dr. Sharon Kelly, Institute of Molecular, Cell and Systems Biology, College of Medical, Veterinary and Life Sciences, University of Glasgow.

5.5.7. *Antibody production*

The antibodies against purified, His-tagged YuaB were raised in rabbits by SeqLab, Gottingen (Germany). The antibodies against purified, tag-less TasA were raised in rabbits by Dundee Cell Products, Dundee.

5.5.8. *Antibody purification*

The antibodies raised against YuaB were purified from the antiserum using purified His_6-tagged YuaB. The following method was obtained from Ellis Jaffray, GRE, College of Life Sciences, Dundee.

5.5.8.1. Column preparation

To prepare the affinity column for antibody purification, the purified YuaB was dialysed against the coupling buffer (Appendix C) overnight using 3 kDa MWCO dialysis tubing (Fisher Scientific). 5 ml of the *N*-hydroxysuccinimidyl-activated agarose beads (Sigma) were activated in 50 ml of 1 mM HCl and washed with 150 ml of coupling buffer by centrifugation (1000 g for 3 min). The protein in the coupling buffer was added to the beads and rotated on a roller for 2 h at 4 °C. The beads with bound YuaB were transferred to a gravity flow column and washed 3 times alternately with 50 ml Ethanolamine and Sodium Acetate buffers (Appendix C). After the last wash, the beads were washed with 50 ml of storage buffer (Appendix C) and kept at 4 °C until needed.

5.5.8.2. Purification

15 ml of the antiserum to be purified was diluted with 135 ml of PBS and filtered through a cellulose syringe filter with pores of 0.2 µm. The affinity column was washed with 100 ml of the coupling buffer (Appendix C). The diluted antiserum was applied onto the column and allowed to pass through the beads twice. The column was washed with 100 ml of 10 mM Tris with 0.5 M NaCl to wash all residual serum from the column. The antibody was eluted from the column with 0.1 M glycine at pH = 2.25. The eluting antibody was collected as 1 ml fractions on top of 100 µl of 1 M Tris at pH = 8.0. The fractions containing the antibody were identified using Bradford protein assay (Thermo Fishier). The antibody-containing fractions were pooled, BSA (Thermo Fisher) was added to a final concentration of 10 mg/ml and glycerol was added to a final concentration of 10%. The antibody was stored at -80 °C until needed.

5.6. Image acquisition and processing, presentation of data

- All graphs were plotted in SigmaPlot 12.0.
- Biofilm images were captured using a Leica MZ16 FA stereoscope fitted with a CLS 150 LS illumination system and a DFC 350 FX digital camera using LAS software version 2.7.1.
- Colour biofilm images were captured using a Nikon D60 digital SLR camera.
- SDS-PAGE gel pictures were captured using a Nikon D60 digital SLR camera.
- Immuno-fluorescence imaging was performed using a Zeiss LSM700 confocal scanning laser microscope fitted with 488nm and 555nm lasers and an EC Plan-Neofluar 40x/1.30 Oil DIC M27 or alfa Plan-Apochromat 100x/1.49 Iol DIC objectives. The images were captured using Zen 2009 software (Zeiss).
- Transmission electron microscopy was performed using JEOL JEM-1200EX electron microscope and captured on an electron-sensitive film.
- Two-dimensional image analysis was conducted using OMERO platform (www.openmicroscopy.org) (Allan *et al.*, 2012).
- Orthogonal views were prepared in Zen 2009 (Zeiss).
- All figures were assembled in Canvas 12 (ACD Systems).

6. References

Absalon, C., K. Van Dellen & P. I. Watnick, (2011) A communal bacterial adhesin anchors biofilm and bystander cells to surfaces. *PLoS pathogens* **7**: e1002210.

Adams, D. G., (1997) Cyanobacteria. In: Bacteria as Multicellular Organisms. J. A. Shapiro & M. Dworkin (eds). Oxford University Press, pp. 109 - 148.

Aguilar, C., H. Vlamakis, A. Guzman, R. Losick & R. Kolter, (2010) KinD is a checkpoint protein linking spore formation to extracellular-matrix production in *Bacillus subtilis* biofilms. *mBio* **1**: e00035-00010.

Aguilar, C., H. Vlamakis, R. Losick & R. Kolter, (2007) Thinking about *Bacillus subtilis* as a multicellular organism. *Curr Opin Microbiol*.

Allan, C., J. M. Burel, J. Moore, C. Blackburn, M. Linkert, S. Loynton, D. Macdonald, W. J. Moore, C. Neves, A. Patterson, M. Porter, A. Tarkowska, B. Loranger, J. Avondo, I. Lagerstedt, L. Lianas, S. Leo, K. Hands, R. T. Hay, A. Patwardhan, C. Best, G. J. Kleywegt, G. Zanetti & J. R. Swedlow, (2012) OMERO: flexible, model-driven data management for experimental biology. *Nat Methods* **9**: 245-253.

Altschul, S. F., T. L. Madden, A. A. Schaffer, J. Zhang, Z. Zhang, W. Miller & D. J. Lipman, (1997) Gapped BLAST and PSI-BLAST: a new generation of protein database search programs. *Nucleic Acids Research* **25**: 3389-3402.

Amati, G., P. Bisicchia & A. Galizzi, (2004) DegU-P represses expression of the motility fla-che operon in *Bacillus subtilis*. *J Bacteriol* **186**: 6003-6014.

Anagnostopoulos, C. & J. Spizizen, (1961) Requirements for Transformation in *Bacillus subtilis*. *Journal of Bacteriology* **81**: 741-746.

Angelini, T. E., M. Roper, R. Kolter, D. A. Weitz & M. P. Brenner, (2009) *Bacillus subtilis* spreads by surfing on waves of surfactant. *P Natl Acad Sci USA* **106**: 18109-18113.

Antelmann, H., H. Tjalsma, B. Voigt, S. Ohlmeier, S. Bron, J. M. van Dijl & M. Hecker, (2001) A proteomic view on genome-based signal peptide predictions. *Genome Res* **11**: 1484-1502.

Arima, K., A. Kakinuma & G. Tamura, (1968) Surfactin, a crystalline peptidelipid surfactant produced by *Bacillus subtilis*: isolation, characterization and its inhibition of fibrin clot formation. *Biochemical and biophysical research communications* **31**: 488-494.

Bai, U., I. Mandic-Mulec & I. Smith, (1993) SinI modulates the activity of SinR, a developmental switch protein of *Bacillus subtilis*, by protein-protein interaction. *Genes Dev* **7**: 139-148.

Bais, H. P., R. Fall & J. M. Vivanco, (2004) Biocontrol of *Bacillus subtilis* against infection of *Arabidopsis* roots by *Pseudomonas syringae* is facilitated by biofilm formation and surfactin production. *Plant Physiol* **134**: 307-319.

Banner, M. A., J. G. Cunniffe, R. L. Macintosh, T. J. Foster, H. Rohde, D. Mack, E. Hoyes, J. Derrick, M. Upton & P. S. Handley, (2007) Localized tufts of fibrils on *Staphylococcus epidermidis* NCTC 11047 are comprised of the accumulation-associated protein. *Journal of Bacteriology* **189**: 2793-2804.

Banse, A. V., A. Chastanet, L. Rahn-Lee, E. C. Hobbs & R. Losick, (2008) Parallel pathways of repression and antirepression governing the transition to stationary phase in *Bacillus subtilis*. *Proc Natl Acad Sci U S A* **105**: 15547-15552.

Barnhart, M. M. & M. R. Chapman, (2006) Curli biogenesis and function. *Annual review of microbiology* **60**: 131-147.

Bassler, B. L., (2002) Small talk. Cell-to-cell communication in bacteria. *Cell* **109**: 421-424.

Bassler, B. L., E. P. Greenberg & A. M. Stevens, (1997) Cross-species induction of luminescence in the quorum-sensing bacterium *Vibrio harveyi*. *Journal of Bacteriology* **179**: 4043-4045.

Bassler, B. L. & R. Losick, (2006) Bacterially speaking. *Cell* **125**: 237-246.

Bassler, B. L., M. Wright, R. E. Showalter & M. R. Silverman, (1993) Intercellular signalling in *Vibrio harveyi*: sequence and function of genes regulating expression of luminescence. *Molecular Microbiology* **9**: 773-786.

Bassler, B. L., M. Wright & M. R. Silverman, (1994) Multiple signalling systems controlling expression of luminescence in *Vibrio harveyi*: sequence and function of genes encoding a second sensory pathway. *Molecular Microbiology* **13**: 273-286.

Beech, I. B. & J. Sunner, (2004) Biocorrosion: towards understanding interactions between biofilms and metals. *Current opinion in biotechnology* **15**: 181-186.

Berk, V., J. C. Fong, G. T. Dempsey, O. N. Develioglu, X. Zhuang, J. Liphardt, F. H. Yildiz & S. Chu, (2012) Molecular architecture and assembly principles of *Vibrio cholerae* biofilms. *Science* **337**: 236-239.

Berne, C., D. T. Kysela & Y. V. Brun, (2010) A bacterial extracellular DNA inhibits settling of motile progeny cells within a biofilm. *Molecular Microbiology*.

Bertani, G., (1951) Studies on lysogenesis. I. The mode of phage liberation by lysogenic *Escherichia coli*. *Journal of Bacteriology* **62**: 293-300.

Bertani, G., (2004) Lysogeny at mid-twentieth century: P1, P2, and other experimental systems. *Journal of Bacteriology* **186**: 595-600.

Besson, F., F. Peypoux, G. Michel & L. Delcambe, (1976) Characterization of iturin A in antibiotics from various strains of *Bacillus subtilis*. *The Journal of antibiotics* **29**: 1043-1049.

Blair, K. M., L. Turner, J. T. Winkelman, H. C. Berg & D. B. Kearns, (2008) A molecular clutch disables flagella in the *Bacillus subtilis* biofilm. *Science* **320**: 1636-1638.

Blanco, L. P., M. L. Evans, D. R. Smith, M. P. Badtke & M. R. Chapman, (2012) Diversity, biogenesis and function of microbial amyloids. *Trends in microbiology* **20**: 66-73.

Bockelmann, U., A. Janke, R. Kuhn, T. R. Neu, J. Wecke, J. R. Lawrence & U. Szewzyk, (2006) Bacterial extracellular DNA forming a defined network-like structure. *FEMS microbiology letters* **262**: 31-38.

Borlee, B. R., A. D. Goldman, K. Murakami, R. Samudrala, D. J. Wozniak & M. R. Parsek, (2010) *Pseudomonas aeruginosa* uses a cyclic-di-GMP-regulated adhesin to reinforce the biofilm extracellular matrix. *Mol Microbiol* **75**: 827-842.

Boucher, J. C., H. Yu, M. H. Mudd & V. Deretic, (1997) Mucoid *Pseudomonas aeruginosa* in cystic fibrosis: characterization of muc mutations in clinical isolates and analysis of clearance in a mouse model of respiratory infection. *Infection and immunity* **65**: 3838-3846.

Branda, S. S., F. Chu, D. B. Kearns, R. Losick & R. Kolter, (2006) A major protein component of the *Bacillus subtilis* biofilm matrix. *Mol Microbiol* **59**: 1229-1238.

Branda, S. S., J. E. Gonzalez-Pastor, S. Ben-Yehuda, R. Losick & R. Kolter, (2001) Fruiting body formation by *Bacillus subtilis*. *Proc Natl Acad Sci U S A* **98**: 11621-11626.

Branda, S. S., J. E. Gonzalez-Pastor, E. Dervyn, S. D. Ehrlich, R. Losick & R. Kolter, (2004) Genes involved in formation of structured multicellular communities by *Bacillus subtilis*. *J Bacteriol* **186**: 3970-3979.

Branda, S. S., S. Vik, L. Friedman & R. Kolter, (2005) Biofilms: the matrix revisited. *Trends in microbiology* **13**: 20-26.

Britton, R. A., P. Eichenberger, J. E. Gonzalez-Pastor, P. Fawcett, R. Monson, R. Losick & A. D. Grossman, (2002) Genome-wide analysis of the stationary-phase sigma factor (Sigma-H) regulon of *Bacillus subtilis*. *Journal of Bacteriology* **184**: 4881-4890.

Brown, W. C., (1973) Rapid methods for extracting autolysins from *Bacillus subtilis*. *Applied microbiology* **25**: 295-300.

Burbulys, D., K. A. Trach & J. A. Hoch, (1991) Initiation of sporulation in *B. subtilis* is controlled by a multicomponent phosphorelay. *Cell* **64**: 545-552.

Burkholder, P. R. & N. H. Giles, (1947) Induced biochemical mutations in *Bacillus subtilis*. *Amer. J. Bot.* **34**: 345.

Byrd, M. S., I. Sadovskaya, E. Vinogradov, H. Lu, A. B. Sprinkle, S. H. Richardson, L. Ma, B. Ralston, M. R. Parsek, E. M. Anderson, J. S. Lam & D. J. Wozniak, (2009) Genetic and biochemical analyses of the *Pseudomonas aeruginosa* Psl exopolysaccharide reveal overlapping roles for polysaccharide synthesis enzymes in Psl and LPS production. *Molecular Microbiology* **73**: 622-638.

Capstick, D. S., A. Jomaa, C. Hanke, J. Ortega & M. A. Elliot, (2011) Dual amyloid domains promote differential functioning of the chaplin proteins during *Streptomyces* aerial morphogenesis. *P Natl Acad Sci USA* **108**: 9821-9826.

Chai, Y., F. Chu, R. Kolter & R. Losick, (2008) Bistability and biofilm formation in *Bacillus subtilis*. *Mol Microbiol* **67**: 254-263.

Chai, Y., R. Kolter & R. Losick, (2009) Paralogous antirepressors acting on the master regulator for biofilm formation in *Bacillus subtilis*. *Mol Microbiol* **74**: 876-887.

Chai, Y., T. Norman, R. Kolter & R. Losick, (2010) An epigenetic switch governing daughter cell separation in *Bacillus subtilis*. *Genes Dev* **24**.

Chai, Y., T. Norman, R. Kolter & R. Losick, (2011) Evidence that metabolism and chromosome copy number control mutually exclusive cell fates in *Bacillus subtilis*. *The EMBO journal* **30**: 1402-1413.

Chapman, M. R., L. S. Robinson, J. S. Pinkner, R. Roth, J. Heuser, M. Hammar, S. Normark & S. J. Hultgren, (2002) Role of *Escherichia coli* curli operons in directing amyloid fiber formation. *Science* **295**: 851-855.

Chater, K. F. & R. Losick, (1997) Mycelial Life Style of *Streptomyces coelicolor* A3(2) and Its Relatives. In: Bacteria as Multicellular Organisms. J. A. Shapiro & M. Dworkin (eds). Oxford University Press, pp. 149 - 182.

Chen, Y., S. Cao, Y. Chai, J. Clardy, R. Kolter, J. H. Guo & R. Losick, (2012) A *Bacillus subtilis* sensor kinase involved in triggering biofilm formation on the roots of tomato plants. *Molecular Microbiology* **85**: 418-430.

Cheng, K. C., A. Demirci & J. M. Catchmark, (2010) Advances in biofilm reactors for production of value-added products. *Applied microbiology and biotechnology* **87**: 445-456.

Chu, F., D. B. Kearns, S. S. Branda, R. Kolter & R. Losick, (2006) Targets of the master regulator of biofilm formation in *Bacillus subtilis*. *Mol Microbiol* **59**: 1216-1228.

Chu, F., D. B. Kearns, A. McLoon, Y. Chai, R. Kolter & R. Losick, (2008) A novel regulatory protein governing biofilm formation in *Bacillus subtilis*. *Mol Microbiol* **68**: 1117-1127.

Chumsakul, O., H. Takahashi, T. Oshima, T. Hishimoto, S. Kanaya, N. Ogasawara & S. Ishikawa, (2010) Genome-wide binding profiles of the *Bacillus subtilis* transition state regulator AbrB and its homolog Abh reveals their interactive role in transcriptional regulation. *Nucleic Acids Res*.

Claessen, D., R. Rink, W. de Jong, J. Siebring, P. de Vreugd, F. G. Boersma, L. Dijkhuizen & H. A. Wosten, (2003) A novel class of secreted hydrophobic proteins is involved in aerial hyphae formation in *Streptomyces coelicolor* by forming amyloid-like fibrils. *Genes & development* **17**: 1714-1726.

Cohen-Gonsaud, M., P. Barthe, F. Pommier, R. Harris, P. C. Driscoll, N. H. Keep & C. Roumestand, (2004) (1)H, (15)N, and (13)C chemical shift assignments of the resuscitation promoting factor domain of Rv1009 from *Mycobacterium tuberculosis*. *Journal of biomolecular NMR* **30**: 373-374.

Cohn, F., (1877) Untersuchungen uber Bacterien. IV. Beitrage zur Biologie der Bacillen. *Beitr. Biol. Pflanz.* **2**: 249-276.

Collinson, S. K., S. C. Clouthier, J. L. Doran, P. A. Banser & W. W. Kay, (1996) *Salmonella enteritidis agfBAC* operon encoding thin, aggregative fimbriae. *Journal of Bacteriology* **178**: 662-667.

Colvin, K. M., Y. Irie, C. S. Tart, R. Urbano, J. C. Whitney, C. Ryder, P. L. Howell, D. J. Wozniak & M. R. Parsek, (2011) The Pel and Psl polysaccharides provide *Pseudomonas aeruginosa* structural redundancy within the biofilm matrix. *Environmental microbiology*.

Conchillo-Sole, O., N. S. de Groot, F. X. Aviles, J. Vendrell, X. Daura & S. Ventura, (2007) AGGRESCAN: a server for the prediction and evaluation of "hot spots" of aggregation in polypeptides. *BMC Bioinformatics* **8**: 65.

Cooper, S., (1991) Synthesis of the cell surface during the division cycle of rod-shaped, gram-negative bacteria. *Microbiological reviews* **55**: 649-674.

Costerton, J. W., (1984) The etiology and persistence of cryptic bacterial infections: a hypothesis. *Rev Infect Dis* **6 Suppl 3**: S608-616.

Costerton, J. W., (2001) Cystic fibrosis pathogenesis and the role of biofilms in persistent infection. *Trends in microbiology* **9**: 50-52.

Costerton, J. W., K. J. Cheng, G. G. Geesey, T. I. Ladd, J. C. Nickel, M. Dasgupta & T. J. Marrie, (1987) Bacterial biofilms in nature and disease. *Annu Rev Microbiol* **41**: 435-464.

Costerton, J. W., Z. Lewandowski, D. E. Caldwell, D. R. Korber & H. M. Lappin-Scott, (1995) Microbial biofilms. *Annu Rev Microbiol* **49**: 711-745.

Costerton, J. W., Z. Lewandowski, D. DeBeer, D. Caldwell, D. Korber & G. James, (1994) Biofilms, the customized microniche. *J Bacteriol* **176**: 2137-2142.

Costerton, J. W., P. S. Stewart & E. P. Greenberg, (1999) Bacterial biofilms: a common cause of persistent infections. *Science* **284**: 1318-1322.

Cucarella, C., C. Solano, J. Valle, B. Amorena, I. Lasa & J. R. Penades, (2001) Bap, a *Staphylococcus aureus* surface protein involved in biofilm formation. *Journal of Bacteriology* **183**: 2888-2896.

Dahl, M. K., T. Msadek, F. Kunst & G. Rapoport, (1991) Mutational analysis of the *Bacillus subtilis* DegU regulator and its phosphorylation by the DegS protein kinase. *J Bacteriol* **173**: 2539-2547.

Danese, P. N., L. A. Pratt & R. Kolter, (2000) Exopolysaccharide production is required for development of *Escherichia coli* K-12 biofilm architecture. *J Bacteriol* **182**: 3593-3596.

Danhorn, T. & C. Fuqua, (2007) Biofilm formation by plant-associated bacteria. *Annu Rev Microbiol* **61**: 401-422.

Davey, M. E. & A. O'Toole G, (2000) Microbial biofilms: from ecology to molecular genetics. *Microbiol Mol Biol Rev* **64**: 847-867.

Davies, D. G., M. R. Parsek, J. P. Pearson, B. H. Iglewski, J. W. Costerton & E. P. Greenberg, (1998) The involvement of cell-to-cell signals in the development of a bacterial biofilm. *Science* **280**: 295-298.

de Jong, W., H. A. Wosten, L. Dijkhuizen & D. Claessen, (2009) Attachment of *Streptomyces coelicolor* is mediated by amyloidal fimbriae that are anchored to the cell surface via cellulose. *Molecular Microbiology* **73**: 1128-1140.

Diggle, S. P., R. E. Stacey, C. Dodd, M. Camara, P. Williams & K. Winzer, (2006) The galactophilic lectin, LecA, contributes to biofilm development in *Pseudomonas aeruginosa*. *Environmental microbiology* **8**: 1095-1104.

Doyle, R. J. & D. C. Birdsell, (1972) Interaction of concanavalin A with the cell wall of *Bacillus subtilis*. *Journal of Bacteriology* **109**: 652-658.

Driks, A., (2002) Maximum shields: the assembly and function of the bacterial spore coat. *Trends in microbiology* **10**: 251-254.

Drobniewski, F. A., (1993) *Bacillus cereus* and related species. *Clin Microbiol Rev* **6**: 324-338.

Dubnau, D., J. Hahn, M. Roggiani, F. Piazza & Y. Weinrauch, (1994) Two-component regulators and genetic competence in *Bacillus subtilis*. *Res Microbiol* **145**: 403-411.

Duc le, H., H. A. Hong, H. S. Atkins, H. C. Flick-Smith, Z. Durrani, S. Rijpkema, R. W. Titball & S. M. Cutting, (2007) Immunization against anthrax using *Bacillus subtilis* spores expressing the anthrax protective antigen. *Vaccine* **25**: 346-355.

Duc le, H., H. A. Hong & S. M. Cutting, (2003a) Germination of the spore in the gastrointestinal tract provides a novel route for heterologous antigen delivery. *Vaccine* **21**: 4215-4224.

Duc le, H., H. A. Hong, N. Fairweather, E. Ricca & S. M. Cutting, (2003b) Bacterial spores as vaccine vehicles. *Infection and immunity* **71**: 2810-2818.

Dueholm, M. S., S. B. Nielsen, K. L. Hein, P. Nissen, M. Chapman, G. Christiansen, P. H. Nielsen & D. E. Otzen, (2011) Fibrillation of the major curli subunit CsgA under a wide range of conditions implies a robust design of aggregation. *Biochemistry* **50**: 8281-8290.

Dueholm, M. S., S. V. Petersen, M. Sonderkaer, P. Larsen, G. Christiansen, K. L. Hein, J. J. Enghild, J. L. Nielsen, K. L. Nielsen, P. H. Nielsen & D. E. Otzen, (2010) Functional amyloid in *Pseudomonas*. *Molecular Microbiology*.

Elliot, M. A., N. Karoonuthaisiri, J. Huang, M. J. Bibb, S. N. Cohen, C. M. Kao & M. J. Buttner, (2003) The chaplins: a family of hydrophobic cell-surface proteins involved in aerial mycelium formation in *Streptomyces coelicolor*. *Genes & development* **17**: 1727-1740.

Elliot, M. A. & N. J. Talbot, (2004) Building filaments in the air: aerial morphogenesis in bacteria and fungi. *Current opinion in microbiology* **7**: 594-601.

Engebrecht, J. & M. Silverman, (1984) Identification of genes and gene products necessary for bacterial bioluminescence. *P Natl Acad Sci USA* **81**: 4154-4158.

Epstein, A. K., B. Pokroy, A. Seminara & J. Aizenberg, (2011) Bacterial biofilm shows persistent resistance to liquid wetting and gas penetration. *P Natl Acad Sci USA* **108**: 995-1000.

Evans, L. R. & A. Linker, (1973) Production and characterization of the slime polysaccharide of *Pseudomonas aeruginosa*. *Journal of Bacteriology* **116**: 915-924.

Fabret, C., V. A. Feher & J. A. Hoch, (1999) Two-component signal transduction in *Bacillus subtilis*: how one organism sees its world. *J Bacteriol* **181**: 1975-1983.

Fernandez-Escamilla, A. M., F. Rousseau, J. Schymkowitz & L. Serrano, (2004) Prediction of sequence-dependent and mutational effects on the aggregation of peptides and proteins. *Nature biotechnology* **22**: 1302-1306.

Flemming, H. C., P. Sriyutha Murthy, R. Venkatesan & K. E. Cooksey, (2009) *Marine and Industial Biofouling*. Springer.

Flemming, H. C. & J. Wingender, (2010) The biofilm matrix. *Nat Rev Microbiol* **8**: 623-633.

Foster, S. J., (1993) Molecular analysis of three major wall-associated proteins of *Bacillus subtilis* 168: evidence for processing of the product of a gene encoding a 258 kDa precursor two-domain ligand-binding protein. *Mol Microbiol* **8**: 299-310.

Friedman, L. & R. Kolter, (2004a) Genes involved in matrix formation in *Pseudomonas aeruginosa* PA14 biofilms. *Mol Microbiol* **51**: 675-690.

Friedman, L. & R. Kolter, (2004b) Two genetic loci produce distinct carbohydrate-rich structural components of the *Pseudomonas aeruginosa* biofilm matrix. *J Bacteriol* **186**: 4457-4465.

Fujita, M., J. E. Gonzalez-Pastor & R. Losick, (2005) High- and low-threshold genes in the Spo0A regulon of Bacillus subtilis. *J Bacteriol* **187**: 1357-1368.

Fux, C. A., J. W. Costerton, P. S. Stewart & P. Stoodley, (2005a) Survival strategies of infectious biofilms. *Trends Microbiol* **13**: 34-40.

Fux, C. A., M. Shirtliff, P. Stoodley & J. W. Costerton, (2005b) Can laboratory reference strains mirror "real-world" pathogenesis? *Trends in microbiology* **13**: 58-63.

Garbuzynskiy, S. O., M. Y. Lobanov & O. V. Galzitskaya, (2010) FoldAmyloid: a method of prediction of amyloidogenic regions from protein sequence. *Bioinformatics* **26**: 326-332.

Gaur, N. K., K. Cabane & I. Smith, (1988) Structure and expression of the *Bacillus subtilis sin* operon. *J Bacteriol* **170**: 1046-1053.

Gerke, C., A. Kraft, R. Sussmuth, O. Schweitzer & F. Gotz, (1998) Characterization of the N-acetylglucosaminyltransferase activity involved in the biosynthesis of the *Staphylococcus epidermidis* polysaccharide intercellular adhesin. *The Journal of biological chemistry* **273**: 18586-18593.

Goldstein, I. J., C. E. Hollerman & J. M. Merrick, (1965) Protein-Carbohydrate Interaction. I. The Interaction of Polysaccharides with Concanavalin A. *Biochimica et biophysica acta* **97**: 68-76.

Gonzalez-Pastor, J. E., E. C. Hobbs & R. Losick, (2003) Cannibalism by sporulating bacteria. *Science* **301**: 510-513.

Grangeasse, C., A. J. Cozzone, J. Deutscher & I. Mijakovic, (2007) Tyrosine phosphorylation: an emerging regulatory device of bacterial physiology. *Trends Biochem Sci* **32**: 86-94.

Graumann, P., (2007) *Bacillus Cellular and Molecular Biology*. Caister Academic Press.

Greene, E. A. & G. B. Spiegelman, (1996) The Spo0A protein of *Bacillus subtilis* inhibits transcription of the *abrB* gene without preventing binding of the polymerase to the promoter. *J Biol Chem* **271**: 11455-11461.

Gupta, R., Q. K. Beg & P. Lorenz, (2002) Bacterial alkaline proteases: molecular approaches and industrial applications. *Applied microbiology and biotechnology* **59**: 15-32.

Guttenplan, S. B., K. M. Blair & D. B. Kearns, (2010) The EpsE flagellar clutch is bifunctional and synergizes with EPS biosynthesis to promote *Bacillus subtilis* biofilm formation. *PLoS Genet* **6**: e1001243.

Hahne, H., S. Wolff, M. Hecker & D. Becher, (2008) From complementarity to comprehensiveness--targeting the membrane proteome of growing Bacillus subtilis by divergent approaches. *Proteomics* **8**: 4123-4136.

Hall-Stoodley, L., J. W. Costerton & P. Stoodley, (2004) Bacterial biofilms: from the natural environment to infectious diseases. *Nature reviews. Microbiology* **2**: 95-108.

Hammar, M., A. Arnqvist, Z. Bian, A. Olsen & S. Normark, (1995) Expression of two *csg* operons is required for production of fibronectin- and congo red-binding curli polymers in *Escherichia coli* K-12. *Molecular Microbiology* **18**: 661-670.

Hammer, N. D., J. C. Schmidt & M. R. Chapman, (2007) The curli nucleator protein, CsgB, contains an amyloidogenic domain that directs CsgA polymerization. *P Natl Acad Sci USA* **104**: 12494-12499.

Hamoen, L. W., A. F. Van Werkhoven, G. Venema & D. Dubnau, (2000) The pleiotropic response regulator DegU functions as a priming protein in competence development in *Bacillus subtilis*. *Proc Natl Acad Sci U S A* **97**: 9246-9251.

Hamon, M. A. & B. A. Lazazzera, (2001) The sporulation transcription factor Spo0A is required for biofilm development in *Bacillus subtilis*. *Mol Microbiol* **42**: 1199-1209.

Hamon, M. A., N. R. Stanley, R. A. Britton, A. D. Grossman & B. A. Lazazzera, (2004) Identification of AbrB-regulated genes involved in biofilm formation by *Bacillus subtilis*. *Mol Microbiol* **52**: 847-860.

Hardie, K. R. & K. Heurlier, (2008) Establishing bacterial communities by 'word of mouth': LuxS and autoinducer 2 in biofilm development. *Nature reviews. Microbiology* **6**: 635-643.

Harshey, R. M., (2003) Bacterial motility on a surface: many ways to a common goal. *Annual review of microbiology* **57**: 249-273.

Harwood, C. R., (2003) *Bacillus subtilis* and its relatives: molecular biological and industrial workhorses. *Trends in Biotechnology* **10**: 247 - 256.

Harwood, C. R. & S. M. Cutting, (1990) Molecular biological methods for *Bacillus*. John Wiley &Sons Ltd. Chichester, England.

Hastings, J. W. & K. H. Nealson, (1977) Bacterial bioluminescence. *Annual review of microbiology* **31**: 549-595.

Hentzer, M., G. M. Teitzel, G. J. Balzer, A. Heydorn, S. Molin, M. Givskov & M. R. Parsek, (2001) Alginate overproduction affects *Pseudomonas aeruginosa* biofilm structure and function. *J Bacteriol* **183**: 5395-5401.

Hinc, K., R. Isticato, M. Dembek, J. Karczewska, A. Iwanicki, G. Peszynska-Sularz, M. De Felice, M. Obuchowski & E. Ricca, (2010) Expression and display of UreA of *Helicobacter acinonychis* on the surface of *Bacillus subtilis* spores. *Microb Cell Fact* **9**: 2.

Hinsa, S. M., M. Espinosa-Urgel, J. L. Ramos & G. A. O'Toole, (2003) Transition from reversible to irreversible attachment during biofilm formation by *Pseudomonas fluorescens* WCS365 requires an ABC transporter and a large secreted protein. *Molecular Microbiology* **49**: 905-918.

Hogardt, M., K. Trebesius, A. M. Geiger, M. Hornef, J. Rosenecker & J. Heesemann, (2000) Specific and rapid detection by fluorescent in situ hybridization of bacteria in clinical samples obtained from cystic fibrosis patients. *Journal of clinical microbiology* **38**: 818-825.

Huber, B., K. Riedel, M. Kothe, M. Givskov, S. Molin & L. Eberl, (2002) Genetic analysis of functions involved in the late stages of biofilm development in *Burkholderia cepacia* H111. *Molecular Microbiology* **46**: 411-426.

Irnov, I. & W. C. Winkler, (2010) A regulatory RNA required for antitermination of biofilm and capsular polysaccharide operons in *Bacillales*. *Mol Microbiol* **76**: 559-575.

Itoh, Y., J. D. Rice, C. Goller, A. Pannuri, J. Taylor, J. Meisner, T. J. Beveridge, J. F. Preston, 3rd & T. Romeo, (2008) Roles of *pgaABCD* genes in synthesis, modification, and export of the *Escherichia coli* biofilm adhesin poly-beta-1,6-N-acetyl-D-glucosamine. *Journal of Bacteriology* **190**: 3670-3680.

Itoh, Y., X. Wang, B. J. Hinnebusch, J. F. Preston, 3rd & T. Romeo, (2005) Depolymerization of beta-1,6-N-acetyl-D-glucosamine disrupts the integrity of diverse bacterial biofilms. *Journal of Bacteriology* **187**: 382-387.

Ivanova, N., A. Sorokin, I. Anderson, N. Galleron, B. Candelon, V. Kapatral, A. Bhattacharyya, G. Reznik, N. Mikhailova, A. Lapidus, L. Chu, M. Mazur, E. Goltsman, N. Larsen, M. D'Souza, T. Walunas, Y. Grechkin, G. Pusch, R. Haselkorn, M. Fonstein, S. D. Ehrlich, R. Overbeek & N. Kyrpides, (2003) Genome sequence of *Bacillus cereus* and comparative analysis with *Bacillus anthracis*. *Nature* **423**: 87-91.

Izano, E. A., M. A. Amarante, W. B. Kher & J. B. Kaplan, (2008) Differential roles of poly-N-acetylglucosamine surface polysaccharide and extracellular DNA in *Staphylococcus aureus* and *Staphylococcus epidermidis* biofilms. *Appl Environ Microbiol* **74**: 470-476.

Jackson, K. D., M. Starkey, S. Kremer, M. R. Parsek & D. J. Wozniak, (2004) Identification of *psl*, a locus encoding a potential exopolysaccharide that is essential for *Pseudomonas aeruginosa* PAO1 biofilm formation. *J Bacteriol* **186**: 4466-4475.

Ji, G., R. C. Beavis & R. P. Novick, (1995) Cell density control of staphylococcal virulence mediated by an octapeptide pheromone. *P Natl Acad Sci USA* **92**: 12055-12059.

Jiang, M., W. Shao, M. Perego & J. A. Hoch, (2000) Multiple histidine kinases regulate entry into stationary phase and sporulation in *Bacillus subtilis*. *Mol Microbiol* **38**: 535-543.

Jones, B. V., R. Young, E. Mahenthiralingam & D. J. Stickler, (2004) Ultrastructure of *Proteus mirabilis* swarmer cell rafts and role of swarming in catheter-associated urinary tract infection. *Infection and immunity* **72**: 3941-3950.

Jones, S., B. Yu, N. J. Bainton, M. Birdsall, B. W. Bycroft, S. R. Chhabra, A. J. Cox, P. Golby, P. J. Reeves, S. Stephens & et al., (1993) The lux autoinducer regulates the production of exoenzyme virulence determinants in Erwinia carotovora and *Pseudomonas aeruginosa*. *The EMBO journal* **12**: 2477-2482.

Julkowska, D., M. Obuchowski, I. B. Holland & S. J. Seror, (2004) Branched swarming patterns on a synthetic medium formed by wild-type *Bacillus subtilis* strain 3610: detection of different cellular morphologies and constellations of cells as the complex architecture develops. *Microbiology* **150**: 1839-1849.

Julkowska, D., M. Obuchowski, I. B. Holland & S. J. Seror, (2005) Comparative analysis of the development of swarming communities of *Bacillus subtilis* 168 and a natural wild type: critical effects of surfactin and the composition of the medium. *J Bacteriol* **187**: 65-76.

Kaplan, J. B., (2011) Antibiotic-induced biofilm formation. *Int J Artif Organs* **34**: 737-751.

Karatan, E. & P. Watnick, (2009) Signals, regulatory networks, and materials that build and break bacterial biofilms. *Microbiol Mol Biol Rev* **73**: 310-347.

Kearns, D. B., (2010) A field guide to bacterial swarming motility. *Nat Rev Microbiol* **8**: 634-644.

Kearns, D. B., F. Chu, S. S. Branda, R. Kolter & R. Losick, (2005) A master regulator for biofilm formation by *Bacillus subtilis*. *Mol Microbiol* **55**: 739-749.

Kearns, D. B., F. Chu, R. Rudner & R. Losick, (2004) Genes governing swarming in *Bacillus subtilis* and evidence for a phase variation mechanism controlling surface motility. *Mol Microbiol* **52**: 357-369.

Kearns, D. B. & R. Losick, (2003) Swarming motility in undomesticated *Bacillus subtilis*. *Mol Microbiol* **49**: 581-590.

Kleerebezem, M., L. E. Quadri, O. P. Kuipers & W. M. de Vos, (1997) Quorum sensing by peptide pheromones and two-component signal-transduction systems in Gram-positive bacteria. *Molecular Microbiology* **24**: 895-904.

Klunk, W. E., R. F. Jacob & R. P. Mason, (1999) Quantifying amyloid by congo red spectral shift assay. *Methods in Enzymology* **309**: 285-305.

Kobayashi, K., (2007a) *Bacillus subtilis* pellicle formation proceeds through genetically defined morphological changes. *J Bacteriol* **189**: 4920-4931.

Kobayashi, K., (2007b) Gradual activation of the response regulator DegU controls serial expression of genes for flagellum formation and biofilm formation in *Bacillus subtilis*. *Mol Microbiol* **66**: 395-409.

Kobayashi, K., (2008) SlrR/SlrA controls the initiation of biofilm formation in *Bacillus subtilis*. *Mol Microbiol* **69**: 1399-1410.

Kobayashi, K. & M. Iwano, (2012) BslA(YuaB) forms a hydrophobic layer on the surface of *Bacillus subtilis* biofilms. *Molecular Microbiology* **85**: 51-66.

Kohler, T., L. K. Curty, F. Barja, C. van Delden & J. C. Pechere, (2000) Swarming of *Pseudomonas aeruginosa* is dependent on cell-to-cell signaling and requires flagella and pili. *Journal of Bacteriology* **182**: 5990-5996.

Kolter, R., (2010) Biofilms in lab and nature: a molecular geneticist's voyage to microbial ecology. *International microbiology : the official journal of the Spanish Society for Microbiology* **13**: 1-7.

Kovacs, A. T. & O. P. Kuipers, (2011) Rok Regulates *yuaB* Expression during Architecturally Complex Colony Development of *Bacillus subtilis* 168. *J Bacteriol* **193**: 998-1002.

Kuehl, R., S. Al-Bataineh, O. Gordon, R. Luginbuehl, M. Otto, M. Textor & R. Landmann, (2009) Furanone at subinhibitory concentrations enhances staphylococcal biofilm formation by *luxS* repression. *Antimicrobial agents and chemotherapy* **53**: 4159-4166.

Kunst, F., N. Ogasawara, I. Moszer, A. M. Albertini, G. Alloni, V. Azevedo, M. G. Bertero, P. Bessieres, A. Bolotin, S. Borchert, R. Borriss, L. Boursier, A. Brans, M. Braun, S. C. Brignell, S. Bron, S. Brouillet, C. V. Bruschi, B. Caldwell, V. Capuano, N. M. Carter, S. K. Choi, J. J. Codani, I. F. Connerton, A. Danchin & et al., (1997) The complete genome sequence of the Gram-positive bacterium *Bacillus subtilis*. *Nature* **390**: 249-256.

Laemmli, U. K., (1970) Cleavage of structural proteins during the assembly of the head of bacteriophage T4. *Nature* **227**: 680-685.

Lam, K. H., K. C. Chow & W. K. Wong, (1998) Construction of an efficient *Bacillus subtilis* system for extracellular production of heterologous proteins. *J Biotechnol* **63**: 167-177.

Larsen, P., J. L. Nielsen, M. S. Dueholm, R. Wetzel, D. Otzen & P. H. Nielsen, (2007) Amyloid adhesins are abundant in natural biofilms. *Environ Microbiol* **9**: 3077-3090.

Lasa, I. & J. R. Penades, (2006) Bap: a family of surface proteins involved in biofilm formation. *Research in microbiology* **157**: 99-107.

Latasa, C., A. Roux, A. Toledo-Arana, J. M. Ghigo, C. Gamazo, J. R. Penades & I. Lasa, (2005) BapA, a large secreted protein required for biofilm formation and host colonization of *Salmonella enterica* serovar Enteritidis. *Molecular Microbiology* **58**: 1322-1339.

Latasa, C., C. Solano, J. R. Penades & I. Lasa, (2006) Biofilm-associated proteins. *C R Biol* **329**: 849-857.

Latifi, A., M. K. Winson, M. Foglino, B. W. Bycroft, G. S. Stewart, A. Lazdunski & P. Williams, (1995) Multiple homologues of LuxR and LuxI control expression of virulence determinants and secondary metabolites through quorum sensing in *Pseudomonas aeruginosa* PAO1. *Molecular Microbiology* **17**: 333-343.

Lazarevic, V., B. Soldo, N. Medico, H. Pooley, S. Bron & D. Karamata, (2005) *Bacillus subtilis* alpha-phosphoglucomutase is required for normal cell morphology and biofilm formation. *Appl Environ Microbiol* **71**: 39-45.

LeDeaux, J. R., N. Yu & A. D. Grossman, (1995) Different roles for KinA, KinB, and KinC in the initiation of sporulation in *Bacillus subtilis*. *J. bacteriol.* **177**: 861-863.

Liew, P. X., C. L. Wang & S. L. Wong, (2012) Functional characterization and localization of a *Bacillus subtilis* sortase and its substrate and use of this sortase system to covalently anchor a heterologous protein to the *B. subtilis* cell wall for surface display. *Journal of Bacteriology* **194**: 161-175.

Linder, M. B., G. R. Szilvay, T. Nakari-Setala & M. E. Penttila, (2005) Hydrophobins: the protein-amphiphiles of filamentous fungi. *FEMS microbiology reviews* **29**: 877-896.

Lopez, D., M. A. Fischbach, F. Chu, R. Losick & R. Kolter, (2009a) Structurally diverse natural products that cause potassium leakage trigger multicellularity in *Bacillus subtilis*. *Proc Natl Acad Sci U S A* **106**: 280-285.

Lopez, D. & R. Kolter, (2010) Extracellular signals that define distinct and coexisting cell fates in *Bacillus subtilis*. *FEMS Microbiol Rev* **34**: 134-149.

Lopez, D., H. Vlamakis & R. Kolter, (2009b) Generation of multiple cell types in *Bacillus subtilis*. *FEMS Microbiol Rev* **33**: 152-163.

Lopez, D., H. Vlamakis & R. Kolter, (2010) Biofilms. *Cold Spring Harb Perspect Biol* **2**: a000398.

Lopez, D., H. Vlamakis, R. Losick & R. Kolter, (2009c) Cannibalism enhances biofilm development in *Bacillus subtilis*. *Mol Microbiol* **74**: 609-618.
Lopez, D., H. Vlamakis, R. Losick & R. Kolter, (2009d) Paracrine signaling in a bacterium. *Genes Dev* **23**: 1631-1638.
Ma, L., H. Lu, A. Sprinkle, M. R. Parsek & D. J. Wozniak, (2007) *Pseudomonas aeruginosa* Psl is a galactose- and mannose-rich exopolysaccharide. *Journal of Bacteriology* **189**: 8353-8356.
Macfarlane, S. & J. F. Dillon, (2007) Microbial biofilms in the human gastrointestinal tract. *J Appl Microbiol* **102**: 1187-1196.
Madigan, M. T., J. M. Martinko & J. Parker, (2000) *Brock Biology of Microorganisms*.
Mann, E. E. & D. J. Wozniak, (2012) *Pseudomonas* biofilm matrix composition and niche biology. *FEMS microbiology reviews* **36**: 893-916.
Mapelli, F., R. Marasco, A. Balloi, E. Rolli, F. Cappitelli, D. Daffonchio & S. Borin, (2012) Mineral-microbe interactions: biotechnological potential of bioweathering. *J Biotechnol* **157**: 473-481.
Matsuyama, T., K. Kaneda, Y. Nakagawa, K. Isa, H. Hara-Hotta & I. Yano, (1992) A novel extracellular cyclic lipopeptide which promotes flagellum-dependent and -independent spreading growth of *Serratia marcescens*. *Journal of Bacteriology* **174**: 1769-1776.
McGuffin, L. J., K. Bryson & D. T. Jones, (2000) The PSIPRED protein structure prediction server. *Bioinformatics* **16**: 404-405.
McLoon, A. L., S. B. Guttenplan, D. B. Kearns, R. Kolter & R. Losick, (2011) Tracing the domestication of a biofilm-forming bacterium. *Journal of Bacteriology* **193**: 2027-2034.
McLoon, A. L., I. Kolodkin-Gal, S. M. Rubinstein, R. Kolter & R. Losick, (2010) Spatial Regulation of Histidine Kinases Governing Biofilm Formation in *Bacillus subtilis*. *J Bacteriol*.
Meile, J. C., L. J. Wu, S. D. Ehrlich, J. Errington & P. Noirot, (2006) Systematic localisation of proteins fused to the green fluorescent protein in *Bacillus subtilis*: identification of new proteins at the DNA replication factory. *Proteomics* **6**: 2135-2146.
Meselson, M. & R. Yuan, (1968) DNA restriction enzyme from *E. coli*. *Nature* **217**: 1110-1114.
Middleton, R. & A. Hofmeister, (2004) New shuttle vectors for ectopic insertion of genes into *Bacillus subtilis*. *Plasmid* **51**: 238-245.
Mijakovic, I., S. Poncet, G. Boel, A. Maze, S. Gillet, E. Jamet, P. Decottignies, C. Grangeasse, P. Doublet, P. Le Marechal & J. Deutscher, (2003) Transmembrane modulator-dependent bacterial tyrosine kinase activates UDP-glucose dehydrogenases. *Embo J* **22**: 4709-4718.
Molle, V., M. Fujita, S. T. Jensen, P. Eichenberger, J. E. Gonzalez-Pastor, J. S. Liu & R. Losick, (2003) The Spo0A regulon of *Bacillus subtilis*. *Mol Microbiol* **50**: 1683-1701.
Morikawa, M., (2006) Beneficial biofilm formation by industrial bacteria *Bacillus subtilis* and related species. *J Biosci Bioeng* **101**: 1-8.
Morris, V. K., Q. Ren, I. Macindoe, A. H. Kwan, N. Byrne & M. Sunde, (2011) Recruitment of class I hydrophobins to the air:water interface initiates a multi-step process of functional amyloid formation. *The Journal of biological chemistry* **286**: 15955-15963.

Morrison, D. C. & J. L. Ryan, (1979) Bacterial endotoxins and host immune responses. *Adv Immunol* **28**: 293-450.

Msadek, T., (1999) When the going gets tough: survival strategies and environmental signaling networks in *Bacillus subtilis*. *Trends Microbiol* **7**: 201-207.

Msadek, T., F. Kunst, D. Henner, A. Klier, G. Rapoport & R. Dedonder, (1990) Signal transduction pathway controlling synthesis of a class of degradative enzymes in *Bacillus subtilis*: expression of the regulatory genes and analysis of mutations in *degS* and *degU*. *J Bacteriol* **172**: 824-834.

Mukai, K., M. Kawata & T. Tanaka, (1990) Isolation and phosphorylation of the *Bacillus subtilis degS* and *degU* gene products. *J Biol Chem* **265**: 20000-20006.

Murray, E. J., T. B. Kiley & N. R. Stanley-Wall, (2009a) A pivotal role for the response regulator DegU in controlling multicellular behaviour. *Microbiology* **155**: 1-8.

Murray, E. J., M. A. Strauch & N. R. Stanley-Wall, (2009b) σX is involved in controlling *Bacillus subtilis* biofilm architecture through the AbrB homologue Abh. *J Bacteriol* **191**: 6822-6832.

Nagorska, K., M. Bikowski & M. Obuchowski, (2007) Multicellular behaviour and production of a wide variety of toxic substances support usage of *Bacillus subtilis* as a powerful biocontrol agent. *Acta Biochim Pol* **54**: 495-508.

Nagorska, K., K. Hinc, M. A. Strauch & M. Obuchowski, (2008) Influence of the σB Stress Factor and *yxaB*, the Gene for a Putative Exopolysaccharide Synthase under σB Control, on Biofilm Formation. *J Bacteriol* **190**: 3546-3556.

Nagorska, K., A. Ostrowski, K. Hinc, I. B. Holland & M. Obuchowski, (2010) Importance of eps genes from *Bacillus subtilis* in biofilm formation and swarming. *J Appl Genet* **51**: 369-381.

Nagy, G. & T. Pal, (2008) Lipopolysaccharide: a tool and target in enterobacterial vaccine development. *Biol Chem* **389**: 513-520.

Nakano, M. M., N. Corbell, J. Besson & P. Zuber, (1992) Isolation and characterization of *sfp*: a gene that functions in the production of the lipopeptide biosurfactant, surfactin, in *Bacillus subtilis*. *Mol Gen Genet* **232**: 313-321.

Neidhaedt, F. C., J. L. Ingraham & S. M., (1990) *Physiology of the Bacterial Cell*. Sinauer Associates Inc.

Nguyen, H. D., T. T. Phan & W. Schumann, (2011) Analysis and application of *Bacillus subtilis* sortases to anchor recombinant proteins on the cell wall. *AMB Express* **1**: 22.

Nicolella, C., M. C. van Loosdrecht & J. J. Heijnen, (2000) Wastewater treatment with particulate biofilm reactors. *J Biotechnol* **80**: 1-33.

Nijland, R., M. J. Hall & J. G. Burgess, (2010) Dispersal of biofilms by secreted, matrix degrading, bacterial DNase. *PLoS One* **5**: e15668.

O'Reilly, M. & K. M. Devine, (1997) Expression of AbrB, a transition state regulator from *Bacillus subtilis*, is growth phase dependent in a manner resembling that of Fis, the nucleoid binding protein from *Escherichia coli*. *J Bacteriol* **179**: 522-529.

Ogura, M. & T. Tanaka, (1996) *Bacillus subtilis* DegU acts as a positive regulator for *comK* expression. *FEBS Lett* **397**: 173-176.

Ohlsen, K. L., J. K. Grimsley & J. A. Hoch, (1994) Deactivation of the sporulation transcription factor Spo0A by the Spo0E protein phosphatase. *Proc Natl Acad Sci U S A* **91**: 1756-1760.

Olmos-Soto, J. & R. Contreras-Flores, (2003) Genetic system constructed to overproduce and secrete proinsulin in *Bacillus subtilis*. *Applied microbiology and biotechnology* **62**: 369-373.

Ostrowski, A., A. Mehert, A. Prescott, T. B. Kiley & N. R. Stanley-Wall, (2011) YuaB functions synergistically with the exopolysaccharide and TasA amyloid fibers to allow biofilm formation by *Bacillus subtilis*. *Journal of Bacteriology* **193**: 4821-4831.

Otsu, N., (1979) Threshold Selection Method from Gray-Level Histograms. *Ieee T Syst Man Cyb* **9**: 62-66.

Overhage, J., M. Bains, M. D. Brazas & R. E. Hancock, (2008) Swarming of *Pseudomonas aeruginosa* is a complex adaptation leading to increased production of virulence factors and antibiotic resistance. *Journal of Bacteriology* **190**: 2671-2679.

Paster, B. J., S. K. Boches, J. L. Galvin, R. E. Ericson, C. N. Lau, V. A. Levanos, A. Sahasrabudhe & F. E. Dewhirst, (2001) Bacterial diversity in human subgingival plaque. *Journal of Bacteriology* **183**: 3770-3783.

Patrick, J. E. & D. B. Kearns, (2009) Laboratory strains of *Bacillus subtilis* do not exhibit swarming motility. *J Bacteriol* **191**: 7129-7133.

Perego, M., (2001) A new family of aspartyl phosphate phosphatases targeting the sporulation transcription factor Spo0A of *Bacillus subtilis*. *Molecular Microbiology* **42**: 133-143.

Perego, M., G. B. Spiegelman & J. A. Hoch, (1988a) Structure of the gene for the transition state regulator, *abrB*: regulator synthesis is controlled by the *spo0A* sporulation gene in *Bacillus subtilis*. *Molecular Microbiology* **2**: 689-699.

Perego, M., G. B. Spiegelman & J. A. Hoch, (1988b) Structure of the gene for the transition state regulator, *abrB*:regulator synthesis is controlled by the *spo0A* sporulation gene in *Bacillus subtilis*. *Molecular Microbiology* **2**: 689-699.

Pestova, E. V., L. S. Havarstein & D. A. Morrison, (1996) Regulation of competence for genetic transformation in *Streptococcus pneumoniae* by an auto-induced peptide pheromone and a two-component regulatory system. *Molecular Microbiology* **21**: 853-862.

Petersen, T. N., S. Brunak, G. von Heijne & H. Nielsen, (2011) SignalP 4.0: discriminating signal peptides from transmembrane regions. *Nat Methods* **8**: 785-786.

Pollard, A. J., K. P. Perrett & P. C. Beverley, (2009) Maintaining protection against invasive bacteria with protein-polysaccharide conjugate vaccines. *Nat Rev Immunol* **9**: 213-220.

Pozsgai, E. R., K. M. Blair & D. B. Kearns, (2012) Modified mariner transposons for random inducible-expression insertions and transcriptional reporter fusion insertions in *Bacillus subtilis*. *Applied and environmental microbiology* **78**: 778-785.

Prigent-Combaret, C., G. Prensier, T. T. Le Thi, O. Vidal, P. Lejeune & C. Dorel, (2000) Developmental pathway for biofilm formation in curli-producing *Escherichia coli* strains: role of flagella, curli and colanic acid. *Environ Microbiol* **2**: 450-464.

Prigent-Combaret, C., O. Vidal, C. Dorel & P. Lejeune, (1999) Abiotic surface sensing and biofilm-dependent regulation of gene expression in *Escherichia coli*. *Journal of Bacteriology* **181**: 5993-6002.

Ramey, B. E., M. Koutsoudis, S. B. von Bodman & C. Fuqua, (2004) Biofilm formation in plant-microbe associations. *Curr Opin Microbiol* **7**: 602-609.

Rather, P. N., (2005) Swarmer cell differentiation in *Proteus mirabilis*. *Environmental microbiology* **7**: 1065-1073.

Reisner, A., J. A. Haagensen, M. A. Schembri, E. L. Zechner & S. Molin, (2003) Development and maturation of *Escherichia coli* K-12 biofilms. *Mol Microbiol* **48**: 933-946.

Ren, D., L. A. Bedzyk, P. Setlow, S. M. Thomas, R. W. Ye & T. K. Wood, (2004) Gene expression in *Bacillus subtilis* surface biofilms with and without sporulation and the importance of *yveR* for biofilm maintenance. *Biotechnol Bioeng* **86**: 344-364.

Rohde, H., C. Burdelski, K. Bartscht, M. Hussain, F. Buck, M. A. Horstkotte, J. K. Knobloch, C. Heilmann, M. Herrmann & D. Mack, (2005) Induction of *Staphylococcus epidermidis* biofilm formation via proteolytic processing of the accumulation-associated protein by staphylococcal and host proteases. *Molecular Microbiology* **55**: 1883-1895.

Romero, D., C. Aguilar, R. Losick & R. Kolter, (2010) Amyloid fibers provide structural integrity to *Bacillus subtilis* biofilms. *Proc Natl Acad Sci U S A* **107**: 2230-2234.

Romero, D., H. Vlamakis, R. Losick & R. Kolter, (2011) An accessory protein required for anchoring and assembly of amyloid fibres in *B. subtilis* biofilms. *Molecular Microbiology*.

Romling, U., Z. Bian, M. Hammar, W. D. Sierralta & S. Normark, (1998a) Curli fibers are highly conserved between *Salmonella typhimurium* and *Escherichia coli* with respect to operon structure and regulation. *J Bacteriol* **180**: 722-731.

Romling, U., W. D. Sierralta, K. Eriksson & S. Normark, (1998b) Multicellular and aggregative behaviour of *Salmonella typhimurium* strains is controlled by mutations in the *agfD* promoter. *Molecular Microbiology* **28**: 249-264.

Roux, A., C. Beloin & J. M. Ghigo, (2005) Combined inactivation and expression strategy to study gene function under physiological conditions: application to identification of new *Escherichia coli* adhesins. *Journal of Bacteriology* **187**: 1001-1013.

Ruzal, S. M. & C. Sanchez-Rivas, (1998) In *Bacillus subtilis* DegU-P is a positive regulator of the osmotic response. *Curr Microbiol* **37**: 368-372.

Saeed, S. M. & G. Fine, (1967) Thioflavin-T for amyloid detection. *Am J Clin Pathol* **47**: 588-593.

Sambrook, J. & D. Russell, (2001) *Molecular Cloning. A laboratory manual*. Cold Springs Harbour Laboratory Press.

Schauder, S. & B. L. Bassler, (2001) The languages of bacteria. *Genes & development* **15**: 1468-1480.

Scheffers, D.-J., (2007) *The Cell Wall of Bacillus subtilis*. Caister Academic Press, Wymondham, U.K.

Schroeder, H. E., (1969) Formation and inhibition of dental calculus. *J Periodontol* **40**: 643-646.

Segrest, J. P. & L. Jackson, (1972) Molecular Weight Determination of Glycoproteins by polyacrylamide Gel Electrophoresis in Sodium Dodecyl Sufate. *Methods in Enzymology* **28**: 54-63.

Segrest, J. P., R. L. Jackson, E. P. Andrews & V. T. Marchesi, (1971) Human erythrocyte membrane glycoprotein: a re-evaluation of the molecular weight as determined by SDS polyacrylamide gel electrophoresis. *Biochemical and biophysical research communications* **44**: 390-395.

Seminara, A., T. E. Angelini, J. N. Wilking, H. Vlamakis, S. Ebrahim, R. Kolter, D. A. Weitz & M. P. Brenner, (2012) Osmotic spreading of *Bacillus subtilis* biofilms driven by an extracellular matrix. *P Natl Acad Sci USA* **109**: 1116-1121.

Serrano, M., R. Zilhao, E. Ricca, A. J. Ozin, C. P. Moran, Jr. & A. O. Henriques, (1999) A *Bacillus subtilis* secreted protein with a role in endospore coat assembly and function. *Journal of Bacteriology* **181**: 3632-3643.

Shank, E. A., V. Klepac-Ceraj, L. Collado-Torres, G. E. Powers, R. Losick & R. Kolter, (2011) Interspecies interactions that result in *Bacillus subtilis* forming biofilms are mediated mainly by members of its own genus. *P Natl Acad Sci USA* **108**: E1236-1243.

Shank, E. A. & R. Kolter, (2009) New developments in microbial interspecies signaling. *Current opinion in microbiology* **12**: 205-214.

Shank, E. A. & R. Kolter, (2011) Extracellular signaling and multicellularity in Bacillus subtilis. *Current opinion in microbiology* **14**: 741-747.

Shapiro, J. A., (1998) Thinking about bacterial populations as multicellular organisms. *Annu Rev Microbiol* **52**: 81-104.

Shimane, K. & M. Ogura, (2004) Mutational analysis of the helix-turn-helix region of *Bacillus subtilis* response regulator DegU, and identification of *cis*-acting sequences for DegU in the *aprE* and *comK* promoters. *J Biochem (Tokyo)* **136**: 387-397.

Shimkets, L. J. & M. Dworkin, (1997) *Myxobacterial* Multicellularity. In: Bacteria as Multicellular Organisms. J. A. Shapiro & M. Dworkin (eds). Oxford Univeristy Press, pp. 220 - 244.

Singh, R., D. Paul & R. K. Jain, (2006) Biofilms: implications in bioremediation. *Trends in microbiology* **14**: 389-397.

Sockett, R. E., (2009) Predatory lifestyle of *Bdellovibrio bacteriovorus*. *Annual review of microbiology* **63**: 523-539.

Solomon, J. M., B. A. Lazazzera & A. D. Grossman, (1996) Purification and characterization of an extracellular peptide factor that affects two different developmental pathways in *Bacillus subtilis*. *Genes Dev* **10**: 2014-2024.

Spizizen, J., (1958) Transformation of Biochemically Deficient Strains of *Bacillus subtilis* by Deoxyribonucleate. *Proc Natl Acad Sci U S A* **44**: 1072-1078.

Stanley, N. R., R. A. Britton, A. D. Grossman & B. A. Lazazzera, (2003) Identification of catabolite repression as a physiological regulator of biofilm formation by *Bacillus subtilis* by use of DNA microarrays. *J Bacteriol* **185**: 1951-1957.

Stanley, N. R. & B. A. Lazazzera, (2005) Defining the genetic differences between wild and domestic strains of *Bacillus subtilis* that affect poly-gamma-dl-glutamic acid production and biofilm formation. *Mol Microbiol* **57**: 1143-1158.

Stein, T., (2005) *Bacillus subtilis* antibiotics: structures, syntheses and specific functions. *Mol Microbiol* **56**: 845-857.

Steinberger, R. E. & P. A. Holden, (2005) Extracellular DNA in single- and multiple-species unsaturated biofilms. *Applied and environmental microbiology* **71**: 5404-5410.

Stevenson, G., K. Andrianopoulos, M. Hobbs & P. R. Reeves, (1996) Organization of the *Escherichia coli* K-12 gene cluster responsible for production of the extracellular polysaccharide colanic acid. *Journal of Bacteriology* **178**: 4885-4893.

Stover, A. G. & A. Driks, (1999a) Control of synthesis and secretion of the *Bacillus subtilis* protein YqxM. *J. bacteriol.* **181**: 7065-7069.

Stover, A. G. & A. Driks, (1999b) Regulation of synthesis of the *Bacillus subtilis* transition-phase, spore-associated antibacterial protein TasA. *Journal of Bacteriology* **181**: 5476-5481.

Stover, A. G. & A. Driks, (1999c) Secretion. localization and antibacterial activity of tasA, a *Bacillus subtilis* spore-associated protein. *J. bacteriol.* **181**: 1664-1672.

Straight, P. D., J. M. Willey & R. Kolter, (2006) Interactions between *Streptomyces coelicolor* and *Bacillus subtilis*: Role of surfactants in raising aerial structures. *J Bacteriol* **188**: 4918-4925.

Strauch, M. A., G. B. Spiegelman, M. Perego, W. C. Johnson, D. Burbulys & J. A. Hoch, (1989) The transition state transcription regulator *abrB* of *Bacillus subtilis* is a DNA binding protein. *Embo J* **8**: 1615-1621.

Studier, F. W. & B. A. Moffatt, (1986) Use of bacteriophage T7 RNA polymerase to direct selective high-level expression of cloned genes. *Journal of molecular biology* **189**: 113-130.

Sunde, M., L. C. Serpell, M. Bartlam, P. E. Fraser, M. B. Pepys & C. C. Blake, (1997) Common core structure of amyloid fibrils by synchrotron X-ray diffraction. *Journal of molecular biology* **273**: 729-739.

Sutherland, I. W., (2001) The biofilm matrix--an immobilized but dynamic microbial environment. *Trends Microbiol* **9**: 222-227.

Tam, N. K., N. Q. Uyen, H. A. Hong, H. Duc le, T. T. Hoa, C. R. Serra, A. O. Henriques & S. M. Cutting, (2006) The intestinal life cycle of *Bacillus subtilis* and close relatives. *Journal of Bacteriology* **188**: 2692-2700.

Terra, R., N. R. Stanley-Wall, G. Cao & B. A. Lazazzera, (2012) Identification of *Bacillus subtilis* SipW as a Bifunctional Signal Peptidase that Controls Surface-Adhered Biofilm Formation. *Journal of Bacteriology*.

Tielker, D., S. Hacker, R. Loris, M. Strathmann, J. Wingender, S. Wilhelm, F. Rosenau & K. E. Jaeger, (2005) *Pseudomonas aeruginosa* lectin LecB is located in the outer membrane and is involved in biofilm formation. *Microbiology* **151**: 1313-1323.

Toledo-Arana, A., J. Valle, C. Solano, M. J. Arrizubieta, C. Cucarella, M. Lamata, B. Amorena, J. Leiva, J. R. Penades & I. Lasa, (2001) The enterococcal surface protein, Esp, is involved in *Enterococcus faecalis* biofilm formation. *Applied and environmental microbiology* **67**: 4538-4545.

Tolker-Nielsen, T., U. C. Brinch, P. C. Ragas, J. B. Andersen, C. S. Jacobsen & S. Molin, (2000) Development and dynamics of *Pseudomonas sp*. biofilms. *J. bacteriol.* **182**: 6482-6489.

Tormo, M. A., E. Knecht, F. Gotz, I. Lasa & J. R. Penades, (2005) Bap-dependent biofilm formation by pathogenic species of *Staphylococcus*: evidence of horizontal gene transfer? *Microbiology* **151**: 2465-2475.

Trach, K. A. & J. A. Hoch, (1993) Multisensory activation of the phosphorelay initiating sporulation in *Bacillus subtilis*: identification and sequence of the protein kinase of the alternate pathway. *Molecular Microbiology* **8**: 69-79.

Tsukahara, K. & M. Ogura, (2007) Characterization of DegU-dependent expression of *bpr* in *Bacillus subtilis*. *FEMS Microbiol Lett*: 1-6.

Tsukahara, K. & M. Ogura, (2008) Promoter selectivity of the *Bacillus subtilis* response regulator DegU, a positive regulator of the *fla/che* operon and *sacB*. *BMC Microbiol* **8**: 8.

van Sinderen, D. & G. Venema, (1994) *comK* acts as an autoregulatory control switch in the signal transduction route to competence in *Bacillus subtilis*. *J Bacteriol* **176**: 5762-5770.

Varki, A., R. D. Cummings, J. D. Esko, H. H. Freeze, P. Stanley, C. R. Bertozzi, G. W. Hart & M. E. Etzler, (2008) *Essentials of glycobiology*. Cold Springs Harbour Laboratory Press.

Veening, J. W., L. W. Hamoen & O. P. Kuipers, (2005) Phosphatases modulate the bistable sporulation gene expression pattern in *Bacillus subtilis*. *Mol Microbiol* **56**: 1481-1494.

Verhamme, D. T., T. B. Kiley & N. R. Stanley-Wall, (2007) DegU co-ordinates multicellular behaviour exhibited by *Bacillus subtilis*. *Mol Microbiol* **65**: 554-568.

Verhamme, D. T., E. J. Murray & N. R. Stanley-Wall, (2009) DegU and Spo0A jointly control transcription of two loci required for complex colony development by *Bacillus subtilis*. *J Bacteriol* **191**: 100-108.

Vidal, O., R. Longin, C. Prigent-Combaret, C. Dorel, M. Hooreman & P. Lejeune, (1998) Isolation of an *Escherichia coli* K-12 mutant strain able to form biofilms on inert surfaces: involvement of a new *ompR* allele that increases curli expression. *J Bacteriol* **180**: 2442-2449.

Vilain, S., J. M. Pretorius, J. Theron & V. S. Brozel, (2009) DNA as an adhesin: *Bacillus cereus* requires extracellular DNA to form biofilms. *Applied and environmental microbiology* **75**: 2861-2868.

Vlamakis, H., C. Aguilar, R. Losick & R. Kolter, (2008) Control of cell fate by the formation of an architecturally complex bacterial community. *Genes Dev* **22**: 945-953.

Vuong, C., S. Kocianova, J. M. Voyich, Y. Yao, E. R. Fischer, F. R. DeLeo & M. Otto, (2004) A crucial role for exopolysaccharide modification in bacterial biofilm formation, immune evasion, and virulence. *The Journal of biological chemistry* **279**: 54881-54886.

Wagner, M., A. Loy, R. Nogueira, U. Purkhold, N. Lee & H. Daims, (2002) Microbial community composition and function in wastewater treatment plants. *Antonie Van Leeuwenhoek* **81**: 665-680.

Wang, X. & M. R. Chapman, (2008) Curli provide the template for understanding controlled amyloid propagation. *Prion* **2**: 57-60.

Whitchurch, C. B., T. Tolker-Nielsen, P. C. Ragas & J. S. Mattick, (2002) Extracellular DNA required for bacterial biofilm formation. *Science* **295**: 1487.

White, D. J., (1997) Dental calculus: recent insights into occurrence, formation, prevention, removal and oral health effects of supragingival and subgingival deposits. *Eur J Oral Sci* **105**: 508-522.

Winson, M. K., M. Camara, A. Latifi, M. Foglino, S. R. Chhabra, M. Daykin, M. Bally, V. Chapon, G. P. Salmond, B. W. Bycroft & et al., (1995) Multiple N-acyl-L-homoserine lactone signal molecules regulate production of virulence determinants and secondary metabolites in *Pseudomonas aeruginosa*. *P Natl Acad Sci USA* **92**: 9427-9431.

Wosten, H. A. & M. L. de Vocht, (2000) Hydrophobins, the fungal coat unravelled. *Biochimica et biophysica acta* **1469**: 79-86.

Wozniak, D. J., T. J. Wyckoff, M. Starkey, R. Keyser, P. Azadi, G. A. O'Toole & M. R. Parsek, (2003) Alginate is not a significant component of the extracellular

polysaccharide matrix of PA14 and PAO1 *Pseudomonas aeruginosa* biofilms. *Proc Natl Acad Sci U S A* **100**: 7907-7912.

Wu, S. C. & S. L. Wong, (2002) Engineering of a *Bacillus subtilis* strain with adjustable levels of intracellular biotin for secretory production of functional streptavidin. *Applied and environmental microbiology* **68**: 1102-1108.

Yamane, K., K. Bunai & H. Kakeshita, (2004) Protein traffic for secretion and related machinery of *Bacillus subtilis*. *Bioscience, biotechnology, and biochemistry* **68**: 2007-2023.

Yasbin, R. E. & F. E. Young, (1974) Transduction in *Bacillus subtilis* by bacteriophage SPP1. *J Virol* **14**: 1343-1348.

Zogaj, X., M. Nimtz, M. Rohde, W. Bokranz & U. Romling, (2001) The multicellular morphotypes of *Salmonella typhimurium* and *Escherichia coli* produce cellulose as the second component of the extracellular matrix. *Mol Microbiol* **39**: 1452-1463.

7. Appendices

7.1. Appendix A: Strains plasmids and oligonucleotides

Table 7.1 List of strains

Strain	Relevant genotype /Description [1]	Source / Construction [2]
	Escherichia coli strains	
BL21(DE3)	*F– ompT gal dcm lon hsdSB(rB- mB-) λ(DE3 [lacI lacUV5-T7 gene 1 ind1 sam7 nin5])*	(Studier & Moffatt, 1986)
DH5α	*F- endA1 glnV44 thi-1 recA1 relA1 gyrA96 deoR nupG Φ80dlacZΔM15 Δ(lacZYA-argF)U169, hsdR17(rK- mK+), λ–*	(Meselson & Yuan, 1968)
MC1061	*F'lacIQ lacZM15 Tn10 (tet)*	*E. coli* Genetic Stock Centre
	Bacillus subtilis strains	
168	*trpC2*	*Bacillus* genetic stock centre
BAL835	JH642 *amyE::Pspac-hy-gfp mut2 (cat)*	(Stanley *et al.*, 2003)
BAL984	JH642 *trpC2 pheA1 tasA::spc*	(Hamon *et al.*, 2004)
DS93	3610 *sinIR::spc*	(Kearns *et al.*, 2005)
JH642	*trpC2 pheA1*	(Perego *et al.*, 1988b)
NCIB3610	prototroph	*Bacillus* Genetic Stock Centre
NRS1314	3610 *degU::pBL204* (cat)	(Verhamme *et al.*, 2007)
NRS1471	JH642 *sacA::Phy-spank-gfp mut2 (kan)*	(Verhamme *et al.*, 2007)
NRS1473	3610 *sacA::Pspac-hy-gfp mut2 (cat)*	SPP1 NRS1471 → 3610
NRS1647	3610 *abrB:: Tn10* (mls)	(Verhamme *et al.*, 2009)
NRS2097	3610 *yuaB::cat*	(Verhamme *et al.*, 2009)
NRS2242	3610 *sacA::PepsA-gfp mut2*(kan)	(Murray *et al.*, 2009b)
NRS2271	JH642 *sacA::PyuaB-gfp mut2* (kan)	pNW511 → JH642
NRS2275	JH642 *sacA::PepsA-gfp mut2* (kan)	pNW510 → JH642
NRS2276	3610 *abrB::Tn10* (mls) *yuaB::cat*	NRS2095 → NRS1647
NRS2283	JH642 *amyE::Phy-spank-yuaB-lacI* (spc)	(Verhamme *et al.*, 2009)
NRS2289	3610 *sacA::PyuaB-gfp mut2* (kan)	SPP1 NRS2271 → 3610
NRS2290	3610 *sacA::PepsA-gfp mut2* (kan)	SPP1 NRS2275 → 3610
NRS2291	3610 *sinIR::spc yuaB::cat*	SPP1 DS93 → NRS2097
NRS2292	3610 *yuaB::cat sacA::PyuaB-gfp mut2* (kan)	SPP1 NRS2271→ NRS2097
NRS2296	3610 *abrB::Tn10* (mls) *sacA::PyqxM-gfp mut2* (kan)	SPP1 NRS2275 → NRS1647
NRS2298	3610 *degU::cat amyE::Phy-spank-yuaB-lacI* (spc)	SPP1 NRS2283 → NRS1314
NRS2299	3610 *yuaB::cat amyE::Phy-spank-yuaB-lacI (spc)*	(Verhamme *et al.*, 2009)
NRS2302	3610 *abrB::Tn10* (mls) *yuaB::cat sacA::PepsA-gfp mut2* (kan)	SPP1 NRS2275 → NRS2276

Strain	Relevant genotype /Description [1]	Source / Construction [2]
NRS2388	168 *sacA::PyqxM-gfp mut2* (kan)	(Murray *et al.*, 2009b)
NRS2391	*168 amyE::Phy-spank-yuaB-flag-lacI (spc)*	pNW603 → 168
NRS2393	3610 *yuaB::cat sacA::PyqxM-gfp mut2* (kan)	SPP1 NRS2388 →NRS 2097
NRS2394	3610 *sacA::PyqxM-gfp mut2* (kan)	(Murray *et al.*, 2009b)
NRS2397	3610 *yuaB::cat amyE::Phy-spank-yuaB-flag-lacI (spc)*	SPP1 NRS2391 → NRS2097
NRS2398	3610 *yuaB::cat sacA::PepsA-gfp* (kan)	SPP1 2095 → NRS2242
NRS2404	168 *yweA::kan*	NSW806/NSW809 → 168
NRS2405	3610 *yweA::kan*	SPP1 NRS2404 →3610
NRS2409	168 *amyE::Phy-spank-yweA-lacI (spc)*	pNW608 → 168
NRS2410	168 *amyE::Phy-spank-BLyuaB-lacI (spc)**	pNW609 → 168
NRS2412	3610 *yuaB::cat amyE::Phy-spank-yweA-lacI (spc)*	SPP1 NRS2409 → NRS2097
NRS2414	3610 *yuaB::cat amyE::Phy-spank-BLyuaB-lacI (spc)**	SPP1 NRS2410 → NRS2097
NRS2415	3610 *tasA::spc*	SPP1 BAL984 → 3610
NRS2417	3610 *yuaB::cat amyE*::*Pspac-hy-gfp mut2 cat*	SPP1 BAL835 → NRS2097
NRS2418	3610 *abrB::Tn10* (mls) *yuaB::cat sacA::PyqxM-gfp mut2* (kan)	SPP1 NRS2388 → NRS2276
NRS2425	3610 *yuaB::cat tasA ::spc*	SPP1 BAL984 → NRS2097
NRS2426	3610 *abrB::Tn10* (mls) *sacA::PyqxM-gfp mut2* (kan)	SPP1 NRS1128 → NRS2394
NRS2427	3610 *sinIR::spc sacA::PepsA-gfp mut2* (kan)	SPP1 DS93 → NRS2290
NRS2428	3610 *sinIR::spc yuaB::cat sacA::PepsA-gfp mut2* (kan)	SPP1 DS93 → NRS2293
NRS2429	3610 *sinIR::spc sacA::PyqxM-gfp mut2* (kan)	SPP1 DS93 → NRS2394
NRS2430	3610 *sinIR::spc yuaB::cat sacA::PyqxM-gfp mut2* (kan)	SPP1 DS93 → NRS2393
NRS2440	168 *amyE::Phy-spank-yuaB*$_{\Delta 2\text{-}28}$*-lacI* (spc)	pNW616 → 168
NRS2441	168 *amyE::Phy-spank-yuaBss-yuaB-lacI* (spc)	pNW617 → 168
NRS2442	168 *amyE::Phy-spank-wapAss-yuaB-lacI* (spc)	pNW618 → 168
NRS2446	3610 *yuaB::cat amyE::Phy-spank-yuaB*$_{\Delta 2\text{-}28}$*-lacI* (spc)	SPP1 NRS2440 → NRS2097
NRS2447	3610 *yuaB::cat amyE::Phy-spank-yuaBss-yuaB-lacI* (spc)	SPP1 NRS2441 → NRS2097
NRS2448	3610 *yuaB::cat amyE::Phy-spank-wapAss-yuaB-lacI* (spc)	SPP1 NRS2442 → NRS2097
NRS2450	3610 *eps(A-O)::tet*	(Branda *et al.*, 2006)
NRS2451	3610 *eps(A-O)::tet tasA::spc*	SPP1 NRS2450 → NRS2415
NRS2452	3610 *eps(A-O)::tet yuaB::cat*	SPP1 NRS2450 → NRS2097
NRS2456	168 *amyE::Phy-spank-BAyuaB-lacI (spc)***	pNW615 → 168
NRS2458	3610 *yuaB::cat amyE::Phy-spank-BAyuaB-lacI (spc)***	SPP1 NRS2456 → NRS2097
NRS2462	168 *amyE::Phy-spank-BPyuaB-lacI (spc)****	pNW620 → 168
NRS2464	3610 *yuaB::cat amyE::Phy-spank-BPyuaB-lacI (spc)****	SPP1 NRS2462 → NRS2097
NRS2543	3610 *eps(A-O)::tet tasA::spc yuaB::cat*	SPP1 NRS2450 → NRS2452
NRS2748	3610 *yuaB::cat abrB::Tn10 (mls) amyE::Phy-spank-yuaB-lacI* (spc)	SPP1 NRS1128 → NRS2299
NRS2749	3610 *yuaB::cat sinR::kan amyE::Phy-spank-yuaB-lacI* (spc)	SPP1 NRS1858 → NRS2299
NRS2953	168 *amyE::Phy-spank-yuaB*$_{\Delta 172\text{-}181}$*-lacI (spc)*	pNW621 →168
NRS2957	3610 *yuaB::cat amyE::Phy-spank-yuaB*$_{\Delta 172\text{-}181}$*-lacI (spc)*	SPP1 NRS2953 → NRS2097
NRS2976	168 *sacA::PyuaB-yuaB (*kan)	pNW518 → 168
NRS2980	3610 *eps(A-O)::tet tasA::spc sacA::PyuaB-yuaB* (kan)	SPP1 NRS2976 → NRS2451
NRS2999	168 *amyE::Phy-spank-yuaB-yweA-lacI (spc)*	pNW639 → 168

Strain	Relevant genotype /Description [1]	Source / Construction [2]
NRS3001	3610 *yuaB::cat amyE::Phy-spank-yuaB-yweA-lacI (spc)*	SPP1 NRS2999 → NRS2097
NRS3790	3610 *yuaB*::*cat amyE*::Phy-spank-*yuaB-lacI* (*spc*) *sacA*::*Phy-spank-gfp mut2 (kan)*	SPP1 NRS1471 → NRS2299
NRS3800	168 *amyE::Phy-spank-yuaB$_{F51Y}$-lacI (spc)*	pNW692 → 168
NRS3801	168 *amyE::Phy-spank-yuaB$_{L76P}$-lacI (spc)*	pNW687 → 168
NRS3809	3610 *yuaB::cat amyE::Phy-spank-yuaB$_{L76P}$-lacI (spc)*	SPP1 NRS3801 → NRS2097
NRS3811	3610 *yuaB::cat amyE::Phy-spank-yuaB$_{F51Y}$-lacI (spc)*	SPP1 NRS3800 → NRS2097
NRS3812	3610 *yuaB::cat sacA:: Phy-spank-gfpmut2 (kan)*	SPP1 NRS1471 → NRS2097
NRS3819	3610 *yuaB::cat amyE::Phy-spank-yuaB$_{LFAT-AAAA}$-lacI (spc)*	SPP1 NRS3967 → NRS2097
NRS3820	3610 *yuaB::cat amyE::Phy-spank-yuaB$_{L76I}$-lacI (spc)*	SPP1 NRS3969 → NRS2097
NRS3821	3610 *yuaB::cat amyE::Phy-spank-yuaB$_{F51P}$-lacI (spc)*	SPP1 NRS3968 → NRS2097
NRS3948	3610 *yuaB::cat amyE::Phy-spank-yuaB$_{L76P}$-lacI (spc) sacA:: Phy-spank-gfp mut2 (kan)*	SPP1 NRS3801 → NRS3812
NRS3952	*168 amyE::Phy-spank-yuaB$_{LGVMEF-AAAAAA}$-lacI (spc)*	pNW696 → 168
NRS3960	3610 *yuaB::cat amyE::Phy-spank-yuaB$_{LGVMEF-AAAAAA}$-lacI (spc)*	SPP1 NRS3952 → NRS2097
NRS3967	168 *amyE::Phy-spank-yuaB $_{LFAT-AAAA}$-lacI (spc)*	pNW1102 →168
NRS3968	168 *amyE::Phy-spank-yuaB$_{F51P}$-lacI (spc)*	pNW1103 →168
NRS3969	168 *amyE::Phy-spank-yuaB$_{L76I}$-lacI (spc)*	pNW1104 →168

[1] Antibiotic resistance cassettes are indicated as follows: *cat*, chloramphenicol resistance; *kan*, kanamycin resistance; *tet*, tetracycline resistance; *mls*, lincomycin/erythromycin resistance; and *spc*, spectinomycin resistance. BSGC represents the *Bacillus* genetic stock centre. *- Allele of *yuaB* cloned from *B. licheniformis* DSM13; **- Allele of *yuaB* cloned from *B. amyloliquefaciens* FZB42; ***- Allele of *yuaB* cloned from *B. pumilus* SAFR-032.

[2] The direction of strain construction is indicated with DNA or phage (SPP1) (→) recipient strain.

Table 7.2 List of plasmids[1]

Plasmid	Harbouring strain	Description	Source/construction[2]
pDR111	NRS1281	B. subtilis integration vector for IPTG-induced expression	(Britton *et al.*, 2002)
pSac-Kan	NRS1038	B. subtilis integration vector	(Middleton & Hofmeister, 2004)
pGEX-6-P	NRS2766	Vector for overexpression of GST-fused proteins	GE Healthcare
pET15bTEV	NRS2838	Vector for overexpression of N-terminally His6-tagged proteins with TEV cleavage site	(Cohen-Gonsaud *et al.*, 2004)
pQE60	NRS1407	Protein expression vector	Qiagen
pQE70	NRS1408	Protein expression vector	Qiagen
pNW512	NRS2278	pDR111-*yuaB*	(Verhamme *et al.*, 2009)
pNW518	NRS2287	pSac-Kan-P_{yuaB}-*yuaB*	Constructed by N. R. Stanley-Wall (NSW646/NSW645 → pSac-Kan)
pNW543	NRS2765	pGEX-6-P-*tasA*	Constructed by N. R. Stanley-Wall (NSW660/NSW661 → pGEX-6-P)
pNW603	NRS2390	pDR111-yuaB-flag	NSW626/NSW801 → pDR111
pNW608	NRS2407	pDR111-*yweA*	NSW810/NSW811 → pDR111
pNW609	NRS2408	pDR111-$yuaB_{Bl}$[3]	NSW812/NSW813 → pDR111
pNW610	NRS2420	pQE60-$yuaB_{His6}$	NSW825/NSW826 → pQE60
pNW611	NRS2432	pQE70-$yuaB_{ss}$	NSW626/NSW828 → pQE70
pNW612	NRS2433	pQE70-$wapA_{ss}$	NSW831/NSW832 → pQE70
pNW613	NRS2434	pQE70-$yuaB_{ss}$-*yuaB*	NSW827/NSW645 → pNW611
pNW614	NRS2435	pQE70-$wapA_{ss}$-*yuaB*	NSW827/NSW645 → pNW612
pNW615	NRS2436	pDR111-$yuaB_{Ba}$[4]	NSW829/NSW830 → pDR111
pNW616	NRS2437	pDR111-$yuaB_{\Delta 2\text{-}28}$	NSW814/NSW645 → pDR111
pNW617	NRS2438	pDR111-$yuaB_{ss}$-*yuaB*	pNW613 → pDR111
pNW618	NRS2439	pDR111-$wapA_{ss}$-*yuaB*	pNW614 → pDR111
pNW619	NRS2460	pGEX-6-P-$yuaB_{29\text{-}181}$	NSW835/NSW836 → pGEX-6-P
pNW620	NRS2461	pDR111-$yuaB_{Bp}$[5]	NSW819/NSW820 → pDR111
pNW621	NRS2465	pDR111-$yuaB_{\Delta 172\text{-}181}$	NSW626/NSW838 → pDR111
pNW622	NRS2952	pQE70-$yuaB_{ss}$-$yuaB_{\Delta 29\text{-}38}$	NSW837/NSW645 →pNW611
pNW623	NRS2954	pDR111-$yuaB_{ss}$-$yuaB_{\Delta 29\text{-}38}$	pNW622 → pDR111
pNW624	NRS2955	pQE70-$yuaB_{ss}$-$yuaB_{\Delta 29\text{-}48}$	NSW839/NSW645 → pNW611
pNW625	NRS2961	pQE70-$yuaB_{ss}$-$yuaB_{\Delta 29\text{-}58}$	NSW840/NSW645 → pNW611
pNW626	NRS2962	pDR111-$yuaB_{ss}$-$yuaB_{\Delta 29\text{-}48}$	pNW624 → pDR111
pNW627	NRS2964	pDR111-$yuaB_{ss}$-$yuaB_{\Delta 29\text{-}58}$	pNW625 → pDR111
pNW628	NRS2965	pDR111-$yuaB_{\Delta 152\text{-}181}$	NSW626/NSW842 → pDR111
pNW629	NRS2970	pDR111-$yuaB_{\Delta 162\text{-}181}$	NSW626/NSW841 → pDR111
pNW630	NRS2981	pQE70-$yuaB_{ss}$-$yuaB_{\Delta 29\text{-}38\ \Delta 172\text{-}181}$	NSW837/NSW838 → pNW611
pNW631	NRS2982	pDR111-$yuaB_{\Delta 29\text{-}38\ \Delta 172\text{-}181}$	pNW630 → pDR111
pNW632	NRS2987	pET15bTEV-$yuaB_{29\text{-}176}$	NSW845/NSW846 → pET15bTEV

Plasmid	Harbouring strain	Description	Source/construction[2]
pNW633	NRS2988	pQE70-*yuaB*$_{1-54}$	NSW626/NSW849 → pQE70
pNW634	NRS2991	pGEX-6-P-*yuaB*$_{29-176}$	NSW847/NSW848 → pNW619
pNW638	NRS2995	pQE70-*yuaB-yweA*	NSW850/NSW811 → pNW633
pNW639	NRS2996	pDR111-*yuaB-yweA*	pNW638 → pDR111
pNW691	NRS3802	pDR111-*yuaB*$_{L76P}$	NSW1301/NSW1302 → pNW512
pNW692	NRS3803	pDR111-*yuaB*$_{F51Y}$	NSW1330/NSW1331 → pNW512
pNW696	NRS3807	pDR111-*yuaB*$_{LGVMEF-AAAAAA}$	NSW1335/NSW1336 → pNW512
pNW1100	NRS3943	pGEX-6-P-*yuaB*$_{29-176\ L76P}$	Constructed by L. Hobley (NSW1301/NSW1302 → pNW634)
pNW1102	NRS3963	pDR111-*yuaB*$_{LFAT-AAAA}$	Constructed by L. Hobley (NSW1316/NSW1317 → pNW512)
pNW1103	NRS3964	pDR111-*yuaB*$_{F51P}$	Constructed by L. Hobley (NSW1328/NSW1329 → pNW512)
pNW1104	NRS3965	pDR111-*yuaB*$_{L76I}$	Constructed by L. Hobley (NSW1337/NSW1338 → pNW512)

[1] All plasmids were constructed and maintained in *E. coli* strain MC1061 [*F'lacIQ lacZM15 Tn10 (tet)].* [2] The PCR product obtained using indicated primers or the insert cut out from an indicated vector was ligated into the target vector as indicated by →; [3] Allele of *yuaB* cloned from *B. licheniformis* DSM13; [4] Allele of *yuaB* cloned from *B. amyloliquefaciens* FZB42; [5] Allele of *yuaB* cloned from *B. pumilus* SAFR-032. BSGC represents the *Bacillus* genetic stock centre.

Table 7.3 Oligonucleotide primers

Primer	Sequence 5' – 3' [1]	Target and use	Coordinates [2]
NSW12	CGATTCAAAACCTCTTTACTG	*amyE* locus	12 → 33
NSW13	GCTTAAGCCCGAGTC	*amyE* locus	1972 → 1957
NSW152	CAGCGAACCATTTGAGGTGATAGG	*kan* cassette amplification	-527 → -503
NSW153	CGATACAAATTCCTCGTAGGCGCTCGG	*kan* cassette amplification	953 → 926
NSW207	CATGACCAGGAGCTTCGT	*sacA* locus	10 → 28
NSW208	CGCACTGGCTGTTACTTC	*sacA* locus	1398→ 1381
NSW660	GCATGGATCCGCATTTAACGACATTAAATCAAA	*tasA* expression	81 → 104
NSW661	GCATCTCGAGTTAATTTTTATCCTCGCTATGCGA	*tasA* expression	786 → 763
NSW626	AGCTAAGCTTCATTTTTTAGGGGGAATTTGTTATG	*yuaB* cloning	-24 → -5
NSW645	AACTGCATGCTTAGTTGCAACCGCAAGGCTGA	*yuaB* cloning	546 → 525
NSW646	ATGCGGATCCGCTTACTATGACTGGCTG	*yuaB* promoter	-281 → -263
NSW647	AACTTCTAGATTAGTTGCAACCGCAAGGCTGA	*yuaB* promoter	1 → -22
NSW801	GCATCGTACGTTATTATTTATCATCATCATCTTTATAATCCGTTG CAACCGCAAGGC	*yuaB-flag tag*	546 → 525
NSW806	CCAAAAGGGGTGGCTCACGGATATAGAGTGC	*yweA* deletion	-482 → 452
NSW807	CCTATCACCTCAAATGGTTCGCTGTTTTAGCATGACATTTCC	*yweA* deletion	9 → -9
NSW808	CGAGCGCCTACGAGGAATTTGTATCGATCCCCGTTAATCG	*yweA* deletion	454 → 468
NSW809	AATCCCGCATTTGAGCGTCATCC	*yweA* deletion	962 → 940
NSW810	GCTCAAGCTTCAATTAGGGGGAAATGTCATGCTAAAA	*yweA* cloning	-19 → 9
NSW811	GCATGCATGCCAAATCTATCGATTAACGGG	*yweA* cloning	477 → 458
NSW812	GCAAAAGCTTTTGGGGGAATTGCTGTGTTG	$yuaB_{Bl}$ cloning	-14 → 6
NSW813	CGTAGCATGCTTGCCTATTTACTTGCAG	$yuaB_{Bl}$ cloning	551 → 534
NSW814	AGCTAAGCTTCATTTTTTAGGGGGAATTTTGTTATGGCTGAATC TACATCAACTAAAGC	$yuaB_{\Delta 2\text{-}28}$ cloning	-24 → 3 84 → 107
NSW819	GCTTAAGCTTGGGGGAAGGAAGAAATGAAAAAAAC	$yuaB_{Bp}$ cloning	-13 → 11
NSW820	GCATGCATGCGCTTTTTTATTTAGCAACCACACG	$yuaB_{Bp}$ cloning	544 → 521
NSW825	CGATCCATGGCTGAATCTACATCAACTAAAGC	$yuaB_{His6}$	84 → 107
NSW826	CGATAGATCTGTTGCAACCGCAAGGCTGAG	$yuaB_{His6}$	543 → 524
NSW827	GCATAGATCTACATCAACTAAAGCTCATACTG	$yuaB_{29\text{-}181}$	90 → 115
NSW828	GCATAGATCTCGCGAAAGAAGCTGTAGGTGC	$yuaB_{ss}$ cloning	84 → 64
NSW829	GCATGTCGACTTTTAGGGGGATTTATGAAAATG	$yuaB_{Ba}$ cloning	-14 → 9
NSW830	CGTAGCATGCGGTCTTTTTTTCGCAATTATTTGC	$yuaB_{Ba}$ cloning	546 → 539
NSW831	AGCTAAGCTTCATTTTTTAGGGGGAATTTTGTTATGAAAAAAAG AAAGAGGCG	$wapA_{ss}$ cloning	1 → 20
NSW832	CGATAGATCTTGCTAGTACATCGGCTGGCAC	$wapA_{ss}$ cloning	97 → 76
NSW835	CGTAGGATCCATGGCTGAATCTACATCAAC	*gst-yuaB* fuison	84 → 101
NSW836	GCATCTCGAGTTAGTTGCAACCGCAAGG	*gst-yuaB* fuison	546 → 529
NSW837	GCATAGATCTTCCACTATGAGAACACAGTC	$yuaB_{\Delta 29\text{-}38}$ *cloning*	118 → 137

Primer	Sequence 5' – 3' [1]	Target and use	Coordinates [2]
NSW838	GCATGCATGCTTAGCGCTTAGCCACGTCAATG	*yuaB* $_{\Delta 172\text{-}181}$ cloning	510 → 429
NSW839	GCATAGATCTTTGTTCGCAACAATCACTGG	*yuaB*$_{\Delta 29\text{-}48}$ *cloning*	148 → 167
NSW840	GCATAGATCTACGGAATGGTCTTTCTC	*yuaB*$_{\Delta 29\text{-}58}$ *cloning*	178 → 194
NSW841	GCATGCATGCTTATGCGTAAAATTTATTTCC	*yuaB* $_{\Delta 162\text{-}181}$ cloning	483 → 466
NSW842	GCATGCATGCTTAAGCGGCAGGAAGTGTTTTG	*yuaB* $_{\Delta 152\text{-}181}$ cloning	423 → 405
NSW845	GCATCATATGGCTGAATCTACATCAACTAAAGC	*TEV-yuaB* cloning	84 → 107
NSW846	GCATCTCGAGTTATTACTGAGTCGGAGGAGTGC	*TEV-yuaB* cloning	528 → 512
NSW847	CTCCTCCGACTCAGTAATGCGGTTGCAAC	P177Z mutagenesis	515 → 543
NSW848	GTTGCAACCGCATTACTGAGTCGGAGGAG	P177Z mutagenesis	543 → 515
NSW849	CGATAGATCTGATTGTTGCGAACAATGAAG	*yuaB*$_{1\text{-}54}$ cloning	163 → 143
NSW850	GCATAGATCTACAGTTAACAGCACGAAAGAG	*yweA*$_{39\text{-}154}$ cloning	115 → 135
NSW872	AGGTGTGGCATAATGTGTGTAATTGTGAGC	*pDR111* MCS	
NSW873	TGAACAATCACGAAACAATAATTGGTACGTACG	*pDR111* MCS	
NSW1301	CCGTCCAAACACGCCTCTCAGCCTTGGCG	L76P mutagenesis	213 → 240
NSW1302	CGCCAAGGCTGAGAGGCGTGTTTGGACGG	L76P mutagenesis	240 → 213
NSW1316	CAGTCTACAGCTTCAGCCGCCGCCGCCATCACTGGCGCCAGC	LFAT-AAAA mutagenesis	133 → 174
NSW1317	GCTGGCGCCAGTGATGGCGGCGGCGGCTGAAGCTGTAGACTG	LFAT-AAAA mutagenesis	174 → 133
NSW1328	GTCTACAGCTTCATTGCCTGCAACAATCACTGGC	F51P mutagenesis	135 → 168
NSW1329	GCCAGTGATTGTTGCAGGCAATGAAGCTGTAGAC	F51P mutagenesis	168 → 135
NSW1330	GTCTACAGCTTCATTGTACGCAACAATCACTGGC	F51Y mutagenesis	135 → 168
NSW1331	GCCAGTGATTGTTGCGTACAATGAAGCTGTAGAC	F51Y mutagenesis	168 → 135
NSW1335	CGTCCAAACACGCTTCTCAGCGCCGCTGCCGCTGCCGCTACATT GCCAAGCGGATTTACT	LGVMEF-AAAAAA mutagenesis	214 → 273
NSW1336	AGTAAATCCGCTTGGCAATGTAGCGGCAGCGGCAGCGGCGCT GAGAAGCGTGTTTGGACG	LGVMEF-AAAAAA mutagenesis	273 → 214
NSW1337	TACCGTCCAAACACGATTCTCAGCCTTGGCG	L76I mutagenesis	211 → 240
NSW1338	CGCCAAGGCTGAGAATCGTGTTTGGACGGTA	L76I mutagenesis	240 → 211

[1] Restriction sites used for cloning engineered into the primer sequences are underlined. [2] Position of primers is indicated in relation to the translational start site (noted as 1) of the named target gene and is shown in 5' to 3' orientation of the primer.

7.2. Appendix B: Antibiotic stock solutions

Antibiotic	Concentration (mg/ml)	Solvent
Ampicillin	100	Water
Chloramphenicol	5	100% Ethanol
Erythromycin	1	100% Ethanol
Lincomycin	12.5	50% Ethanol
Kanamycin	10	Water
Spectinomycin	100	Water

7.3. Appendix C: Buffers and solutions

10 mM dNTPs stock	10 mM dATP 10 mM dCTP 10 mM dTTP 10 mM dGTP
AbDil	TBS 2% BSA 0.1% Azide
Acetate buffer	100 mM Sodium acetate 500 mM NaCl
Antibody column storage buffer	PBS 500 mM NaCl 0.1% (w/v) Sodium azide
B. subtilis lysis buffer	100 mM NaCl 50 mM EGTA
B. subtilis transformation buffer	T-Base 2mM EGTA
B. subtilis transformation wash buffer	T-Base 1 mM Mg_2SO_4
CD buffer	3.8 mM NaH_2PO_4 16.2 mM Na_2HPO_4
Coomassie destain	50% (v/v) Methanol 10% (v/v) Acetic acid
Coomassie protein stain	50% (v/v) Ethanol 7.5% (v/v) Acetic acid 0.1% (w/v) Bromophenol Blue
ECL solution 1	100 mM Tris –HCl (pH 8.5) 2.5 mM Luminol in DMSO 0.4 mM p-Coumaric acid in DMSO
ECL solution 2	100 mM Tris-HCl (pH 8.5) 0.064% (v/v) H_2O_2
Electroblotting buffer	25 Mm Tris 192 mM Glycine 0.2% (v/v) Tween-20 20% (v/v) Methanol

Ethanolamine buffer	500 mM Ethanolamine (pH 8.3) 500 mM NaCl
GST purification binding buffer (Also Gel Filtration buffer)	25 mM Tris-HCl (pH 7.5) 250 mM NaCl
GST purification elution buffer	25 mM Tris-HCl (pH 7.5) 250 mM NaCl 50 mM Glutathione
HIS_6 purification Buffer A	25 mM Tris-HCl (pH 7.5) 250 mM NaCl 35 mM imidazole
HIS_6 purification Buffer B	25 mM Tris-HCl (pH 7.5) 250 mM NaCl 500 mM imidazole
Mounting Medium	0.5% P-phenylenediamine (Free base) 20mM Tris-HCl pH 8.8 90% Glycerol
NHS beads coupling buffer	200 mM $NaHCO_3$ (pH 8.3) 500 mM NaCl
PBS	0.137M NaCl 2.68 mM KCl 10.436 mM $NaHPO_4$ 1.764 mM KH_2PO_4
Protein purification lysis buffer	25 mM Tris-HCl (pH 7.5) 250 mM NaCl Complete EDTA-free Proteinase Inhibitor Cocktail 5 mg DNase I
SDS loading buffer	60 mM Tris-HCl (pH 8.8) 4% (v/v) β-Mercaptoethanol 2% (w/v) SDS 10% Glycerol 0.04% Bromophenol Blue
SDS running buffer	25 mM Tris 192 mM Glycine 0.% (v/v) SDS
TAE	40 mM Tris-acetate

	1 mM EDTA
T-Base	15 mM $(NH_4)2SO_4$
	80 mM K_2HPO_4
	44 mM KH_2PO_4
	3.4 mM Sodium citrate
TBS	20 mM Tris-HCl (pH 8.0)
	150 mM NaCl

7.4. Appendix D: Publications

JOURNAL OF BACTERIOLOGY, Sept. 2011, p. 4821–4831 Vol. 193, No. 18
0021-9193/11/$12.00 doi:10.1128/JB.00223-11

YuaB Functions Synergistically with the Exopolysaccharide and TasA Amyloid Fibers To Allow Biofilm Formation by *Bacillus subtilis*▽

Adam Ostrowski,[1] Angela Mehert,[2] Alan Prescott,[3] Taryn B. Kiley,[1] and Nicola R. Stanley-Wall[1]*

Division of Molecular Microbiology, College of Life Sciences, University of Dundee, Dundee DD1 5EH, United Kingdom[1]; Division of Biological Chemistry and Drug Discovery, College of Life Sciences, University of Dundee, Dundee DD1 5EH, United Kingdom[2]; and Division of Cell Signalling and Immunology, College of Life Sciences, University of Dundee, Dundee DD1 5EH, United Kingdom[3]

Received 16 February 2011/Accepted 28 June 2011

During biofilm formation by *Bacillus subtilis*, two extracellular matrix components are synthesized, namely, the TasA amyloid fibers and an exopolysaccharide. In addition, a small protein called YuaB has been shown to allow the biofilm to form. The regulatory protein DegU is known to initiate biofilm formation. In this report we show that the main role of DegU during biofilm formation is to indirectly drive the activation of transcription from the *yuaB* promoter. The N terminus of YuaB constitutes a signal peptide for the Sec transport system. Here we show that the presence of the signal peptide is required for YuaB function. In addition we demonstrate that upon export of YuaB from the cytoplasm, it localizes to the cell wall. We continue with evidence that increased production of TasA and the exopolysaccharide is not sufficient to overcome the effects of a mutation in *yuaB*, demonstrating the unique involvement of YuaB in forming a biofilm. In line with this, YuaB is not involved in correct synthesis, export, or polymerization of either the TasA amyloid fibers or the exopolysaccharide. Taken together, these findings identify YuaB as a protein that plays a novel role during biofilm formation. We hypothesize that YuaB functions synergistically with the known components of the biofilm matrix to facilitate the assembly of the biofilm matrix.

Biofilms are complex communities of microbial cells. The formation of a biofilm can result in the establishment of chronic infections in mammalian hosts but can also be exploited for bioremediation and biocontrol processes (3, 17). A key feature of a biofilm is the synthesis of a self-produced extracellular matrix. The biofilm matrix is composed of polysaccharides, proteins, and sometimes DNA (6). It serves to provide structural integrity and protection to the microbes from mechanical, chemical, and immunological stress (13, 14). There have been significant advances in understanding the regulatory pathways and key building blocks required for the growth of biofilms for many species of bacteria (26). However, it is still not understood how the extracellular and cell-associated components physically interact to allow a three-dimensional biofilm to develop.

Bacillus subtilis is a soil-dwelling Gram-positive bacterium that forms biofilms containing differentiated cells in the form of rugose pellicles at the liquid-air interface or colonies with a complex three-dimensional architecture (25). The formation of a *B. subtilis* biofilm is tightly controlled at the level of transcription (20). Initiation of biofilm formation is dependent on the activation of three transcription factors called Spo0A, DegU, and ComA (26, 30). Spo0A is active in its phosphorylated state (9). Phosphorylation of Spo0A during biofilm formation is controlled in part by KinC, which detects a signal that is triggered by starvation and the extracellular lipopeptide surfactin (9, 28), whereas the synthesis of surfactin is controlled by quorum sensing through the regulator ComA (28). How Spo0A influences a cell depends on the concentration of the phosphorylated form of Spo0A in the cell (18, 20, 21). When a low level of phosphorylated Spo0A is reached, it regulates two parallel pathways of antirepression. This culminates in the initiation of transcription from the operons needed for the synthesis of the extracellular matrix in a subpopulation of cells in the maturing biofilm (28). A second signaling pathway required to activate biofilm formation is controlled by the response regulator DegU (30). When the cognate sensor kinase of DegU, DegS, detects a specific environmental signal, it autophosphorylates (30). Transfer of the phosphate group from DegS to DegU is subsequently facilitated by a small protein called DegQ (23). Upon phosphorylation, DegU dimerizes and activates transcription of *yuaB* and *yvcA*, the products of which are required for biofilm formation (30). In addition to DegU-mediated regulation, transcription of *yuaB* is also indirectly activated by the regulators Spo0A (40) and Rok (24).

We are interested in how the biofilm matrix assembles into a three-dimensional structure. For *B. subtilis*, the biofilm matrix is known to be composed of at least two components, an exopolysaccharide (EPS) of an as yet undefined sugar composition and linkage, which is synthesized by the products of the 15-gene *epsABCDEFGHIJKLMNO* operon (here called *epsA–O*), and a protein called TasA (27), which is a product of the *tapA-sipW-tasA* operon (here called the *tapA* operon). TasA is currently the only defined protein component of the biofilm matrix and is posttranslationally modified by SipW, a signal peptidase that releases mature TasA into the extracellular environment (4). TasA has recently been shown to form long intercellular amyloid fibers that provide structure to the bio-

* Corresponding author. Mailing address: Division of Molecular Microbiology, College of Life Sciences, University of Dundee, Dundee DD1 5EH, United Kingdom. Phone: 44 (0)1382 386335. Fax: 44 (0)1382 386375. E-mail: n.r.stanleywall@dundee.ac.uk.
▽ Published ahead of print on 8 July 2011.

TABLE 1. *B. subtilis* strains used in this study

Strain	Relevant genotype/description[a]	Reference, source, or construction[b]
JH642	*trpC2 pheA1*	33
168	*trpC2*	BGSC
NCIB3610	Prototroph	BGSC
BAL984	JH642 *trpC2 pheA1 ΔtasA::spc*	18
BAL835	JH642 *amyE*::$P_{hy\text{-}spank}$-*gfpmut2 cat*	37
DS93	3610 *ΔsinIR::spc*	21
NRS1314	3610 *degU::pBL204 (cat)*	39
NRS1647	3610 *abrB*::Tn*10 (mls)*	40
NRS2097	3610 *yuaB::cat*	40
NRS2242	3610 *sacA*::P_{epsA}-*gfp* (*kan*)	31
NRS2271	JH642 *sacA*::P_{yuaB}-*gfp mut2* (*kan*)	pNW511 → JH642
NRS2275	JH642 *sacA*::P_{epsA}-*gfp mut2* (*kan*)	pNW510 → JH642
NRS2276	3610 *abrB*::Tn*10 (mls) yuaB::cat*	NRS2095 → NRS1647
NRS2283	JH642 $P_{hy\text{-}spank}$-*yuaB-lacI (spc)*	40
NRS2289	3610 *sacA*::P_{yuaB}-*gfp mut2* (*kan*)	SPP1 NRS2271 → 3610
NRS2290	3610 *sacA*::P_{epsA}-*gfp mut2* (*kan*)	SPP1 NRS2275 → 3610
NRS2291	3610 *ΔsinIR::spc yuaB::cat*	SPP1 DS93 → NRS2097
NRS2292	3610 *yuaB::cat sacA*::P_{yuaB}-*gfp mut2* (*kan*)	SPP1 NRS2271 → NRS2097
NRS2296	3610 *abrB*::Tn*10 (mls) sacA*::P_{tapA}-*gfp mut2* (*kan*)	SPP1 NRS2275 → NRS1647
NRS2298	3610 *degU::cat amyE*::$P_{hy\text{-}spank}$-*yuaB-lacI (spc)*	SPP1 NRS2283 → NRS1314
NRS2299	3610 *yuaB::cat amyE*::$P_{hy\text{-}spank}$-*yuaB-lacI (spc)*	40
NRS2302	3610 *abrB*::Tn*10 (mls) yuaB::cat sacA*::P_{epsA}-*gfp mut2* (*kan*)	SPP1 NRS2275 → NRS2276
NRS2388	168 *sacA*::P_{tapA}-*gfp mut2* (*kan*)	31
NRS2393	3610 *yuaB::cat sacA*::P_{tapA}-*gfp mut2* (*kan*)	SPP1 NRS2388 → NRS 2097
NRS2394	3610 *sacA*::P_{tapA}-*gfp mut2* (*kan*)	31
NRS2398	3610 *yuaB::cat sacA*::P_{epsA}-*gfp* (*kan*)	SPP1 2095 → NRS2242
NRS2415	3610 *tasA::spc*	SPP1 BAL984 → 3610
NRS2417	3610 *yuaB::cat amyE*::$P_{hy\text{-}spank}$-*gfpmut2 cat*	SPP1 BAL835 → NRS2097
NRS2418	3610 *abrB*::Tn*10 (mls) yuaB::cat sacA*::P_{tapA}-*gfp mut2* (*kan*)	SPP1 NRS2388 → NRS2276
NRS2426	3610 *abrB*::Tn*10 (mls) sacA*::P_{tapA}-*gfp mut2* (*kan*)	SPP1 NRS1128 → NRS2394
NRS2427	3610 *ΔsinIR::spc sacA*::P_{epsA}-*gfp mut2* (*kan*)	SPP1 DS93 → NRS2290
NRS2428	3610 *ΔsinIR::spc yuaB::cat sacA*::P_{epsA}-*gfp mut2* (*kan*)	SPP1 DS93 → NRS2293
NRS2429	3610 *ΔsinIR::spc sacA*::P_{tapA}-*gfp mut2* (*kan*)	SPP1 DS93 → NRS2394
NRS2430	3610 *ΔsinIR::spc yuaB::cat sacA*::P_{tapA}-*gfp mut2* (*kan*)	SPP1 DS93 → NRS2393
NRS2440	168 *amyE*::$P_{hy\text{-}spank}$-*Δ2-28-yuaB-lacI* (*spc*)	pNW616 → 168
NRS2441	168 *amyE*::$P_{hy\text{-}spank}$-*yuaBss-yuaB-lacI* (*spc*)	pNW617 → 168
NRS2442	168 *amyE*::$P_{hy\text{-}spank}$-*wapAss-yuaB-lacI* (*spc*)	pNW618 → 168
NRS2446	3610 *yuaB::cat amyE*::$P_{hy\text{-}spank}$-*Δ2-28-yuaB-lacI* (*spc*)	SPP1 NRS2440 → NRS2097
NRS2447	3610 *yuaB::cat amyE*::$P_{hy\text{-}spank}$-*yuaBss-yuaB-lacI* (*spc*)	SPP1 NRS2441 → NRS2097
NRS2448	3610 *yuaB::cat amyE*::$P_{hy\text{-}spank}$-*wapAss-yuaB-lacI* (*spc*)	SPP1 NRS2442 → NRS2097
NRS2450	3610 *epsA–O::tet*	4
NRS2451	3610 *epsA–O::tet tasA::spc*	SPP1 NRS2450 → NRS2415
NRS2452	3610 *epsA–O::tet yuaB::cat*	SPP1 NRS2450 → NRS2097
NRS2543	3610 *epsA–O::tet tasA::spc yuaB::cat*	SPP1 NRS2450 → NRS2452
NRS2748	3610 *yuaB::cat abrB*::Tn*10 (mls) amyE*::$P_{hy\text{-}spank}$-*yuaB-lacI (spc)*	SPP1 NRS1128 → NRS2299
NRS2749	3610 *yuaB::cat ΔsinR::kan amyE*::$P_{hy\text{-}spank}$-*yuaB-lacI* (*spc*)	SPP1 NRS1858 → NRS2299
NRS2976	168 *sacA*::P_{yuaB}-*yuaB (kan)*	pNW518 → 168
NRS2980	3610 *epsA–O::tet tasA::spc sacA*::P_{yuaB}-*yuaB (kan)*	SPP1 NRS2976 → NRS2451

[a] Drug resistance cassettes are indicated as follows: *cat*, chloramphenicol resistance; *kan*, kanamycin resistance; *tet*, tetracycline resistance; *mls*, lincomycin/erythromycin resistance; and *spc*, spectinomycin resistance.

[b] BGSC represents the *Bacillus* genetic stock center. The direction of strain construction is indicated with DNA or phage (SPP1) (→) recipient strain.

film matrix (34). In addition to the EPS and TasA, YuaB is a small protein that is needed for biofilm formation but for which analysis of the primary amino acid sequence does not provide any information concerning biochemical function. We began our investigation of the role that YuaB plays during biofilm formation by identifying *yuaB* transcription as the main target of the DegU regulon during the activation of biofilm formation. We go on to show that, in contrast to the major biofilm matrix protein TasA, YuaB is located within the cell wall. We continue by showing that the absence of YuaB cannot be compensated for by overproduction of either TasA or EPS. Finally we demonstrate that YuaB must act in a synergistic manner with the TasA amyloid fibers and the EPS polymer to allow biofilm development through the facilitation of the assembly or function of the matrix.

MATERIALS AND METHODS

General strain construction and growth conditions. The *B. subtilis* strains used and constructed in this study are detailed in Table 1. *Escherichia coli* strain MC1061 [*F' lacI*^{q} *lacZ*M15 Tn*10*(*tet*)] was used for the construction and maintenance of plasmids. *B. subtilis* JH642 and 168 derivatives were generated by transformation of competent cells with plasmids or DNA using standard protocols (19). SPP1 phage transductions, for the introduction of DNA into *B. subtilis* strain NCIB 3610, were conducted as described previously (39). Both *E. coli* and *B. subtilis* strains were routinely grown in Luria-Bertani (LB) medium (10 g

NaCl, 5 g yeast extract, and 10 g tryptone per liter) or MSgg medium (5 mM potassium phosphate and 100 mM MOPS [morpholinepropanesulfonic acid] at pH 7.0 supplemented with 2 mM $MgCl_2$, 700 μM $CaCl_2$, 50 μM $MnCl_2$, 50 μM $FeCl_3$, 1 μM $ZnCl_2$, 2 μM thiamine, 0.5% glycerol, 0.5% glutamate) (4) at 37°C. When appropriate, antibiotics were used as required at the following concentrations: ampicillin at 100 μg ml^{-1}, chloramphenicol at 5 μg ml^{-1}, erythromycin at 1 μg ml^{-1} with lincomycin at 25 μg ml^{-1}, kanamycin at 25 μg ml^{-1}, and spectinomycin at 100 μg ml^{-1}.

Biofilm analysis. Analysis of the biofilm architecture was performed as described previously (5, 39). For coculture experiments, strains were grown in LB to mid-late exponential phase. Strains for coculture were mixed in a 1:1 ratio based on their optical density values at 600 nm (OD_{600}). A total of 10 μl of the combined cell mix was spotted onto an MSgg agar plate. The agar plates were incubated at 37°C for 48 h prior to photography. For pellicle cocultures, the mixed strains were inoculated into liquid MSgg as described previously and incubated at 25°C for 96 h (4).

Plasmid construction. (i) Delivery plasmid for YuaB expression under the native promoter. The DNA encoding the *yuaB* promoter region and the coding region was amplified from the chromosome of NCIB 3610 using primers NSW646 (5′-ATGC**GGATCC**CGCTTACTATGACTGGCTG-3′) and NSW 647 (5′-AACT**TCTAGA**TTAGTTGCAACCGCAAGGCTGA-3′). The resulting fragment was digested with the restriction sites EcoRI and BamHI (shown in bold in the primer sequences above), which had been incorporated in the primer sequences, and cloned into pSac-Kan (29) to generate pNW518.

(ii) Signal peptide swapping plasmids. The DNA encoding the signal sequence of YuaB was amplified from the chromosome of NCIB 3610 using primers NSW626 (5′-AGCT**AAGCTT**CATTTTTTAGGGGGAATTT TGTTATG-3′) and NSW828 (5′-GCAT**AGATCT**CGCGAAAGAAGCT GTAGGTGC-3′). The resulting PCR product was digested with the restriction sites HindIII and BglII, which had been incorporated in the primer sequences (indicated in bold), and cloned into pQE-70 (Qiagen) (pNW611). The DNA encoding the WapA signal sequence was cloned in an identical manner using primers NSW831 (5′-AGCT**AAGCTT**CATTTTTTAGGGGGAATTTTGTTATGAAA AAAAG AAAGAGGCG-3′) and NSW832 (5′-CGAT**AGATCT**TG CTAGTACATCGG CTGGCAC-3′) to generate plasmid pNW612. Subsequent to this, the DNA coding the mature YuaB region was amplified from the chromosome of NCIB 3610 using primers NSW827 (5′-GCAT**AGATCT**ACATCAACTAAAG CTCA TACTG-3′) and NSW645 (5′-AACT**GCATGC**TTAGTTGCAAC CGCAAGGC TGA-3′). The PCR product was digested with BglII and SphI, which had been incorporated into the primer sequence (indicated in bold), and cloned into pNW611 to generate plasmid pNW613 harboring the reconstructed *yuaB* allele and into pNW612 to generate plasmid pNW614 harboring a recombinant allele of *yuaB* with the signal sequence from *wapA*. Plasmid pNW617 for ectopic expression of reconstructed *yuaB* was constructed by excision of the insert fragment from pNW613 with HindIII and SphI and cloning of the fragment into pDR111 (kindly provided by David Rudner) (7). Plasmid pNW618 for ectopic expression of the *yuaB* allele with the signal sequence from *wapA* was generated by excision of the insert fragment from pNW614 with HindIII and SphI and cloning of the fragment into pDR111.

To construct plasmid pNW616 for ectopic expression of *yuaB* lacking amino acids 2 to 28, DNA was amplified from the chromosome of NCIB 3610 using primers NSW814 (5′-AGCT**AAGCTT**CATTTTTTAGGGGGAATTTTGTTAT GGCTGAATCTACATCAACTAAAGC-3′) and NSW645. The resulting PCR product was digested with the restriction sites HindIII and SphI, which had been incorporated in the primer sequences (indicated in bold), and cloned into pDR111. All constructs were introduced into *B. subtilis* strain 168 via double recombination at the *amyE* locus using the spectinomycin resistance cassette associated with pDR111. Double crossovers at the *amyE* locus were confirmed by PCR analysis. All plasmids were sequenced.

(iii) Protein expression vectors. A DNA fragment encoding YuaB lacking the signal peptide starting at position A29 was amplified from NCIB 3610 genomic DNA using primers NSW835 (5′-CGTAGGATCCATGGCTGAATCTACATC AAC-3′) and NSW836 (5′-GCATCTCGAGTTAGTTGCAACCGCAAGG-3′). The resulting PCR product was digested with BamHI and XhoI and cloned into pGEX-6P-1 (GE Healthcare) to generate pNW619 harboring the coding region for a glutathione *S*-transferase (GST)-YuaB fusion protein. An additional stop codon was introduced at amino acid position P177 in YuaB to truncate the encoded protein. The last 10 C-terminal amino acids of YuaB were found to contribute to protein instability and are not required for YuaB function (data not shown). Introduction of the stop codon was achieved using the QuikChange protocol (Stratagene) and primers NSW847 (5′-CTCCTCCGACTCAGTAATG CGGTTGCAAC-3′) and NSW848 (5′-GTTGCAACCGCATTACTGAGTCGG AGGAG-3′) to generate pNW634.

A DNA fragment encoding TasA lacking the signal peptide was amplified from NCIB 3610 genomic DNA using primers NSW660 (5′-GCATGGATCCG CATTTAACGACATTAAATCAAA-3′) and NSW661 (5′-GCATCTCGAGTT AATTTTTATCCTCGCTATGCGA-3′). The resulting PCR product was digested with BamHI and XhoI and cloned into pGEX-6P-1 to generate pNW543 harboring the coding region for a GST-TasA fusion protein.

Protein overexpression and purification and antibody production. To overexpress YuaB or TasA, the *E. coli* BL21(DE3) strain was freshly transformed with plasmid pNW634 or pNW543, respectively, and grown in LB plus antibiotics at 30°C until an OD_{600} of 0.3. At this point, expression was induced with 100 μM IPTG (isopropyl-β-D-thiogalactopyranoside), and the cells were transferred to 20°C for incubation overnight with shaking. Cells were collected by centrifugation and suspended in lysis buffer (250 mM NaCl, 25 mM Tris [pH 7.5]) with DNase I and EDTA-free proteinase inhibitor cocktail (Roche). Cells were lysed by French pressing, and the cellular debris was removed by centrifugation. The supernatant was filtered using a 0.45-μm syringe filter. Glutathione Sepharose 4B (GE Healthcare) beads were added, and the samples were incubated for 2 h at 4°C with rolling and then collected using a disposable chromatography column. The beads were washed with 150 ml of wash buffer (250 mM NaCl, 25 mM Tris [pH 7.5]) and transferred to the elution buffer (wash buffer supplemented with 50 mM reduced glutathione [Sigma]). After 2 h incubation at 4°C with rolling, the beads were recollected and the flowthrough containing eluted protein was retained. GST was removed using 50 μg of PreScission protease (GE Healthcare) during overnight dialysis into the wash buffer. The cleaved protein mix was treated once more with glutathione Sepharose to bind the cleaved GST and PreScission protease, and target protein was eluted. Remaining impurities were removed using gel filtration on Superdex75. The identity of purified proteins was confirmed by matrix-assisted laser desorption ionization–time of flight mass spectrometry (MALDI-TOF MS). For the purpose of raising polyclonal antibodies, samples of the purified proteins were submitted to Dundee Cell Products for antibody production in rabbits.

Antibody purification. To purify the YuaB antiserum, affinity chromatography was used. *N*-hydroxysuccinimidyl-activated agarose beads (Sigma) were activated with 50 ml of 1 mM hydrochloric acid and washed with 100 ml of coupling buffer (200 mM sodium carboxide, 500 mM sodium chloride [pH 8.3]). Purified recombinant YuaB was dialyzed into the coupling buffer and brought to 2 mg ml^{-1} in 20 ml of the buffer. Activated beads were added to the protein solution and incubated at 4°C with rolling for 2 h. The beads were transferred into a disposable column, washed with 50 ml of wash buffer A (500 mM sodium chloride, 500 mM ethanolamine [pH 8.3]), and washed with 50 ml of wash buffer B (500 mM sodium chloride, 100 mM sodium acetate [pH 4.0]). Washes were repeated 2 times further. After the last wash with wash buffer B, the column was washed with storage buffer (500 mM sodium chloride in phosphate-buffered saline [PBS]). A total of 15 ml of the antiserum raised against YuaB was diluted in 135 ml of PBS and filtered through a 0.2-μm syringe filter. The column was washed with 100 ml of the coupling buffer, after which the diluted antiserum was passed through the column twice. The column was washed with 100 ml of 500 mM sodium chloride buffered with 10 mM Tris-HCl, pH 7.5, and the antibodies were eluted with 100 mM glycine, pH 2.25. One-milliliter fractions were collected on top of 0.1 ml of Tris-HCl, pH 8.0. Glycerol was added to the purified antibody solution to a final concentration of 10%, and the solution was supplemented with 10 mg ml^{-1} of bovine serum albumin (BSA).

Spore quantification. To determine the percentage of sporulation in complex colonies, strains were grown on MSgg agar for 72 h (41), and the number of spores was calculated as previously described (22, 41).

Western blot analysis. (i) Pellicle fractionation and protein extraction. Pellicles were grown in 10 ml of MSgg medium as described previously (5). The pellicle was fractionated as described previously (4), with the following changes. Proteins from each fraction were precipitated by mixing 5 ml of each fraction with 5 ml of a 1:1 chloroform-methanol solution and centrifuged for 5 min at 5,000 × *g*. The proteins from the phase interface were collected and washed with 100% methanol and air dried. The precipitants were dissolved in SDS-PAGE loading dye, resolved on a 14% SDS-PAGE gel, and transferred onto a polyvinylidene difluoride (PVDF) membrane (Millipore) by electroblotting. The membrane was incubated overnight in 3% powdered milk in Tris-buffered saline (TBS) (20 mM Tris-HCl [pH 8.0], 0.15 M NaCl) at 4°C. This was followed by incubation for 1.5 h in the primary antibody raised against TasA at a dilution of 1:10,000 or the affinity-purified antibody raised against YuaB at a dilution of 1:1,500 in 3% powdered milk in wash buffer (TBS plus 0.05% Tween 20). The membrane was washed using wash buffer and incubated for 45 min with the secondary goat anti-rabbit antibody conjugated to horseradish peroxidase (Pierce Scientific) at a dilution of 1:3,000. The membrane was washed, developed, and exposed to X-ray film.

(ii) Lithium chloride extraction of surface proteins. To extract proteins noncovalently bound to the cell wall, cells were extracted from biofilms which were grown and fractionated as described above. Extracted cells were washed in PBS centrifuged for 10 min at 5,000 × *g* and suspended in 15 ml of 5 M lithium chloride (Sigma). After a 15-min incubation, cells were collected by centrifugation, and the supernatant was filtered through a 0.2-μm syringe filter (Millipore) and retained as the cell wall wash fraction. The cells were lysed using BugBuster master mix (Novagen), the cellular debris was removed by centrifugation, and the supernatant was retained as the combined cytoplasmic and membrane fraction. Samples were precipitated with the methanol-chloroform mix as described above and suspended in PBS plus 0.1% SDS. Samples were diluted in SDS-loading dye to 1 μg μl^{-1}, and 10 μg of each sample was resolved on a 14% SDS-PAGE gel and electroblotted as described above. YuaB was detected as described above, and DegU was detected by an antibody raised in a sheep against DegU (39) at a dilution of 1:5,000 in 3% powdered milk in wash buffer. The membrane was washed and exposed to the secondary anti-sheep antibody raised in rabbits and conjugated to HRP (Pierce Scientific) as described above.

Electron microscopy and immunolabeling. (i) Transmission electron microscopy (TEM) analysis of TasA amyloid fibers. To visualize the TasA fibers, the method described by Romero et al. (34) was adapted. Mutant strains derived from the NCIB 3610 isolate, namely, the *epsA–O* (strain NRS2450), *epsA–O tasA* (NRS2451), and *epsA–O yuaB* (NRS2452) mutants, were grown in liquid MSgg medium for 24 h at 25°C. Cells were absorbed with a Pasteur pipette and spotted on a glow-discharged Pioloform nickel grid. Grids were blocked in the blocking agent (PBS with 0.1% Tween 20 and 3% milk) for 20 min and exposed to the anti-TasA antibody at a 1:150 dilution in the blocking agent for 90 min. Grids were washed 3 times in PBS and exposed to Immunogold conjugate protein A (10-nm gold particles; BBInternational) at a 1:50 dilution in the blocking agent. Grids were washed in PBS followed by water, stained with 3% uranyl acetate, and finally washed 5 times with water. The images were acquired using a JEOL JEM-1200EX electron microscope.

(ii) TEM analysis of YuaB localization. To determine the localization of YuaB, strains derived from the NCIB 3610 isolate, namely, the *epsA–O* (NRS2450) and the *epsA–O yuaB* (NRS2452) mutants, were grown in liquid MSgg medium for 24 h at 25°C. Cells were collected by centrifugation and fixed in 4% paraformaldehyde in piperazine-*N*,*N*′-bis(2-ethanesulfonic acid). The fixed pellets were transferred to 1 M sucrose and incubated at 4°C overnight. The cell pellets were snap-frozen in liquid nitrogen and sectioned using a Leica Ultracut EMFCS cryomicrotome into 80-nm sections. Sections were collected onto carbon-coated copper grids and blocked with 0.5% fish skin gelatin (Sigma) in PBS. For efficient labeling of YuaB, the YuaB-specific antibody was concentrated 10-fold, and the blocked grids were incubated in a 10-μl drop of the antibody solution for 30 min. Grids were washed 3 times in PBS and exposed to Immunogold conjugate protein A (10-nm gold particles; BBInternational) diluted 1:50 with the blocking agent. Next the grids were washed in PBS followed by water, stained with methyl cellulose-uranyl acetate (250 μl 3% uranyl acetate in 900 μl 2% methyl cellulose), and finally washed 5 times with water. The images were acquired using the JEOL JEM-1200EX electron microscope.

Analysis of exopolysaccharide production. To isolate the biofilm matrix, pellicles were grown in 10 ml of MSgg medium for 16 h at 37°C. The entire biofilm was collected by centrifugation at 3,500 × *g* for 10 min, and the growth medium replaced with 10 ml of double-distilled water (ddH_2O). Samples were subjected to gentle sonication (such that the cells did not lyse [4]), and the cell pellet was collected by centrifugation for 20 min, at 9,000 × *g* at 4°C. The supernatant was retained as the matrix fraction and was lyophilized. The dried matrix fraction was hydrated in 250 μl of ddH_2O, and the samples were normalized using the wet weight of the cell pellet collected during separation of the biofilm matrix from the biomass. To obtain an estimation of the size of the exopolysaccharide in the biofilm matrix, gel electrophoresis followed by Schiff's reagent (Sigma) staining was utilized (36).

Electromobility shift assay. For the assessment of phosphorylated DegU (DegU~P) binding to the *yuaB* promoter, a PCR product corresponding to the promoter region of *yuaB* (P_{yuaB}) was amplified using primers NSW627 (5′-ATGCGAATTCGCTTACTATGACTGGCTG-3′) and NSW628 (5′-ATGCAAGCTTGCGTTTCATAACAAAATTC-3′) and purified by gel extraction. Additionally, a PCR product corresponding to the promoter region of *aprE* (P_{aprE}) was amplified using primers NSW61 (5′-GGTAAAGCCTATGAATTCTCCATTTTCTTC-3′) and NSW654 and purified as above. The promoter DNA was labeled using 50 μCi [γ-^{32}P]ATP (Perkin-Elmer) and T4 polynucleotide kinase (New England BioLabs). Unincorporated ATP was removed from the labeled DNA using an Illustra Microspin G-25 column (GE Healthcare). Phosphorylated purified DegU was produced essentially as described previously (16), with the exception that a final concentration of 15 μM purified DegU~P and 3.18 μM purified DegS were added to the phosphorylation reaction mixture. The phosphorylation reaction, DNA binding, and mobility shift assay were performed as described previously (22).

RESULTS AND DISCUSSION

YuaB production restores biofilm formation to the *degU* mutant. The response regulator DegU has dual roles in controlling biofilm formation, functioning as both an activator and an inhibitor (38). Exactly how this occurs is unclear, but it has previously been shown that DegU activates the transcription of *yuaB* and *yvcA*, which are needed for biofilm formation (23, 39). We had previously shown that heterologous expression of *yvcA* is not sufficient to facilitate biofilm formation in the *degU* mutant (39). Therefore, to establish if uncoupling *yuaB* transcription from DegU-mediated control was sufficient to compensate for the absence of *degU*, the coding region for *yuaB* was placed under the control of the IPTG-inducible promoter $P_{hy\text{-}spank}$ at a heterologous location on the chromosome. Upon the induction of transcription of *yuaB* with IPTG, the biofilm gradually increased in complexity when both colony formation and pellicle formation were assessed (Fig. 1A). As *yvcA* production is also regulated by DegU during biofilm formation (39), we checked if heterologous induction of *yuaB* transcription influenced *yvcA* transcription using a reporter fusion. Consistent with data published previously (39), expression from the *yvcA* promoter was abolished in the *degU* mutant. The level of transcription from the *yvcA* promoter was unaffected by addition of the *yuaB* mutation (data not shown). In addition, induction of *yuaB* expression had no effect on the level of expression from the *yvcA* promoter (data not shown). These results demonstrate that the presence of YuaB does not affect the transcription of *yvcA* and that the overexpression of YuaB in the *degU* mutant background can compensate for the lack of *yvcA*. Together with the results published previously (40), these findings indicate that the promoter element of *yuaB* is the main target controlled either directly or indirectly by DegU during the activation of biofilm formation.

To investigate if DegU~P bound to the promoter region of *yuaB* directly to control transcription, we applied an *in vitro* electromobility shift assay (EMSA) as described previously (22). The activity of the purified DegU-His_6 protein was determined using a known DegU target, the *aprE* promoter region (32) (data not shown). Next the promoter region of *yuaB* was used. This was the same region of the NCIB 3610 chromosome previously used in constructing the transcriptional reporter fusion to monitor expression of *yuaB*, which was shown to be regulated by DegU (40). The experiments indicated that DegU~P did not cause visible delay in the migration of the *yuaB* promoter (Fig. 1B). While we cannot completely rule out the possibility that DegU~P does bind to the *yuaB* promoter region, the simplest conclusion is that the regulation of *yuaB* by DegU~P is indirect.

YuaB is required for spore formation in the biofilm. During the development of the biofilm by *B. subtilis*, subpopulations of differentiated cells develop. The last subpopulation to form are the sporulating cells (41). The formation of endospores in the biofilm is dependent on the biosynthesis and assembly of the extracellular matrix (41). The synthesis of the matrix appears to allow the cells to grow more rapidly; thus, they become

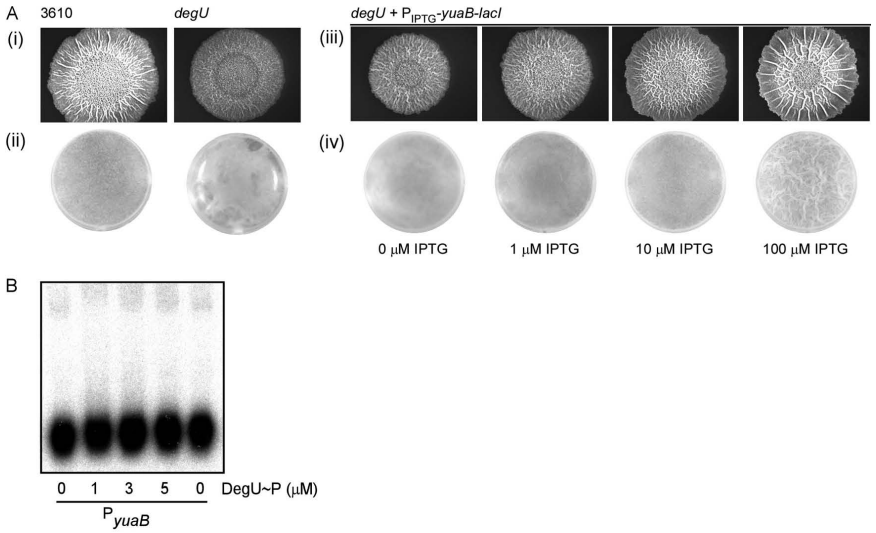

FIG. 1. (A) Heterologous expression of *yuaB* restores biofilm formation to the *degU* mutant. Prior to photography, the wild-type (NCIB 3610), *degU* mutant (NRS1314), and *degU amyE*::$P_{hy\text{-}spank}$-*yuaB-lacI* mutant (NRS2298) strains were incubated for 48 h at 37°C on solid MSgg (i and iii) or in liquid MSgg overnight at 37°C (ii and iv) in the presence of IPTG as indicated. (B) Electrophoretic mobility shift analysis of the *yuaB* operon promoter region. DNA binding reactions were conducted with γ-^{32}P-labeled DNA corresponding to the region of bp −281 to +11. Labeled DNA (1 ng) was loaded into each lane, with or without purified DegU~P.

starved for nutrients, and sporulation is promoted (1). In consequence, the degree of sporulation in the biofilm can be considered an indication of biofilm maturation and matrix production. The biofilm formed by the *yuaB* mutant lacks the structural complexity apparent in the wild-type strain (23, 40), which is a phenotype associated with mutants of *B. subtilis* that cannot synthesize the matrix (25). Using the level of sporulation as a proxy to test if the biofilm matrix formed correctly in the absence of *yuaB*, the level of sporulation in the *yuaB* mutant was quantified relative to the wild-type strain after 72 h incubation. The sporulation rate of the *yuaB* mutant (13%) was 6-fold lower ($n = 3$; $P < 0.05$) than that of the wild-type strain (81%) (Fig. 2). The reduction in sporulation could be complemented by the heterologous induction of *yuaB* transcription (Fig. 2). It should be noted that a 2-fold reduction in the total number of cells present in the biofilm of the *yuaB* mutant in comparison to that of the wild-type strain was measured (data not shown). A reduction in the number of cells in the biofilm of a strain unable to synthesize the biofilm matrix has independently been observed previously (1). To rule out the possibility that deletion of *yuaB* affected the sporulation process *per se*, sporulation assays were performed using planktonic cultures grown for 72 h in MSgg. Under these conditions, no difference in the sporulation efficiencies of the wild type and *yuaB* mutant was detected (Fig. 2). Thus, YuaB is needed for biofilm maturation, not sporulation *per se*.

YuaB is located in the cell wall. TasA, the major protein component of the biofilm matrix, is released to the extracellular environment during biofilm formation (4). It assembles into amyloid fibers and forms a structural component of the biofilm matrix (34). A nonbiased study of the secretome of *B. subtilis* tentatively identified YuaB as an extracellular protein (2). To test if YuaB was also located within the biofilm matrix, the wild-type biofilm was fractionated into cell, biofilm matrix, and growth medium samples, and the location of YuaB was as-

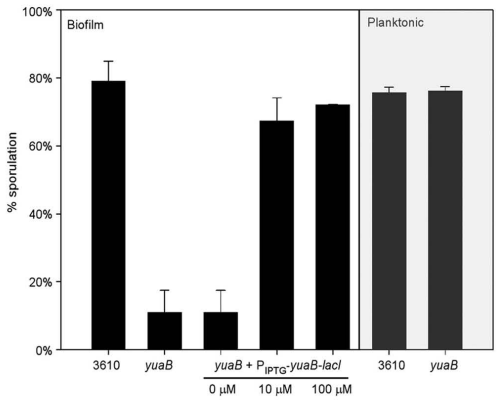

FIG. 2. YuaB is required for sporulation during biofilm formation. The sporulation efficiencies of the wild type (NCIB 3610), *yuaB* mutant (NRS2097), and complemented *yuaB amyE*::$P_{hy\text{-}spank}$-*yuaB-lacI* (NRS2299) strain were determined after 72 h growth during planktonic and biofilm growth conditions. Plotted is the average sporulation efficiency from three independent experiments, where the error bars represent the standard error of the mean. The level of IPTG used is indicated, as appropriate.

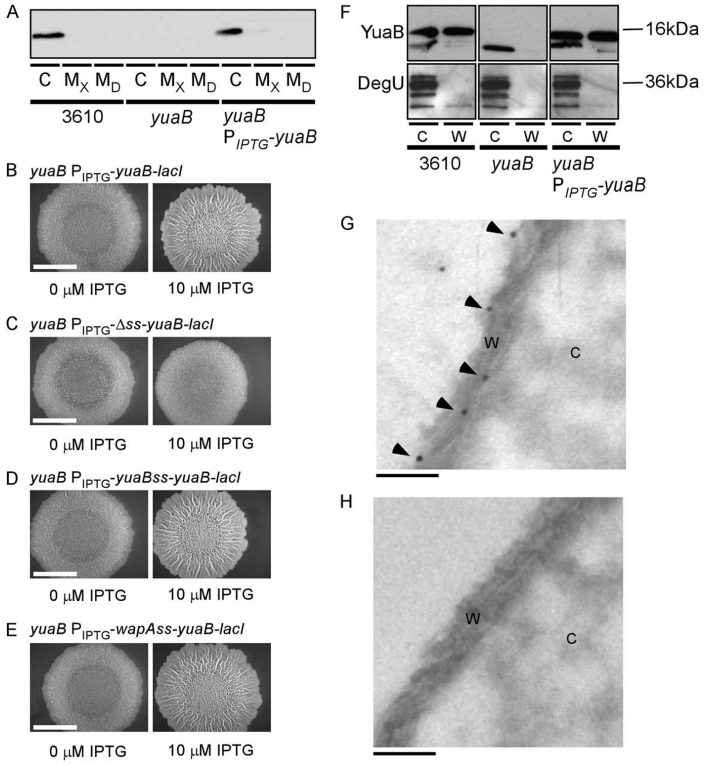

FIG. 3. YuaB is a cell wall protein. (A) Wild-type (NCIB 3610), *yuaB* mutant (NRS2097), and complemented *yuaB amyE*::$P_{hy\text{-}spank}$-*yuaB-lacI* (NRS2299) strain pellicles were separated into cell (C), matrix (M_X), and growth medium (M_D) fractions. Localization of YuaB was determined by Western blotting. (B to E) Representative images of biofilms formed after 48 h of incubation at 37°C on solidified MSgg medium, in the presence or absence of 10 μM IPTG as indicated, by the *yuaB* mutant carrying at the *amyE* locus under the control of the IPTG-inducible promoter $P_{hy\text{-}spank}$ the wild-type *yuaB* allele (NRS2299) (B), an allele of *yuaB* lacking the N-terminal signal sequence (ss) (NRS2446) (C), a recombinant *yuaB* signal sequence-*yuaB* construct (NRS2447) (D), and a *wapA* signal sequence-*yuaB* recombinant protein (NRS2448) (E). Scale bars represent 1 cm. (F) Cells from wild-type (NCIB 3610), *yuaB* mutant (NRS2097), and complemented *yuaB amyE*::$P_{hy\text{-}spank}$-*yuaB-lacI* (NRS2299) strain pellicles were extracted and subjected to a lithium chloride wash to isolate proteins noncovalently bound to the cell wall. Localization of YuaB was determined by Western blot analysis. YuaB was detected in both cellular (C) and cell wall wash (W) fractions, whereas the cytoplasmic response regulator DegU could be detected only in the cytoplasmic fraction. Protein masses are indicated by mass markers. The wild-type *yuaB* cells (NRS2450) (G) and mutant *yuaB* cells (NRS2452) (H) were collected from early-stage biofilms. YuaB was visualized by immuno-gold labeling and can be seen as dark spots indicated by the arrowheads. The images show fragments of cell wall (W) and cytoplasm (C) of representative cells of each strain. The scale bars represent 0.1 μm.

sessed by Western blotting. A band corresponding to the molecular mass of YuaB was detected in the fraction representing the cell lysate but not in the biofilm matrix fraction or the growth medium (Fig. 3A). The band was absent from the *yuaB* mutant cell lysate but returned when expression of *yuaB* was driven by the presence of the IPTG-inducible promoter (Fig. 3A). These results clearly indicate that, in contrast to TasA, YuaB is a cell-associated protein.

The findings presented above are in contradiction with the proteomic study which identified YuaB as a member of the secretome (2). Therefore, to test if YuaB did in fact need to be exported to facilitate biofilm formation, a mutant allele of *yuaB*, in which the DNA coding for the signal sequence was removed, was constructed. The putative signal peptide sequence for the Sec transport system was identified as the 28 N-terminal residues by SignalP (15). The induction of expression of the truncated *yuaB* gene could not restore the wild-type phenotype (Fig. 3C), unlike when wild-type *yuaB* was expressed (Fig. 3B and D). It should, however, be noted that when the signal sequence is removed, YuaB cannot be detected in the cytoplasm using Western blot analysis (data not shown), presumably due to proteolytic activity. Therefore, we next tested if replacing the native YuaB signal sequence with a signal sequence from a known cell wall protein (WapA) could restore function to YuaB. The chimeric WapA-YuaB fusion protein was capable of complementing the *yuaB* mutation with

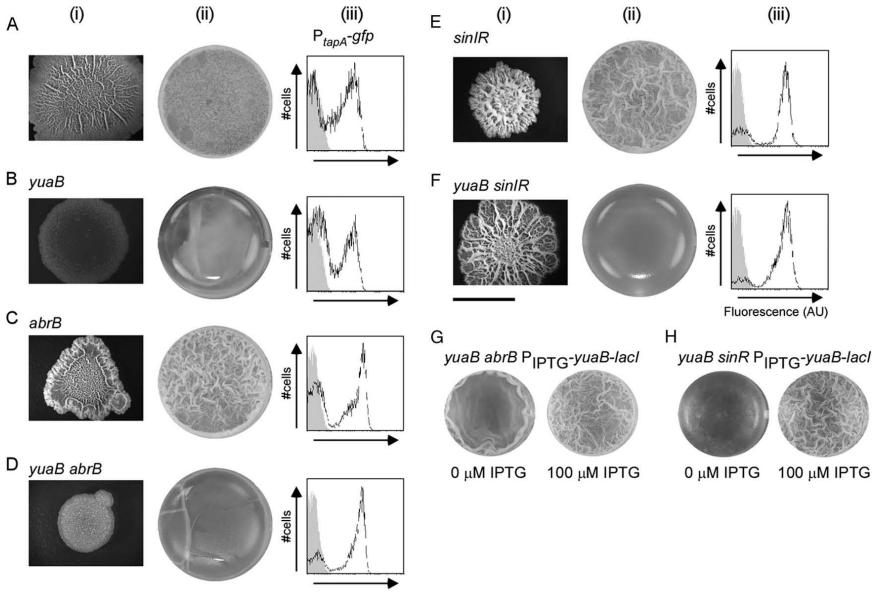

FIG. 4. Overproduction of TasA and the exopolysaccharide cannot compensate for the absence of YuaB. Wild-type (NCIB 3610) (A), *yuaB* mutant (NRS2097) (B), *abrB* mutant (NRS1647) (C), *yuaB abrB* mutant (NRS2276) (D), *sinIR* mutant (DS93) (E), and *yuaB sinIR* mutant (NRS2291) (F) strains. In column i, representative images of colony morphology after 48 h incubation at 37°C are shown. In column ii, representative images of the pellicle formed after 24 h incubation at 37°C in MSgg are shown. The graphs in column iii provide representative flow cytometry data, for which the level of expression from the *tapA* promoter was measured after 18 h incubation on MSgg plates. (See Materials and Methods and Table 1 for full details.) The *x* axis of each graph represents the level of fluorescence in arbitrary units (AU) in the logarithmic scale. The *y* axis of each graph represents the number of cells. For each graph the fluorescence profile generated by the nonfluorescent control strain NCIB 3610 is shown as the light gray peak. Representative images of the pellicle formed after 24 h incubation at 37°C in MSgg in the presence and absence of 100 μM IPTG are shown for the *yuaB*::*cat abrB amyE*::$P_{hy\text{-}spank}$-*yuaB-lacI* mutant (NRS2748) (G) and the *yuaB*::*cat abrB amyE*::$P_{hy\text{-}spank}$-*yuaB-lacI* (NRS2749) mutant (H).

the same efficiency as wild-type YuaB (Fig. 3E). We conclude that it is necessary for YuaB to be exported from the cytoplasm to function during biofilm formation.

As YuaB has a functional signal sequence (Fig. 3B) but is cell associated (Fig. 3A), we predicted that YuaB was located in the cell wall. To establish if this was the case, we utilized two methods. First, lithium chloride was used with whole cells to remove surface proteins that are not covalently bound to the peptidoglycan or anchored in the membrane (8), and second, immunogold electron microscopy was implemented. For the first method, cells were collected from the biofilm and subjected to a lithium chloride wash. YuaB was detected in both the fraction representing the cytoplasm and the membrane fractions as well as in the fraction of proteins removed from the peptidoglycan. In contrast, the cytoplasmatic marker, DegU, was detected only in the cytoplasmatic/membrane fraction (Fig. 3F). To confirm that YuaB was localized to the cell wall, cells extracted from pellicles were prepared for immunogold-labeling with anti-YuaB antibodies followed by TEM analysis. The strains used carried a deletion of the *epsA–O* operon to avoid the electron-thick background caused by presence of the exopolysaccharide (EPS) (34). For the YuaB-positive strain (NRS2450), gold particles were found associated with the cell wall for each cell examined (Fig. 3G). The abundance of the protein was low, which fits with the level of transcription observed for the *yuaB* promoter (40). However, the labeling was not seen when the YuaB-minus strain (NRS2452) was tested (Fig. 3H), confirming the specificity of the immunogold interaction ($n = 35$ cells for the wild type and the *yuaB* mutant; $P < 0.001$). We therefore conclude that YuaB is a cell wall-associated protein.

Overproduction of TasA and EPS cannot compensate for the absence of YuaB. We next tested if the absence of YuaB could be compensated for by increasing the level of the EPS and TasA amyloid fiber within the matrix. This was achieved by deleting *yuaB* from the *abrB* (NRS2274) and *sinIR* (NRS2291) mutant strain backgrounds. AbrB and SinR are direct repressors of transcription from the *epsA–O* and *tapA* operon promoters, and deletion of either *abrB* or *sinR* results in increased production of the biofilm matrix (4, 18, 21). It was predicted that if YuaB was essential for biofilm formation to proceed, a reduction in biofilm architecture would be observed with the double mutant strains. Consistent with the postulated assumption, deletion of *yuaB* from the *abrB* mutant (NRS2276) led to a reduction in the complexity of the biofilm architecture exhibited by both the pellicle and the colony (compare Fig. 4C

and D). This phenotype could be specifically complemented by introduction of the *amyE*::$P_{hy\text{-}spank}$-*yuaB-lacI* construct in the presence of the inducer IPTG (NRS2748) (Fig. 4G). Deletion of *yuaB* from the *sinIR* mutant background (NRS2291) also reduced the complexity of the pellicle formed. The raised ridges and furrows characteristic of the absence of SinR did not develop (compare Fig. 4E and F). Introduction of the *amyE*::$P_{hy\text{-}spank}$-*yuaB-lacI* construct to the *yuaB sinIR* mutant strain restored the furrows and raised ridges to the pellicle formed in the presence of IPTG (NRS2749) (Fig. 4H). On solid media the alteration in morphology between the *yuaB sinIR* (NRS2291) and *sinIR* (DS93) mutant strains was apparent but was more subtle than that between the *yuaB abrB* double mutant and its parental *abrB* mutant strain (compare Fig. 4E with F and Fig. 4C with D). This difference presumably reflects the difference in the levels of EPS and TasA produced in the *abrB* (12, 18) and *sinIR* (11) mutant strains.

To rule out the possibility that the reduced complexity of the *yuaB abrB* and *yuaB sinIR* mutant strains was somehow linked to a reduction in expression from either the *epsA–O* or *tapA* operon promoter, the level of transcription was determined at the single-cell level by flow cytometry using a P*eps-gfp* and a P*tapA-gfp* transcriptional reporter fusion. It is known that deletion of either *abrB* or *sinR* increases transcription from the *epsA–O* and *tapA* operon promoters (27), and this is manifested by an increase in the number of cells that transcribe these operons and the level of expression (10). It was found that deletion of *yuaB* did not negatively influence the transcription profile from either the *epsA–O* promoter (data not shown) or the *tapA* operon promoter in the absence of AbrB or SinR (Fig. 4). Therefore, the loss of complexity of biofilm formed by the *yuaB abrB* and *yuaB sinIR* mutant strains was not a consequence of a reduction in transcription of the *epsA–O* and *tapA* operons. The simplest explanation for these findings is that YuaB is required in addition to EPS and TasA to allow biofilm maturation.

The function of YuaB benefits all members of the biofilm. The data presented above support the hypothesis that YuaB, TasA, and the EPS are all needed for biofilm maturation. A wild-type biofilm formation can be restored when an *epsA–O* mutant strain is cocultured with a *tasA* mutant strain (4). This is consistent with the fact that both EPS and TasA are extracellular components of the matrix and that they are produced only by a subpopulation of the cells in the community (10, 41). To establish if the function of YuaB could also be shared within the biofilm community, despite YuaB being localized to the cell wall (Fig. 2) and produced by each cell rather than in a bimodal manner (24), the following approach was taken. A strain carrying mutations in both *epsA–O* and *tasA* (NRS2451) was cocultured with the *yuaB* mutant strain (NRS2097). A mature biofilm was observed to form when the coculture was grown on solid media. This is depicted by the complex architecture shown in Fig. 5I and demonstrates that the activity of the mature YuaB protein can be shared within the biofilm, as only 50% of the cell population in the experiment was wild type for YuaB. To establish the maturity of the biofilm and to test if the biofilm matrix had assembled correctly, we determined the number of cells in the biofilm that had sporulated. Consistent with the visual appearance of the biofilm, an average of 82% sporulation efficiency was seen (data not shown). This is

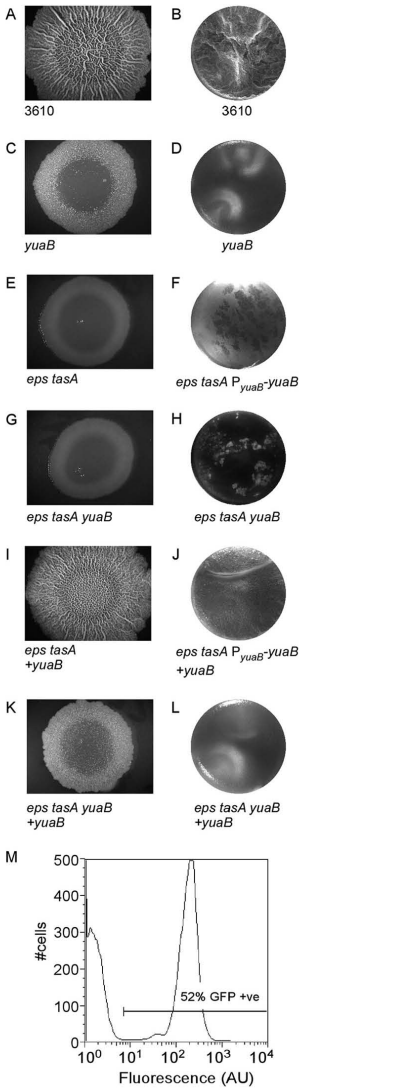

FIG. 5. Wild-type biofilm formation can be restored on coculture. Representative images of colony morphology after 48 h incubation at 37°C and pellicles after 96 h incubation at 25°C are shown. Wild type (NCIB 3610) (A and B), *yuaB* mutant (NRS2097) (C and D), *epsA–O tasA* mutant (NRS2451) (E), *epsA–O tasA* P_{yuaB}-*yuaB* mutant (NRS2980) (F), *epsA–O tasA yuaB* mutant (NRS2453) (G and H), *epsA–O tasA* mutant (NRS2451) cocultured with the *yuaB* mutant (NRS2097) (I), *epsA–O tasA* P_{yuaB}-*yuaB* mutant (NRS2980) cocultured with the *yuaB* mutant (NRS2097) (J), and *epsH tasA yuaB* mutant (NRS2431) cocultured with the *yuaB* mutant (NRS2097) (K and L). (M) Flow cytometry of the *epsA–O tasA* strain (NRS2451) cocultured with the *yuaB* green fluorescent protein (GFP)-positive strain (NRS2417) after 30 h incubation on solid media at 37°C. The percentage of GFP-positive cells is indicated and represents the number of *yuaB* cells in the biofilm.

a level similar to that seen for the wild-type strain alone (Fig. 2). In addition we determined if the biofilm formed after coculture was composed of equal numbers of the *epsA–O tasA* (NRS2451) and *yuaB* cells (NRS2097). To do this, a constitutively transcribed copy of *gfp* was introduced into the *yuaB* strain (NRS2417). Cells were collected from the coculture biofilm grown on solid MSgg after 30 h incubation (see Materials and Methods), and the proportion of fluorescent to nonfluorescent cells was calculated by flow cytometry. The mature biofilm formed after coculture was composed of both strains in the starting inoculum in equal numbers (Fig. 5M). We also ensured that the strains recovered from the coculture experiment retained the drug markers associated with the mutations (data not shown). Interestingly we could not entirely replicate the complex colony coculture complementation when pellicle formation was used as a measure of biofilm formation (Fig. 5). We hypothesized that this might be caused by a low concentration of YuaB in the biofilm when only 50% of the cells are capable of synthesizing YuaB. Therefore, we constructed a strain in the *epsA–O tasA* genetic background that carried an additional copy of *yuaB* under its native promoter at an ectopic locus (NRS2980). When this strain was cocultured with the *yuaB* mutant (NRS2097), it was able to partially restore pellicle formation in liquid media. This is depicted by increased thickness and the more wrinkled surface of the pellicle (Fig. 5J). We presume that the success of the coculture complementation in the complex colony and only partial success in the pellicle is due to YuaB being located in the cell wall. One can imagine that in the complex colony the cells have a closer juxtaposition, and therefore, YuaB will be able to exert its impact on neighboring cells more efficiently. In contrast, in the pellicle environment the cells are likely to have a looser association, and therefore, the impact of the cell wall-associated protein YuaB is less apparent when not present in all of the cells. The exact mechanism of how the function of YuaB is shared between the biofilm members is the subject of current investigation.

Before moving on, we ensured that the success of the complex colony coculture experiments was specifically a result of YuaB being synthesized by the *epsA–O tasA* strain (NRS2451) and the EPS and TasA being made by the *yuaB* strain (NRS2097); we cocultured a strain that contained a mutation in *yuaB* as well as *epsA–O* and *tasA* (NRS2453) with the single *yuaB* mutant (NRS2097). Biofilm formation was not restored (Fig. 5K and L). Using spore formation as a proxy for biofilm maturation of the complex colony, it was determined that only 20% of the cell population had sporulated (data not shown). This represents a 4-fold decrease in comparison to that for coculture experiments using the *yuaB* mutant and *epsA–O tasA* double mutant. These findings support the biofilm analysis and indicate that a mature biofilm is formed only when the products of the *epsA–O*, *tapA*, and *yuaB* operons are synthesized.

YuaB does not affect production of EPS or TasA. Having clearly shown that YuaB is needed for biofilm formation and that its absence cannot be compensated for by increased production of TasA and EPS, we wanted to start to define the mechanism of function. We proposed two simple hypotheses: first, that YuaB influenced EPS biosynthesis and, second, that YuaB controlled TasA biosynthesis or localization. This would be at the posttranscriptional level, as we have shown that transcription from the *epsA* and *tapA* promoters was not influenced by the absence of YuaB (Fig. 4 and data not shown). Disruption of the correct production of either of these components would explain the biofilm defect observed for the *yuaB* mutant. To investigate if the *yuaB* mutation affected production of the EPS, carbohydrates from the matrix fraction of the biofilm were extracted and analyzed by Schiff's staining after gel electrophoresis (36). For this analysis the wild-type (NCIB 3610), *yuaB* mutant (NRS2097), *sinIR* mutant (DS93), and *yuaB sinIR* double mutant (NRS2291) strains were used alongside the *epsA–O* (NRS2450) strain as a negative control. From the analysis, we did not detect a significant difference in the amount or size of EPS produced in the absence of *yuaB* in either the wild-type or *sinR* mutant background (Fig. 6A).

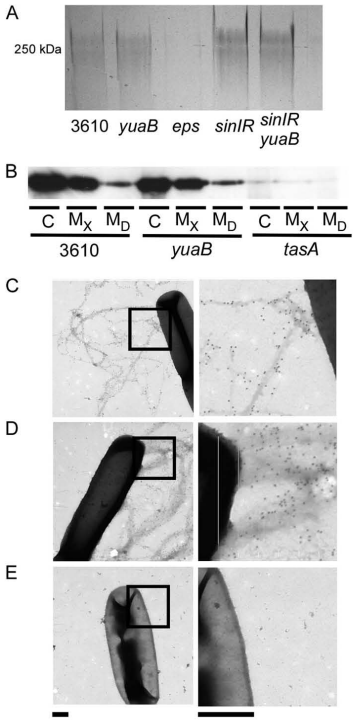

FIG. 6. YuaB is not required for the production of the EPS or TasA amyloid fibers. (A) EPS was extracted from the biofilm pellicles of the wild type (NCIB 3610) and the *yuaB* (NRS2097), *epsA–O* (NRS2450), *sinIR* (DS93), and *sinIR yuaB* (NRS2291) mutants, resolved by SDS-PAGE, and stained using Schiff's method. (B) Pellicles of the wild type (NCIB 3610), *yuaB* mutant (NRS2097), and *tasA* mutant (NRS2415) were collected and separated into cell (C), matrix (M_X), and growth medium (M_D) fractions. Localization of TasA was identified by Western blotting. TasA fibers were visualized for the wild type (NRS2450) (C), *yuaB* mutant (NRS2452) (D), and *tasA* mutant (NRS2451) (E) by immunogold labeling. The images are of representative cells of each strain and surrounding extracellular space where the gold-decorated TasA fibers are visible. The images on the right in panels C, D, and E represent magnifications of the images on the left, as indicated by black boxes. The scale bars represent 0.5 μm.

Therefore, we conclude that YuaB does not influence the quantity or size of the EPS synthesized, but we cannot eliminate the possibility that YuaB influences the linkage of the monosaccharides within the EPS polymer.

To analyze if TasA was produced, localized, and assembled correctly in the *yuaB* mutant, the biofilms from wild-type and *yuaB* mutant strains were fractionated into cell, matrix, and growth medium fractions and analyzed by Western blot analysis (Fig. 6B). Consistent with previous data (4), TasA was detected in abundance in the matrix and cell lysate fractions from both pellicles. A small amount was located in the growth medium, which represents detached TasA fibers (34). No difference in band intensities could be observed in the absence of *yuaB* (Fig. 6B). The *tasA* strain was used as a negative control to ensure band specificity. Outside the cell, TasA assembles into amyloid fibers that are attached to the cell surface and can be visualized by immunogold EM analysis (34). The analysis was conducted using strains mutated for the *epsA–O* operon. TasA amyloid fibers decorated with gold particles were found in abundance for both wild-type (NRS2450) (Fig. 6C) and *yuaB* mutant (NRS2452) strains (Fig. 6D) but not when the *tasA* (NRS2451) control strain was used (Fig. 6E). Therefore, no difference in the assembly or anchoring of the TasA fibers was observed in the absence of *yuaB*, and we conclude that YuaB is not involved in synthesis, localization, or polymerization of TasA.

Concluding remarks. The principal conclusion of this work is that the *B. subtilis* cell wall protein YuaB acts in a synergistic manner with the TasA amyloid fibers and the EPS polymer to allow biofilm development. This conclusion is based on the findings that production of the EPS and TasA amyloid fibers is not affected by the absence of YuaB but biofilm formation is ablated (Fig. 5 and 6). The role that YuaB plays during biofilm formation is unique when it is considered alongside TapA (recently renamed from YqxM [35]), as anchoring of TasA fibers to the cell is not affected by the absence of YuaB as it is by the absence of TapA (Fig. 6). The simplest interpretation of our findings is that synthesis of the EPS and the TasA amyloid fibers is not sufficient to allow the biofilm matrix to assemble and that YuaB is also required. We have also demonstrated that activation of transcription of *yuaB* is the major function of the response regulator DegU during the activation of biofilm formation. This was apparent, as ectopic expression of *yuaB* from an IPTG-driven promoter in the *degU* genetic background was sufficient to restore the wild-type biofilm architecture (Fig. 1A). It was shown that transcription of *yuaB* is indirectly activated by DegU~P (Fig. 1B); therefore, it will be of interest to determine how DegU~P triggers activation of *yuaB* transcription. It is possible that DegU~P either activates transcription of an activator or inhibits expression of a repressor protein that directly controls transcription from the *yuaB* promoter. Moreover, we cannot completely rule out the possibility that DegU~P, in fact, does bind to the promoter of *yuaB in vivo* but not *in vitro*. Transcription of *yuaB* is also directly repressed by AbrB (40) and indirectly activated by Rok (24). The relief of the AbrB-mediated *yuaB* transcription repression is under the control of the regulator Spo0A (40). Spo0A also directs the production of the EPS and TasA amyloid fibers (25, 27). Perhaps this genetic circuitry has evolved to ensure that when the EPS and TasA are produced, YuaB is also generated since the products of all three operons are needed for biofilm formation. There are various models that can be proposed to explain how YuaB may act synergistically with TasA and the EPS to facilitate biofilm formation. For example, once synthesized and transported to the cell wall, YuaB may promote the attachment of the EPS to the cell surface by acting as an adhesion. Furthermore YuaB may allow an interaction between the TasA amyloid fibers and the EPS to occur, thereby provoking the assembly of a functional matrix. It will be of interest in the future to characterize at the molecular level how YuaB is regulated and how it facilitates biofilm formation. This will begin to address the complex question of how extracellular molecules interact in a specific manner to form an organized and structured community.

ACKNOWLEDGMENTS

This work was supported by the Biotechnology and Biological Sciences Research Council (grant number BB/C520404/1). A.O. is the recipient of a Biotechnology and Biological Sciences Research Council Doctoral Training Account grant (BB/D526161/1).

We thank Dan Kearns for strain DS93, Roberto Kolter for the *epsA–O::tet* mutant strain, and Daan van Aalten and members of the NSW lab for helpful discussions.

REFERENCES

1. **Aguilar, C., H. Vlamakis, A. Guzman, R. Losick, and R. Kolter.** 2010. KinD is a checkpoint protein linking spore formation to extracellular-matrix production in *Bacillus subtilis* biofilms. mBio **1:**e00035–10.
2. **Antelmann, H., et al.** 2001. A proteomic view on genome-based signal peptide predictions. Genome Res. **11:**1484–1502.
3. **Bais, H. P., R. Fall, and J. M. Vivanco.** 2004. Biocontrol of *Bacillus subtilis* against infection of *Arabidopsis* roots by *Pseudomonas syringae* is facilitated by biofilm formation and surfactin production. Plant Physiol. **134:**307–319.
4. **Branda, S. S., F. Chu, D. B. Kearns, R. Losick, and R. Kolter.** 2006. A major protein component of the *Bacillus subtilis* biofilm matrix. Mol. Microbiol. **59:**1229–1238.
5. **Branda, S. S., J. E. Gonzalez-Pastor, S. Ben-Yehuda, R. Losick, and R. Kolter.** 2001. Fruiting body formation by *Bacillus subtilis*. Proc. Natl. Acad. Sci. U. S. A. **98:**11621–11626.
6. **Branda, S. S., S. Vik, L. Friedman, and R. Kolter.** 2005. Biofilms: the matrix revisited. Trends Microbiol. **13:**20–26.
7. **Britton, R. A., et al.** 2002. Genome-wide analysis of the stationary-phase sigma factor (sigma-H) regulon of *Bacillus subtilis*. J. Bacteriol. **184:**4881–4890.
8. **Brown, W. C.** 1973. Rapid methods for extracting autolysins from *Bacillus subtilis*. Appl. Microbiol. **25:**295–300.
9. **Burbulys, D., K. A. Trach, and J. A. Hoch.** 1991. Initiation of sporulation in *B. subtilis* is controlled by a multicomponent phosphorelay. Cell **64:**545–552.
10. **Chai, Y., F. Chu, R. Kolter, and R. Losick.** 2008. Bistability and biofilm formation in *Bacillus subtilis*. Mol. Microbiol. **67:**254–263.
11. **Chu, F., D. B. Kearns, S. S. Branda, R. Kolter, and R. Losick.** 2006. Targets of the master regulator of biofilm formation in Bacillus subtilis. Mol. Microbiol. **59:**1216–1228.
12. **Chu, F., et al.** 2008. A novel regulatory protein governing biofilm formation in Bacillus subtilis. Mol. Microbiol. **68:**1117–1127.
13. **Costerton, J. W., et al.** 1987. Bacterial biofilms in nature and disease. Annu. Rev. Microbiol. **41:**435–464.
14. **Davey, M. E., and A. G. O'Toole.** 2000. Microbial biofilms: from ecology to molecular genetics. Microbiol. Mol. Biol. Rev. **64:**847–867.
15. **Emanuelsson, O., S. Brunak, G. von Heijne, and H. Nielsen.** 2007. Locating proteins in the cell using TargetP, SignalP and related tools. Nat. Protoc. **2:**953–971.
16. **Gueriri, I., S. Bay, S. Dubrac, C. Cyncynatus, and T. Msadek.** 2008. The Pta-AckA pathway controlling acetyl phosphate levels and the phosphorylation state of the DegU orphan response regulator both play a role in regulating *Listeria monocytogenes* motility and chemotaxis. Mol. Microbiol. **70:**1342–1357.
17. **Hall-Stoodley, L., J. W. Costerton, and P. Stoodley.** 2004. Bacterial biofilms: from the natural environment to infectious diseases. Nat. Rev. Microbiol. **2:**95–108.
18. **Hamon, M. A., N. R. Stanley, R. A. Britton, A. D. Grossman, and B. A. Lazazzera.** 2004. Identification of AbrB-regulated genes involved in biofilm formation by *Bacillus subtilis*. Mol. Microbiol. **52:**847–860.
19. **Harwood, C. R., and S. M. Cutting.** 1990. Molecular biological methods for *Bacillus*. John Wiley & Sons Ltd., Chichester, England.

20. **Karatan, E., and P. Watnick.** 2009. Signals, regulatory networks, and materials that build and break bacterial biofilms. Microbiol. Mol. Biol. Rev. **73:**310–347.
21. **Kearns, D. B., F. Chu, S. S. Branda, R. Kolter, and R. Losick.** 2005. A master regulator for biofilm formation by *Bacillus subtilis*. Mol. Microbiol. **55:**739–749.
22. **Kiley, T. B., and N. R. Stanley-Wall.** 2010. Post-translational control of *Bacillus subtilis* biofilm formation mediated by tyrosine phosphorylation. Mol. Microbiol. **78:**947–963.
23. **Kobayashi, K.** 2007. Gradual activation of the response regulator DegU controls serial expression of genes for flagellum formation and biofilm formation in *Bacillus subtilis*. Mol. Microbiol. **66:**395–409.
24. **Kovács, A. T., and O. P. Kuipers.** 2011. Rok regulates *yuaB* expression during architecturally complex colony development of *Bacillus subtilis* 168. J. Bacteriol. **193:**998–1002.
25. **Lopez, D., and R. Kolter.** 2010. Extracellular signals that define distinct and coexisting cell fates in *Bacillus subtilis*. FEMS Microbiol. Rev. **34:**134–149.
26. **Lopez, D., H. Vlamakis, and R. Kolter.** 2010. Biofilms. Cold Spring Harb. Perspect. Biol. **2:**a000398.
27. **Lopez, D., H. Vlamakis, and R. Kolter.** 2009. Generation of multiple cell types in *Bacillus subtilis*. FEMS Microbiol. Rev. **33:**152–163.
28. **Lopez, D., H. Vlamakis, R. Losick, and R. Kolter.** 2009. Paracrine signaling in a bacterium. Genes Dev. **23:**1631–1638.
29. **Middleton, R., and A. Hofmeister.** 2004. New shuttle vectors for ectopic insertion of genes into Bacillus subtilis. Plasmid **51:**238–245.
30. **Murray, E. J., T. B. Kiley, and N. R. Stanley-Wall.** 2009. A pivotal role for the response regulator DegU in controlling multicellular behaviour. Microbiology **155:**1–8.
31. **Murray, E. J., M. A. Strauch, and N. R. Stanley-Wall.** 2009. σX is involved in controlling *Bacillus subtilis* biofilm architecture through the AbrB homologue Abh. J. Bacteriol. **191:**6822–6832.
32. **Ogura, M., K. Shimane, K. Asai, N. Ogasawara, and T. Tanaka.** 2003. Binding of response regulator DegU to the aprE promoter is inhibited by RapG, which is counteracted by extracellular PhrG in Bacillus subtilis. Mol. Microbiol. **49:**1685–1697.
33. **Perego, M., G. B. Spiegelman, and J. A. Hoch.** 1988. Structure of the gene for the transition state regulator, *abrB*: regulator synthesis is controlled by the *spo0A* sporulation gene in *Bacillus subtilis*. Mol. Microbiol. **2:**689–699.
34. **Romero, D., C. Aguilar, R. Losick, and R. Kolter.** 2010. Amyloid fibers provide structural integrity to *Bacillus subtilis* biofilms. Proc. Natl. Acad. Sci. U. S. A. **107:**2230–2234.
35. **Romero, D., H. Vlamakis, R. Losick, and R. Kolter.** 2011. An accessory protein required for anchoring and assembly of amyloid fibres in *B. subtilis* biofilms. Mol. Microbiol. **80:**1155–1168.
36. **Segrest, J. P., and L. Jackson.** 1972. Molecular weight determination of glycoproteins by polyacrylamide gel electrophoresis in sodium dodecyl sufate. Methods Enzymol. **28:**54–63.
37. **Stanley, N. R., R. A. Britton, A. D. Grossman, and B. A. Lazazzera.** 2003. Identification of catabolite repression as a physiological regulator of biofilm formation by *Bacillus subtilis* by use of DNA microarrays. J. Bacteriol. **185:**1951–1957.
38. **Stanley, N. R., and B. A. Lazazzera.** 2005. Defining the genetic differences between wild and domestic strains of *Bacillus subtilis* that affect poly-gamma-DL-glutamic acid production and biofilm formation. Mol. Microbiol. **57:**1143–1158.
39. **Verhamme, D. T., T. B. Kiley, and N. R. Stanley-Wall.** 2007. DegU coordinates multicellular behaviour exhibited by *Bacillus subtilis*. Mol. Microbiol. **65:**554–568.
40. **Verhamme, D. T., E. J. Murray, and N. R. Stanley-Wall.** 2009. DegU and Spo0A jointly control transcription of two loci required for complex colony development by *Bacillus subtilis*. J. Bacteriol. **191:**100–108.
41. **Vlamakis, H., C. Aguilar, R. Losick, and R. Kolter.** 2008. Control of cell fate by the formation of an architecturally complex bacterial community. Genes Dev. **22:**945–953.